MATHEMATICAL MODELS FOR WILDLIFE DISEASE MANAGEMENT

by
Eleanor Tanner

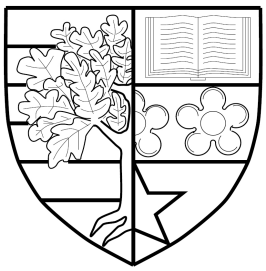

Submitted for the degree of
Doctor of Philosophy

Department of Mathematics
School of Mathematical and Computer Sciences
Heriot-Watt University

May , 2019

Abstract

Endemic diseases in wildlife present both intra- and inter-species management problems with risk to conservation of endangered species and spillover of virulent disease to other wildlife, farmed and domestic populations. Mathematical models have been developed to aid understanding of the transmission and persistence of such endemic disease. We review such models with an emphasis on models of tuberculosis. The understanding gained from previous model studies is used to formulate a new mathematical model for the wild boar reservoir of tuberculosis in central Spain where the disease persists at high prevalence and impacts other wild and domestic species. This model is used to investigate the efficacy of hunting and vaccination as management techniques to control tuberculosis in wild boar. Insight from the specific wild boar TB model generates a general result for compensatory population growth following culling of a population harbouring endemic disease. We show that compensatory growth due to a reduction in disease-induced mortality following culling could be a new mechanism for producing the 'Hydra' effect. We extend the wild boar TB model to reflect the situation in Asturias where wolf predation may influence the disease dynamics leading to lower prevalence of tuberculosis in wild boar. In conclusion we review how our findings can provide insight for disease management and control, and consider how the model could be extended to investigate emerging diseases for which wild boar may also be a reservoir.

Acknowledgements

Primarily I would like to thank my supervisor Prof. Andy White for his care, patience and direction during my research. It has been a privilege to work with Andy and benefit from his wealth of skill and experience.

I have been very fortunate to work on such an exciting project in cooperation with veterinarians in Spain. I am very grateful to Prof. Christian Gortázar whose knowledge and ideas have been invaluable, and who, along with his team, extended such a warm welcome when we have visited Spain. I would also like to thank Christian for the use of his fabulous photographs to illustrate this thesis.

I would not have been able to perform this research without support from the MIGSAA programme at the Maxwell Institute. They have provided both funding and academic support throughout my PhD, and encouraged me to reach beyond the confines of my research topic. I am indebted to Prof. Jonathan Sherratt who initially put my name forward for the MIGSAA programme, and who has provided such interesting courses during my pursuit of MIGSAA credits. I would also like to thank my fellow MIGSAA students at Heriot-Watt University: Eleni Moraki, Jamie Bennett, and Antonios Ververis. We shared an office, coffee, frustrations and successes and they have been a wonderful support network.

Finally I would like to thank my friends and family who have been a constant support, although perhaps a little surprised that a mathematics PhD can involve wild boar.

ACADEMIC REGISTRY
Research Thesis Submission

Name*:*	Eleanor Tanner		
School:	MACS		
Version: *(i.e. First, Resubmission, Final)*	Final	Degree Sought:	PhD

Declaration

In accordance with the appropriate regulations I hereby submit my thesis and I declare that:

1. The thesis embodies the results of my own work and has been composed by myself
2. Where appropriate, I have made acknowledgement of the work of others
3. Where the thesis contains published outputs under Regulation 6 (9.1.2) these are accompanied by a critical review which accurately describes my contribution to the research and, for multi-author outputs, a signed declaration indicating the contribution of each author (complete Inclusion of Published Works Form – see below)
4. The thesis is the correct version for submission and is the same version as any electronic versions submitted*.
5. My thesis for the award referred to, deposited in the Heriot-Watt University Library, should be made available for loan or photocopying and be available via the Institutional Repository, subject to such conditions as the Librarian may require
6. I understand that as a student of the University I am required to abide by the Regulations of the University and to conform to its discipline.
7. Inclusion of published outputs under Regulation 6 (9.1.2) shall not constitute plagiarism.
8. I confirm that the thesis has been verified against plagiarism via an approved plagiarism detection application e.g. Turnitin.

* *Please note that it is the responsibility of the candidate to ensure that the correct version of the thesis is submitted.*

Signature of Candidate*:*		Date:	

Submission

Submitted By *(name in capitals):*	ELEANOR TANNER
Signature of Individual Submitting:	
Date Submitted:	

For Completion in the Student Service Centre (SSC)

Received in the SSC by *(name in capitals):*			
Method of Submission *(Handed in to SSC; posted through internal/external mail):*			
*E-thesis Submitted (**mandatory for final theses)***			
Signature:		Date:	

ACADEMIC REGISTRY

Inclusion of Published Works

Declaration

This thesis contains one or more multi-author published works. In accordance with Regulation 6 (9.1.2) I hereby declare that the contributions of each author to these publications is as follows:

Citation details	Iratxe Díez-Delgado, Iker A. Sevilla, Beatriz Romero, Eleanor Tanner, Jose A. Barasona, Andrew R. White, Peter W.W. Lurz, Mike Boots, José de la Fuente, Lucas Dominguez, Joaquin Vicente, Joseba M. Garrido, Ramón A. Juste, Alicia Aranaz, Christian Gortázar, "Impact of piglet oral vaccination against tuberculosis in endemic free-ranging wild boar populations", Preventive Veterinary Medicine, *155*, pp.11-20 (2018)
Iratxe Díez-Delgado	Vaccine trial development, field data collection and ecological analysis
Eleanor Tanner	Mathematical analysis
Andy White	Mathematical analysis
Sevilla, I.A., Romero, B., Barasona, J.A., Lurz, P.W., Boots, M., de la Fuente, J., Dominguez, L., Vicente, J., Garrido, J.M., Juste, R., Aranaz, A., Gortázar, C.	Vaccine trial development and ecological analysis
Signature:	
Date:	

Citation details	Eleanor Tanner, Andy White, Peter W.W. Lurz, Christian Gortázar, Iratxe Díez-Delgado, and Mike Boots, "The critical role of infectious disease in compensatory population growth in response to culling", The American Naturalist, (July 2019), https://doi.org/10.1086/703437
Eleanor Tanner	Mathematical analysis
Andy White	Mathematical analysis
Peter W.W. Lurz, Christian Gortázar, Iratxe Díez-Delgado, and Mike Boots	Ecological analysis
Signature:	
Date:	

Citation details	Eleanor Tanner, Andy White, Pelayo Acevedo, Ana Balseiro, Jaime Marcos and Christian Gortázar, ” Wolves contribute to disease control in a multi-host system”, Scientific Reports, In preparation, (Accepted May 2019)
Eleanor Tanner	Mathematical analysis
Andy White	Mathematical analysis
Pelayo Acevedo, Ana Balseiro, Jaime Marcos and Christian Gortázar	Ecological analysis
Signature:	
Date:	

Contents

1 Introduction **1**

2 Introduction to modelling tuberculosis in wildlife **6**

2.1 Deterministic modelling of TB in badger populations 8

2.1.1 Susceptible Exposed Infected model 12

2.1.2 SEI The Basic Reproductive Rate R_0 for the Disease 12

2.1.3 SEI Transmission Coefficient $\boldsymbol{\beta}$ 13

2.1.4 Results for SEI model 13

2.1.5 Vertical transmission in SEI model 13

2.1.6 SEI vertical transmission R_0 15

2.1.7 SEI vertical transmission results 15

2.1.8 SEI with free-living particles 16

2.1.9 SEI model with constant density of free-living particles 17

2.1.10 SEI model with varying density of free-living particles 18

2.2 Stochastic modelling of TB in Badgers 20

2.3 Stochastic modelling of TB in wild boar 20

2.4 Stochastic modelling of TB in cattle 21

2.5 Summary of models 22

Appendices to Chapter 2 25

2A.1 Steady states for logistic growth model 25

2A.2 Steady states for logistic growth model with enhanced density dependent effects 25

2A.3 SEI Steady State and Stability Analysis 26

2A.4 SEI with vertical transmission steady state and stability analysis . . . 27

2A.5 SEI with free-living steady state and stability analysis 28

2B.1 Stochastic SEI model 29

2B.1.1 Stochastic SEI results 30

2B.2 Spatial Stochastic SEI model 32

2B.2.1 Spatial Array 33

2B.2.2 Spatial parameters and boundary conditions 34

2B.2.3 Spatial Stochastic Results 35

3 Developing a wild boar TB model **40**

3.1 The Piglet-Yearling-Adult (PYA) model 42

3.1.1 PYA model: Default parameter set . . . 45
3.1.2 Sensitivity of c_β and c_ε to model changes . . . 48
3.1.3 Sensitivity of total population to model changes . . . 49
3.1.4 Sensitivity of individual class populations to model changes . 50
3.2 PYA model: discussion of age structure . . . 51
3.3 PYA Model: the response of infection to changes in population size . 51
3.4 PYA model: birth from the generalised class . . . 52
3.4.1 PYA model: pseudo-vertical transmission . . . 55
3.5 PYA model enhancement to PYAG model . . . 56
3.6 PYAG model: varying key model parameters . . . 58
3.6.1 Varying virulence of the disease α . . . 58
3.6.2 Varying progression to generalised ε_A . . . 59
3.6.3 Varying disease transmission β_A . . . 59
3.6.4 Varying natural death rate d . . . 61
3.6.5 Varying free-living decay rate μ . . . 61
3.7 PYAG wild boar TB model discussion . . . 61
Appendices to Chapter 3 . . . 63
3A.1 SIGF: critical population threshold . . . 63

4 Management of tuberculosis in wild boar 65
4.1 Wild boar TB management: Vaccination . . . 65
4.1.1 Piglet vaccination modelling . . . 67
4.1.2 Piglet vaccination model parameters . . . 69
4.1.3 Piglet vaccination model results . . . 70
4.2 Wild boar TB management: Hunting . . . 71
4.3 Discussion . . . 74

5 Population compensatory growth as a result of culling 76
5.1 Abstract . . . 76
5.2 Introduction . . . 77
5.3 Methods . . . 78
5.4 Results . . . 82
5.4.1 The effects of culling in populations with virulent infection and no recovery . . . 82
5.4.2 The effects of culling in populations with virulent infection and recovery to immunity . . . 84
5.4.3 The impact of culling on population management . . . 85
5.4.4 The impact of culling on disease management . . . 86
5.4.5 Generality of model findings . . . 87
5.5 Case Study . . . 89
5.6 Discussion . . . 91

Appendices to Chapter 5 . . . 95
5A.1 System steady states and restrictions . . . 95
5A.2 Continuous culling . . . 96
5A.2.1 Steady state condition for the demographic effects only model 97
5A.2.2 Steady states for continuous culling with DD transmission . . 98
5A.2.3 N_{DD} and N_{dis} decrease as γ increases . . . 99
5A.2.4 The relationship between N_{DD} and N_e . . . 100
5A.2.5 The relationship between N_{DD} and N_{dis} . . . 100
5A.2.6 The relationship between N_{DD} and N_{dem} . . . 100
5A.2.7 The relationship between N_{dis} and N_{dem} . . . 101
5A.2.8 Steady states for continuous culling with FD transmission . . 101
5A.2.9 The relationship between N_{FD} and N_e . . . 102
5A.2.10 The relationship between N_{FD} and N_{dem} . . . 102
5A.2.11 Conclusion: the relationships between N_e, N_{DD}, N_{FD}, N_{dem} and N_{dis} . . . 102
5A.2.12 Indiscriminate continuous culling results for $b(N) = b(1 - qN)$ 102
5A.3 Free living transmission . . . 103
5A.4 The impact of targeted culling of infecteds . . . 105
5A.4.1 Continuous targeted infected culling steady states . . . 105
5A.4.2 Steady states for continuous targeted infected culling with DD transmission . . . 106
5A.4.3 Steady states for continuous targeted infected culling with FD transmission . . . 106
5A.4.4 The relationship between N_{DD}^T and N_{FD}^T . . . 107
5A.4.5 Conclusion, the relationships between N_{DD}^T, N_{FD}^T and N_e . . . 107
5A.4.6 Targeted infected continuous culling results for $b(N) = b(1-qN)$ 107
5A.5 Density dependent mortality . . . 110
5A.5.1 Why the demographic effects only model remains invariant to changes in q_b . . . 113
5A.5.2 Density dependent mortality with FD transmission . . . 114
5A.5.3 Density dependent mortality with DD transmission . . . 114
5A.6 Parameter sensitivity . . . 115
5A.7 Wild boar TB model . . . 116
5A.7.1 Wild boar TB model parameters . . . 118

6 Wild boar model with predation **120**
6.1 Abstract . . . 121
6.2 Introduction . . . 121
6.3 Methods . . . 124
6.3.1 Ethics statement . . . 124
6.3.2 Study area and target species . . . 124

6.3.3 TB prevalence . . . 124
6.3.4 Asturias: estimating wolf population . . . 125
6.3.5 Mathematical Modelling . . . 125
6.4 Results . . . 127
6.4.1 Wolf population . . . 127
6.4.2 Wild boar population . . . 128
6.4.3 TB prevalence . . . 128
6.4.4 The model comparison to data for regions with wolves . . . 129
6.4.5 The impact of wolves on TB prevalence in the long-term . . . 130
6.4.6 Model comparison to data in areas of Asturias without wolves 132
6.4.7 The potential impact of predation in regions of high TB prevalence in wild boar . . . 132
6.5 Discussion . . . 134
6.6 Data availability . . . 137
6.7 Acknowledgements . . . 137
6.8 Author contributions statement . . . 138
Appendices to Chapter 6 . . . 139
6A.1 Wild boar TB model parameters . . . 139
6A.2 Asturias: prey selection . . . 141

7 Discussion **143**

Bibliography **149**

List of Tables

2.1 Badger SEI model parameters . . . 9
2.2 Stochastic SEI model events . . . 30
2.3 Spatial array of patches . . . 33
2.4 Spatial stochastic model events . . . 34

3.1 PYA model yearling class sensitivity . . . 47

List of Figures

1.1 Wild boar (*Sus Scrofa*) 5

2.1 Numerical solutions of Equation (2.1) for different growth rates 10
2.2 Solutions of Equation (2.3) for different values of density-dependence . 11
2.3 Numerical solutions for SEI model (Equations (2.5)) varying the transmission coefficient 14
2.4 Solutions for SEI model (Equations (2.7)) with vertical transmission . 15
2.5 Equations (2.7): R_0 versus probability p of vertical transmission . . . 16
2.6 SEI model (Equations (2.10)) with different values of $\beta_w W^*$ and constant level of free-living particles 17
2.7 SEI model (Equations (2.9)) for different values of μ and varying density of free-living particles 18
2.8 SEI model (Equations (2.9)) for different excretion rates with varying density of free-living particles 19
2.9 SEI model (Equations (2.9)) for different transmission rates and varying density of free-living particles 19
2B.1 Stochastic SEI model on a patch 1x1 km^2 30
2B.2 Stochastic SEI model on a patchwork 10x10km^2 31
2B.3 Stochastic SEI model (Equations (2B1)) probability for disease die-out in 10x10km^2 region 32
2B.4 Spatial stochastic model (Equations (2B2)) for spatial array of 20x20 1x1km^2 patches 35
2B.5 Spatial stochastic model represented by Equations (2B2) on a spatial array of 20x20 1x1km^2 patches 37
2B.6 Spatial stochastic model (Equations (2B2)) population density 38
2B.7 Spatial stochastic model (Equations (2B2)) population density on a spatial array of 20x20 1x1km^2 patches 38
2B.8 Spatial stochastic model (Equations (2B2)) on a spatial array of 20x20 1x1km^2 patches 39

3.1 Wild boar at central Spain water hole 40
3.2 SIGF system 43
3.3 Schematic for PYA wild boar TB model 44
3.4 PYA model total population and level of free-living 48

3.5 PYA model: sensitivity of transmission parameters 49
3.6 PYA model choice: temporal changes in population 50
3.7 PYA total population and prevalence varying with carrying capacity . 52
3.8 PYA model birth from generalised 53
3.9 PYA model response to change in population size with generalised birth 54
3.10 PYA model sensitivity to c_β and c_ε 54
3.11 PYA model sensitivity to fecundity of generalised individuals 55
3.12 PYA model schematic including pseudo-vertical transmission 56
3.13 PYA model effect of pseudo-vertical transmission 57
3.14 PYAG parameter sensitivity 60

4.1 Central Spain water hole and vaccination cages 66
4.2 Temporal trend of tuberculosis (TB) lesion prevalence of piglets and total population by site. 66
4.3 Schematic representation of the wild boar TB vaccination model . . . 67
4.4 Extended modelling results for wild boar vaccination against tuberculosis 70
4.5 Wild boar TB model response to culling 72
4.6 Wild boar TB model: response to hunting 73

5.1 SI and SIR model response to culling 81
5.2 SI model phase plane and force of infection 83
5.3 SI model compensatory growth 84
5.4 SIR model compensatory growth 86
5.5 SIRS model response to culling 87
5.6 Wild boar TB model case study results 90
5A.1 SI model response to continuous culling 96
5A.2 SI an SIR compensatory response to continuous culling 98
5A.3 SI model discrete versus continuous results 99
5A.4 SI model discrete versus continuous sensitivity to culling rate 104
5A.5 SI model results with free-living transmission 104
5A.6 SI and SIR model response to targeted infected culling 108
5A.7 SI and SIR model targeted culling compensation 109
5A.8 SI and SIR model targeted culling compensation sensitivity to culling rate 111
5A.9 SI model with density dependent death 113
5A.10 SI and SIR model parameter sensitivity 116

6.1 Wolf (*Canis lupus*) 120
6.2 Wolf (*Canis lupus*) distribution maps in the Iberian Peninsula 123
6.3 Asturias wild boar hunting harvest 125
6.4 Asturias: the rate of increase in wolf attacks 128
6.5 Asturias: mean TB prevalence for wild boar and cattle 129

6.6 Asturias wild boar TB model with wolf predation 131
6.7 Asturias wild boar TB model with no wolf predation 133
6.8 Varying wolf predation in area with high TB prevalence 133
6A.1 Asturias: effect of wolves preying on all classes of wild boar 142
6A.2 Asturias: effect of wolves preying on wild boar piglets only 142
6A.3 High TB prevalence area: effect of wolves preying on wild boar 142

7.1 Wild boar TB model response to culling combined with vaccination . 148

Chapter 1

Introduction

In a world of rising human population the increasing domestic demand for land is encroaching on hitherto wildlife habitat thus provoking a greater risk of conflict arising from these interactions. This shared use of space is often presented as a struggle between conserving a natural environment for increasingly endangered species and the human need to build more housing and increase food production. At the boundary between wild habitat and human existence direct conflict arises when natural predators prey on livestock and occasionally even humans.

However, less overt but nonetheless critical, there is another battle that occurs at this interface: the existence of pathogens that wild animals can harbour in so-called wildlife reservoirs of disease. These infectious diseases can pose different risks depending on their nature. There are diseases that cause a threat to a particular wild species but do not cross the wild-domestic boundary thereby depressing a wildlife species that is endangered or is a specific hunting target, e.g. facial tumour disease in Tasmanian devils [18] and chronic wasting disease (CWD) in cervids [136]. Some diseases may pass from wild to domestic livestock, and although they don't infect humans they can have significant negative impact on human food production e.g. African swine fever (ASF) in wild boar (*Sus scrofa*, Figure 1.1) and domestic pigs [61]. Finally there are zoonotic diseases that intersect the wildlife-livestock-human interface that may cause significant economic losses to agriculture and even severe threat to life e.g. rabies, tuberculosis [74].

Globally, humans have long sought to control, or even eradicate, infectious disease in wildlife using a range of management measures. In contrast to humans, of whom specific individuals can be targeted for vaccination to prevent disease occurrence or promptly administered medication to combat disease, wildlife cannot be accessed so easily making management of their diseases more complex. Of management techniques used in combating disease in wildlife, culling is widely used though it can be a blunt tool. The theory behind culling is that by reducing the density of a wild population this will reduce the number of infectious individuals and therefore reduce the chance of disease spread both within and between species.

Culling can be more successful if diseased individuals can be easily identified in the population. This form of control can be very contentious depending on the perceived 'value' of the species in its locale. For example, in the attempt to control bovine tuberculosis, the culling of possums in New Zealand, a non-indigenous species viewed as a pest, garners far more acceptance than the culling of badgers in Great Britain, one of their few large native mammals. Vaccination has also been used when available, with the aim of reducing the number of individuals in the population that are susceptible to disease. However, administering vaccines to wildlife in sufficient number to be effective is a complex task, can be expensive, and its success depends on the feasibility of accessing sufficient numbers of uninfected animals. Finally diseased animals may be targeted and removed from the general population and quarantined. However, locating and identifying infectious animals is not a simple task, for example in larger dispersed populations this may not be a feasible solution or for diseases that do not present with visible symptoms.

To ascertain the effectiveness of a particular management technique good concrete data are difficult to gather for wildlife populations. Such information can be patchy and estimates tend to be made at a group level by sampling a proportion of the population leading to a greater risk of inaccuracy. In the absence of empirical data, mechanistic mathematical models are a key tool used to develop understanding of complex disease dynamics in both single and multiple hosts, and test the effectiveness of management interventions. Mathematical models therefore can be used to predict the efficacy of interventions, and forecast future outcomes based on proposed control methods.

The development of mathematical modelling of population growth has a long history reaching deep into the last millennium. As Murray (2002) [103] notes, change in population has been explored mathematically as far back as Leonardo of Pisa in the 13th century regarding rabbit populations; by Malthus over 200 years ago postulating the exponential growth function to describe how total populations expand over time; and this refined by Verhulst in the 19th century who realised that populations are limited by resources, giving rise to the *logistic growth* function where populations rise to a notional *carrying capacity* beyond which there are not sufficient resources to sustain the population. Over the last century there has been an explosion in mathematical modelling of population change, in both single and multiple species, too numerous to enumerate here. Pertinent to this thesis are: developments in sustainable harvesting of fish and the effect of harvesting on fish stocks, notably Ricker (1954) [121] who developed his 'stock and recruitment' model showing how fish population growth compensated for mortality caused by repeated harvesting; May (1973) [96] examined dynamics of population growth in ecosystems; and originally published in 1976 but updated as May & McLean (2007) [95] the population dynamics of both single and multiple-species ecological systems including

predator prey type models.

Alongside population growth, models to investigate the effects of infectious disease on population dynamics have also been developed to understand factors affecting disease outbreak and die-back, disease prevalence and incidence, abundance of population with endemic disease, and dissemination of disease. Keeling & Rohani (2008) [84] detail models of a wide variety of infectious disease, affecting a range of different species, including modelling disease control measures. They note the history of disease modelling through early work by Bernoulli in the 18th century investigating immunisation against smallpox, and the development of compartmental Susceptible Infected Recovered (SIR) models through work by Kermack and McKendrick (1927) [85], Dietz (1967) [47] leading to Anderson and May (1979) [9] and further developed for diseases affecting humans Anderson & May (1991) [10]. These works form the foundation to develop mathematical tools to investigate management strategies for wildlife populations: culling, vaccination and targeted diseased removal, and the research for this thesis is a direct descendent of such models. These SIR type models partition populations into different classes dependent on their disease classification: susceptible, infected or recovered. Susceptible individuals may become infected by a probability that transmission occurs proportional to the total number of infected individuals in the population using the law of mass action. Infected individuals recover at a constant rate.

Models come in various guises dependent on the species, geographical spread and disease presentation, and can be classified further as deterministic or stochastic type models. Deterministic models will render the same result given the same initial conditions. They can be simpler to analyse mathematically, and also may reveal the underlying mechanisms driving changes to populations suffering endemic disease and management intervention. As deterministic models always achieve the same end result from a given starting position, they may not seem as attuned to real-life situations. Stochastic models address this by introducing real-life randomness into a system so are more able to represent disease outbreak and die-back. This model type may be more important when the population is small or when prevalence is low. Analysis of these models is more complex, and has to consider the variability between the different model outcomes. The choice of which model type to use is dependent on the type of disease and target population distribution, and also may be driven by the amount of data available to inform such models.

The research for this thesis has been motivated by veterinary research in central and southern Spain where tuberculosis (TB) is endemic in wild boar populations reaching high prevalence levels of greater than 50% [106]. It also persists, but at a lower prevalence, in other host species such as red deer, but wild boar are seen as the key wildlife reservoir of TB. These host species tend to gather around scant water resources, particularly during dry seasons. Current understanding is that

most infection occurs through contact with free-living *Mycobacterium tuberculosis* complex (MTC) shed by infected wild boar that utilise the same water sources [138]. Areas used for supplementary feeding are also implicated because of similar congregating effects though are not implicated to the same degree as water sources [138]. The high prevalence of TB in wildlife populations can lead to transmission and infection of adjacent livestock. This can have significant financial implications for the farming industry and motivates the need to develop management plans to control TB levels in reservoir wildlife systems. In this area there is a long cultural history of hunting wild boar and deer in both managed hunting estates and large unmanaged areas where both wild and domestic species may mingle. Despite annual culls returning large hunting bags, the density of wild boar has been rising and prevalence of TB has remained high. Trials vaccinating 3-6 month old piglets have taken place showing some success in reducing prevalence, however TB still remains endemic in the wild boar population. To help unpick the drivers influencing these rising wild boar densities and high TB prevalence, and understand the long-term impact of management interventions, veterinarians working in this area envisaged mathematical modelling as a key tool. This foresight has led to the collaboration of mathematicians (Andy White, supervisor of this research, and the author) with veterinarians based in Ciudad Real, Spain (led by Christian Gortázar) to help inform future management of wild boar in this area.

Bovine tuberculosis has been a persistent problem in a number of locations worldwide, hosted in a variety of worldwide reservoirs. Given the risk of spill-over to the human population and the severe economic cost to agriculture to prevent and contain cross-infection it is not surprising that a variety of mathematical models have already been developed, specific to species and locale, in efforts to understand the dynamics of MTC infection and effects of its management and control. Prior to developing a new mathematical model to help understand the wild boar TB system in Spain, it was necessary to review previous models of tuberculosis in wildlife reservoirs, which has been separated into an introductory chapter on modelling TB in wildlife in Chapter 2. Following this initial research we developed a model encapsulating the key processes regulating the wild boar TB system, collaborating with veterinarians to determine suitable characterisation of the population and parameterisation for the model. This model is detailed in Chapter 3. We have used this model to aid understanding of the wild boar TB system when culling and vaccination are uses as a management control, the results of which can be found in Chapter 4.

As research in one area can feed another, the work detailing the effect of culling wild boar suffering endemic tuberculosis stimulated a more general result regarding population compensation in response to culling wildlife harbouring virulent disease. This has become a piece of work that is separate from the main wild boar model,

though uses the wild boar TB model as a case study. It establishes a new means to a 'Hydra' effect [2] and can be found in Chapter 5. This research gave new knowledge of the underlying mechanisms that help bolster the abundance of a wildlife population suffering endemic disease despite significant culling. Armed with this new understanding of compensatory population regrowth, in Chapter 6 we apply the use of our wild boar TB model, specifically designed for the situation in central and southern Spain, to a different area of Spain, Asturias, where TB prevalence is much lower and the wild boar population density is growing. This area is also inhabited by a growing wolf population, and we combine empirical data gathered over a decade for wolf and wild boar populations to tailor our model to this region and examine the possibility that wolf preying on wild boar can assist the fight against TB infection.

In conclusion, Chapter 7, this thesis examines further directions that the wild boar TB model can be taken for the management of tuberculosis in wild boar and also contemplates how this model can be translated to inform about other diseases that may be transmitted via both close contact and through free-living pathogens.

Figure 1.1: Wild boar (*Sus scrofa*)

Chapter 2

Introduction to modelling tuberculosis in wildlife

Living in the present day you could be forgiven for thinking that TB was a pernicious disease that had dire effect in our ancestors of the 19th and early 20th centuries, but was eradicated due to the advancement of pasteurisation and public health programmes in the 20th century. This general impression can only have been compounded by the cessation of the routine BCG immunisation of schoolchildren in 2005. However, contrary to this belief, the disease still affects a sizeable number of individuals each year in the United Kingdom. Public Health England [116] report that in 2013 there were 7,892 noted cases of tuberculosis (12.3 per 100,000), the greatest proportion of which occurred in individuals not born in the United Kingdom or living in the most deprived populations. Nearly all of these incidences of TB were caused by the strain *Mycobacterium tuberculosis*, however 0.6% were identified as being caused by *Mycobacterium bovis*.

Mycobacterium bovis (a strain of MTC) is hosted in domestic and wild animals and can cause zoonotic TB, mainly through inhalation though also potentially through open wounds [44]. This disease used to be endemic in the human population in the United Kingdom but was brought under control largely through pasteurisation of cow's milk and strict controls on cattle livestock with yearly testing of cattle in high risk areas, 4-year testing in lower risk areas and compulsory slaughter of affected cattle [46]. There are also routine checks made of carcasses at slaughterhouses. This has resulted in an extremely low risk to the general human population of contracting zoonotic tuberculosis. However, those who by choice still consume non-pasteurised dairy products, or those who work in the cattle industry are at greater risk from infection, particularly given that the incidence of tuberculosis in cattle herds has been rising [44]. Clearly government has great interest in preventing any outbreak of zoonotic tuberculosis in the general population, therefore attention is being given to how domestic livestock becomes infected by the bacteria.

The greatest effect of MTC infection is through the development of TB in

domestic cattle. The compulsory slaughter of affected herds is a financial strain on the agricultural industry and wide-scale testing procedures are required following a TB positive test. The incidence of TB in cattle herds in the United Kingdom is rising and therefore the United Kingdom government and agricultural industry place great importance on preventing infection in domestic livestock. Thus attention is focused on those wild animal populations in which TB infection is endemic and which live in close proximity to domestic animals giving the potential for cross-infection of the disease.

In the United Kingdom the badger has been identified as the key reservoir of TB, being a prime suspect in the high incidence of cattle herd breakdown due to TB in the south-west and midlands of England. Donnelly & Hone (2010) [50] show strong evidence for badger to cattle transmission of the disease. Current estimates are that in the areas of England where TB is endemic a third of the badger population is infected [45]. The process of badger to cattle (and *vice versa*) infection is unclear as physical contact between the two species is rare. However, they do inhabit the same environment. Badgers roam cattle pasture in the search for earthworms [11] and have been known to visit farm outbuildings in the search for food.

This problem is by no means confined to the United Kingdom: there are certain wildlife populations throughout the world known to be reservoirs of MTC infection, notably brush-tailed possums in New Zealand, white-tailed deer in North America and wild boar in Spain. Each particular population is subject to different biological, environmental and cultural factors that contribute to the success or failure of controlling the disease. For example in contrast to the badger in the United Kingdom there is far more appetite for culling non-native species like the brush-tailed possums in New Zealand which are widely regarded as a pest rather than a special part of the country's fauna. A programme of culling in New Zealand reduced the number of herds infected with TB from 1700 in the 1990s to 66 in 2011/12 [45].

It would be hard to imagine any government in the United Kingdom, where the badger is indigenous, having the political appetite to authorise culling to the same extent as the brush-tail possum. Indeed, in Wales there has been a positive move towards a vaccination strategy instead [53]. In England, the Randomised Badger Culling Trial (RBCT) was initiated in 1998 to investigate the results of various methods of culling in three relatively small areas in south-west England. This test cull was furiously contested and abandoned. Results from the trial have been mixed, in particular showing that the cull has increased the levels of TB in areas surrounding the test site [27] [49]. Widespread licensed badger culling in England restarted in autumn 2018, with a view to significantly reduce the badger population to reduce the chance of spill-over of TB to cattle. Results from this round of culling are still being analysed but already there is disagreement between scientists and government as to their validity.

In researching models of MTC infection we will focus on the methods of Anderson and Trewhella (1985) [11] who examined the dynamics and persistence of TB in badger populations in England. This work outlines several key concepts in modelling disease in ecological systems and in particular details model structures to represent direct transmission of infection passed from one badger to another in social contact; vertical transmission of infection where a badger cub is infected from birth; and free-living transmission where bacteria excreted by badgers survives in the environment and acts as source of infection without involving immediate contact between badgers. These frameworks underpin recent, more complicated, model set-ups that additionally include stage-structure, stochasticity and spatial structure, and we additionally review these models in a stochastic framework as well as separate stochastic models of TB in wild boar and in cattle.

2.1 Deterministic modelling of TB in badger populations

In the 1985 paper by Anderson and Trewhella [11] an examination is made of the growth rates of badger populations in disease-free conditions and also in the presence of bovine tuberculosis (TB) infection. This paper works through a progression of models examining different factors that need to be considered to produce an effective model for the disease in badgers. We review the key life history and disease parameters and their estimated values below.

The intrinsic growth rate captures the ability for a population to grow without any limitation on resources. It is calculated using an estimate for the per capita birth rate, γ, and the per capita natural death rate, b:

γ The birth rate for English habitats is estimated to be 0.6 per capita of population per year, deduced from unpublished data taken from the south-west of England. This is comparable to data from Sweden that Anderson & Trewhella also quote [11].

b The natural death rate is determined by fitting an exponential decay curve to the same unpublished data [11], giving an estimate of average life expectancy of 2.5 years, thus the per capita death rate as 0.4 per capita per year.

The resultant intrinsic growth rate is then assumed to be $r = 0.2$.

Highest known densities in the most favourable conditions are found to be 20 adults per square kilometre. Lower densities of 5 to 8 adults per square kilometre are perhaps more common in reasonably favourable conditions. Adults make up roughly half the population.

Migration of badgers between social groupings is fairly uncommon. When we consider dispersal we assume that it occurs on average once in an individuals lifetime.

When a susceptible individual becomes infected it initially incubates the disease but is not infectious. After the incubation period an individual becomes infectious and can transmit the disease. Infectious individuals also incur an additional death rate due to the disease:

α The disease-induced mortality rate is relatively low compared to other diseases. Life expectancy for an infectious badger is estimated as 1 year from onset of infectiousness.

σ The disease incubation period, estimated to be 3 months.

β The disease transmission rate determined from the diseased population density and taken to be 1.54 and 0.308 km^2 per capita per year respectively.

There is some disagreement on population density in the presence of disease. Values of 1 and 5 per kilometre squared are considered.

It should be noted that though there is some basis for these parameter estimates, Anderson & Trewhella [11] refer to the data they are based on as sparse, particularly in relation to disease dynamics. Table 2.1 contains the standard set of parameters used in the models discussed in this chapter. Prior to considering the impact of

Parameter	*Symbol*	*Default value*	*units*
incubation rate	σ	4	$year^{-1}$
disease induced mortality rate	α	1	$year^{-1}$
endemic disease susceptible density	K_T	5	km^{-2}
transmission coefficient	β	0.308	$km^2 year^{-1} density^{-1}$
carrying capacity	K	20	km^{-2}
natural death rate	b	0.4	$year^{-1}$
birth rate	γ	0.6	$year^{-1}$
intrinsic growth rate	r	0.2	$year^{-1}$
density-dependence constraint	c	7	dimensionless

Table 2.1: The model parameters based on Anderson & Trewhella 1985 [11], their default values and their units. Rates are expressed *per capita*.

bovine tuberculosis (TB) on the UK badger system Anderson and Trewhella (1985) [11] examined the population growth dynamics in the absence of the disease. The first model to consider is for the natural growth of a population of badgers with density N/km^2 when no disease is present. This is modelled using logistic growth.

$$\frac{dN}{dt} = rN\left(1 - \frac{N}{K}\right) \tag{2.1}$$

Here r represents the maximum growth rate in the absence of any density dependence. The logistic growth model acts to reduce the growth rate as the population density increases, decreasing to zero when $N = K$ where K is defined as

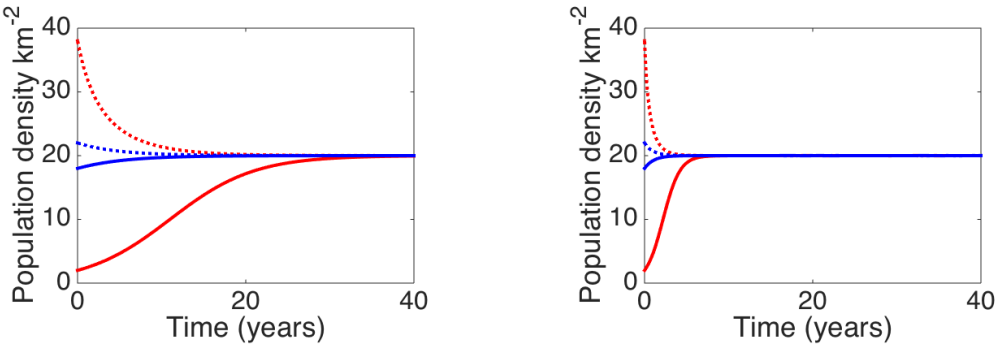

(a) (b)

Figure 2.1: Numerical solutions of Equation (2.1) showing the population dynamics over time for (a) $r = 0.2$ and (b) $r = 1.0$ starting from different initial conditions. The approach to the steady state $N_s = K = 20$ is more rapid for higher values of r.

the carrying capacity of the population. Steady states occur at $N_s = 0$ and $N_s = K$ (analysis can be found in Appendix 2A.1).

The solution to Equation (2.1) is

$$N(t) = \frac{KN(0)}{N(0) + (K - N(0))e^{-rt}} \tag{2.2}$$

where $N(0)$ is the population density at time $t = 0$ then . As $t \uparrow \infty$ then $e^{-rt} \downarrow 0$ so that the population density $N(t)$ returns towards the equilibrium density K as time increases. The order of magnitude of this return time is $\frac{1}{r}$ [11]. This confirms the pictorial evidence in Figure 2.1 that a larger intrinsic growth rate leads to a faster return to equilibrium after perturbation.

The previous model assumes a linear dependence between the net growth rate $r(1-\frac{N}{K})$ and the population density N. However as discussed in Fowler [57] "species with low reproductive rates, long life-spans and populations that are more limited by resources (large mammals in particular) indicate that most density-dependent changes in vital rates occur at levels of the population quite close to the carrying capacity". Therefore Anderson & Trewhella [11] considered a modification to the logistic model where the severity of the density-dependent effects could be adjusted. This led to the following model.

$$\frac{\mathrm{d}N}{\mathrm{d}t} = rN\left(1 - \left(\frac{N}{K}\right)^c\right) \tag{2.3}$$

Here the terms are as defined for Equation (2.1) with the addition of the constant c which reflects the severity of density-dependent effects. When $c > 1$ it implies that density dependence is less pronounced than the linear model for all population

densities less than K. Therefore, greater rates of change to the density occur at lower population levels. When $c = 1$ the logistic growth, Equation (2.1) is recovered. The steady states again are $N_s = 0$ and $N_s = K$ (analysis can be found in Appendix 2A.2).

The solution to Equation (2.3) can be expressed as

$$N(t)^c = \frac{K^c N(0)^c}{N(0)^c + (K^c - N(0)^c)e^{-crt}} \tag{2.4}$$

where $N(0)$ is the population density at time $t = 0$. As $t \uparrow \infty$ then $e^{-crt} \downarrow 0$ so that the population density $N(t)$ returns towards the equilibrium density K as time increases. The order of magnitude of this return time is $\frac{1}{cr}$ and explains why the return to equilibrium is reduced as c increases.

Figure 2.2 shows that for larger values of c, the population growth rate remains higher as the population increases, leading to a greater rate of change in the population density and a faster return to the equilibrium population density. After considering the available data for badger populations recovering from a catastrophic population crash after severe drought, in particular the effect on badgers in South-west England after the exceedingly dry summer of 1976, Anderson & Trewhella [11] recommend that c is set to 7.

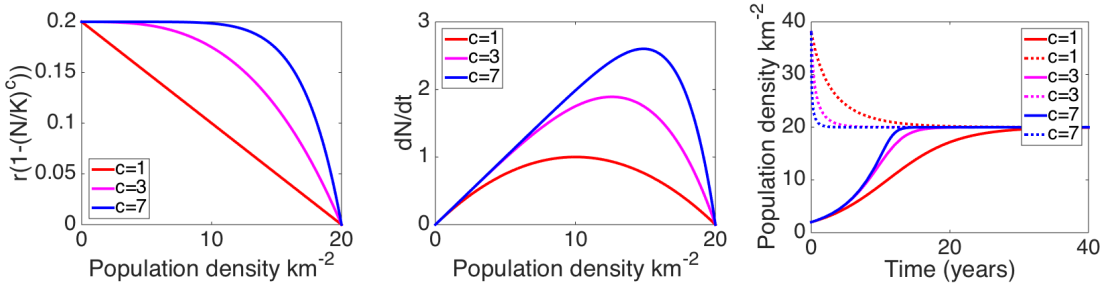

(a) (b) (c)

Figure 2.2: Solutions of Equation (2.3) for $K = 20$ and different values of density-dependence constant $c = 1, 3$ and 7 showing (a) growth rate as population density increases, (b) the rate of change of population density and (c) the time taken for return to stable equilibrium. For greater value of c faster population growth at lower density leads to faster return to the equilibrium density. Other model parameters are set to default values (Table 2.1).

We now extend the models of population growth to include disease dynamics and consider incorporating various ways that TB spreads within a badger population.

2.1.1 Susceptible Exposed Infected model

The first model that Anderson and Trewhella(1985) [11] consider to represent the dynamics of TB in badgers is a Susceptible-Exposed-Infectious model (Equations (2.5)) where X represents the density of susceptible badgers, H represents the density of badgers incubating the disease but not yet infectious (exposed), Y represents the density of infectious badgers and the total population $N = X + H + Y$.

$$\frac{\mathrm{d}X}{\mathrm{d}t} = \hat{r}(N)N - bX - \beta XY \tag{2.5a}$$
$$\frac{\mathrm{d}H}{\mathrm{d}t} = \beta XY - (b+\sigma)H \tag{2.5b}$$
$$\frac{\mathrm{d}Y}{\mathrm{d}t} = \sigma H - (b+\alpha)Y \tag{2.5c}$$

In the absence of infection the host badger population undergoes population growth dynamics as in Equation (2.3). This requires that $\hat{r}(N) = \gamma - dN^c$ where $d = \frac{\gamma - b}{K^c}$ and $c = 7$. Infection occurs at a rate proportional to the density of susceptibles and the density of infected with transmission coefficient β. After infection the host enters the incubating (exposed) class. The host progresses from the exposed class to the infectious class at rate σ and when infectious the host has a disease induced mortality rate α. Members of all classes have a natural death rate of b. Steady state and stability analysis can be found in Appendix 2A.3.

2.1.2 SEI The Basic Reproductive Rate R_0 for the Disease

The stability of the SEI model in Equations (2.5) can be represented in terms of the basic reproductive ratio of the disease, R_0, which can be defined as the number of secondary cases generated by one infectious individual being added to a susceptible population at equilibrium. When $R_0 < 1$ the disease dies out, whereas when $R_0 > 1$ the disease can spread. For Equations (2.5) adding a small amount of infection to the disease-free equilibrium, the disease can spread if the following condition holds.

$$R_0 = \frac{K\sigma\beta}{(b+\alpha)(b+\sigma)} > 1 \tag{2.6}$$

When $R_0 < 1$ the Jacobian for the disease-free steady state has three eigenvalues with negative real part so the disease-free state is stable and the endemic steady state unstable so the disease dies out. When $R_0 > 1$ the endemic steady state now becomes stable, and the disease-free steady state unstable allowing the disease

to proliferate. Here we have defined R_0 from the stability analysis (see Appendix, Equation (2A13)), but it can also be calculated directly as the rate at which cases occur in a population at disease-free equilibrium βK multiplied by the proportion that become infectious $\frac{\sigma}{b+\sigma}$ multiplied by the life expectancy of an infectious $\frac{1}{b+\alpha}$.

2.1.3 SEI Transmission Coefficient β

As mentioned in Chapter 2.1 an actual value for the transmission coefficient β is hard to derive from badger population data. Instead we can estimate it by assuming that when at endemic equilibrium each susceptible produces one secondary infection so that $\frac{\sigma\beta X_T}{(b+\alpha)(b+\sigma)} = 1$. To find this value, estimates are made of the endemic susceptible density steady state. Anderson & Trewhella [11] refer to this as the critical threshold density and consider critical densities of 1 and 5 with the resulting transmission coefficient, $\beta = 1.54$ and $\beta = 0.308$ respectively derived from them. However, it should be remembered that there is contention about the data on which these numbers are based.

2.1.4 Results for SEI model

Results for different rates of transmission are shown in Figure 2.3. This shows the epidemiological dynamics when 1 infectious individual is added to a population at the disease-free steady state. The numerical simulations confirm the findings of the stability analysis that, as the parameters are set so that $R_0 > 1$, the disease-free steady state is unstable and the endemic steady state stable. The addition of an infected individual suppresses the host population density, which settles at the stable endemic steady state. This suppression of the susceptible density is due to the virulence of the disease leading to higher rate of mortality for infectious individuals. The greater transmission coefficient in Figure 2.3b leads to a greater suppression of the susceptible population density since more individuals become infected. For both transmission coefficients the population density at the endemic steady state exhibits damped oscillations, these being of shorter period and greater amplitude for the lower transmission rate in Figure 2.3a. Note that the disease remains endemic but at low density.

2.1.5 Vertical transmission in SEI model

Vertical transmission is the infection of newborn offspring by its mother when still a developing fetus or during birth. In the badger system this should really be referred to as pseudo-vertical transmission as there is no evidence that badger cubs can be infected with TB before or at birth, rather that they can catch the disease shortly after birth from an infected individual in the sett (which is most likely the maternal

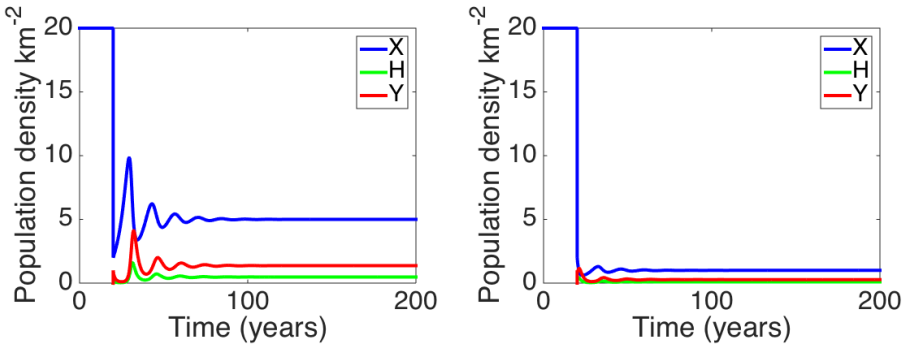

(a) (b)

Figure 2.3: Results for the SEI model represented by Equations (2.5) for different values of transmission coefficient β: (a) $\beta = 0.308$, $R_0 = 4$ (b) $\beta = 1.54$, $K = 20$. The blue line shows susceptible density, green exposed density and red the infectious density. At time 20 years, one infected individual is inserted in to a susceptible population at disease-free steady state $K = 20$. As $R_0 > 1$, the disease-free steady state is unstable so the diseases proliferates leading to the population density falling to the stable endemic steady state. Both transmission coefficients lead to damped oscillations about an endemic steady state, the lower transmission coefficient in (a) resulting in a shorter period of oscillation with greater amplitude. The higher transmission coefficient in (b) exhibits a greater level of suppression of susceptibles since a greater number become infected and suffer from the increased mortality associated with the disease. Other model parameters are set to default values (Table 2.1).

parent). The classical framework for modelling vertical transmission nevertheless is a good approximation for this. Vertical transmission of the disease can be added to the SEI model Equations (2.5), by splitting the birth function so that a proportion, p of the cubs born to an infectious mother, $p\hat{r}(N)Y$, enter the disease incubating class, H, immediately with the remainder entering the susceptible class. This new model is represented in Equations (2.7).

$$\frac{\mathrm{d}X}{\mathrm{d}t} = \hat{r}(N)\left[X + H + (1-p)Y\right] - bX - \beta XY \tag{2.7a}$$

$$\frac{\mathrm{d}H}{\mathrm{d}t} = p\hat{r}(N)Y + \beta XY - (b+\sigma)H \tag{2.7b}$$

$$\frac{\mathrm{d}Y}{\mathrm{d}t} = \sigma H - (b+\alpha)Y \tag{2.7c}$$

The other terms are the same as in Equations (2.5). Steady state and stability analysis can be found in Appendix 2A.4.

2.1.6 SEI vertical transmission R_0

As with the SEI model in Section 2.1.2 the stability of the SEI with vertical transmission model in Equations (2.7) can be represented in terms of the basic reproductive ratio of the disease, R_0. For Equations (2.7) adding a small amount of infection to the disease-free equilibrium, the disease can spread if,

$$R_0 = \frac{K\beta\sigma + pb\sigma}{(b+\alpha)(b+\sigma)} > 1 \tag{2.8}$$

2.1.7 SEI vertical transmission results

Solutions for different values of p can be seen in Figure 2.4. These show that for all values of $p > 0$ vertical transmission acts as a population suppressor and the greater the probability of vertical transmission of the disease, the greater the suppression of the susceptible population density.

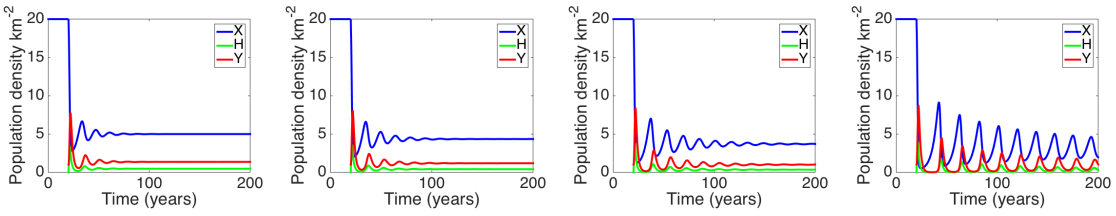

(a) (b) (c) (d)

Figure 2.4: Solutions for SEI model with vertical transmission represented by Equations (2.7), showing the effect on population densities given different probability p of vertical transmission. (a) $p = 0$, (b) $p = \frac{1}{3}$ (c) $p = \frac{2}{3}$, (d) $p = 1$. (a) shows the SEI model. The greater the probability p of vertical transmission, the greater the suppression of the endemic steady state of susceptibles, and the less damping of oscillations about the endemic steady state. Other model parameters are set to default values (Table 2.1).

For all values of p, the density of susceptibles exhibits damped oscillations about the endemic steady state, the damping occurring at a slower rate for higher probabilities of vertical transmission. Also the period of the oscillations is greater for higher probability of vertical transmission as is the amplitude of oscillation.

When there is greater probability of vertical transmission, the oscillations about the endemic steady state are far more exaggerated with longer period. Therefore a population with a high probability of vertical transmission is at greater risk of extermination due to a random reduction of susceptibles as their density falls to a much lower density at the trough of an oscillation.

This suppression of the susceptible density is reflected in the strength of the disease, R_0. Figure 2.5 illustrates that as p increases from 0 to 1 then R_0 increases. Therefore, comparing the model with vertical transmission ($p > 0$) to that without ($p = 0$) indicates that the disease can persist for a wider range of parameters when vertical transmission is included.

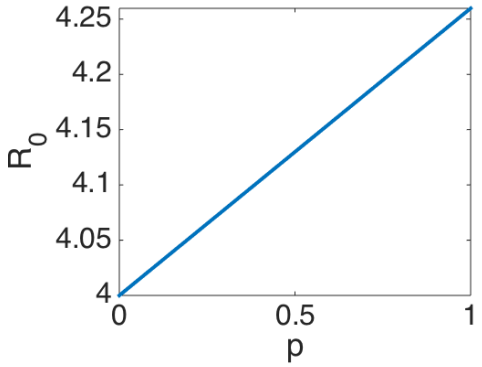

Figure 2.5: R_0 versus probability p of vertical transmission for the model represented by Equations (2.7). As p increases from no vertical transmission, $p = 0$, to all births to infectious mothers resulting in an infected individual, $p = 1$, the basic reproductive ratio R_0 increases. K=20, other model parameters are set to default values (Table 2.1).

2.1.8 SEI with free-living particles

Field studies have shown that direct physical interactions between badgers and livestock are fairly rare [52], so indirect contact through free-living particles could be an important source of the transmission of infection.

To add this potential source of infection in to the SEI model, a new class is added, W, which represents the density of free-living infective particles. This new model is represented in Equations (2.9).

$$\frac{\mathrm{d}X}{\mathrm{d}t} = \hat{r}(N)N - bX - \beta_w XW - \beta XY \tag{2.9a}$$

$$\frac{\mathrm{d}H}{\mathrm{d}t} = \beta_w XW + \beta XY - (b+\sigma)H \tag{2.9b}$$

$$\frac{\mathrm{d}Y}{\mathrm{d}t} = \sigma H - (b+\alpha)Y \tag{2.9c}$$

$$\frac{\mathrm{d}W}{\mathrm{d}t} = \lambda Y - \mu W - \beta_w NW \tag{2.9d}$$

This model is the same as the SEI model Equations (2.5) but additionally includes the possibility of transmission by consumption of free-living particles with

transmission coefficient β_w. Free-living particles are assumed to be shed from infective individuals at rate λ and infective particles decay at rate μ.

Anderson and Trewhella [11] argue that as changes to the density of the bacteria occur over a much shorter timescale than changes in the densities of infected and infectious badgers, the density of the bacilli is taken as the equilibrium value W^* and accordingly they set $\frac{\mathrm{d}W}{\mathrm{d}t} = 0$ in the model.

2.1.9 SEI model with constant density of free-living particles

Considering the density of free-living bacteria as a constant, W^*, leads to the following reduced set of ODEs in Equations (2.10).

$$\frac{\mathrm{d}X}{\mathrm{d}t} = \hat{r}(N)N - bX - \beta_w XW^* - \beta XY \tag{2.10a}$$

$$\frac{\mathrm{d}H}{\mathrm{d}t} = \beta_w XW^* + \beta XY - (b+\sigma)H \tag{2.10b}$$

$$\frac{\mathrm{d}Y}{\mathrm{d}t} = \sigma H - (b+\alpha)Y \tag{2.10c}$$

Steady state and stability analysis can be found in Appendix 2A.5. Results for the addition of free-living particles at different levels can be found in Figure 2.6. These show that lower values of $\beta_w W^*$ lead to greater oscillations about the endemic steady state, which is lower for higher values of $\beta_w W^*$. When the level of free-particles passes the critical threshold in Figure 2.6d, the level of free-living particles induces a level of infection in the host population that leads to population extinction.

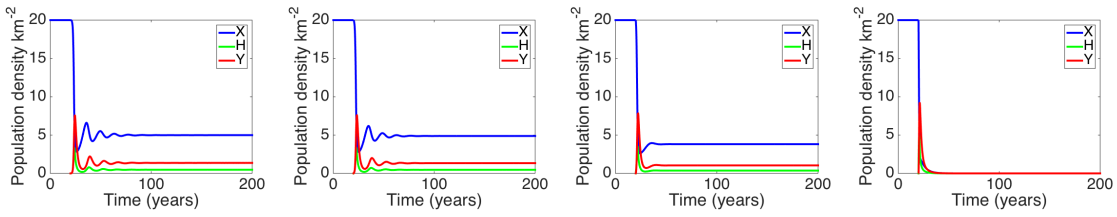

(a) (b) (c) (d)

Figure 2.6: Different values of $\beta_w W^*$ in the SEI model with constant level of free-living particles represented by Equations (2.10). (a) $\beta_w W^* = 0.001$, (b) $\beta_w W^* = 0.01$, (c) $\beta_w W^* = 0.1$, (d) $\beta_w W^* = 1$. A greater value of $\beta_w W^*$ leads to a greater suppression of the host population. In (d) the level of free-living particles is so great that the number of infections they induce leads to population extinction. Other model parameters are set to default values (Table 2.1).

2.1.10 SEI model with varying density of free-living particles

In this section we consider the model detailed in Equations (2.9) where the density of free-living particles is dynamic in time. The eigenvalues for the disease-free populated state are more complicated and it is difficult to determine them explicitly. Similarly for the endemic steady state and its stability. Therefore we look to numerical solutions of Equations (2.9) to gain understanding of the disease dynamics with dynamic free-living particles.

Allowing the density of free-living particles to vary in time gives the problem of trying to determine suitable parameters for the free-living component of the model represented by Equations (2.9). To do this we use the default set of parameters in Table 2.1 and look at the effect on stability and critical thresholds whilst varying the free-living parameters, λ, μ and β_w.

First considering μ, the death rate of the bacteria in the environment. The survival rates for the bacteria in the environment is not well known, and has different characteristics depending on the season. Anderson & Trewhella [11] quote statistics that imply a maximum survival rate of 2.5 months.

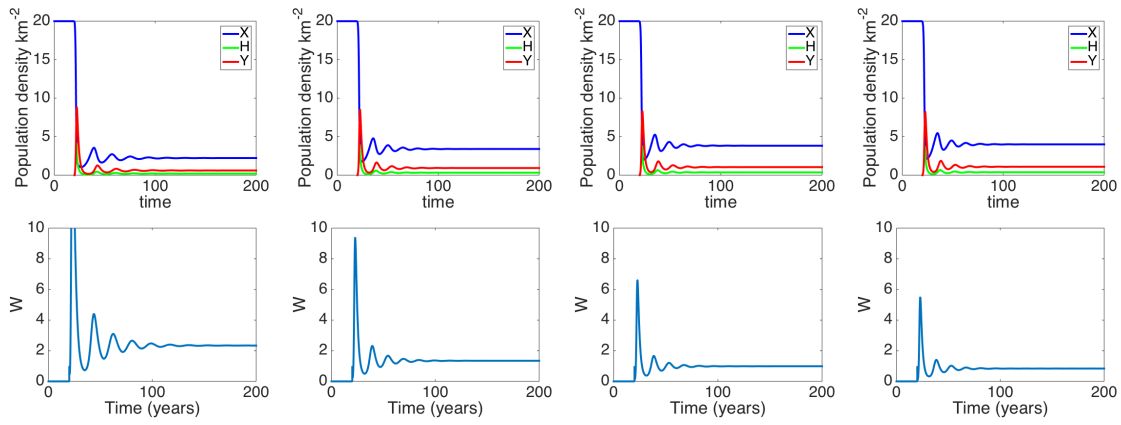

Figure 2.7: Different values of μ in the SEI model with varying density of free-living particles represented by Equations (2.9). (a) $\mu = 1$, (b) $\mu = 3$, (c) $\mu = 4.8$, (d) $\mu = 6$. Lower levels of μ, the decay rate of the free-living particles, leads to greater suppression of the host population. Here $\lambda = 5$, $\beta_w = 0.1$ and other model parameters are set to default values (Table 2.1).

Figure 2.7 has solutions for different values of μ, showing that for lower values of μ (implying free-living particles living longer in the environment), there is a greater level of suppression of the susceptible badger population with a corresponding rise in the density of the free-living particles.

Figure 2.8 has solutions for different values of λ, the excretion rate of bacilli by badgers. As would be expected, greater values of λ lead to a higher density

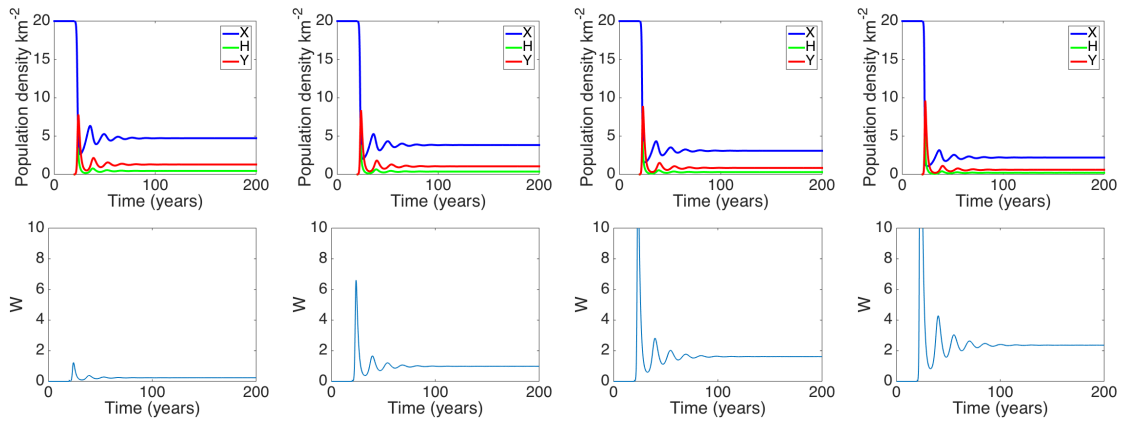

Figure 2.8: Different values of λ in SEI model with varying density of free-living particles represented by Equations (2.9). (a) $\lambda = 1$, (b) $\lambda = 5$, (c) $\lambda = 10$, (d) $\lambda = 20$. A greater level of λ, the average excretion rate of free particles by infectious individuals, leads to a greater level of free-particles, W, in the environment and a greater suppression of the host population. Here $\mu = 4.8$, $\beta_w = 0.1$ and other model parameters are set to default values (Table 2.1).

of free-living particles in the environment with a corresponding depression of the susceptible badger population.

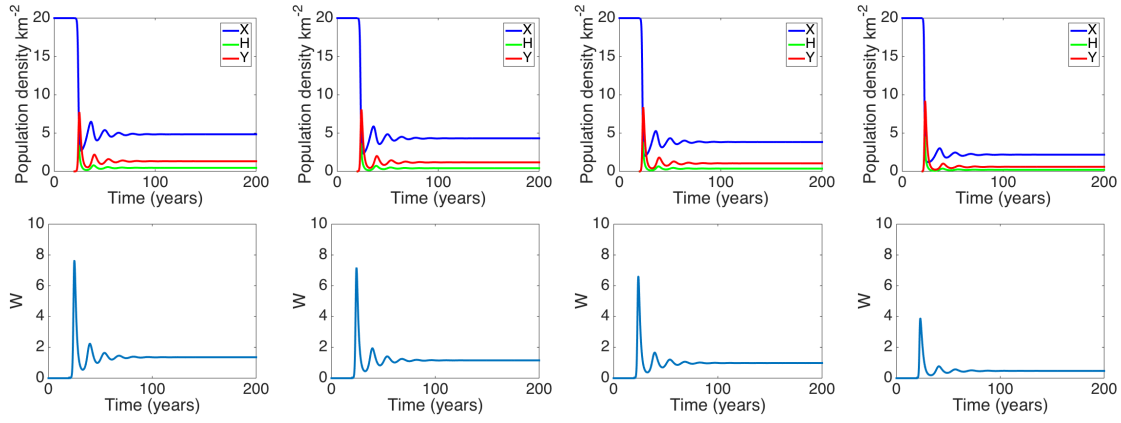

Figure 2.9: Different values of β_w in SEI model with varying density of free-living particles represented by Equations (2.9). (a) $\beta_w = 0.01$ (b) $\beta_w = 0.05$, (c) $\beta_w = 0.1$, (d) $\beta_w = 0.5$. A greater value of $beta_w$, the transmission rate of free particles from the environment to susceptibles, leads to a greater suppression of the host population, and a lower level of free particles, W, in the environment. $\mu = 4.8$, $\lambda = 5$ and other model parameters are set to default values (Table 2.1).

Figure 2.9 has solutions for different values of β_w, the rate that individuals become infected from free-living particles in the environment. The higher the transmission rate, the greater the suppression of the susceptible population. This has the side-effect that the higher transmission rate also corresponds to a reduction

in the steady state for the free-living particles themselves.

Both of our free-living models demonstrate that an increase of the pathogen in the environment can lead to an increase in infection and a corresponding suppression of the host population. However, for the constant level of free-living particles model there is a limit to the amount of the pathogen that the host population can survive. If the level of bacteria in the environment is too great, the rate of population density loss due to the infection leads to population extinction.

2.2 Stochastic modelling of TB in Badgers

The models we have so far reviewed in this chapter have all concerned MTC infection described by deterministic models. A common factor in all these models is that the disease remains endemic in the population at very low densities. Therefore, there may be a need to examine the effects of stochasticity in the models of badger TB interaction.

Badgers live in small social groupings with their range depending on the abundance of food supply [11]. It is therefore sensible to consider the disease dynamics at the local level, but this therefore implies low infected densities which could cause the disease to die out. To incorporate this possibility into the models for badgers we modify the SEI model (Equations (2.5)) to include stochasticity. This is a novel extension to the work of Anderson & Trewhalla (1985) [11] and the model formulation and results are presented in Appendix 2B.1. In summary these results show that in a grid of patches, where the SEI model runs in each patch, but where dispersal may occur between neighbouring patches, TB infection can die-out and re-emerge in each individual patch. However, if the system of patches is viewed as a whole, the disease prevalence and population suppression due to disease shows the same pattern as the deterministic model.

2.3 Stochastic modelling of TB in wild boar

Anderson et al (2013) [6] developed an individual based model to investigate the efficacy of vaccination against TB in wild boar in south-western Spain. Wild boar in this area are a known reservoir of MTC infection with exceedingly high prevalence recorded in some areas [106]. Wild boar live in two main types of area: managed hunting estates where high wild boar density is encouraged by enforced enclosure and supplementary feeding; and areas that are not fenced where wild boar are able to roam freely, but do not receive any extra sustenance. The wild boar population is structured into different classes to account for age, reproductive and disease status. (Note that this allows for vaccination of piglets at 6 months old.) Probabilities are set for birth, death, infection and progression to excretor level, and also for

dispersal between squares. Where possible, these model parameters are derived from unpublished empirical data in Spain and published sources from the rest of Europe. For unknown parameters relating to probability of disease transmission, sensitivity was performed by randomly varying the parameter for 5,000 iterations of the model. As this sensitivity showed that the target results (the proportion of latent and infected wild boar after 35 years) were not significantly influenced by changes to these disease parameters, the average parameter value over the iterations was taken as the actual value.

The model is run on a 2-D grid of 1 km^2 squares whose starting wild boar population is set to the carrying capacity, parameterised either for the managed situation or unmanaged with the age and disease status of the population initialised to predetermined percentages. Individuals may become infected by contact with a local excretor, via an excretor from a neighbouring square or by contact with an external source. Trial runs are made over a time period split into quarter-year intervals, with densities adjusted each season to account for the probability of birth, death, disease and dispersal. An annual cull of 30%, skewed so that adult males with large tusks are more likely to be taken, is applied in the Autumn.

In contrast to the results obtained for the previous models of badger populations where changes are reported for total density, results are reported for the change in percentage of excretors in the population after a vaccination programme, showing that longer vaccination programmes lead to a lower percentage of excretors in the population. Sensitivity tests show that the length of the vaccination programme and the percentage of piglets successfully vaccinated are independently significant predictors of the resultant proportion of excretors in the managed situation. However, for the unmanaged situation where wild boar live more sparsely, the interaction between these two variables was a significant predictor of the percentage of excretors in the population. In this stochastic patch model, infection is able to be eradicated at certain levels of vaccination.

2.4 Stochastic modelling of TB in cattle

Brooks-Pollock et al (2014) [28] developed a stochastic metapopulation SEI model capturing the dynamics of MTC infection caused by the transfer of cattle between herds in Great Britain and is a complex model involving both local infection and long-range transmission of infection due to transfer of cattle to different farms. It is a dynamic model so that previous model behaviour affects future events. Data obtained from the Cattle Tracing System [26] provides comprehensive information on cattle movements and thus is used to show how infection is spread by the flow of cattle round Great Britain. The model is fitted using data gained from extensive records of reactors and failed cattle herd tests and parameters are generated using

a MCMC approach. The model considers both intra and inter-farm infection, where disease transmission on a particular farm occurs by frequency dependent transmission between individuals on the farm and free-living transmission from both the local farm environment and the local region.

Different cattle management strategies are applied to the model: culling the entire herd; vaccination; decreasing environmental transmission (approximating culling of a local wildlife reservoir, most likely to be badgers); and preventing movement of infected cattle. The model highlights the complexities of the spread of TB in Great Britain with different sources of infection. Current vaccination only offers partial protection and therefore the model predicts that it is not sufficient to reduce TB infection to a large extent. Decreasing local environmental transmission in the model showed little effect as it only affects one route to infection. The most effective routes to controlling TB infection in the model were those that affected all routes of infection like culling or vaccination of the whole herd or more herd testing to prevent the movement of infected cattle. They concluded that in this system controlling local badger populations only had a constrained effect on reducing herd breakdown.

2.5 Summary of models

Taking inspiration from Anderson & Trewhella [11] we have investigated a number of models that illustrate the potential transmission routes and dynamics of TB and highlight how this chronic infection can remain endemic in a population. The SEI deterministic model demonstrates the suppression of a host population in the presence of disease which can then remain endemic in the population at very low numbers. The persistence of the disease can be interpreted in terms of the basic reproductive ratio of the disease, R_0, which represents the number of secondary infecions from the introduction of one infected individual. This expression for R_0 provides a condition for when the disease can persist, and its value indicates the strength of the infection. We also examined additions to the SEI model, reflecting aspects of badger lifestyle and disease transmission that could affect the course of the disease in a host population. These included the possibility of vertical transmission where a proportion of newborn individuals are infected, and free-living transmission where infectious individuals release live bacteria into the environment that can subsequently infect a susceptible. These modifications enhance the ability of the disease to persist by increasing the value of R_0. All the models have as a common theme that the disease remains endemic in the host population at very low numbers. In the real world populations at low abundance are at risk from extinction and so it is possible that stochastic processes may lead to disease (or population) extinction. This led to considering a stochastic approach based on the deterministic SEI model.

On a single small area, this stochastic model could show disease epidemics but the disease would fade out and was not able to remain endemic in the population (Section 2B.1.1). We therefore added a spatial component to the stochastic model by considering a spatial array of patches allowing dispersal of individuals between neighbouring patches. This model demonstrated a continual pattern of infection followed by disease die-out then subsequently after a number of years re-infection on an individual patch level. Considering the spatial array as a whole, we showed that the disease remains endemic in the metapopulation, demonstrating that migration of individuals promotes the spread of infection (Section 2B.2.3). This illustrates problems experienced during trial badger culling where it has been shown that culling increases population dispersal as remaining badgers disperse to re-form social groups. This increase in dispersal can increase disease transmission and promote the persistence of the disease. Indeed results from the RBCT in south-west England indicated that disease prevalence has increased following culling [45].

It should be remembered that Anderson & Trewhella [11] produced this piece of work in 1985, when the area of mathematical biology was in relative infancy. It also was written before notable crises in the cattle industry in the United Kingdom, the onset of BSE and then the foot-and-mouth outbreak, both of which caused considerable economic damage to the cattle farming industry in the United Kingdom. The United Kingdom government clearly wants to avoid any further damage to livestock herds and therefore are increasingly looking to model the dynamics of disease in both domestic and wild animals to inform about disease management. In 1985 there was concern about the level of bovine tuberculosis in cattle, particularly in the south-west of England where environmental conditions appeared to enhance its affect on the population, and badgers were already being cited as a contributor to the rise in TB infection in cattle. Anderson & Trewhella [11] use the results in their paper to recommend, among other strategies, test culling to ascertain whether reduction in badger density resulted in a reduction in cattle herd breakdown due to TB.

Since 1985 there has been an increase in cattle herd breakdown due to TB, and an increased spotlight placed on badgers as a key TB reservoir. This has led to the development of further mathematical models in order to examine the dynamics of the disease within the badger population and of the interactions between badger and cattle. Smith *et al* (2001) [129] produced a spatial stochastic model introducing more classes of population: age and sex were introduced in separate classes as well as the concept of a super-excretor. Their model was used to examine different control strategies, concluding that proactive culling, before TB is detected in livestock in a region, is more effective than reactive. Cox *et al* (2005) [41] produced a deterministic model to describe TB infection between cattle and badgers to model the effect on cattle of culling badgers. This model was used to estimate the reproductive rate of

TB in cattle. Brooks-Pollock (2014) [28], (see Section 2.4) produced a stochastic metapopulation model of cattle within farms, connected via cattle movements, but not including transmission of TB via badgers. This model resulted in a number of cattle control strategies, and concluded that the spread of TB within livestock was the primary factor for the increase in herd breakdown in the United Kingdom. While wildlife reservoir populations were a factor in the overall persistence of disease they contributed only weakly to the generation of new cases. Therefore, Brooks-Pollock reported that control of local badger populations would have a limited effect on reducing overall TB incidence.

Further afield, Barlow (2000) [17] produced a deterministic model for TB in brush-tail possums in New Zealand, where culling of possums has been actively pursued to reduce cattle TB infection. The prevalence of TB in possums is lower than in badgers and possums have a high rate of disease induced mortality. Results from this model are used to show that dramatically reducing the host possum population and keeping the density low is sufficient to stop TB infection. The model predictions are borne out by results in the field where large scale culling of possums in New Zealand has reduced the number of herds infected with TB from 1700 in the 1990s to 66 in 2011/12 [45]. This highlights the importance of developing system specific models in order to develop disease control strategies.

Further to investigating models of MTC infection in host reservoirs, the research goal of this thesis is to develop a model for the spread of TB in wild boar in Spain. The wild boar TB system has the potential for direct, vertical and free-living transmission and the age-class at which an individual becomes infected is critical in determining the infectious status of an individual. The model will therefore be able to draw on the techniques of Anderson & Trewhella (1985) [11] and subsequent modelling techniques applied to the badger and possum systems: Smith *et al* (2001) [129], Brooks-Pollock (2014) [28] and Barlow (2000) [17]. The aim of this new model is to understand the primary mechanisms of disease transmission and then suggest management practice that can reduce disease prevalence.

Appendices to Chapter 2

2A.1 Steady states for logistic growth model

Steady states for Equation 2.1 occur when $\frac{\mathrm{d}N}{\mathrm{d}t} = 0$, giving the steady states for this model:

$$N_s = 0, N_s = K \tag{2A1}$$

Letting $f(N) = rN\left(1 - \frac{N}{K}\right)$, local stability requires that $f'(N_s) < 0$.

$$f'(0) = r \Rightarrow \quad N_s = 0 \quad \text{locally unstable} \tag{2A2}$$

$$f'(K) = -r \Rightarrow \quad N_s = K \quad \text{locally stable} \tag{2A3}$$

For $0 \leq N < K$, $\frac{\mathrm{d}N}{\mathrm{d}t} > 0$ and for $N > K$, $\frac{\mathrm{d}N}{\mathrm{d}t} < 0$, and we can find a candidate Lyapunov function $V(N) = r(1 - \frac{N}{K})^2$ so that the local stability extends to global [96]. Illustrations for this growth pattern for different values of r can be seen in Figure 2.1. Higher intrinsic growth rate leads to faster growth and hence a faster return to the stable steady state $N_s = 20$. This analysis assumes that $r > 0$, which in turn says that the birth rate γ should be greater than the death rate b as specified in Section 2.1.

2A.2 Steady states for logistic growth model with enhanced density dependent effects

The steady states for Equation 2.3 are:

$$N_s = 0, N_s = K \tag{2A4}$$

Now letting $f(N) = rN(1 - (\frac{N}{K})^c)$,

$$f'(0) = r \Rightarrow \quad N_s = 0 \quad \text{locally unstable} \tag{2A5}$$

$$f'(K) = -rc \Rightarrow \quad N_s = K \quad \text{locally stable} \tag{2A6}$$

In the same manner as for Equation 2.1, $N_s = K$ is also globally stable.

2A.3 SEI Steady State and Stability Analysis

The steady states of Equations 2.5 can be found by setting the right hand sides of the equations equal to zero. These are

$$(X_s, H_s, Y_s) = \begin{cases} (0,0,0) & \text{zero population} \\ (K,0,0) & \text{disease-free populated state} \\ (\frac{(b+\sigma)(b+\alpha)}{\sigma\beta}, H_T, \frac{\sigma}{b+\alpha}H_T) & \text{endemic state} \end{cases} \tag{2A7}$$

where H_T is the solution to the following equation:

$$\left(\gamma - \frac{\gamma - b}{K^c}\left(K_T + \frac{\sigma + b + \alpha}{b+\alpha}H_T\right)^c\right)\left(K_T + \frac{\sigma+b+\alpha}{b+\alpha}\right) - bK_T - \frac{\beta K_T \sigma}{b+\alpha}H_T = 0 \tag{2A8}$$

To determine the stability of the steady states we find the eigenvalues of the Jacobian, J, evaluated at the steady states.

$$J(0,0,0) = \begin{pmatrix} \gamma - b & \gamma & \gamma \\ 0 & -(b+\sigma) & 0 \\ 0 & \sigma & -(b+\alpha) \end{pmatrix} \tag{2A9}$$

and the eigenvalues are

$$\begin{gathered} \gamma - b \\ -(b+\sigma) \\ -(b+\alpha) \end{gathered} \tag{2A10}$$

The steady state is stable if all eigenvalues have negative real part. As we assume that $\gamma > b$ then there is always one positive eigenvalue and so the steady state is always unstable.

$$J(K,0,0) = \begin{pmatrix} -c(\gamma-b) & -(c+1)(\gamma-b) & -(c+1)(\gamma-b)+\gamma-\beta K \\ 0 & -(b+\sigma) & \beta K \\ 0 & \sigma & -(b+\alpha) \end{pmatrix} \tag{2A11}$$

and the eigenvalues are

$$\begin{gathered} -c(\gamma-b) \\ -(2b+\alpha+\sigma) - \sqrt{(2b+\alpha+\sigma)^2 - 4((b+\sigma)(b+\alpha)-\sigma\beta K)} \\ -(2b+\alpha+\sigma) + \sqrt{(2b+\alpha+\sigma)^2 - 4((b+\sigma)(b+\alpha)-\sigma\beta K)} \end{gathered} \tag{2A12}$$

As we assume that $\gamma > b$ then all three eigenvalues have negative real parts and hence the disease-free steady state is stable if $(b+\sigma)(b+\alpha) - \sigma\beta K > 0$ which is equivalent to

$$R_0 = \frac{K\sigma\beta}{(b+\sigma)(b+\alpha)} < 1. \tag{2A13}$$

For the endemic disease equilibrium, $J(X_T, H_T, Y_T)$ is more complicated and it is difficult to determine the eigenvalues explicitly. We assume that the endemic steady state is stable when the disease-free steady state is unstable. We highlight this with numerical simulations in Figure 2.3 which show that the susceptible, exposed and infectious density solutions show damped oscillations about the steady state.

2A.4 SEI with vertical transmission steady state and stability analysis

Again, the steady states of Equations 2.7 can be found by setting the right hand sides of the equations equal to zero. These are

$$(X_s, H_s, Y_s) = \begin{cases} (0,0,0) & \text{zero population} \\ (K,0,0) & \text{disease-free populated state} \\ (X_T, H_T, \frac{\sigma}{b+\alpha}H_T) & \text{endemic state} \end{cases} \tag{2A14}$$

The zero population steady state has the same stability characteristics as without vertical transmission in Equation. 2.5.

Adding vertical transmission into the SEI model now changes the Jacobian for the disease-free populated steady state to,

$$J(K,0,0) = \begin{pmatrix} -c(\gamma-b) & -c(\gamma-b)+b & -c(\gamma-b)+b(1-p)-\beta K \\ 0 & -b-\sigma & K\beta+bp \\ 0 & \sigma & -(b+\alpha) \end{pmatrix} \tag{2A15}$$

and the eigenvalues are

$$\begin{gathered} -c(\gamma-b) \\ -\tfrac{1}{2}\left((b+\alpha)+(b+\sigma)\right) - \tfrac{1}{2}\sqrt{4K\beta\sigma+4bp\sigma+\alpha^2-2\alpha\sigma+\sigma^2} \\ -\tfrac{1}{2}\left((b+\alpha)+(b+\sigma)\right) + \tfrac{1}{2}\sqrt{4K\beta\sigma+4bp\sigma+\alpha^2-2\alpha\sigma+\sigma^2} \end{gathered} \tag{2A16}$$

As we assume that $\gamma > b$ then all three eigenvalues have negative real parts and hence the disease-free steady state is stable if

$$\sqrt{4K\beta\sigma+4bp\sigma+\alpha^2-2\alpha\sigma+\sigma^2} - \left((b+\alpha)+(b+\sigma)\right) < 0 \tag{2A17}$$

or, after some rearrangement the following condition holds.

$$R_0 = \frac{K\beta\sigma + pb\sigma}{(b+\alpha)(b+\sigma)} < 1 \tag{2A18}$$

For the endemic disease equilibrium both the steady state and the Jacobian are more complicated so we do not evaluate them here. It is also difficult to determine the eigenvalues explicitly. We assume that the endemic steady state is stable when the disease-free steady state is unstable. We highlight this with numerical simulations in Figure 2.4 which shows that the susceptible, exposed and infectious density solutions show damped oscillations about the steady state for various values of p.

2A.5 SEI with free-living steady state and stability analysis

In the same method as we used for the SEI model in Section 2A.2 we look for the steady states of Equations 2.9. This time, as the disease is always present there is no populated disease-free steady state. The steady states now are,

$$(X_s, H_s, Y_s) = \begin{cases} (0,0,0) & \text{zero population} \\ \left(\frac{(b+\sigma)(b+\alpha)Y_T}{\sigma(\beta_w W^* + \beta Y_T)}, \frac{b+\alpha}{\sigma}Y_T, Y_T\right) & \text{endemic state} \end{cases} \tag{2A19}$$

We now have to look at the zero population steady state to determine stability characteristics. The Jacobian matrix is as follows.

$$J(0,0,0) = \begin{pmatrix} \gamma - b - \beta_w W^* & \gamma & \gamma \\ \beta_w W^* & -(b+\sigma) & 0 \\ 0 & \sigma & -(b+\alpha) \end{pmatrix} \tag{2A20}$$

Unfortunately the algebraic results for the eigenvalues of this matrix are too complicated. However on inserting the default parameters from Table 2.1 we find that the eigenvalues for $J(0,0,0)$ change from having one eigenvalue with positive real part when $\beta_w W^* = 0.4$ to all eigenvalues having negative real part when $\beta_w W^* = 0.5$, indicating that the zero populated steady state is unstable for $\beta_w W^* = 0.4$, but stable for $\beta_w W^* = 0.5$. Results for a series of values of $\beta_w W^*$ in Figure 2.6 confirm this change in stability for the zero populated steady state.

Again the Jacobian for the endemic steady state is too complicated, so we contend that when the zero populated steady state is unstable (when $\beta_w W^*$ is less than the critical level between 0.4 and 0.5), the endemic steady state is stable. We can deduce from Equation 2.10 that the disease will only proliferate if the equilibrium

density of susceptibles, X_s satisfies,

$$X_s > \frac{(b+\alpha)(b+\sigma)}{\sigma(\beta_w W^* + \beta)} \tag{2A21}$$

2B.1 Stochastic SEI model

The deterministic models examined in Chapter 2 inform about levels of suppression of the population by disease, and give a good model for the low level of disease endemic in a population acting as a reservoir of MTC . However, an aspect of real life that is not captured by these models is the tendency for the disease to die out; the disease to die out but then re-emerge a number of years later; or for a population to be driven to extinction by disease.

To account for these possibilities it is necessary to develop a stochastic version of the model which can capture the possibility of such random events. Anderson & Trewhella [11] report results from stochastic simulations based on the SEI model, Equations (2.5), however do not specify the method used.

Here we will introduce stochastic behaviour in to the SEI model, Equations (2.5), by using a Gillespie algorithm [67] which models the system as a Poisson process, treating each of the changes to the susceptible, infected and infectious densities in the ODEs, Equations (2B1), as event rates. This is also described by Renshaw [120].

To implement this, the terms that represent changes to the rates of change of susceptible, infected and infectious classes caused by birth, death and transition between classes, numbered 1-7 in Equations (2B1), are turned into probabilistic events.

$$\frac{\mathrm{d}X}{\mathrm{d}t} = \underbrace{\hat{r}(N)N}_{1} - \underbrace{bX}_{2} - \underbrace{\beta XY}_{3} \tag{2B1a}$$

$$\frac{\mathrm{d}H}{\mathrm{d}t} = \underbrace{\beta XY}_{3} - \underbrace{bH}_{4} - \underbrace{\sigma H}_{5} \tag{2B1b}$$

$$\frac{\mathrm{d}Y}{\mathrm{d}t} = \underbrace{\sigma H}_{5} - \underbrace{bY}_{6} - \underbrace{\alpha Y}_{7} \tag{2B1c}$$

The events are detailed in Table 2.2 which indicates how the rates are turned into probabilities by dividing by the sum of all the rates R. The stochastic dynamics are generated using a Gillespie algorithm. The event is chosen using a uniform random variable, $u_1 \sim U[0,1]$ which specifies which event occurs. The population levels are updated accordingly and the event probabilities are recalculated. The time to the next event, Δt, is an exponential random variable with mean value $\frac{1}{R}$ ($\Delta t \sim Exp(R)$). In practice this is implemented with inverse sampling: $\Delta t = \frac{-ln(u_2)}{R}$ where $u_2 \sim U[0,1]$. This process is then repeated until an end condition is reached, for example the total population has become extinct.

Event No	*Event*	*Probability*	*XHY change*
1	Birth of badger	$\frac{\hat{r}(N)N}{R}$	if $\hat{r}(N) > 0 \quad X \to X+1$
2	Natural death of susceptible	$\frac{bX}{R}$	$X \to X-1$
3	Infection of susceptible	$\frac{\beta XY}{R}$	$X \to X-1, H \to H+1$
4	Natural death of infected	$\frac{bH}{R}$	$H \to H-1$
5	Infected becomes infectious	$\frac{\sigma H}{R}$	$H \to H-1, Y \to Y+1$
6	Natural death of infectious	$\frac{bY}{R}$	$Y \to Y-1$
7	Death due to infection	$\frac{\alpha Y}{R}$	$Y \to Y-1$

Table 2.2: The possible events in the stochastic SEI model Equations (2B1), the probability of these events and the change in abundance due to each event. Here R represents the total of all event rates

2B.1.1 Stochastic SEI results

Figure 2B.1 shows four realisations of the stochastic population dynamics when an infected individual is added to a purely susceptible population. Compared with the deterministic case in Figure 2.3, none of the paths taken show the disease remaining endemic in the population. As this is an aspect of TB that we would like to preserve in our model dynamics, modelling densities that represent a 1x1km^2 patch do not seem sufficient to allow disease persistence.

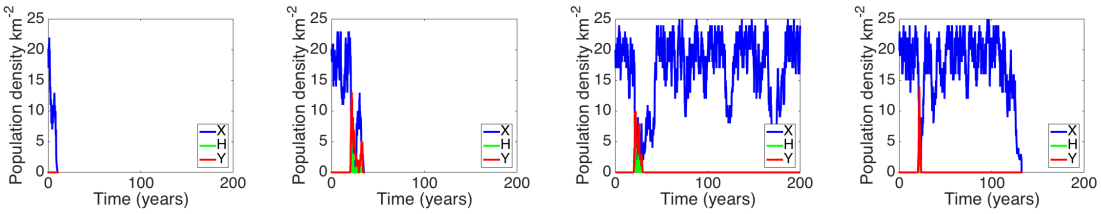

Figure 2B.1: Results for the stochastic SEI model represented by Equations (2B1) with 1 infectious individual added at time 20 years on a patch 1x1 km^2 at disease-free steady state density. Four sample paths are shown for susceptible(X), exposed(H) and infectious(Y) densities showing possibility of (a) population dying out without influence of disease, (b) disease mediated population extinction, (c) the host population recovering from a period of suppression due to infection and (d) the host population recovering from the disease but subsequently suffering extinction due to other random event. Model parameters are set to default values (Table 2.1).

To increase the population size Anderson & Trewhella [11] performed stochastic modelling over an area of 10x10km^2, by altering the carrying capacity K accordingly to $100K$. Note that for the model Equations (2B1) to balance, the transmission coefficient β must be adjusted accordingly to $\frac{\beta}{100}$ as it is still derived from the

endemic steady state susceptible density.

Figure 2B.2 shows two model realisations which highlight the typical population dynamics at the 10x10km^2 scale: the disease never becoming established (Figure 2B.2a); and the disease remaining endemic in the population (Figure 2B.2b). In comparison with the deterministic case in Figure 2.3, when the disease remains endemic (Figure 2B.2b) the oscillations in the population are no longer damped and are of shorter period.

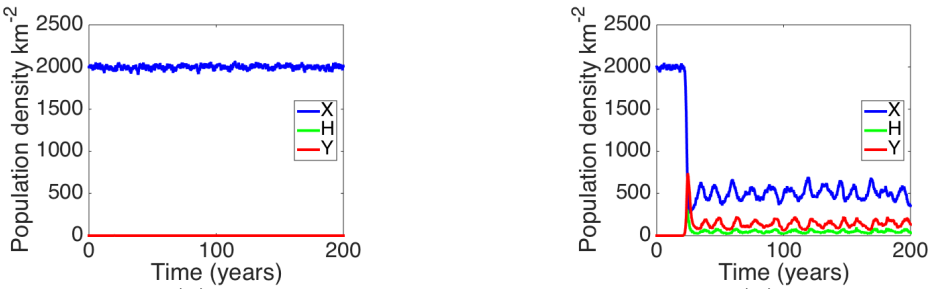

Figure 2B.2: Results for the stochastic SEI model represented by Equations (2B1) with 1 infectious individual added at time 20 years on a patch 10x10km^2 at disease-free steady state density. Two sample paths are shown for susceptible(X), exposed(H) and infectious(Y) densities showing possibility of (a) the disease never getting a foothold in the population and (b) the disease remaining endemic in the population. K = 20x100, $\beta = \frac{0.308}{100}$. Other model parameters are set to default values (Table 2.1).

As a key aspect of developing a model to describe TB dynamics in the badger population is to show the low-level endemic nature of the infection, we investigated the probability of the disease dying out in this stochastic model. Figure 2B.3 shows the probability of the disease dying out within 5, 10 or 30 years after 1 infected has been added to a population of susceptibles of density at a range of carrying capacities on an area of 10x10km^2. Two different values for the transmission coefficient β were used to compare and contrast the behaviour. For the smaller transmission coefficient, $\beta = \frac{0.308}{100}$, for populations with a population of 1,000 or more, the disease does not die out for over 40% of the runs. However, for a larger transmission coefficient, $\beta = \frac{1.54}{100}$, and hence lower critical threshold density, there is a greater chance of the disease dying out.

Our motivation for adding stochasticity to the deterministic SEI model (Equations (2.5)) was to introduce the possibility of the disease dying out. Figures 2B.1 & 2B.2 show that although our stochastic model achieves this when considering small numbers of badgers, the disease does not persist. When we consider our model over a larger area, so considering a larger host population, the disease can persist. This is because as the size of the host population increases, the size of the infectious population increases accordingly so is less likely to get to zero. However, increasing the the population size makes the model's behaviour more like the deterministic SEI model in negating the chance of disease extinction. Therefore this approach,

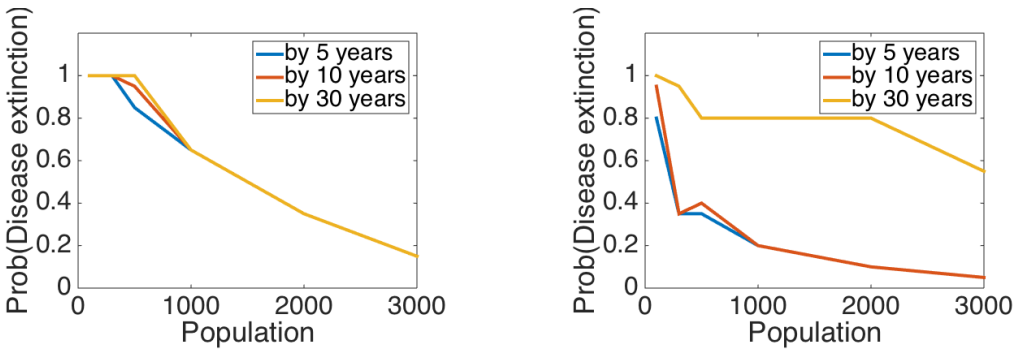

(a) (b)

Figure 2B.3: Probability for disease die-out in 5, 10 or 30 years after 1 infected is added to the equilibrium population at time=0 years on when considering a 10x10km^2 region using model represented by Equations (2B1). The probability was derived from 20 simulations over a 100 year period for each value of K. Sample paths taken from 20 independent runs for each population level. (a) shows results for $\beta = \frac{0.308}{100}$, (b) shows results for $\beta = \frac{1.54}{100}$. The greater transmission coefficient in (b) shows a greater probability of disease extinction. Other model parameters are set to default values (Table 2.1).

although capturing some of the real world behaviour that we want, may not be a good fit.

We therefore look at other facets of badger behaviour that may influence the course of the disease. Anderson & Trewhella [11] considered the effect on a single 10x0km^2 area of a constant rate of 1 infectious badger migrating into the patch each year showing that this reduces the probability of disease extinction. We take the idea of potential badger migration further by considering a number of adjoining patches in a spatial array as in White & Lurz (2014) [142]. We will explore whether migration between such patches leads to a model that captures the possibility of disease persistence in Appendix 2B.2.

2B.2 Spatial Stochastic SEI model

The stochastic SEI model in Appendix 2B.1 considered the population dynamics within one bounded patch which was adjusted in area to model different sizes of populations. It was shown that the disease could persist if we dealt with a larger patch size, allowing a larger number of individuals to be considered per patch. A more realistic way to consider different population sizes in stochastic systems is to consider a collection of spatially linked patches.

To represent this system we consider a spatial array of 1x1 km^2 patches, within each of which the population and disease exhibit the same dynamics as the stochastic SEI model, Equations (2B1), but with the extra possibility of an individual dispersing to a neighbouring patch.

2B.2.1 Spatial Array

The spatial set-up contains a PxP grid of linked patches as in White & Lurz (2014) [142]. Let us consider a patch at position (i, j), referred to as $p_{i,j}$ in Table 2.3. The disease dynamics for this particular patch (i, j) can be represented as follows

		j		
	$p_{i-1,j-1}$	$p_{i-1,j}$	$p_{i-1,j+1}$	
i	$p_{i,j-1}$	$p_{i,j}$	$p_{i,j+1}$	
	$p_{i+1,j-1}$	$p_{i+1,j}$	$p_{i+1,j+1}$	

Table 2.3: Spatial array of patches.

in Equations (2B2):

$$\frac{\mathrm{d}X_{i,j}}{\mathrm{d}t} = \underbrace{\hat{r}(N_{i,j})N_{i,j}}_{1} - \underbrace{bX_{i,j}}_{2} - \underbrace{\beta X_{i,j}Y_{i,j}}_{3} - \underbrace{\sum_{\substack{i-1\le k\le i+1\\ j-1\le l\le j+1\\ k>0,l>0\\ (k,l)\neq(i,j)}} m_{(i,j),(k,l)}X_{i,j} + \sum_{\substack{i-1\le k\le i+1\\ j-1\le l\le j+1\\ k>0,l>0\\ (k,l)\neq(i,j)}} m_{(k,l),(i,j)}X_{k,l}}_{4}, \tag{2B2a}$$

$$\frac{\mathrm{d}H_{i,j}}{\mathrm{d}t} = \underbrace{\beta X_{i,j}Y_{i,j}}_{3} - \underbrace{bH_{i,j}}_{5} - \underbrace{\sigma H_{i,j}}_{6} - \underbrace{\sum_{\substack{i-1\le k\le i+1\\ j-1\le l\le j+1\\ k>0,l>0\\ (k,l)\neq(i,j)}} m_{(i,j),(k,l)}H_{i,j} + \sum_{\substack{i-1\le k\le i+1\\ j-1\le l\le j+1\\ k>0,l>0\\ (k,l)\neq(i,j)}} m_{(k,l),(i,j)}H_{k,l}}_{7}, \tag{2B2b}$$

$$\frac{\mathrm{d}Y_{i,j}}{\mathrm{d}t} = \underbrace{\sigma H_{i,j}}_{6} - \underbrace{bY_{i,j}}_{8} - \underbrace{\alpha Y_{i,j}}_{9} - \underbrace{\sum_{\substack{i-1\le k\le i+1\\ j-1\le l\le j+1\\ k>0,l>0\\ (k,l)\neq(i,j)}} m_{(i,j),(k,l)}Y_{i,j} + \sum_{\substack{i-1\le k\le i+1\\ j-1\le l\le j+1\\ k>0,l>0\\ (k,l)\neq(i,j)}} m_{(k,l),(i,j)}Y_{k,l}}_{10}. \tag{2B2c}$$

Here $m_{(i,j),(k,l)}$ is the rate of dispersal from patch p_{ij} to its neighbouring patch p_{kl}. As in Chapter 2B.1 the rates in the deterministic model can be turned into probabilities of events. These events are specified in Table 2.4.

Event No	*Event*	*Probability*	*XHY change*
1	Birth of badger	$\frac{\hat{r}(N_{ij})N_{ij}}{R}$	if $\hat{r} > 0 \quad X_{ij} \to X_{ij} + 1$
2	Natural death of susceptible	$\frac{bX_{ij}}{R}$	$X_{ij} \to X_{ij} - 1$
3	Infection of susceptible	$\frac{\beta X_{ij} Y_{ij}}{R}$	$X_{ij} \to X_{ij} - 1, H_{ij} \to H_{ij} + 1$
4	Migration from patch	$\frac{m_{(ij),(kl)} X_{ij}}{R}$	$X_{ij} \to X_{ij} - 1, X_{kl} \to X_{kl} + 1$
5	Natural death of incubator	$\frac{bH_{ij}}{R}$	$H_{ij} \to H_{ij} - 1$
6	Infected becomes infectious	$\frac{\sigma H_{ij}}{R}$	$H_{ij} \to H_{ij} - 1, Y_{ij} \to Y_{ij} + 1$
7	Migration from patch	$\frac{m_{(ij),(kl)} H_{ij}}{R}$	$H_{ij} \to H_{ij} - 1, H_{kl} \to H_{kl} + 1$
8	Natural death of infectious	$\frac{bY_{ij}}{R}$	$Y_{ij} \to Y_{ij} - 1$
9	Death due to infection	$\frac{\alpha Y_{ij}}{R}$	$Y_{ij} \to Y_{ij} - 1$
10	Migration from patch	$\frac{m_{(ij),(kl)} Y_{ij}}{R}$	$Y_{ij} \to Y_{ij} - 1, Y_{kl} \to Y_{kl} + 1$

Table 2.4: The possible events for patch (i,j) in the spatial stochastic model represented by Equations (2B2). Here R represents the total of all event rates summed over all patches.

2B.2.2 Spatial parameters and boundary conditions

We have considered this model with a constant migration rate, m. It is difficult to estimate this value and so as a baseline we assume it equals the natural death rate leading to an assumption that dispersal to a different patch will on average occur once in a badgers lifetime. This constant rate m means that in an internal patch a badger will migrate to a particular neighbouring patch at rate $\frac{m}{8}$. Consideration has to be given to how migration proceeds from patches at the boundary. Comins, Hassell & May [38] consider three types of boundary conditions: absorbing, reflective and cyclical whilst modelling an insect population. Absorbing conditions lead to the individual leaving the spatial array altogether; cyclical conditions mean that an individual leaving the spatial array on one edge, re-enters on the corresponding opposite edge; and with reflective conditions an individual does not leave the array but reflects into the neighbouring edge patch (or back into the focal patch).

Of these three types of boundary conditions, reflective would be the closest to the model you might expect for badgers, however it would not seem likely that a badger would try to migrate out of a boundary that would just lead to it returning to the original patch. It would seem more reasonable to consider that a migrating badger has some notion of where it might go to, or at least have existing paths to follow. Therefore at the boundary for a non-corner patch we take the migration rate to each of the five neighbouring patches as $\frac{m}{5}$, and for a corner patch the migration rate to each of the three neighbouring patches as $\frac{m}{3}$.

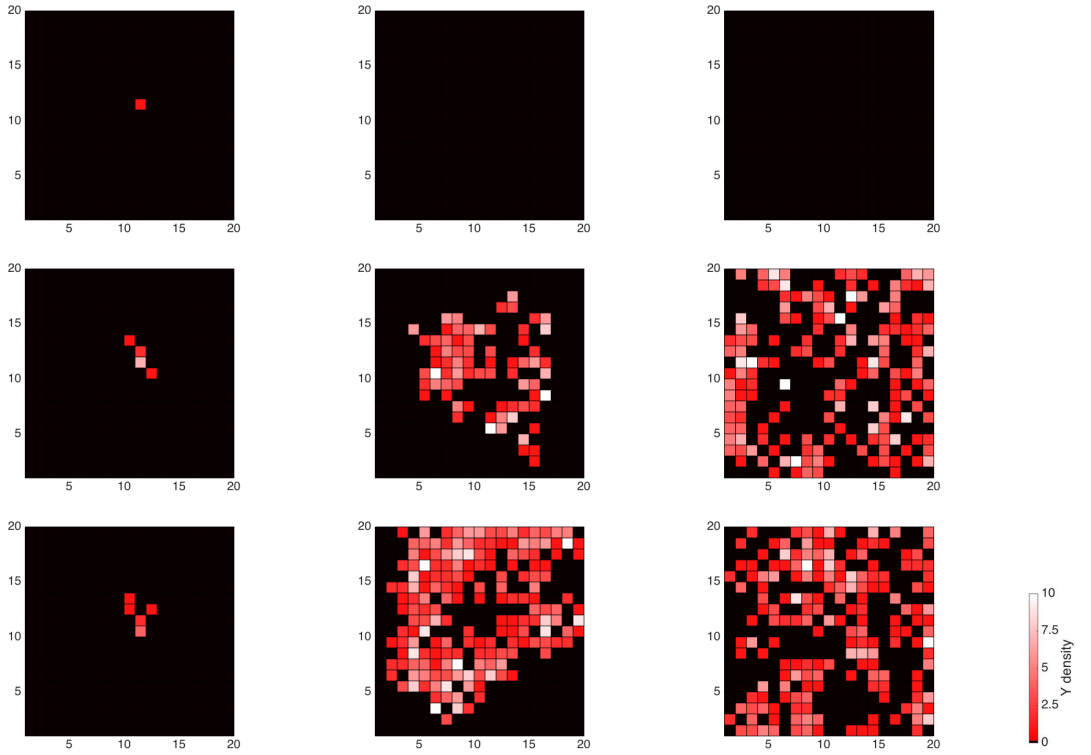

(a) (b) (c)

Figure 2B.4: Results from the spatial stochastic model represented by Equations (2B2) showing levels of infectious (Y) individuals on a spatial array of 20x20 1x1km^2 patches. Each patch starts at the disease-free steady state with $X = K$, 1 infected added at 10 years. Column a) shows level of infected in patches at start of infection, b) level of infected in the spatial array after 15 years, c) level of infected in the spatial array after 30 years. Row 1 shows an infection that never managed to proliferate, migration rate m; row 2 results from migration at $\frac{m}{2}$; row 3 results from migration rate m, the same as the natural death rate. Guided by the colour bar on the bottom right, patches coloured black are disease-free, those coloured darker red are patches with low number of infected individuals rising through pink to white showing patches where the greatest density of infected individuals lies. Disease can be seen to move from the centre of the infection out to the edges. Some patches in the centre can be seen to become disease-free, however in time disease migrates back to these patches. The lower migration rate leads to a slower proliferation of the disease. Other model parameters are set to default values (Table 2.1).

2B.2.3 Spatial Stochastic Results

Figure 2B.4 shows snapshots from sample runs on a 20x20 spatial array at the introduction of disease, 15 years after first infection and then 30 years after first infection. The spatial array is initialised to a disease-free state with susceptible population density at 20 individuals in each patch. Patches coloured black illustrate a disease-free patch; coloured red a small number of infectious individuals; and coloured pink through to white show patches with a higher number of infectious individuals. Correspondingly Figure 2B.5 illustrates the density levels of the

susceptible population on the spatial array where bright yellow illustrates susceptible density at 20 or more, moving down to blue showing a lower level of susceptibles and dark navy blue no susceptibles in a patch. To initiate the disease, 1 infectious individual is added to a patch at the centre of the spatial array. The top row shows a sample run when the disease does not spread into other patches. In this case the infectious individual dies before it managed to promote an epidemic. The middle and bottom rows show sample runs when the disease manages to proliferate throughout the spatial array. In both cases the disease spreads out in all directions spreading the disease into hitherto healthy patches. At 15 years after infection it can be seen that some patches at the centre of the spatial array actually become disease-free but after 30 years disease has migrated into the patches again. In this way the spatial stochastic model represents disease die-off and re-infection that was not captured in the earlier models considered in this project. The course of the disease is shown for one particular patch in Figure 2B.6. There are repeated local disease epidemics that the host population recovers from only to become infected again due to the migration of an infectious individual from a neighbouring patch.

It is also interesting to compare the total population dynamics over the whole array with the dynamics of the deterministic system (Equation (2.5)). Examining a spatial array of 20x20 patches the total susceptible population over time is shown in Figure 2B.7 for sample runs when the disease does not proliferate and in Figure 2B.8 when disease becomes endemic in the spatial system.

When no epidemic has occurred, for the cases when the migration rate is non-zero (Figures 2B.7b & 2B.7c) the population settles to a stable level (but note this is below the level it would be in a deterministic system of 8,000 individuals). Interestingly, when the migration rate is zero (Figure 2B.7a) the total population trend appears to be very slowly diminishing over time. This is due to the small probability of the population dying out in a patch through natural causes, and a birthing event not occurring in time to revitalise the population. As there is no migration of susceptibles to re-populate the patch the population slowly declines. This result highlights that migration of individuals helps maintain the total population in the spatial system in the absence of disease.

When the disease has managed to spread and become endemic in the population we compare the totals for three different migration rates in Figure 2B.8. The general pattern emerging from this is akin to results from the deterministic model (Equations (2.5)) illustrated in Figure 2.3. The onset of the disease causes the density of susceptibles to crash, oscillating about a lower density. Different migration rates also have an effect on the average susceptible population: a higher migration rate leads to a faster crash in the susceptible population; a slightly lower average susceptible population; and a shorter oscillatory period.

In summary, if we consider a spatial stochastic model it allows us to represent

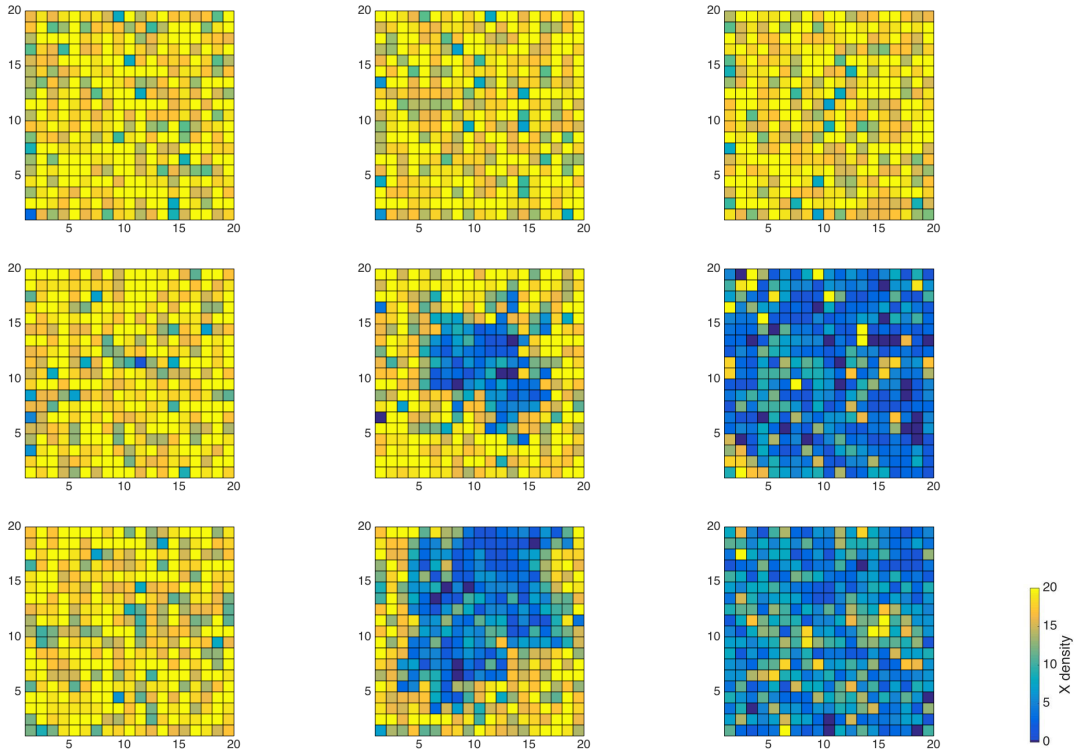

Figure 2B.5: Results from the spatial stochastic model represented by Equations (2B2) showing levels of susceptible (X) individuals on a spatial array of 20x20 1x1km^2 patches corresponding to the levels of infectious in Figure 2B.4. Each patch starts at the disease-free steady state $X = K$, 1 infected added at 10 years. Column a) shows level of susceptibles at start of infection, b) levels of susceptibles in the spatial array after 15 years, c) levels in susceptibles in the spatial array after 30 years. Row 1 shows an infection that never managed to proliferate; row 2 results from migration at $\frac{m}{2}$; row 3 results from migration rate m, the same as the natural death rate. Guided by the colour bar on the bottom right, patches coloured bright yellow are patches with the density of susceptibles at disease-free level, those coloured light blue are patches with a lower density of susceptibles indicating a patch where disease has proliferated dropping to dark navy blue indicating a patch with 0 susceptibles where disease and migration has led to the population being wiped out. As disease moves from the centre out to the edges, some patches in the centre can be seen to recover from the infection, however in time disease migrates back to these patches. The lower migration rate leads to a slower proliferation of the disease. Other model parameters are set to default values (Table 2.1).

the disease dynamics of the badger TB system. In particular the disease can be maintained in populations at relatively low density. This occurs through a process of local repeated disease epidemics followed by recovery of the population.

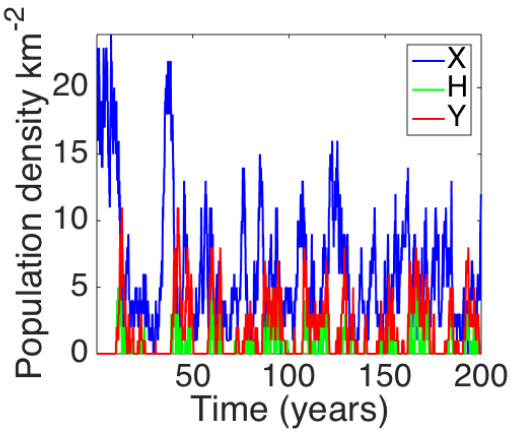

Figure 2B.6: Results from the spatial stochastic model represented by Equations (2B2) showing the population for the patch in the spatial array that incurred the initial infection of 1 infectious at time 10 years. Susceptible density is shown in blue, infected in green and infectious in red. Repeated disease epidemics are followed by recovery of the population. After extinction of the disease, migration of an infectious individual from a neighbouring patch starts another outbreak of the disease. Model parameters are set to default values (Table 2.1).

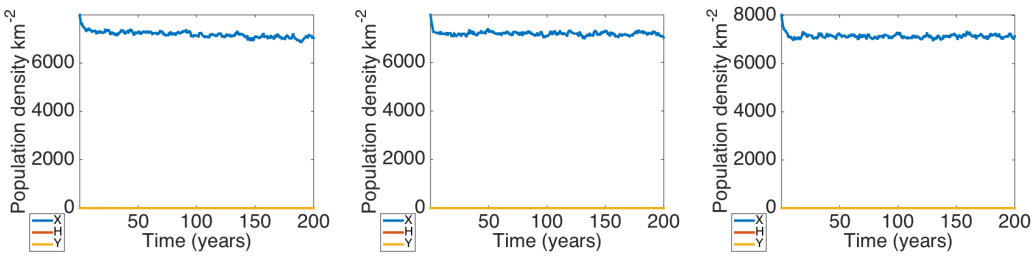

Figure 2B.7: Results from the spatial stochastic model represented by Equations (2B2) showing total levels of susceptible(X), exposed(H) and infectious(Y) on a spatial array of 20x20 1x1km^2 patches. Each patch starting at the disease-free steady state $X = 20$, 1 infected added at 10 years but the disease dying out after initial infection at the centre of the spatial array. Column (a) no migration; column (b) migration rate m; column (c) migration rate $\frac{3m}{2}$. As disease has died out, total levels of susceptibles only affected by migration of non-infected individuals. Non-zero migration rate ((b),(c)) does not affect population density levels when compared with zero migration density ((a)). Other model parameters are set to default values (Table 2.1).

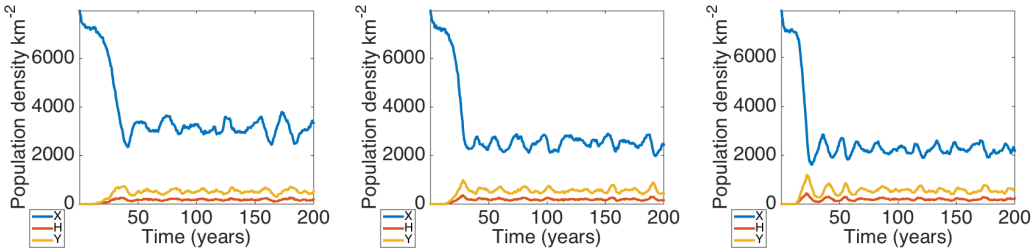

(a) (b) (c)

Figure 2B.8: Results from the spatial stochastic model represented by Equations (2B2) showing total levels of susceptible(X), exposed(H) and infectious(Y) on a spatial array of 20x20 1x1km^2 patches. Each patch starts at the disease-free steady state $X = K$, 1 infected added at 10 years. Column (a) migration rate $\frac{m}{2}$; column (b) migration rate m; column (c) migration rate $2m$. A higher level of migration causes greater proliferation of the disease, therefore suppressing the density of the susceptible population to a greater extent. Other model parameters are set to default values (Table 2.1).

Chapter 3

Developing a wild boar TB model

Figure 3.1: Wild boar and deer at a water hole in central Spain.

In central Spain tuberculosis (TB) is endemic in wild boar populations reaching high prevalence levels of greater than 50% [106, 137]. It also persists, but at a lower prevalence, in other host species such as red deer, however as this prevalence follows changes in wild boar prevalence, red deer are not seen as the prime host reservoir [76, 56]. Wild boar affected by TB can be separated into two classes. The first class are infected, but largely asymptomatic and shed a negligible amount of MTC particles. The second class are wild boar that have progressed from the infected to the generalised (super-shedder) state. These animals typically shed large quantities of MTC and also suffer from increased mortality associated with generalised infection [126]. While wild boar tend to congregate in separate social groups during the dry season different groups share scarce water resources ([14]; Figure 3.1). Free-living MTC particles can survive in mud and water for long periods [55, 126] and so the interaction between the population and the infectious agent is well-mixed. Infection through contact with free-living MTC particles (particularly at water holes) is seen as the key factor that leads to the high disease prevalence of TB infection in wild boar in central Spain [138, 14]. While infection through direct boar to boar contact is also possible it is likely to be at a lower level than infection through contact with free-living pathogen (and can to some extent be approximated by the free-living

infection process). We endeavour to produce a mathematical model that reflects TB being spread through contact with free-living particles and aim to use the model to identify ways to reduce the level of generalised infection in the wild boar population, and hence inform strategies to reduce overall TB prevalence. This chapter outlines the process of the initial model development and undertakes a sensitivity of key parameters on population and disease status.

As detailed in Chapter 2 a wide range of studies have developed models to examine the infection dynamics of TB. These have examined specific systems, notably badgers, possums, deer and cattle, and used a range of mechanistic (strategic) and rule-based (tactical) modelling approaches. In general they consider the disease transmission through direct host-host contact. Anderson et al. (2013) [6] developed a rule-based model to assess the wild boar TB dynamics in central Spain. Here disease transmission was through contact between susceptible and local excretor hosts, through dispersal of an excretor and through contact with an external source. In our study we will develop an alternative model for the wild boar TB dynamics in central Spain. We will use a mechanistic approach in which the underlying dynamics are represented by a system of differential equations. An advantage of the mechanistic approach is that it allows for a more thorough exploration of the possible population outcomes and a better characterisation of the key processes that determine the dynamics. Our model will focus on disease transmission through contact between susceptible hosts and free-living infective particles that are released by infected, excretor hosts. This is based on research showing that high TB prevalence in wild boar is associated with multiple wild boar social groups accessing common water and supplementary food sources, thus spreading and coming into contact with MTC pathogen via the environment [138, 137].

In central Spain TB is more prevalent in the more intensely managed hunting estates where wild boar tend to live at higher density [138]. Our initial modelling will focus on an area representative of such estates. As such we consider a single geographical area that supports a homogeneously mixed population of wild boar with total population density N. In the presence of infection the total population is reduced to a density below this disease-free state as a result of disease-induced mortality. Reflecting evidence from the field [126], the progression of TB in wild boar can be split into two phases: on initial infection the wild boar do not shed a high concentration of infected particles and do not suffer disease virulence; and secondly a proportion of these infected wild boar will progress to a generalised phase where they become super-shedders and can shed a high concentration of infected particles into the environment and also suffer from additional disease mortality. We will model these separate phases of infection using three distinct classes of wild boar: susceptible individuals who have never been infected by TB having density S;

infected individuals who were susceptible but became infected via exposure to TB in the environment have population density I; and those individuals whose infection has progressed to the generalised state, with population density G. We construct the model to reflect that the generalised individuals (super-shedders) are the sole producer of the free-living pathogen which exists in the environment at density F. The total wild boar population is therefore $N = S + I + G$, and individuals from all classes may reproduce into the susceptible class (although generalised individuals may reproduce at a reduced rate). All of the population classes may suffer death due to natural causes with the generalised class additionally incurring disease-induced mortality. A schematic representation of the system is shown in Figure 3.2.

Translating this system into a deterministic mathematical model would produce a system of four coupled non-linear ordinary differential equations. However, by considering all ages of wild boar together we lose important specific details of the system. As evidenced by Vicente et al. (2013) [137] and Che'Amat et al. (2015) [34] different age classes of wild boar have different susceptibility to MTC infection with yearlings most likely to present as super-shedders [94], and therefore we infer that the infection rate and the progression to generalised infection in piglets and yearlings is faster than that for adults. Also, pertinent to being able to target specific age groups in the model we note that vaccination to prevent MTC infection is applied to piglets only [60]; and that hunting typically targets larger more mature (trophy) individuals [140]. These considerations are highlighted by biological and ecological literature regarding TB in wild boar and other wild animals in the Iberian peninsula [75]. Therefore we look to refine this simple model by splitting the susceptible and infected classes into separate age categories.

3.1 The Piglet-Yearling-Adult (PYA) model

In a similar manner to the model of Anderson et al. (2013) [6], we split our susceptible and infected classes into separate age classes to reflect different transmission parameters for younger and older wild boar, and also to reflect what age classes of wild boar are known to reproduce. Taking a longer view for the model, we also envisage that separate age classes will be important when incorporating management strategies, for example vaccination affecting only piglets, and hunting being focused on adult wild boar. We divide both the susceptible and infected populations into three age classes: piglets (aged 0-1 year) P, yearlings (aged 1-2 years) Y, and adults (aged 2 years+) A, with our susceptible classes having population density P_S, Y_S and A_S respectively and infected classes population density P_I, Y_I and A_I respectively. Susceptible piglets, P_S, mature into susceptible yearlings, Y_S, which mature into susceptible adults, A_S, at rates m_{P_S} and m_{Y_S} respectively, and similarly infected piglets, P_I, mature into infected yearlings, Y_I,

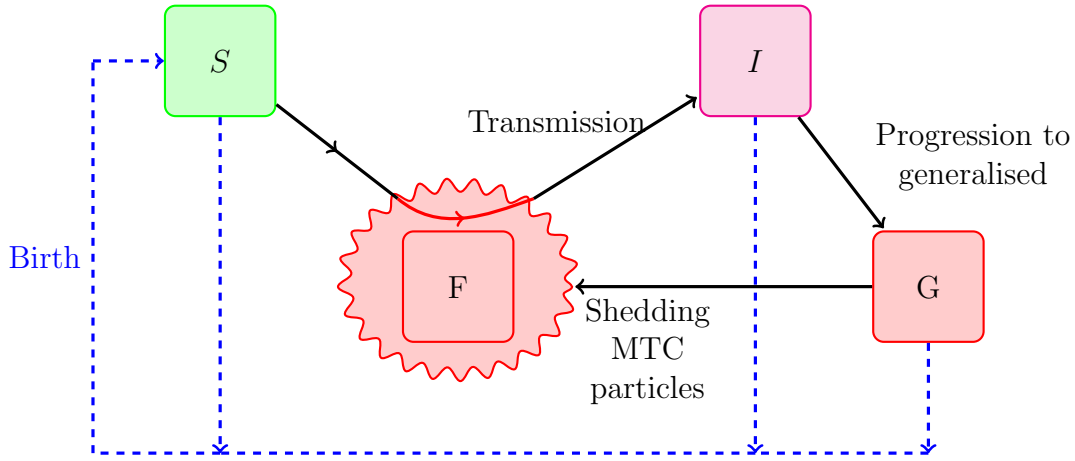

Figure 3.2: SIGF system: susceptible (S) wild boar become infected (I) via contact with free-living particles (F). Infected wild boar (I) may progress to generalised (G) who are super-shedders, the sole producers of free-living particles (F). Each of the population classes can die due to natural causes, with generalised experiencing an added mortality rate due to the disease. Each population class may reproduce with all new-borns entering the susceptible class.

which mature into infected adults, A_I, at rates m_{P_I} and m_{Y_I} respectively. In the generalised class we do not separate the age classes because once generalised the key functional trait is the release of pathogen particles and additional level of mortality, whose properties are less dependent on age-class.

Each susceptible class may become infected through contact with infectious free-living particles at rates β_P, β_Y and β_A respectively. Infected wild boar of any age class, P_I, Y_I and A_I, can progress to the generalised class, G, and occurs at rates ε_P, ε_Y and ε_A respectively.

The total population, N, can therefore be defined as $N = P_S+P_I+Y_S+Y_I+A_S+A_I+G$, which is at steady state, $N = P_S + Y_S + A_S = K$, in the absence of disease. All the densities are expressed in terms of population per the geographical area. We define the total prevalence, $p_{tot} = \frac{P_I+Y_I+A_I+G}{N}$, as the proportion of the total population infected with TB; the prevalence of infected but not generalised $p_{inf} = \frac{P_I+Y_I+A_I}{N}$; and the prevalence of generalised $p_{gen} = \frac{G}{N}$; such that $p_{tot} = p_{inf} + p_{gen}$.

Free-living infected particles exist in the environment at density F and have a natural decay rate of μ. The density of free-living particles increases through generalised wild boar shedding particles at rate λ.

Yearlings and adults (both susceptible and infected) and generalised, give birth to susceptible piglets at rates b_Y, b_A and b_G respectively. The birth rate is modified to represent density-dependent constraints through the term, q, which acts to stabilise the total population at $N = K$ in the absence of disease. Piglets, yearlings, adults and generalised classes may die of natural causes at rates d_P, d_Y, d_A and d_G respectively, and generalised individuals suffer an additional mortality rate due

to the disease of α.

$$\frac{\mathrm{d}P_S}{\mathrm{d}t} = (b_Y(Y_S + Y_I) + b_A(A_S + A_I) + b_G G)(1 - qN) - m_{P_S}P_S - d_P P_S - \beta_P P_S F \tag{3.1a}$$

$$\frac{\mathrm{d}P_I}{\mathrm{d}t} = \beta_P P_S F - m_{P_I}P_I - d_P P_I - \varepsilon_P P_I \tag{3.1b}$$

$$\frac{\mathrm{d}Y_S}{\mathrm{d}t} = m_{P_S}P_S - m_{Y_S}Y_S - d_Y Y_S - \beta_Y Y_S F \tag{3.1c}$$

$$\frac{\mathrm{d}Y_I}{\mathrm{d}t} = \beta_Y Y_S F + m_{P_I}P_I - m_{Y_I}Y_I - d_Y Y_I - \varepsilon_Y Y_I \tag{3.1d}$$

$$\frac{\mathrm{d}A_S}{\mathrm{d}t} = m_{Y_S}Y_S - d_A A_S - \beta_A A_S F \tag{3.1e}$$

$$\frac{\mathrm{d}A_I}{\mathrm{d}t} = m_{Y_I}Y_I + \beta_A A_S F - d_A A_I - \varepsilon_A A_I \tag{3.1f}$$

$$\frac{\mathrm{d}G}{\mathrm{d}t} = \varepsilon_P P_I + \varepsilon_Y Y_I + \varepsilon_A A_I - \alpha G - d_G G \tag{3.1g}$$

$$\frac{\mathrm{d}F}{\mathrm{d}t} = \lambda G - \mu F \tag{3.1h}$$

The population dynamics are described by Equations (3.1). A schematic representation of the model is shown in Figure 3.3.

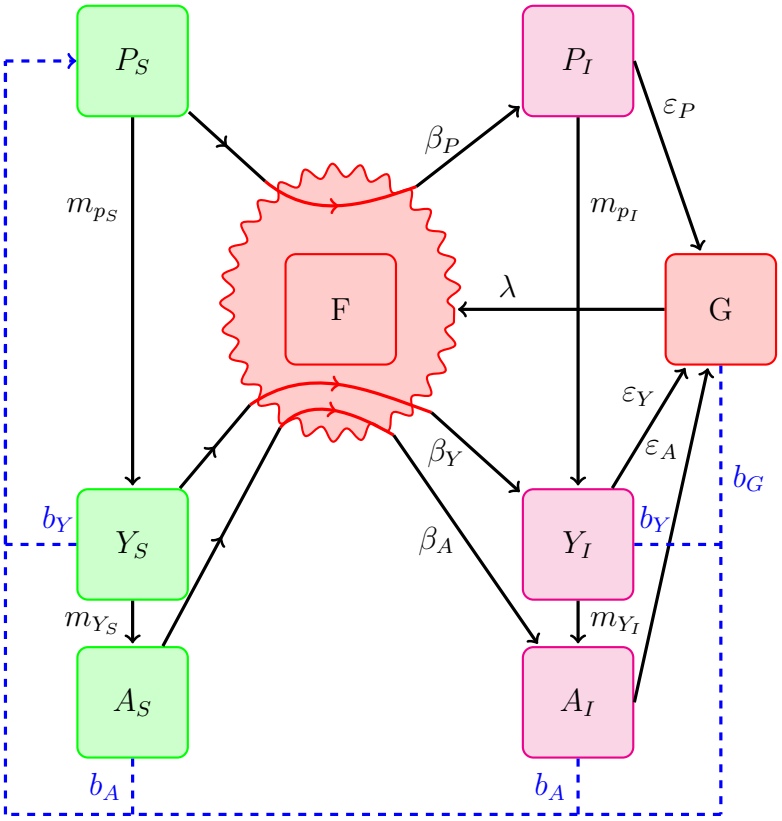

Figure 3.3: A schematic representation of the wild boar TB model with piglet, yearling and adult classes represented by Equations (3.1).

3.1.1 PYA model: Default parameter set

There are many parameters in this model and in this section we aim to determine best estimate parameters from empirical data. Where empirical data are not available we investigate which parameter sets can achieve disease prevalence levels of $p_{tot} = 50\%$ and $p_{gen} = 25\%$ (as these are representative of the wild boar TB system in central Spain). We use the following default parameters,

'target area'=3x3km^2 We consider a single geographical managed estate containing a homogeneously mixed wild boar population covering an area of 3x3km^2.

$b_Y = b_A = b = log(4)$ The population birth rate in a disease-free population when resources are unlimited. This constant rate means that for each reproductive member of the population, 3 piglets will be born, averaged over the population over a year. (This has been derived by assuming that there is a 50% sex ratio and that each female produces an average of 6 offspring per year when resources are not limited [105, 64].)

$b_G = 0$ For the default parameters we assume that members of the generalised class cannot reproduce.

$K = 500$ The steady state for the total population in the target area in the absence of disease. (Note that there are no ecological data to back this value up. With this value of K the corresponding endemic population is representative of wild boar densities observed on hunting estates in central Spain of around 20/km^2 [3]. We perform a sensitivity analysis on this parameter in Section 3.3.)

$q = \frac{1}{K}\left(1 - \frac{d_A(d_P+m_{P_S})(d_Y+m_{Y_S})}{m_{P_S}\left(b_A m_{Y_S}+b_Y d_A\right)}\right)$ This parameter limits the total population to carrying capacity K in the populated disease-free steady state, and is derived from steady-state analysis of the model without infection.

$m_{P_S} = m_{P_I} = m_{Y_S} = m_{Y_I} = m = 1$ The rate that piglets mature to yearlings and yearlings mature to adults for both susceptible and infected classes. These rates assume that it takes on average 1 year to enter the next age group using standard classification for wild boar juveniles and adults [94].

$d_P = d_Y = d_A = d = \frac{1}{7}$ The natural death rate of all classes which implies an average life expectancy of 7 years [134].

$\beta_A = \frac{20}{K}$ The infection rate for adults, adjusted dependent on K. (Note this parameter has been adjusted so that the model produces the required disease prevalence in conjunction with the other default values. We undertake sensitivity analysis of this parameter as part of the model evaluation.)

$\beta_P = \beta_Y = c_\beta \beta_A$ The infection rate for both piglets and yearlings. For the default parameter set we assume that $c_\beta = 3$ and so disease transmission to piglets and yearlings is three times that of the adult rate. We undertake a sensitivity analysis of c_β in the results below and let it range from $1 < c_\beta \leq 10$, as we assume that transmission is higher for piglets and yearlings than it is for adults. This is inferred from data from the field where a high proportion of piglets on hunting estates were already infected at 3-6 months old [34], and also data that shows that yearlings show the greatest proportion of infecteds [137].

$\varepsilon_A = \frac{2}{3}$ This is the rate that infectious adults become generalised. This rate implies that it takes on average in 1.5 years for an adult to become generalised following infection. Alongside β_A this value has been adjusted so that the model produces the required disease prevalence in conjunction with the other default values. We undertake a sensitivity analysis of this parameter.

$\varepsilon_P = \varepsilon_Y = c_\varepsilon \varepsilon_A$ The rate that infected piglets and yearlings become generalised. For the default parameter set we assume $c_\varepsilon = 3$. This assumes that it takes on average 6 months for an infected piglet or yearling to progress to the generalised class. We undertake a sensitivity of c_ε in the results below and let it range from $1 < c_\varepsilon \leq 10$ as we assume that progression to generalised is faster for piglets and yearlings than for adults, inferred from data from the field showing that juveniles suffer the greatest proportion of generalised [106].

$\alpha = 1$ This is the additional disease induced death rate of the generalised class and assumes that on average individuals spend 1 year in the generalised class before death. Barasona et al. (2016) [12] gathered data on the causes of mortality of 45 adult wild boar that were monitored over a period of 3 years using GPS collars, noting that MTC infection was confirmed in 72% of the wild boar for which postmortem data were available. In the game estates, similar to our focal area, the mean survival time was roughly 300 days with 72% of these deaths being from harvesting, whereas 22% were caused by tuberculosis. However, the mean survival time for the wild boar monitored in areas with much lower hunting pressure was over double that of the game estates, and the proportion of deaths from TB was 45%. TB is a chronic disease in wild boar, and from these figures we infer that wild boar can remain in the generalised phase for a significant period of time. We perform a sensitivity analysis of this parameter.

$\lambda = 1$ We normalise this value to 1. This is valid as we explore a range of values for β_P, β_Y and β_A which scale with the size of λ and the density of free-particles, F. Therefore λ, μ, β_P, β_Y and β_A depend on each other and are to some

extent fitted to provide reasonable underlying results. There are no empirical estimates for this parameter.

$\mu = 6$ This is the decay rate for free-living particles, indicating that they have a life expectancy of 2 months. Fine et al. (2011) [55] examined the survival of *Mycobacterium bovis* in natural conditions in Michigan, USA over a 12-month period. They report that *Mycobacterium bovis* persisted for 88 days in soil and 58 days in water, although under hotter conditions this reduced to 11 and 48 days respectively. Ghodbane et al. (2014) [65] show under controlled laboratory conditions MTC species can survive in soil for over 12 months, however it is commonly understood that MTC exhibits lower survival times in natural conditions [132]. Under natural conditions moisture is a key factor in the survival to *Mycobacterium bovis* [132, 126] and in central Spain high levels of MTC were found in the mud of waterholes with the presence of diseased animals heightening this risk [14]. As our continuous model aims to average the system behaviour over a year, we set the default value of survival to 2 months which is between the highest and lowest values recorded by Fine et al. (2011) [55]. It should be noted that we explore a range of values for β_P, β_Y and β_A which are dependent on the density of free-living particles, F, so that the decay rate μ influences the fitted values for the transmission rates. We perform a sensitivity analysis for this parameter.

Using parameters set to these values, we examine what happens to a disease-free population of 500 individuals in the target area, when 1 infected yearling is added at a time t=10 years. The effect of the disease on the population can be seen in Figure 3.4.

When the disease is introduced the total population is suppressed with the number of infected and generalised individuals and susceptible individuals stabilising to a stable endemic state. At the endemic steady state we have $p_{tot} \approx 53\%$, $p_{gen} \approx 28\%$ and $p_{inf} \approx 25\%$. The level of free-living particles follows a similar pattern to that of the total infected population.

	Model	β_Y	ε_Y	b_Y
1	Default model	β_P	ε_P	b_A
2	Yearlings with piglet parameters	β_P	ε_P	0
3	Yearlings with adult parameters	β_A	ε_A	b_A

Table 3.1: Variants of the PYA model that are tested to examine the importance of the yearling class.

As well as ensuring that our target disease prevalence, $p_{tot} = 50\%$ and $p_{gen} = 25\%$ is achievable with this model, it is also a valuable exercise to check that the three

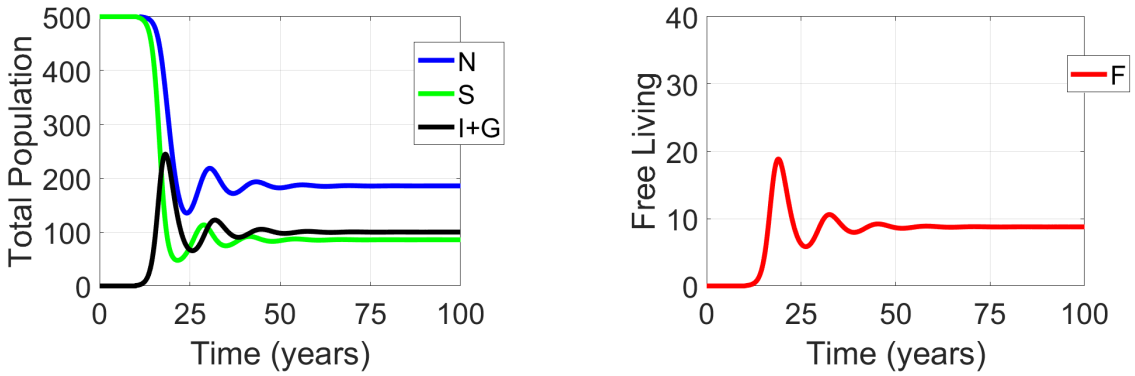

(a) (b)

Figure 3.4: (a) The population against time for the total population $N = S + I + G$ (blue), susceptibles $S(= P_S + Y_S + A_S)$ (green) and total infected and generalised $I(= P_I + Y_I + A_I) + G$ (red). (b) The level of free-living, F, against time. Here 1 infected yearling is introduced to a susceptible population at its carrying capacity at $t = 10$. Default parameter values.

class PYA model is not over complicated. To investigate this we use the default parameter set in Section 3.1.1 as a starting point. These parameters assume that yearlings have the same rates for transmission and progression to generalised as piglets, and that yearlings (classes Y_S and Y_I) can give birth at the same rate as adults (classes A_S and A_I). Evidence suggests this is a realistic combination, as discussed in the default parameters Section 3.1.1 piglets and yearlings present higher rates of infection and progression to generalised, also yearlings have a slightly lower but similar birth rate to adults on hunting estates [124]. We call this model 1 in Table 3.1 and compare this model with model 2 where the yearling class has the same parameters as the piglet class, and with model 3 where the yearling class has the same parameters as the adult class. If the results for model 1 are analogous to either of these other models it would indicate that the model could be simplified by combining the yearling class with one of the other classes.

3.1.2 Sensitivity of c_β and c_ε to model changes

To examine the differences between these three models we look at the sensitivity to changes in the values of c_β and c_ε. We do this by examining heat charts for our target disease prevalences p_{tot}, p_{inf} and p_{gen} (Figure 3.5) as the sensitivity parameters c_β and c_ε vary. The areas of the charts highlighted bright green show the combinations of c_β and c_ε that achieve our target disease prevalence: $p_{tot} = 50\%$, $p_{inf} = 25\%$ and $p_{gen} = 25\%$. The intersection of these three green areas highlight the values of c_β and c_ε that satisfy our requirements.

Comparing heat charts from Figure 3.5 we see significant differences between

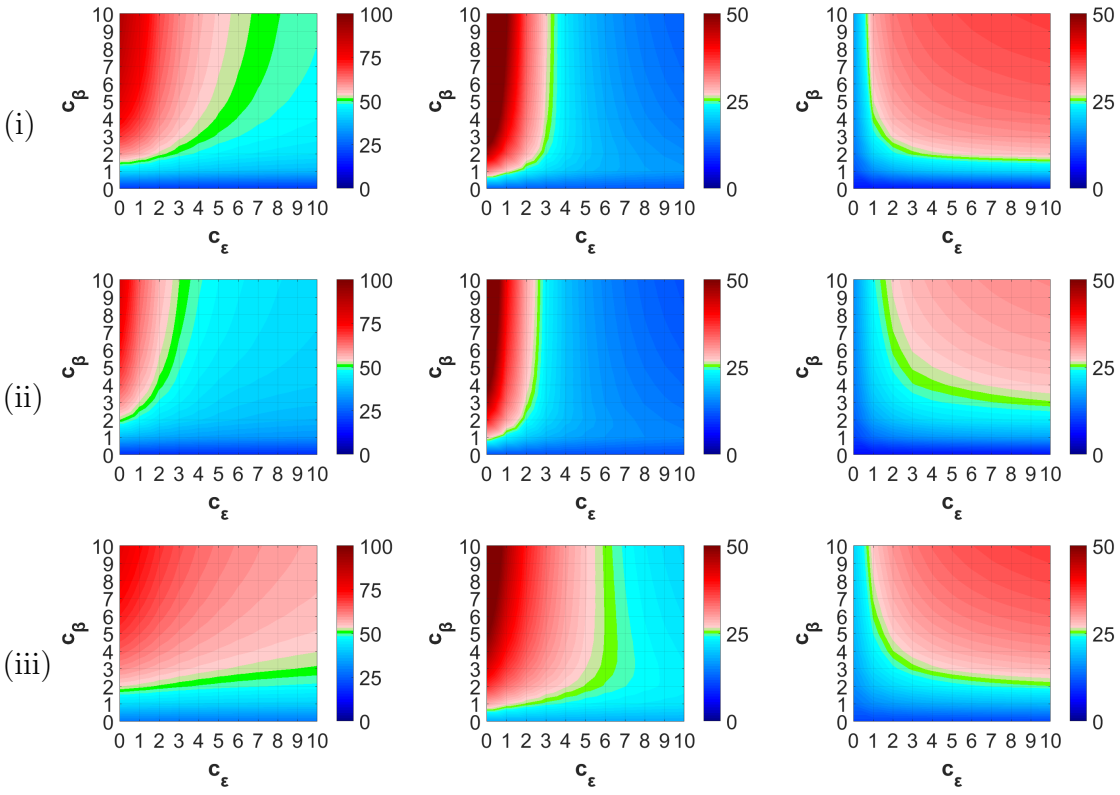

Figure 3.5: Sensitivity of transmission parameters to changes in parameters for the Y class. Heat charts show variation in (a) p_{tot} (b) p_{inf} and (c) p_{gen} given changes in c_β and c_ε. (i) shows results for model 1; (ii) shows results for model 2; and (iii) shows results for model 3 as described in Table 3.1. Other parameters set to the default parameter values.

the models. In particular the pattern of total prevalence, p_{tot} is markedly different between the three models. Model 2, where yearlings have the same parameters as piglets, shows that $p_{tot} = 50\%$ requires a narrow range of c_ε whereas model 3, where yearlings have adult parameters, requires a narrow range of c_β to achieve $p_{tot} = 50\%$. The results for default model 1 are between these extremes. This provides evidence that there is sufficient difference between the dynamics of the three models and therefore that the default model in which yearlings have different parameters to both adults and piglets should be used.

3.1.3 Sensitivity of total population to model changes

While we intend to focus on model 1, some useful information about the general behaviour of the model can be gained by examining changes in the total population over time for the different models (Figure 3.6i). The results indicate that the three

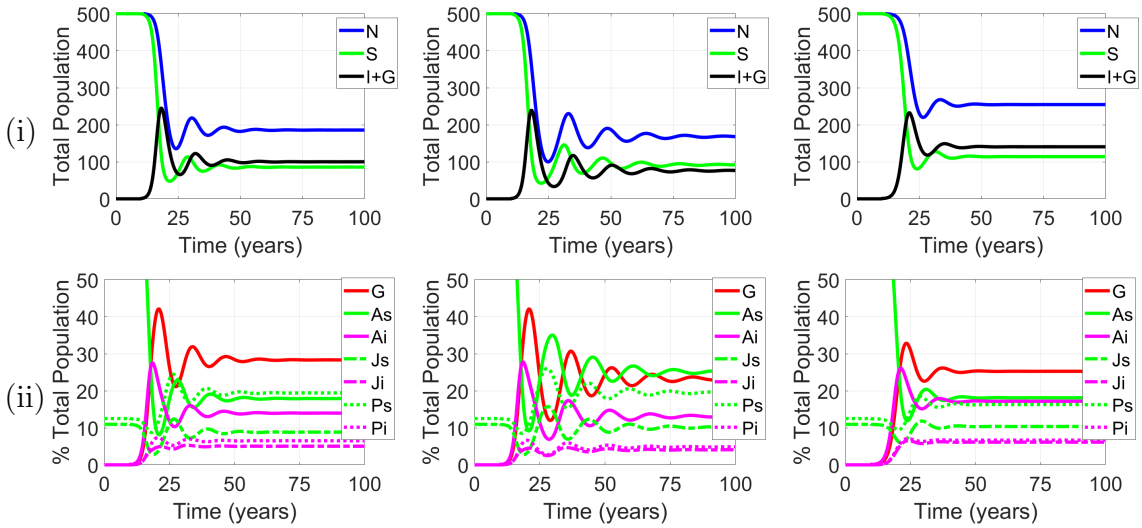

Figure 3.6: Changes in the total population over time for: (a) model 1; (b) model 2; and (c) model 3 as described in Table 3.1. 1 infected yearling is inserted into a disease-free population at steady state at time t=10 years. (i) shows the total population N (blue), susceptibles $S = P_S + Y_S + A_S$ (green) and infectious $I + G = P_I + Y_I + A_I + G$ (black). (ii) shows changes to individual classes which are indicated in the key to the figure but more generally the generalised class is red, infected classes are magenta, susceptible classes green with adult classes shown by a continuous line, yearling classes by a dot-dash line and piglet classes by a dotted line. Parameters not specific to models 1, 2 and 3 are set to the default parameter values.

models are qualitatively similar. Model 1 shows a higher level of infecteds and overall higher total population than model 2 which is a consequence of yearling reproduction in model 1 (the additional reproduction provides additional piglets that are susceptible to infection). Model 3 shows higher total population when compared to the default model which is a consequence of the reduced likelihood of infection as yearlings are assumed equivalent to adults in terms of susceptibility to infection in model 3. To gain greater insight into the differences between the three models we examine the changes to the individual classes.

3.1.4 Sensitivity of individual class populations to model changes

To examine the population density in individual classes for models 1, 2 and 3 we plot the percentage of the total population for each class (Figure 3.6ii). The results indicate that model 1 (default parameters) produces the greatest percentage of generalised individuals. This arises since in model 1 yearlings have the same susceptibility to infection and rate of progression to the generalised class as piglets

and they can also reproduce like adults and so increase the supply of individuals that are most susceptible to infection. In comparison, model 2 in which yearlings do not reproduce shows a decrease in overall levels of infection. This highlights how a sufficient supply of new susceptible individuals is required to support high infection levels. Model 3, in which yearlings reproduce but have the same susceptibility to infection and progression to generalised infection as adults shows a reduction in the level of generalised individuals and an increase in infected adults (and an increase in the proportion of adult individuals in general compared to model 1).

3.2 PYA model: discussion of age structure

In developing a model to represent the wild boar TB system we have considered a framework where the only route to infection is through transmission from free-living infected particles. We have considered a model that splits the population into susceptible, infected and generalised classes and considered age structure that represents piglets, yearlings and adults separately for susceptible and infected classes. We have confirmed that with this model we can achieve our target prevalences of p_{tot}=50%, p_{gen}=25%.

We compared the results from three models that represented different parameterisations of the PYA model described by Equations (3.1). We show (Figures 3.5 and 3.6) that the results are sufficiently different so that it is important to consider the three age class system (model 1), and we will proceed with this model for the remaining analysis in this chapter.

Considering a model with three age classes does increase the complexity of the system but we mitigate this somewhat by assuming yearlings have the same transmission coefficients for infection ($\beta_Y = \beta_P$) and same rate of progression to generalised infection ($\varepsilon_Y = \varepsilon_P$) as piglets, and that yearlings have the same rate of reproduction as adults ($b_Y = b_A$). This reduces the number of parameters and also represents the key differences between the age classes observed in the natural system.

3.3 PYA Model: the response of infection to changes in population size

We examine how the population and infection dynamics of the PYA model vary when the underlying density of the host varies. In particular we are interested in determining a threshold level in host population at which the pathogen is supported and the trend in infection prevalence as the host population increases. Field work has shown that the disease prevalence has increased with increases in underlying wild

boar densities [76] and the response to population changes will also be important when we add management procedures to the model that affect the population size.

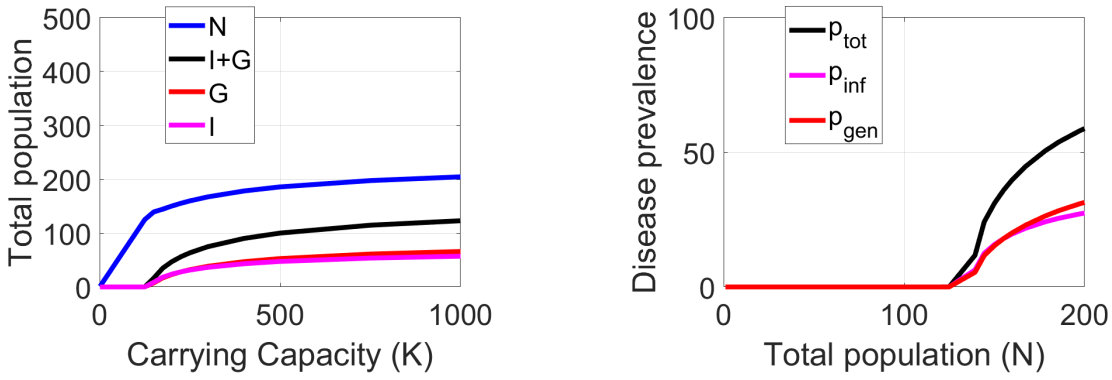

(a) (b)

Figure 3.7: PYA model response to change in population size. (a) shows plot of resultant total population against change in carrying capacity (K). (b) shows plot of prevalence against resultant population size N. Default parameter values.

To do this, we run the model using the default parameter set from Section 3.1.1 for a range of values of K between 0 and 1000, and plot the resultant values of total population N against the input value of K, and also the disease prevalence indicators p_{tot}, p_{gen} and p_{inf} against the resultant N.

Figure 3.7a shows that for increasing values of K, the resultant total population N saturates due to the effect of endemic infection at a level around $N = 200$. There is a critical value of K where the host population is unable to support the pathogen. This is borne out in Figure 3.7b showing the resultant disease prevalence attained for each resultant value of the total population N. Figure 3.7b shows a critical threshold for $N \approx 120$ below which the host cannot support the pathogen. Above this critical threshold the disease can be supported and increases as N increases. As N increases from 120 to 200 it is observed that p_{tot} increases from 0-60%. The prevalence of generalised individuals, p_{gen}, and the other infected individuals, p_{inf}, increase with N but remain approximately equal (to each other) until N approaches 200.

3.4 PYA model: birth from the generalised class

Evidence from the field indicates that individuals with generalised infection may be able to reproduce (albeit at a reduced rate). Additional reproduction may be a key driver in enhancing the level of infection and the prevalence of generalised infection. Since the generalised class forms a significant proportion of the population it is important to examine how reproduction from this class may affect the infection dynamics.

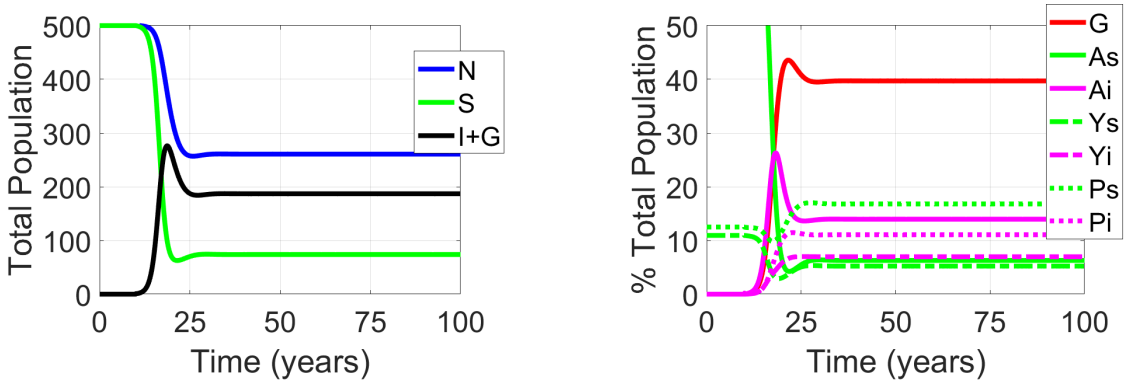

(a) (b)

Figure 3.8: Results for the PYA model with default parameters and birth from generalised ($b_G = b_A$) where 1 infected yearling is inserted into a disease-free population at steady state at time t=10 years. (a) plots total population against time for total population N (blue), susceptibles $S = P_S + Y_S + A_S$ (green) and infectious $I = P_I + Y_I + A_I + G$ (black). (b) plots individual class densities against time which are indicated in the key to the figure but more generally the generalised class is red, infected classes are magenta, susceptible classes green with adult classes shown by a continuous line, yearling classes by a dot-dash line and piglet classes by a dotted line.

To provide an upper bound on the effect of birth from the generalised class we set $b_G = b_A$ ($b_G = 0$ in the previous default results). Figure 3.8a with $b_G = b_A$ can be compared to Figure 3.6a(i) in which $b_G = 0$. It is clear that birth from the generalised class increases the overall population ($N \approx 270$ compared to $N \approx 190$). The increase in population is driven by an increase in the number of infected and generalised individuals, with the level of susceptibles largely unchanged. The transfer of new susceptibles, recruited by increased reproduction, into increased levels of infected individuals is a feature of classical epidemiological models [10, 84].

Figure 3.8b shows the percentage of total population for each of the population classes when $b_G = b_A$ (and can be compared with Figure 3.6a(ii) in which $b_G = 0$) where the proportion of generalised has risen to 40% (from below 30%), whereas the proportion of adult susceptibles has dropped below 10% (from $\sim$ 18%) which results from a relatively unchanged level of susceptibles but an increase in the total host population level. Figure 3.9 highlights how birth from the generalised class may play an important role in generating the high levels of prevalence seen in the wild boar TB system.

We examine the sensitivity of the PYA model with birth from the generalised class to changes in the values of c_β and c_ε. Figure 3.10 shows heat charts for our target disease prevalences p_{tot}, p_{inf} and p_{gen} and can be compared with Figure 3.5i. The prevalence of the generalised class has increased dramatically and this leads to an increase in the overall prevalence with levels above our target values for much of

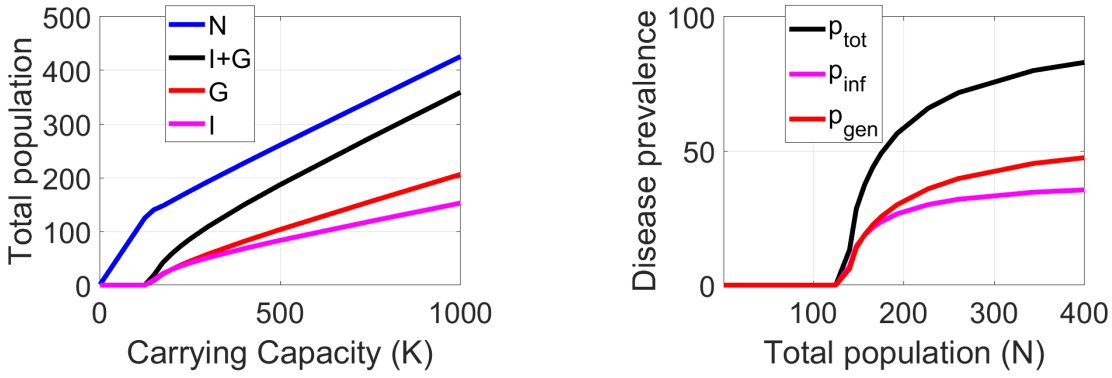

(a) (b)

Figure 3.9: PYA model response to change in population size with generalised birth ($b_G = b_A$). (a) shows plot of resultant total population against change in carrying capacity (K). (b) shows plot of prevalence against resultant population size N. Default parameter values and birth from generalised ($b_G = b_A$).

the parameter space.

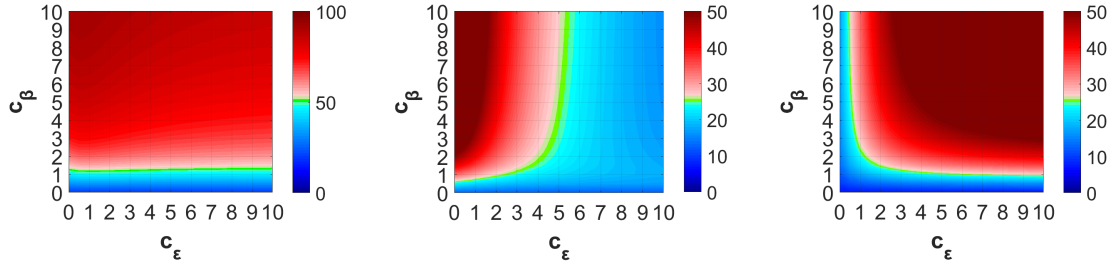

(a) (b) (c)

Figure 3.10: Heat charts show variation in p_{tot}, p_{gen} and p_{inf} given changes in c_β and c_ε for the PYA model with default parameter values and birth from the generalised class ($b_G = b_A$).

The implication of these results is that birth from the generalised class could have a major effect on the resultant total population as well as the disease prevalence which could increase well beyond our initial target of $p_{tot} = 50\%$. However, we have assumed that the birth rate for the generalised class is the same as that for adults which is an upper bound as there is evidence that those with a generalised infection reproduced at a reduced rate. To investigate this we set $b_G = fb_A$, where $f \in [0, 1]$ is the proportion of adult reproduction for the generalised class, and examine changes in the prevalence of TB as f is varied.

Figure 3.11 shows that the prevalence of TB increases as f increases. The greatest increase is in the prevalence of generalised individuals, p_{gen}, and this drives the increase in total prevalence. The rate of increase of prevalence is greatest at higher values of K, as here the underlying birth rate is higher due to reduced (intra-specific) density dependent pressures. Figure 3.11 illustrates that for increasing values of K the total population density increases, and for each K as

the fecundity f increases then so does the total population density, driven by the increase in reproduction from the generalised class.

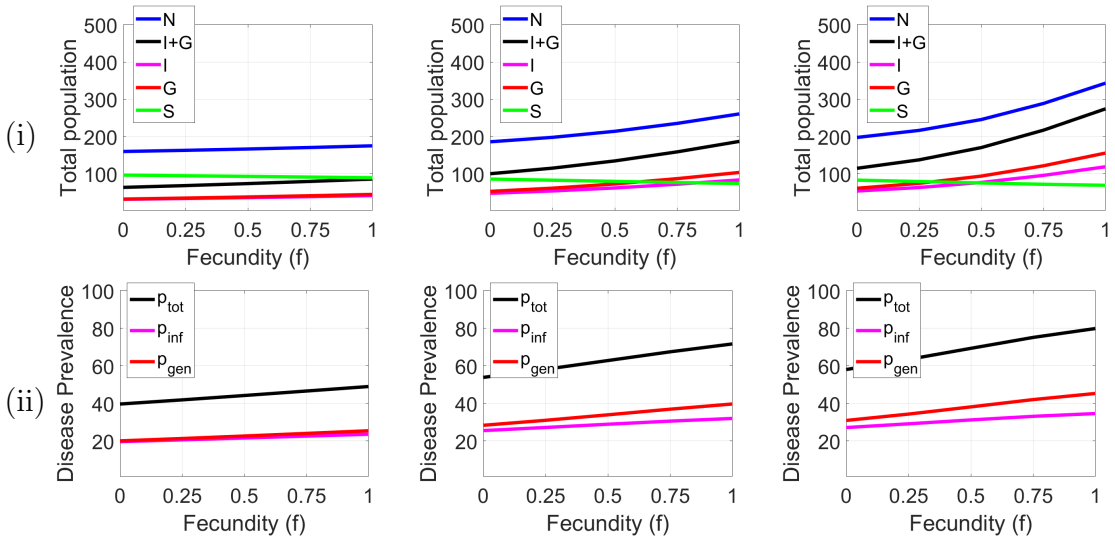

Figure 3.11: For (a) $K = 250$; (b) $K = 500$; and (c) K=750, changes in (i) the total population and (ii) disease prevalence, plotted against the level of fecundity of the generalised, where $f = 0$ is equivalent to no birth from the generalised class, $f = 1$ is equivalent to birth from the generalised class at the same level as the adult class. All other parameters from the default parameter set.

3.4.1 PYA model: pseudo-vertical transmission

A key goal of our study was to develop a wild boar TB model in which infection was via free-living infected particles. However, due to the large quantities of infected particles shed by generalised individuals and the close contact between mothers and their initially susceptible piglets, we also wish to assess the importance of the transfer of infection to piglets through close contact with a generalised parent. We model this as pseudo-vertical transmission whereby a proportion of the births from the generalised class are born into the infected piglet class. Figure 3.12 updates the schematic of the model processes to include pseudo-vertical transmission where birth from the generalised class results in infected piglets with probability p_{vt}, and susceptible piglets with probability $(1-p_{vt})$. This change modifies the piglet classes in Equations (3.1) with the modifications underlined in Equations (3.2).

$$\frac{\mathrm{d}P_S}{\mathrm{d}t} = (b_Y(Y_S + Y_I) + b_A(A_S + A_I) + \underline{(1-p_{vt})}b_G G)(1 - qN) - m_{P_S}P_S - d_P P_S - \beta_P P_S F \tag{3.2a}$$

$$\frac{\mathrm{d}P_I}{\mathrm{d}t} = \underline{p_{vt}b_G G(1-qN)} + \beta_P P_S F - m_{P_I}P_I - d_P P_I - \varepsilon_P P_I \tag{3.2b}$$

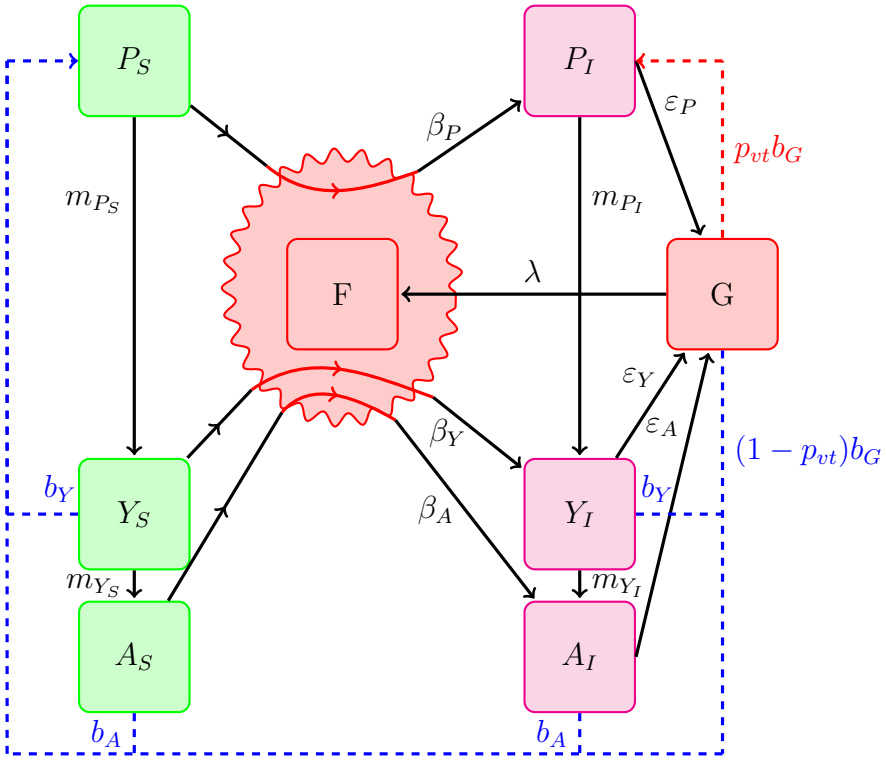

Figure 3.12: A schematic of the PYA model including pseudo-vertical transmission from the generalised class with probability p_{vt}.

For increasing levels of pseudo-vertical transmission there is an approximately linear increase in p_{tot}, with p_{gen} showing greater increase than p_{inf} (Figure 3.13ii). Corresponding to the increase in infection there is a decrease in the total population (Figure 3.13i). When the birth rate from the generalised class is relatively low ($f = 0.25$) there is only a small increase in total prevalence as p_{vt} increases from 0 to 1. For higher birth rates from the generalised class ($f = 0.5$ or 1) the increase in total prevalence and the prevalence of the generalised class is more significant.

3.5 PYA model enhancement to PYAG model

Over a number of conference calls and a site visit to central Spain we had discussions regarding the suitability of the structure and parameters for the PYA model. The veterinarians involved with wild boar testing advised on the age-specific disease dynamics and were able to give guidance on parameter values and target population density and prevalence. Using the model results from Figures 3.4 to 3.13 we wanted to understand whether the model gave a suitable representation of the wild boar TB system. It was agreed that this initial model captured the qualitative behaviour of the wild boar TB system but that birth from generalised should be included in the model as there is evidence from the field that generalised wild boar are nearly as fecund as healthy individuals [124]. The higher prevalence this can generate would

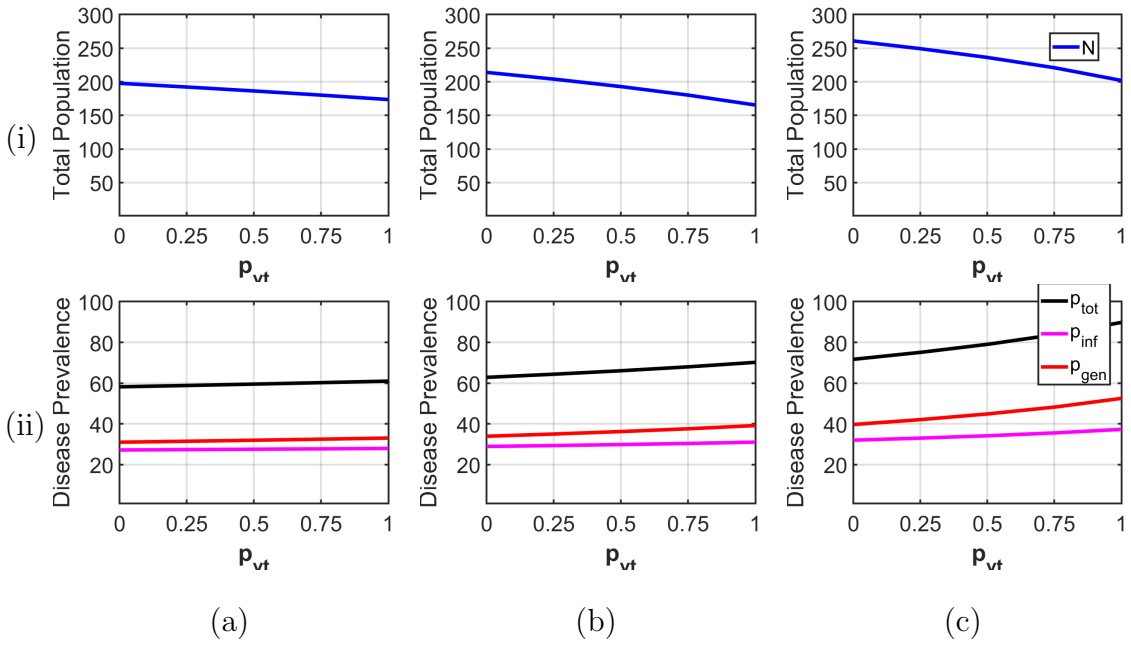

Figure 3.13: Effect of pseudo-vertical transmission from the generalised class on (i) the total population and (ii) the disease prevalence, for different levels of generalised fecundity: (a) $f = 0.25$, (b) $f = 0.5$, and (c) $f = 1$. The default parameter set is used.

agree with reported values in some regions where total TB prevalence could reach 90% [139]. It was also agreed that as it was unclear as to the level of pseudo-vertical transmission that may occur in reality, and as the model can render high prevalence and high levels of generalised without this feature, the model by default should not include an element of pseudo-vertical transmission. We therefore decompose the generalised class into piglet, yearlings and adults and set $b_G = b_Y = b_A = b$, and set $p_{vt} = 0$. Note that by splitting the generalised G class up into separate age classes will reduce the overall birth from generalised slightly as the P_G class will not be reproductive, however this is not a significant change.

We will therefore perform further sensitivity tests with the enhanced PYA model, which we will refer to as the PYAG model described by:

$$\frac{\mathrm{d}P_S}{\mathrm{d}t} = b(Y_S + Y_I + A_S + A_I + (1-p_{vt})(Y_G + A_G))(1-qN) - mP_S - dP_S - \beta_P P_S F \tag{3.3a}$$

$$\frac{\mathrm{d}P_I}{\mathrm{d}t} = p_{vt} b(Y_G + A_G)(1-qN) + \beta_P P_S F - mP_I - dP_I - \varepsilon_P P_I \tag{3.3b}$$

$$\frac{\mathrm{d}P_G}{\mathrm{d}t} = \varepsilon_P P_I - mP_G - dP_G - \alpha P_G \tag{3.3c}$$

$$\frac{\mathrm{d}Y_S}{\mathrm{d}t} = mP_S - mY_S - dY_S - \beta_Y Y_S F \tag{3.3d}$$

$$\frac{\mathrm{d}Y_I}{\mathrm{d}t} = \beta_Y Y_S F + mP_I - mY_I - dY_I - \varepsilon_Y Y_I \tag{3.3e}$$

$$\frac{\mathrm{d}Y_G}{\mathrm{d}t} = \varepsilon_Y Y_I + mP_G - mY_G - dY_G - \alpha Y_G \tag{3.3f}$$

$$\frac{\mathrm{d}A_S}{\mathrm{d}t} = mY_S - dA_S - \beta_A A_S F \tag{3.3g}$$

$$\frac{\mathrm{d}A_I}{\mathrm{d}t} = \beta_A A_S F + mY_I - dA_I - \varepsilon_A A_I \tag{3.3h}$$

$$\frac{\mathrm{d}A_G}{\mathrm{d}t} = \varepsilon_A A_I + mY_G - dA_G - \alpha A_G \tag{3.3i}$$

$$\frac{\mathrm{d}F}{\mathrm{d}t} = \lambda(P_G + Y_G + A_G) - \mu F \tag{3.3j}$$

3.6 PYAG model: varying key model parameters

Analysis of our simpler SIGF system in Figure 3.2 detailed in Appendix 3A.1 shows that for this system

$$R_0 = \frac{\beta K \varepsilon \lambda}{\mu(d+\varepsilon)(d+\alpha)} \tag{3.4a}$$

and so changes to the parameters β, ε, $\frac{\lambda}{\mu}$, d, and α will affect the dynamics of the disease. Our PYAG system (Equations (3.3)) is more complex but still has the same underlying dependence on a similar set of parameters. We want to test how changes to each of these parameters individually affects the disease and population dynamics, assuming that all other parameters are fixed to their default value.

3.6.1 Varying virulence of the disease α

The parameter α models the additional cost of the TB infection to generalised wild boar, giving an additional mortality rate α to the generalised class. By increasing this parameter, we increase the virulence of the disease. It should be remembered that the default parameter set value $\alpha = 1$ represents generalised wild boar on average dying in 1 year due to the effects of the disease, whereas $\alpha = 4$ represents

generalised wild boar dying on average in 3 months due to the disease. From the SIGF value of R_0, a measure of the strength of the disease, we see that as alpha grows larger, and hence the virulence of the disease grows stronger, R_0 grows smaller and thus the impact on the total population reduces. We see that as α increases beyond 2 the generalised class die out more rapidly resulting in less population suppression due to the disease, lower disease prevalence p_{tot} and reduced generalised prevalence p_{gen} (Figure 3.14i). However, as α gets smaller it plays a significant role in the number of generalised in the population and hence the disease prevalence p_{tot}. In this case, as α gets smaller, the generalised class live longer in the population and thus can infect more susceptibles leading to much greater disease prevalence p_{tot} and p_{gen}. As the additional mortality on the generalised class reduces, the cost of the disease to the population reduces and thus the total population suppression due to the disease reduces to 0 as α reduces to 0.

3.6.2 Varying progression to generalised ε_A

The parameter ε_A models the rate of progression to the generalised class of infected adults. The default parameter set has $\varepsilon_A = \frac{2}{3}$ which translates to infected adults becoming generalised on average in 1.5 years. The piglet and yearling rate is set to 3 times this value, $\varepsilon_P = \varepsilon_Y = 3\varepsilon_A$, meaning that they become generalised on average in 6 months. As the rate of progression to generalised increases, so does the effect of the disease on the total population density, and hence the total population density N decreases (Figure 3.14ii). As ε_A grows from 0 to 1 (and thus progression to generalised increases) the proportion of generalised in the population, p_{gen}, grows saturating at 40% as ε_A increases beyond 1, although notably the actual number of generalised individuals saturates when ε_A is less than 0.5. In contrast, p_{inf} decreases to below 20% as ε_A increases beyond 1. As the rate of progression to generalised decreases, less infecteds become generalised until $\varepsilon_A \sim 0.5$ where $p_{gen} = p_{inf}$. As ε_A decreases to 0, the cost to the total population of the disease lessens to a point where although $p_{inf} = p_{tot}$ is relatively high, p_{gen} is very low and thus there is very little suppression of the total population density N from the disease-free steady state.

3.6.3 Varying disease transmission β_A

β_A is the disease transmission rate from free-living particles to the adult class. As the R_0 value for the SIGF system in Equation (3.4) has β in the numerator we expect that as β grows, so should the strength of the disease and thus increase the suppression of the total population density. When β_A is 0 there is no disease transmission and therefore no suppression of the population density from its disease free steady state (Figure 3.14iii). As β_A increases from 0, there is a threshold below which the disease is not able to spread and become endemic in the population.

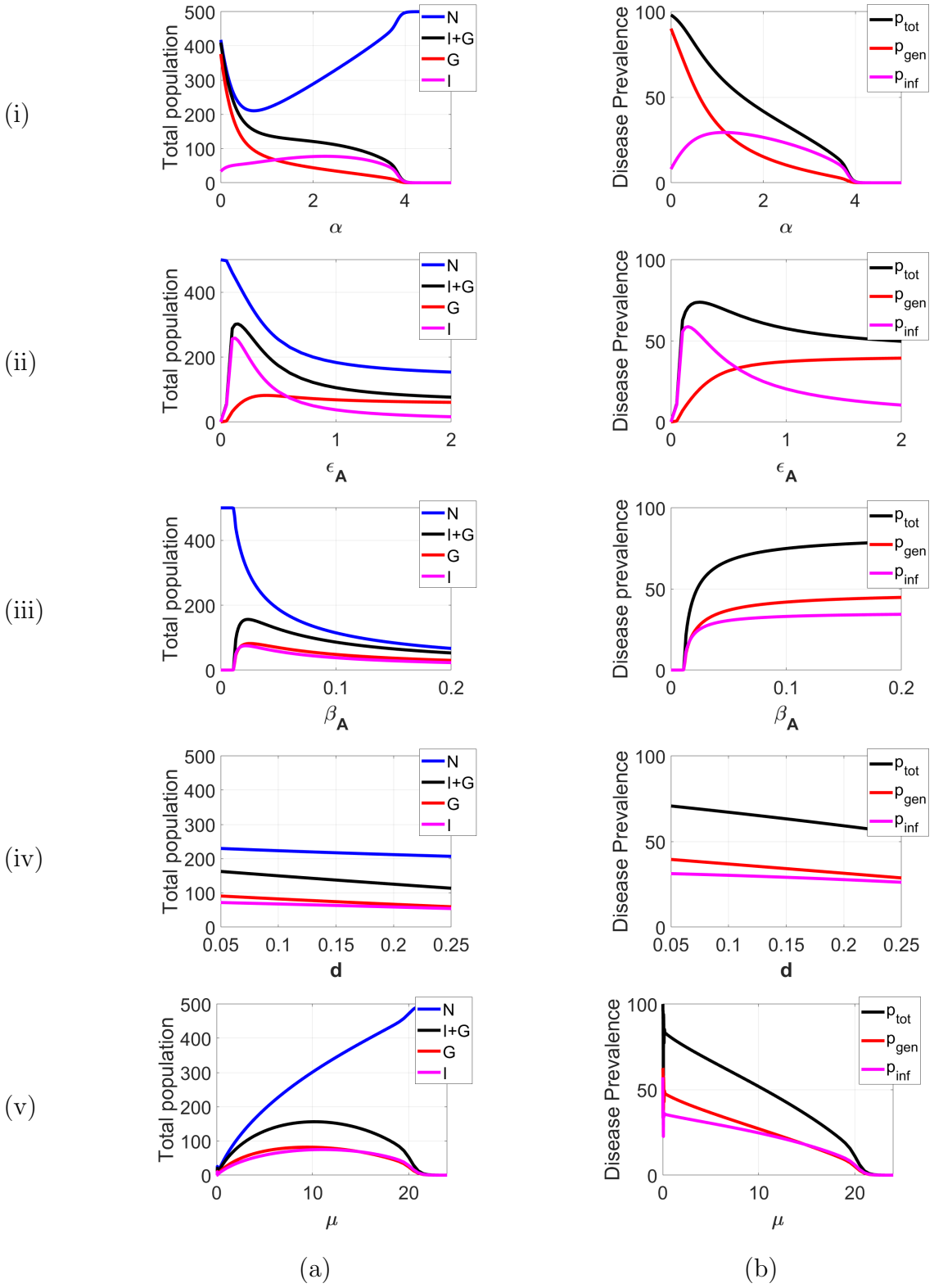

Figure 3.14: PYAG parameter sensitivity showing response in (a) total population and (b) disease prevalence when varying individual key model parameters: (i) additional disease mortality rate (α), (ii) progression rate to generalised for adults (ε_A), (iii) transmission rate for adults (β_A), (iv) natural death rate (d), and (v) free-living decay rate (μ). Non-varied parameters are set to the default values.

From the SIGF value of R_0, this is effectively when $R_0 < 1$. When β_A is increased above this threshold the disease is able to spread, inducing a suppression in the total

population density, and a rise in the disease prevalence. As β_A increases, the disease prevalence increases saturating at $p_{tot} \approx 75\%$. For lower values of β_A, p_{gen} and p_{inf} are approximately equal with p_{gen} becoming greater than p_{inf} when β_A increases above 0.025.

3.6.4 Varying natural death rate d

All the population classes suffer natural death at the same rate. As lifespan decreases (d increases) the population levels and prevalence levels decrease slightly (Figure 3.14iv). However there is little suppression of the total population N as d increases, echoing the expression for R_0 for the SIGF system in Equation (3.4) which although it has d in the denominator, is dominated by the values of α and ε which are greater. For all values of d between 0.05 and 0.25 p_{gen} is greater than p_{inf}, as d increases, the difference between them decreases.

3.6.5 Varying free-living decay rate μ

Our free-living control parameters are λ and μ, but as we set $\lambda = 1$ and scale β_A accordingly, parameter variation for the free living class focuses on the parameter μ, the natural decay rate of free-living particles. Discounting the oscillatory behaviour at very low values of μ which occurs for unrealistic levels, as μ increases from 2 to 12 the total population density increases as does the density of generalised and infected, however as the density of susceptibles increases at a greater rate the prevalence p_{tot}, p_{gen} and p_{inf} all decrease as μ increases (Figure 3.14v). This is due to an increase in μ leading to a reduction in the level of free-living particles in the system and hence a reduction in infection. As μ increases from 12 the susceptible density continues increasing and the disease prevalence drops until the density of the infected and generalised class drops to 0, showing in our system that the disease dies out when $\mu > 21$. This echoes the R_0 value for the SIGF model in Equation (3.4) where $R_0 \propto \frac{1}{\mu}$, showing for sufficiently large μ $R_0 < 1$ and therefore the disease cannot spread.

3.7 PYAG wild boar TB model discussion

We have developed the PYAG model in consultation with veterinarians in central Spain, using their guidance over sources for parameter values and key delineation of population classes. It could be argued that this has generated a model that has too much complexity, however we foresee that the extra population classes will help the implementation of management controls that are targeted at specific age groups. Also, having performed sensitivity analysis on the PYAG model (Equations (3.3)), with the default parameter set as the base parameter set with $b_G = b_Y = b_A = b$

and $p_{vt} = 0$, we understand the impact of changes in parameters and can use this to help understand the population response to TB management. We also note that the model results are qualitatively similar for a range of parameters around our default values. We therefore can have confidence that our key (qualitative) findings are not restricted to a specific set of parameters. Therefore, the PYAG model with this parameter setup will be the wild boar TB model used to test the effect of TB management controls in Chapters 4, 5 and 6.

Appendices to Chapter 3

3A.1 SIGF: critical population threshold

To provide baseline information into the disease dynamics we undertake a steady state and stability analysis of the reduced model shown in Figure 3.2 which has the following form:

$$\frac{\mathrm{d}S}{\mathrm{d}t} = (b(S+I)+b_G G)(1-q(S+I+G)) - dS - \beta SF \tag{3A1a}$$

$$\frac{\mathrm{d}I}{\mathrm{d}t} = \beta SF - dI - \epsilon I \tag{3A1b}$$

$$\frac{\mathrm{d}G}{\mathrm{d}t} = \epsilon I - dG - \alpha G \tag{3A1c}$$

$$\frac{\mathrm{d}F}{\mathrm{d}t} = \lambda G - \mu F \tag{3A1d}$$

Steady states are:

$$(S,I,G,F) = (0,0,0,0) \qquad \text{zero density} \tag{3A2a}$$

$$= \left(\left(\frac{b-d}{bq}\right),0,0,0\right) \qquad \text{disease-free populated steady state} \tag{3A2b}$$

$$= \left(S^* = \frac{\mu(d+\epsilon)(d+\alpha)}{\beta\epsilon\lambda}, I^*, G^*, F^*\right) \qquad \text{endemic disease state} \tag{3A2c}$$

As we want to set the disease-free total population to K we therefore set $q = \frac{b-d}{Kb}$. We examine the eigenvalues of the Jacobian to determine the stability of these steady states. For the zero density steady state the Jacobian is,

$$J(0,0,0) = \begin{pmatrix} b-d & b & b_G & 0 \\ 0 & -d-\epsilon & 0 & 0 \\ 0 & \epsilon & -\alpha-d & 0 \\ 0 & 0 & \lambda & -\mu \end{pmatrix} \tag{3A3}$$

The eigenvalues are, $b-d$, $-d-\epsilon$, $-\alpha-d$ and $-\mu$, therefore making the zero density state unstable when $b > d$.

For the disease-free steady state the Jacobian is,

$$J(K,0,0,0) = \begin{pmatrix} -b+d & -b+2d & -\frac{b^2-bd-b_G d}{b} & -\beta K \\ 0 & -d-\epsilon & 0 & \beta K \\ 0 & \epsilon & -\alpha-d & 0 \\ 0 & 0 & \lambda & -\mu \end{pmatrix} \tag{3A4}$$

Finding eigenvalues for this matrix is not trivial, but given its structure we know

that one of them is $-(b-d)$, which by enforcing $b > d$, our condition for growth from the zero density state, is always negative. Therefore we are concerned with whether any eigenvalues of the sub-matrix

$$\begin{pmatrix} -d-\epsilon & 0 & \beta K \\ \epsilon & -\alpha-d & 0 \\ 0 & \lambda & -\mu \end{pmatrix} \tag{3A5}$$

are positive. This time we spot that the trace of this matrix

$$\text{trace}(J) = -(d+\epsilon) - (d+\alpha) - \mu \tag{3A6}$$

is always negative and real so we know that the sum of the eigenvalues is always negative and real, as the elements of the matrix are all real. Also, the product of the eigenvalues, equal to the determinant of this matrix

$$\det(J) = \beta K \epsilon \lambda - \mu(d+\epsilon)(d+\alpha) \tag{3A7}$$

and is always real. As the trace of the Jacobian is always negative there must be at least one eigenvalue with negative real part for all parameter combinations. Therefore the stability of the steady state depends on the sign of the real part of one eigenvalue changing. This occurs when the determinant of the Jacobian changes sign. Therefore the steady state becomes unstable when $\det(J)$ becomes positive which can be written as:

$$R_0 = \frac{K\beta\epsilon\lambda}{\mu(d+\epsilon)(d+\alpha)} > 1 \tag{3A8}$$

This condition is used in Section 3.6.

Chapter 4

Management of tuberculosis in wild boar

Following the work to develop a wild boar TB model, in Chapter 3, that is representative of the situation in central Spain, we now wish to test management strategies to see their affect on the overall population density and disease prevalence in both the short and long-term. In this chapter we will test both vaccination and culling strategies as these are controls that are either culturally well-embedded or are being actively trialled in the region. We will examine their effects independently to understand the underlying mechanisms that drive the population response to each control separately.

4.1 Wild boar TB management: Vaccination

Vaccination acts to reduce the number of susceptible hosts in a population and therefore lower the potential for disease transmission which lessens the overall population level burden of disease-induced mortality [8, 10]. The work in this section was performed in collaboration with veterinarians based in central Spain and used to support and extend results from a trial of piglet vaccination against TB. The field trial and associated mathematical modelling was published in *Preventive Veterinary Medicine* as Díez-Delgado (2018) [48] on which I am a co-author and led the mathematical modelling and analysis that was included in the paper.

The field trial tested two orally delivered vaccines, heat-inactivated *Mycobacterium bovis* (IV) and BCG, in four different sites so that each vaccine type was trialled in both a managed and a more natural or unmanaged setting. Each trial ran for four years. As well as the four test locations, TB was monitored in fifteen separate unvaccinated control sites for one year immediately prior to the trial starting. Piglets aged 2-6 months were targeted as the recipients of vaccine baits, deployed using selective piglet feeders (Figure 4.1a) placed at key sites known to be regularly frequented by wild boar groups with piglets (Figure 4.1b).

(a) (b)

Figure 4.1: (a) a vaccination cage that only piglets can enter to eat the treated bait. (b) Andy White, Eleanor Tanner and Peter Lurz at a water hole beside which a vaccination cage was placed.

Results for the trials (Figure 4.2) showed that TB prevalence increased in unvaccinated sites, while a significant decline occurred in the managed IV site. Changes in TB prevalence recorded in the remaining sites were not significant leading to the conclusion that IV could become one of the tools to control TB, dependent on the context in which it is deployed. As these trials only ran for four years, empirical data could only show the short-term impact of vaccination. These field observations were complemented by mathematical modelling, representative of the field system, to examine the long-term impact on disease prevalence and population abundance.

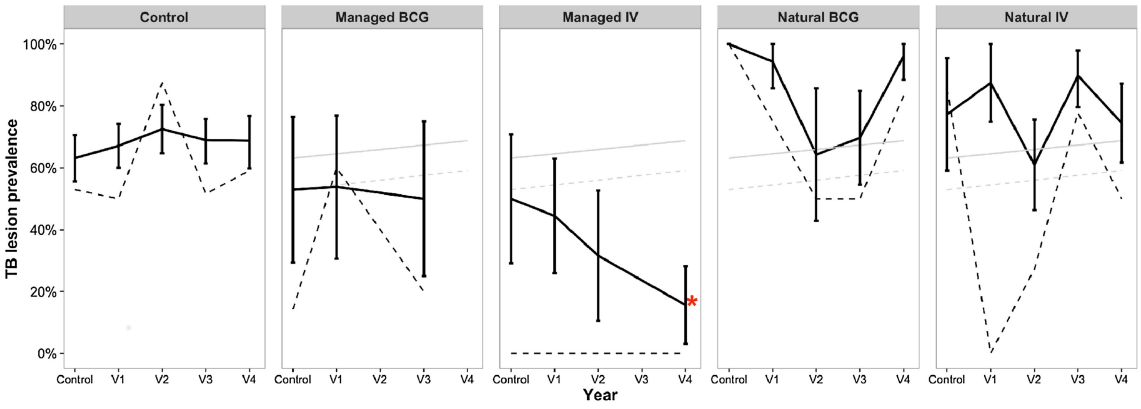

Figure 4.2: Reproduced from Díez-Delgado (2018) [48]: Temporal trend of tuberculosis (TB) lesion prevalence of piglets and total population by site. The dashed line represents piglet age class and the solid line the total population. Background information: the average trend for total population (solid line) and piglets (dashed line) found on the control site appears in light grey in the vaccine site figures. Error bars are bootstrap 95% confidence intervals (CI). Asterisk indicates a significant at $p < 0.01$ decline in prevalence as compared to pre-vaccination levels.

The reader is referred to Díez-Delgado (2018) [48] to discover in-depth biological details about the vaccine, its administration and more in-depth analysis of the empirical data. In this thesis we reproduce the modelling contributions from the paper. The model is an extended version of the PYAG model, Equations (3.3), that

includes a vaccinated class of piglets. The model results can increase understanding of the vaccination trial results and also offer insight into the long-term potential outcomes of the vaccination programme.

4.1.1 Piglet vaccination modelling

The model reflects a single geographical managed estate containing a homogeneously mixed population covering an area representative of a hunting estate. The model is deterministic and compartmental and considers the population density of wild boar separated into different age classes to capture distinct disease and reproductive characteristics for piglets (aged 0-1 year) P, yearlings (aged 1-2 years) Y, and adults (aged 2 years+) A. Further, the age-classes are split into susceptible, infected and generalised classes (subscripts S, I, G, respectively) to reflect the disease status of the population. The population dynamics of the wild boar TB system are represented by the following set of non-linear differential equations which is an extension of classical disease modelling frameworks (see Anderson & May 1979 [9]; Keeling & Rohani 2008 [84]) and a schematic representation is shown in Figure 4.3:

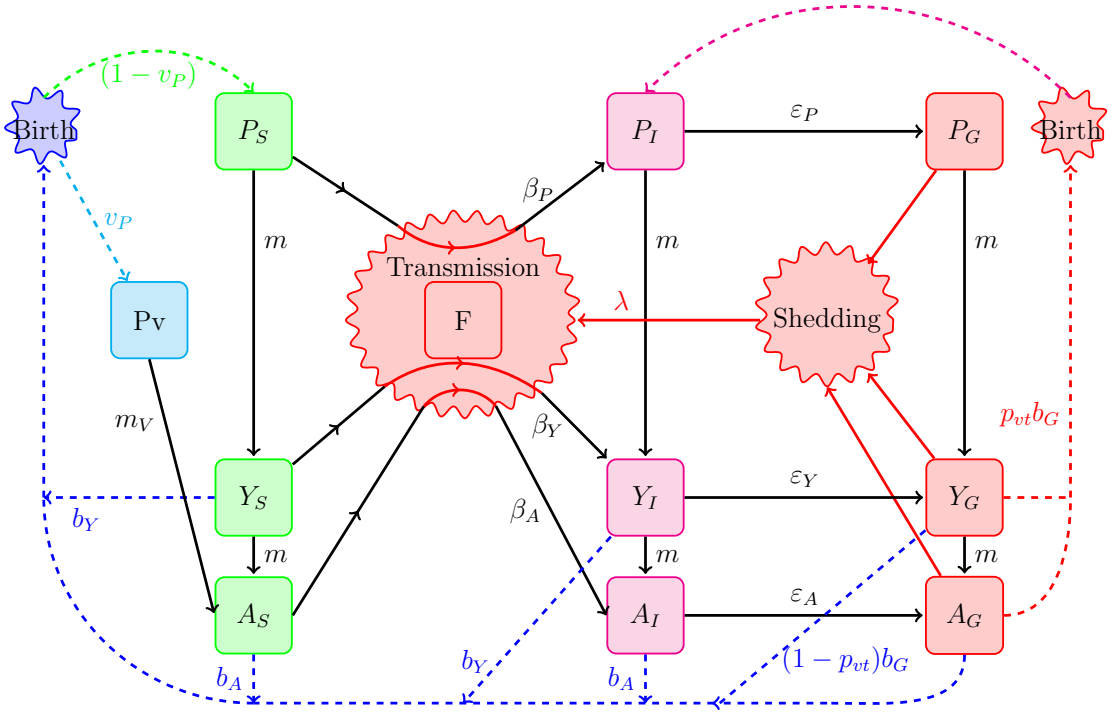

Figure 4.3: A schematic representation of the wild boar TB vaccination model represented by Equations (4.1). The model represents the density of piglets P, yearlings Y, and adults A with age-classes split into susceptible, infected and generalised classes (subscripts S, I, G, respectively). The class P_V represents vaccinated piglets and F represents the density of free-living TB particles. The parameters are detailed in Section 4.1.2.

$$\frac{\mathrm{d}P_S}{\mathrm{d}t} = (1-v_P)(b_Y(Y_S+Y_I)+b_A(A_S+A_I)+(1-p_{vt})b_G(Y_G+A_G))(1-qN) - mP_S - d_P P_S - \beta_P P_S F \tag{4.1a}$$

$$\frac{\mathrm{d}P_I}{\mathrm{d}t} = p_{vt} b_G(Y_G+A_G)(1-qN) + \beta_P P_S F - mP_I - d_P P_I - \varepsilon_P P_I \tag{4.1b}$$

$$\frac{\mathrm{d}P_G}{\mathrm{d}t} = \varepsilon_P P_I - mP_G - \alpha P_G - d_P P_G \tag{4.1c}$$

$$\frac{\mathrm{d}P_V}{\mathrm{d}t} = v_P(b_Y(Y_S+Y_I)+b_A(A_S+A_I)+(1-p_{vt})b_G(Y_G+A_G))(1-qN) - m_V P_V - d_P P_V \tag{4.1d}$$

$$\frac{\mathrm{d}Y_S}{\mathrm{d}t} = mP_S - mY_S - d_Y Y_S - \beta_Y Y_S F \tag{4.1e}$$

$$\frac{\mathrm{d}Y_I}{\mathrm{d}t} = \beta_Y Y_S F + mP_I - mY_I - d_Y Y_I - \varepsilon_Y Y_I \tag{4.1f}$$

$$\frac{\mathrm{d}Y_G}{\mathrm{d}t} = \varepsilon_Y Y_I + mP_G - mY_G - \alpha Y_G - d_Y Y_G \tag{4.1g}$$

$$\frac{\mathrm{d}A_S}{\mathrm{d}t} = mY_S + m_V P_V - d_A A_S - \beta_A A_S F \tag{4.1h}$$

$$\frac{\mathrm{d}A_I}{\mathrm{d}t} = \beta_A A_S F + mY_I - d_A A_I - \varepsilon_A A_I \tag{4.1i}$$

$$\frac{\mathrm{d}A_G}{\mathrm{d}t} = \varepsilon_A A_I + mY_G - \alpha A_G - d_A A_G \tag{4.1j}$$

$$\frac{\mathrm{d}B}{\mathrm{d}t} = \lambda(P_G+Y_G+A_G) - \mu F \tag{4.1k}$$

Here, N represents the total wild boar population. Susceptible and infected yearlings and adults give birth to susceptible piglets at rates b_Y and b_A respectively. Generalized yearlings and adults give birth to piglets at rate b_G with a proportion p_{vt} assumed infected (through pseudo-vertical transmission from parent to offspring) and the remainder, $(1-p_{vt})$, assumed susceptible. In this study we assume that $b_Y = b_A = b_G$. The total population is regulated through a crowding parameter, q, that acts to stabilise the total population to a carrying capacity, $N = K$, in the absence of disease. Maturity from piglets to yearlings and yearlings to adults occurs at rate m and piglets, yearlings and adults may die of natural causes at rates d_P , d_Y , d_A respectively. Here we assume $d_P = d_Y = d_A$.

The prime driver for infection in the wild boar TB system is through environmental contact with free-living TB particles, with density B. We assume that free-living particles are shed from generalised wild boar at rate λ and decay at rate μ. Susceptibles may become infected through contact with free-living TB particles with transmission coefficients β_P, β_Y and β_A and infecteds can progress to the

generalised class at rates ε_P, ε_Y and ε_A for the different age classes respectively. We assume that individuals in the generalised class suffer an additional disease induced mortality at rate α. We assume piglets and yearlings are more susceptible to TB infection than adults and so set $\beta_P = \beta_Y$, which we assume to be three times greater than transmission for adults, $\beta_A = 3\beta_Y$. Similarly we set the rate of progression to generalised infection for piglets and yearlings to be the same, $\varepsilon_P = \varepsilon_Y$, and three times the rate for adults, $\varepsilon_A = \frac{1}{3}\varepsilon_Y$. In this way we have set the model so that the yearling class is the same as the piglet class in terms of disease characteristics, but the yearling class is the same as the adult class in terms of reproductive processes.

We represent vaccination in the model by assuming a proportion, v_P, of susceptible births enter the immune piglet class P_V. The vaccinated piglets lose their immunity at rate m_V maturing into the susceptible adult class. This implicitly assumes that when immunity is lost individuals have reached maturity and are able to reproduce but also have a reduced susceptibility to infection. Note, our vaccination coefficient combines the effects of both coverage and efficacy by representing the proportion of successful inoculations. In the model the vaccination process is represented as a continuous process whereas in the field vaccination is applied to piglets aged 3-6 months. Therefore, there is a chance of infection prior to vaccination and we approximate this with the inclusion of pseudo-vertical transmission from generalised individuals.

4.1.2 Piglet vaccination model parameters

We set values to approximate the observed prevalence and to be representative of the wild boar TB system in central Spain. The parameters for the model are the same as the default parameter set in Section 3.1.1 with birth from generalised $b_G = b_A$ and the following vaccination and pseudo-vertical transmission related parameters:

v_P The proportion of susceptible births successfully vaccinated. We explore the full range of possible values of v_P in this study.

$m_V = 1$ The rate that vaccinated piglets mature into the susceptible adult class. This assumes that when immunity is lost individuals are able to reproduce but also have the same reduced susceptibility to infection as adults.

p_{vt} The proportion of generalised births that result in pseudo-vertical transmission. In this study we assume $p_{vt} = 0$ or 1. When $p_{vt} = 0$ piglets have a low chance of infection prior to vaccination and when $p_{vt} = 1$ a greater proportion of piglets are infected prior to vaccine uptake.

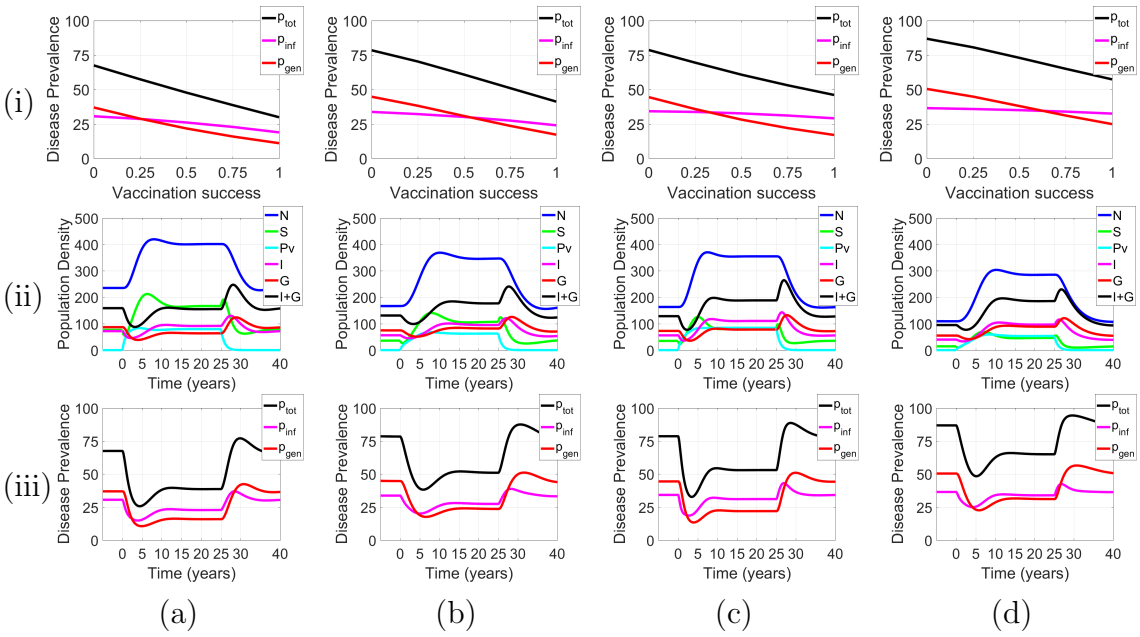

Figure 4.4: Using default parameter values described in Section 4.1.2 with (a) 0% pseudo-vertical transmission; (b) 100% pseudo-vertical transmission; (c) 0% pseudo-vertical transmission with disease transmission twice the default value; and (d) 100% pseudo-vertical transmission with disease transmission twice the default value. Row (i) shows disease prevalence against proportional vaccination success, v_p, with results determined at the stable endemic steady state when the specified level of vaccination is included; (ii) shows changes in density against time for the wild boar TB vaccination model for a vaccination level of 75%, ($v_p = 0.75$); and (iii) shows changes in disease prevalence against time for the wild boar TB vaccination model for a vaccination level of 75%, ($v_p = 0.75$). Here p_{tot}(black) is the proportion of the total population infected with TB; p_{inf}(magenta) the prevalence of infected but not generalised; p_{gen}(red) the prevalence of generalised; N(blue) is the total population density, I(magenta) the total density of infected but not generalised; G(red) the total density of generalised; S(green) is the total density of susceptibles; and P_V(cyan) is the total density of vaccinated piglets.

4.1.3 Piglet vaccination model results

We obtain numerical results for the model as the proportion of successfully vaccinated piglets v_P is varied. We use the default parameter set detailed in Section 4.1.2 under conditions of 0 or 100% pseudo-vertical transmission, $p_{vt} = 0$ or 1. We consider results for both the default transmission coefficient, which results in a medium disease prevalence at steady state (similar to Managed sites), and twice the default transmission value to reflect a greater risk of TB infection associated with increased mixing of groups of wild boar at water holes during periods of drought or at feeding stations when extra food is made available resulting in a higher disease prevalence at the endemic steady state (similar to Natural sites). We run the model until it has reached a stable endemic steady state then include vaccination for a period of 25 years to achieve a stable vaccinated steady state. We examine how vaccination affects the disease prevalence statistics p_{tot}, p_{inf} and p_{gen}

and the epidemiological dynamics.

We examine results for the model described by Equations (4.1) in different combinations of disease transmissions rates and pseudo-vertical transmission. Figure 4.4 shows that the impact of vaccination on reducing TB prevalence is reduced when the transmission rate, initial prevalence and level of pseudo-vertical transmission is increased. It also indicates that there is an initial reduction in the level of infected and generalised individuals, which lowers disease transmission and consequently leads to a decrease in prevalence. The impact of vaccination is largest when there is a reduced chance of piglet infection prior to vaccination and a lower initial prevalence. In the set-up that is most similar to Managed site IV the model predicts a 35% decrease in TB prevalence after 4 years (Figure 4.4a(iii)). This is comparable with the 34% decrease reported in the field study. A consequence of the vaccine induced reduction in prevalence is a reduction in population mortality due to a decrease in disease-induced death. This drives an increase in total population density which in the long-term allows the density of infected and generalised individuals to return to their pre-vaccination levels. Therefore, the long-term reduction in disease prevalence shown in Figure 4.4iii is a consequence of an increase in total population density rather than a decrease in the density of infected and generalised individuals. These model results highlight how observations from the early years of a vaccination programme may not provide a clear picture of the effectiveness of a long-term vaccination strategy, since the benefits of vaccination on reducing the level of infection in the early years are countered by the subsequent increase in total population density. The model results also indicate that when the vaccination programme is stopped there is an initial increase in disease prevalence and density of infected and generalised wild boar before levels return to those prior to vaccination. This is a consequence of the elevated population density resulting from vaccination and of the temporary nature of vaccine-derived immunity.

In the four scenarios considered in this study (Figure 4.4 a-d) the proportion of piglets at the end of the vaccination period is (a) 26%, (b) 31%, (c) 33% and (d) 34% respectively. The proportion of individuals that are piglets is substantial and therefore vaccination of piglets against TB is an effective method of TB control. We note that as transmission opportunities increase, the burden of disease induced mortality reduces the adult population and therefore the proportion of individuals that are piglets increases.

4.2 Wild boar TB management: Hunting

On managed hunting estates in central Spain harvesting takes place once a year during the autumn over a short period of a few weeks. Young wild boar are not targeted during these hunts as the prime hunting prize are mature individuals

with well developed tusks. We represent hunting in the model as an instantaneous reduction in the adult and yearling (susceptible, infected and generalised) population of a given percentage. Piglets are left unaffected. We note that alongside examining the effect of hunting on our model we also need to verify that our model continues to give results that are consistent with empirical data, given that data gained from the field includes the effects of annual harvesting.

We run the model (Equations (4.1)) using the default parameter set from Section 3.1.1 with birth from generalised ($b_G = b_A$) and no vaccination ($v_P = 0$). Figure 4.5 shows results for hunting bags of 10%, 25% and 50% of adult and yearling wild boar, run over a period of 45 years. Initally we assume no hunting for 5 years and so the population is stable at the endemic steady state. We then assume hunting for 30 years followed by a period of no hunting for 10 years. At the start of the culling

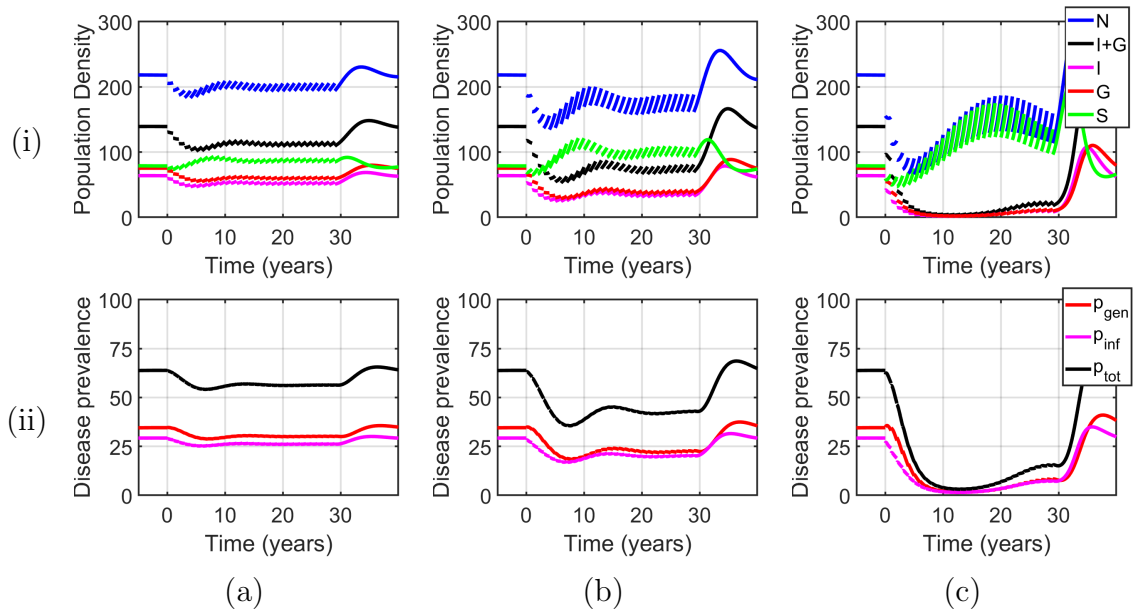

Figure 4.5: Changes in (i) population density and (ii) disease prevalence when (a) 10%, (b) 25%, and (c) 50% of adults and yearlings are removed instantaneously from the population by hunting every year for 30 years for the wild boar TB model (Equations (4.1)) with default parameters $b_G = b_A$ and no vaccination $v_P = 0$.

regime there is a sharp decline in both population and disease prevalence, however both the prevalence and population recover until for both 10% and 25% culls a new (periodic) endemic solution is reached. For a culling level of 50% this recovery takes longer so the system does not reach a 'stable' periodic level within the 30 years of the culling regime. When the annual culls stop both population and disease prevalence rise above the initial endemic steady state before stabilising to their initial levels. Figure 4.6 plots the resultant population and prevalence after 30 years of annual cull followed by population growth. In this case we show results for different levels of pseudo-vertical transmission, p_{vt}=0, 0.25 and 0.5 from which we can see that this extra level of transmission does not have a significant influence on the resultant

population and prevalence. We can immediately see that an increase in hunting bag leads to a decrease in disease prevalence until a point when the culling decreases the population below the threshold for which the disease can persist, such that for high levels of hunting the disease is eradicated. However, as well as examining the disease prevalence we must also examine the population density which shows a slightly different pattern in response to hunting. For lower levels of hunting the population does not decrease as quickly as the disease prevalence and remains reasonably high for hunting levels up to 50%. When hunting levels increase above 50%, it decreases the population below a level that can support the disease, above 75% the population is also eradicated.

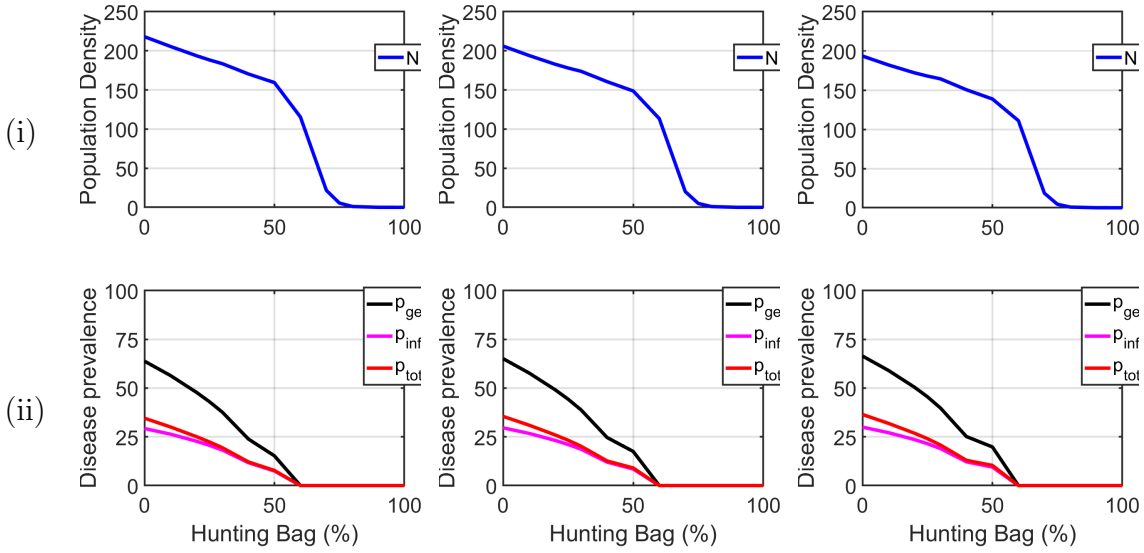

(a) $p_{vt=0}$ (b) $p_{vt=0.25}$ (c) $p_{vt=0.5}$

Figure 4.6: The wild boar TB model response to culling against different levels of hunting bag (annual cull). (i) shows resultant population density and (b) shows resultant disease prevalence p_{tot}, p_{gen} and p_{inf} at the end of 30 years annual hunt and regrowth plotted against percentage level of hunting. (a) shows results for $p_{vt} = 0$; (b) shows results for $p_{vt} = 0.25$; (c) shows results for $p_{vt=0.5}$. Model parameters set to default values and $b_G = b_A$.

In summary, including hunting in our model reduces the total number of infected and generalised wild boar but this does not cause a similar reduction in the total population. Since culling reduces the level of generalised individuals in the population it reduces the level of free living pathogen and therefore the potential for disease transmission. Culling is thereby inducing a compensatory response at a total population level whereby some of the death that occurs due to culling is compensated by less death as a result of the infection. We examine this phenomena in general in the next chapter.

4.3 Discussion

In this chapter we examined the effect of vaccination and culling on the population and disease dynamics of wild boar. A key finding is that it is important to examine both the prevalence and population density to understand the potential risk of spillover infection from a reservoir host. This is because results that focus on prevalence alone may conclude that disease management has been successful in terms of a prevalence reduction. However, this may result from an increase in total density and relatively stable levels of infection which in wildlife disease reservoirs would indicate an unchanged risk of spillover. In fact under several scenario of vaccination (Figure 4.4) while prevalence did decrease the density of infected individuals increased following vaccination in response to a large increase in total density. Our findings also indicated that there may be differences between short-term and long-term dynamics. Here the short-term effect is more marked than the long-term impact of intervention. Moreover, if disease control is halted the systems can initially exhibit enhanced levels of prevalence and infected density before settling to pre control levels. Therefore in many systems disease control will need to be a long-term commitment.

The model results show that vaccination can cause the wild boar population to become healthier due to a decrease in disease prevalence. This is driven by a rise in the total population rather than a decrease in the number of infected individuals in the population. This echoes earlier work by Smith & Cheeseman (2002) [128] using a model with density dependent transmission of TB in badgers who noted that as vaccinated animals can still reproduce then the total number of susceptibles in a population under vaccination control will be greater than without such control, and therefore harder to eradicate the disease [8]. We provide further insight showing that as the total number of generalised is not greatly reduced, the level of pathogen excreted into the environment is not reduced and therefore the force of infection is not reduced. If the force of infection remains the same this means that a susceptible wild boar has the same risk of contracting the disease both before and during a vaccination control programme. Also, as the level of excreted pathogen in the environment remains at a similar high level, the risk of cross-infection to other co-habiting susceptible species is not reduced either. It is also notable that none of the models we used to represent the population and disease dynamics of the wild boar TB system in central Spain showed the disease could be eradicated. Our results showed that higher levels of vaccination success produced a greater reduction in the prevalence of generalised in the population. Separate work by Anderson *et al.* (2013) [6] using a stochastic rule-based model showed that over a 25 year period with sufficient levels of piglet vaccination it was possible for the disease to be eradicated. In comparison with our model, results were reported just in terms of disease prevalence so changes to the total population were unavailable.

A major difference between our model results and those of Anderson *et al.* (2013) [6] is that the latter also includes an annual cull of 30%. We have deliberately isolated the vaccination results from culling, however this is an indicator that further research into the effects of combined management controls may be beneficial to further understanding.

Our results for hunting support the observations in the field that despite high annual culling levels of 20-30% the wild boar population density in central Spain has remained buoyant over a long period of time, and endemic TB persists. Culling can eradicate the disease, but a high level of culling is required. Once the disease is eradicated the population density of wild boar reduces rapidly with increased levels of culling. In comparison to vaccination culling does not reduce disease prevalence as dramatically since under vaccination the population density can increase. As Anderson *et al.* (1981) notes, the goal of culling a population to eradicate disease is to reduce the population below a level at which the disease will persist. However, as culling reduces the level of infection it means that the population suffers less disease mortality and so can support a higher than expected population. This may make it hard to eradicate a virulent disease. We will explore this aspect in general in the next chapter.

Chapter 5

Population compensatory growth as a result of culling

Following the initial wild boar TB vaccination and hunting modelling, it became apparent that the wild boar TB system was potentially exhibiting behaviour that could be abstracted into a more general result and merited further investigation beyond the wild boar TB model. The content in this chapter is the outcome of this research. This work has been accepted for publication in *The American Naturalist*: 'The critical role of infectious disease in compensatory population growth in response to culling' by Eleanor Tanner, Andy White, Peter Lurz, Christian Gortázar, Iratxe Díez-Delgado and Mike Boots. I played the lead role in developing the work and writing the article and undertook the mathematical modelling and analysis. The paper is reproduced verbatim in this chapter with the supplementary information from the published article reproduced in Appendices 5A.1-5A.7.

5.1 Abstract

Despite the ubiquity of disease in nature, the role that disease dynamics play in the compensatory growth response to harvesting has been ignored. We use a mathematical approach to show that harvesting can lead to compensatory growth due to a release from disease-induced mortality. Our findings imply that culling in systems that harbour virulent parasites can reduce disease prevalence and increase population density. Our models predict that this compensation occurs for a broad range of infectious disease characteristics unless disease induces long-lasting immunity in hosts. Our key insight is that a population can be regulated at a similar density by disease or at reduced prevalence by a combination of culling and disease. We illustrate our predictions with a system-specific model representing wild boar tuberculosis infection, parameterised for central Spain, and find significant compensation to culling. Given that few wildlife diseases are likely to induce long-lived immunity, populations with virulent diseases may often be resilient to

harvesting.

5.2 Introduction

It is well known that harvesting may be compensated by an increased growth rate at lower density [1]. This phenomenon of compensatory growth in response to culling was first modelled by Ricker (1954) [121] who showed that for moderate harvesting levels the population can stabilise to a level that exceeds the density in the absence of harvesting. Despite the ubiquity of infectious disease in nature, little work has considered the impact of harvesting and culling in populations with virulent infectious disease and the compensatory potential of changes to disease dynamics. Since culling affects the disease dynamics there is considerable potential to generate feedbacks on host population dynamics. Moreover, as culling is also used as a management strategy to control emergent wildlife diseases, it is vital to understand the interplay between culling, disease and population dynamics [16, 145]. In this study we develop mathematical models to examine the impact of culling in systems that support endemic diseases and for the first time detail how culling can lead to compensatory growth due to a reduction in disease-induced mortality.

It is difficult to gather field data to test theories about the population-level implications of complex disease dynamics [1, 97]. Mathematical models are therefore important tools for explaining the impact of culling and harvesting in systems with endemic parasites. There is an extensive modelling literature focussed on the control of disease through culling, for example chronic wasting disease in deer in North America [141, 113, 130, 136]; acutely virulent classical swine fever in wild boar [35, 25, 40]; and lethal facial tumour disease in Tasmanian devils [18]. While these studies recognise that culling in systems with endemic disease can induce compensation through demographic processes, they have not examined how culling may lead to compensatory effects that arise directly from changes in disease dynamics.

The limited work that has examined the effect of culling on disease dynamics has shown that culling may increase prevalence due to a decrease in long-lasting immunity or vaccine coverage [35, 25, 113], with Potapov *et al.* (2012) [113] showing that prevalence can decrease in a system with no immunity. However, these studies have not examined compensatory effects due to disease and have only considered a limited range of disease characteristics. Here, we model in general the impacts of culling and harvesting in systems that support a wide range of endemic diseases. A novel aspect of our study is that we isolate the compensatory effects following culling due to changes in the disease dynamics resulting from a population level release from disease-induced mortality. This facet is vital if we are to understand the response of harvesting in managed and natural systems that harbour virulent parasites. We show that significant host compensation occurs in response to culling for infections

that do not cause long-lasting immunity and therefore such host populations can be more sustainable. However, when there is long-lasting immunity the disease can decrease the population's resilience to harvesting and increase its extinction risk when culling is used to manage a disease. We develop a system-specific model of *Sus scrofa* (wild boar) tuberculosis interactions that illustrates our predictions in a specific disease context. Our work highlights the importance of understanding the nature of immunity to infectious disease for sustainable harvesting of populations and the management of disease through culling.

5.3 Methods

We examine a classical compartmental SIRS model of disease [9, 84] that considers a total population (N) split into separate classes representing different disease stages: the class of susceptibles (S), of infecteds (I) and of recovereds/immunes (R), such that the total population density is $N = S + I + R$. In this model all classes reproduce and all newborns are susceptible. The maximum per capita birth rate b decreases with increasing density through parameter q and all population classes incur natural death at rate d. A susceptible individual becomes infected with transmission rate function $\theta(I, N)$ which can represent density-dependent (DD) or frequency-dependent (FD) disease transmission (Equations (5.2a) and (5.2b) respectively). Infected individuals incur additional disease-induced mortality (virulence) at rate α and can recover from infection to become immune from the disease at rate γ. Immunity can be lost causing recovereds to become susceptible again at rate η. This model is represented with the following system of ordinary differential equations:

$$\frac{\mathrm{d}S}{\mathrm{d}t} = bN(1 - qN) - dS - \theta(I, N)S + \eta R \tag{5.1a}$$

$$\frac{\mathrm{d}I}{\mathrm{d}t} = \theta(I, N)S - dI - \alpha I - \gamma I \tag{5.1b}$$

$$\frac{\mathrm{d}R}{\mathrm{d}t} = \gamma I - dR - \eta R. \tag{5.1c}$$

A strength of our model is that it can be adapted to represent a range of classical infection frameworks: SI by setting $\gamma = 0$; SIR by setting $\gamma > 0$ and $\eta = 0$; and SIRS with both $\gamma > 0$ and $\eta > 0$. The system is normalised to a common endemic steady state $N = N_e$ ($S = S_e$, $I = I_e$, $R = R_e$ and we choose $N_e = 1$ without loss of generality) when the initial prevalence prior to culling is $p_i \left(= \frac{I_e}{N_e}\right)$, see Appendix 5A.1 for further details. The endemic transmission functions are defined as follows:

$$\text{DD transmission}: \quad \theta(I,N) = \frac{(d+\alpha+\gamma)}{N_e\left(1-p_i\left(\frac{\gamma}{d+\eta}+1\right)\right)}I \tag{5.2a}$$

$$\text{FD transmission}: \quad \theta(I,N) = \frac{(d+\alpha+\gamma)}{\left(1-p_i\left(\frac{\gamma}{d+\eta}+1\right)\right)}\frac{I}{N}. \tag{5.2b}$$

Under this set-up we can compare results for systems that have the same initial density and initial level of prevalence prior to culling.

We examine the dynamics exhibited by the model (Equations (5.1)) when the population is subject to indiscriminate culling (i.e. an equal proportion is removed from each class in the model). We implement the culling regime as a discrete event that removes a fixed percentage of the population with continuous population regrowth between each cull event. Culling occurs at unit time intervals leading to $\frac{1}{d}$ culls during the average lifetime of an individual in the absence of the disease. We run the culling regime for 30 consecutive periods of instantaneous cull followed by regrowth and examine the effect on the disease prevalence and the population density both during and at the end of this culling regime. In particular, we define the 'resultant density' as the population density at the end of the 30 consecutive cull and subsequent regrowth events. Note, our results are qualitatively similar if we assume culling occurs continuously rather than as a discrete event (see below and Appendix 5A.2). Our results are produced numerically using MATLAB ODE solvers.

In addition to assessing the impact of culling on the dynamics in the full model (Equations (5.1)) we also develop a model whose dynamics can respond to culling through demographic effects only:

$$\frac{\mathrm{d}N}{\mathrm{d}t} = bN(1-qN) - dN - \alpha p_i N. \tag{5.3}$$

This 'demographic effects only model' has the equivalent level of mortality to the full model (Equations (5.1)) at the endemic steady state but it cannot respond to changes in disease prevalence and therefore allows us to isolate the importance of changes to the disease dynamics as a result of culling. The parameters b, d, q and α are the same as in the full model (Equations (5.1)), p_i is the initial prevalence in the full model (which is constant in this model) and therefore prior to culling both models have the same steady state density $N = N_e$. Importantly, the density-dependent per capita birth rate, $b(1-qN)$, has an identical response in both models and therefore any changes to the density in response to culling lead to the same change in the per capita birth rate.

We now note that the dynamics of the total density in the full model (found by

summing Equations (5.1) can be written as:

$$\frac{\mathrm{d}N}{\mathrm{d}t} = bN(1-qN) - dN - \alpha\frac{I}{N}N. \tag{5.4}$$

Prior to culling the level of mortality is the same, since $p_i = \frac{Ie}{Ne}$. Critically, however, culling can lead to a change in the disease dynamics and therefore a change in disease prevalence $\frac{I}{N}$. This can lead to a change in the rate of mortality in the full model but not in the demographic effects model since p_i does not change. A comparison of the full model and the demographic effects only model therefore allows us to determine the importance of changes due to the disease dynamics as a result of culling.

We also develop a 'disease effects only' model which has the same disease dynamics as the full model (Equations (5.1)) but has a fixed per capita birth rate $b(1-qN_e)$ and therefore dynamic population density does not affect the rate of reproduction. This model is the same as Equations (5.1) except for Equation (5.1a) which is modified as follows:

$$\frac{\mathrm{d}S}{\mathrm{d}t} = bN(1-qN_e) - dS - \theta(I,N)S + \eta R \tag{5.5}$$

For DD transmission the disease effects only model has the same endemic steady state, N_e, as the full model and therefore we can compare results between the disease effects only model and the full model to understand the contribution of demographic effects on compensatory growth. However, for FD transmission, the disease effects only model does not have a comparable non-zero endemic steady state so this comparison is not valid. (In a similar manner a model that cannot respond through disease or demographic effects cannot be compared to the full model, as culling would lead to population extinction.)

Analysing the results for these models allows us to compare the compensatory growth following culling that is due to: both demographic and disease effects (represented by the full model, Equations (5.1)); demographic effects only (represented by Equation (5.3)); and disease effects only (represented by Equation (5.5)). The difference between the population densities in response to culling in these models allows us to partition compensatory growth due to disease dynamics only, namely a population level release from disease-induced mortality, and compensatory growth due to demographic effects. In this study we wish to understand the importance of compensatory growth due to a release from disease-induced mortality in response to culling for a range of key infection representations.

We examine the behaviour of the model, Equations (5.1), with DD and FD transmission for a SI framework (no recovery from infection) and for a SIR framework which represents life-long immunity to infection. Later we consider a SIRS framework in which immunity can wane over time; targeted culling on infected individuals only; and density-dependent mortality in addition to density-dependent

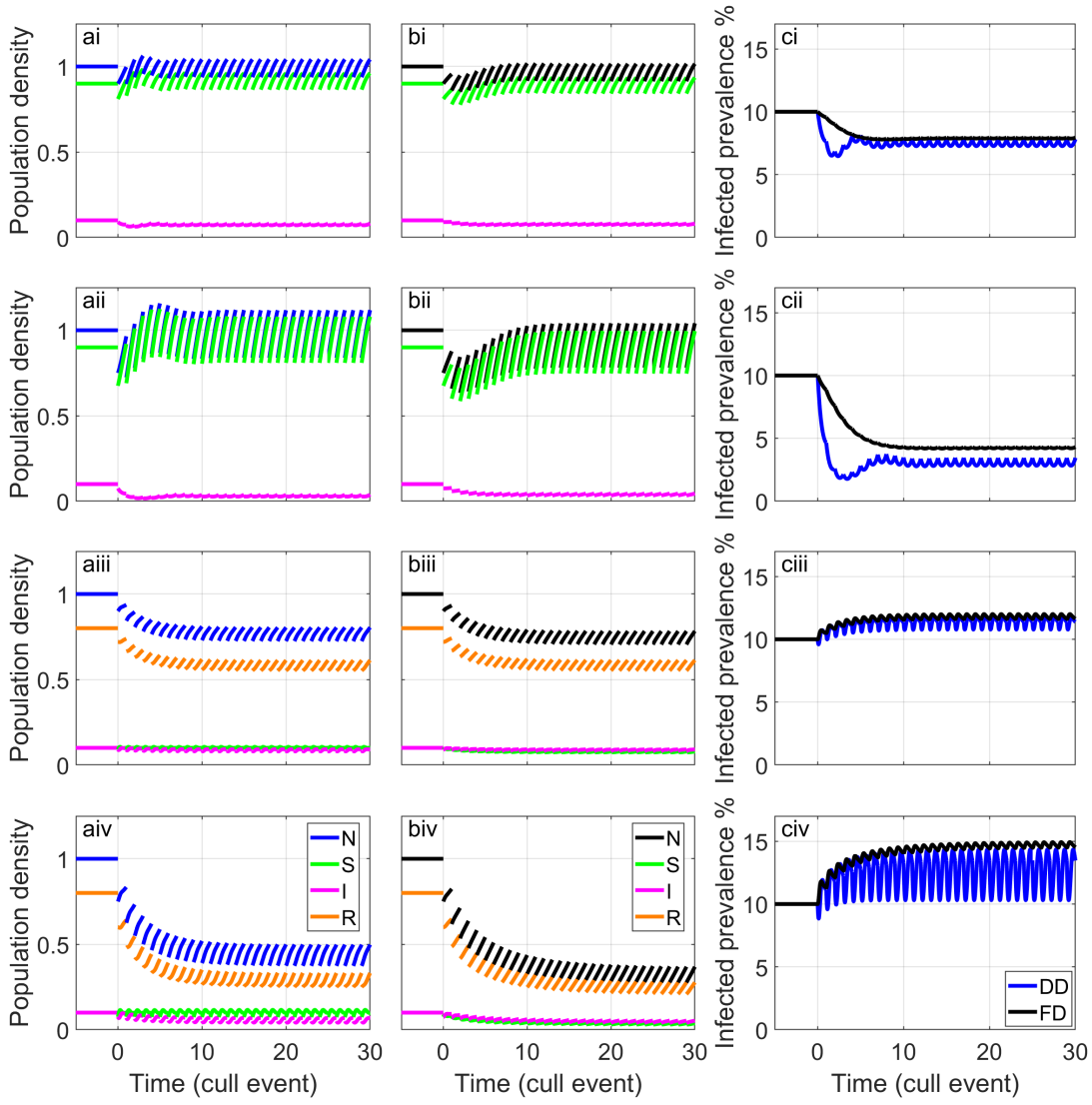

Figure 5.1: The population density and infected prevalence ($\frac{I}{N}$) response to culling for Equations (5.1). (i),(ii) show results for the SI model, (iii),(iv) show results for the SIR model. Results are shown for a 10% cull (i,iii) and a 25% cull (ii,iv). (a) shows DD transmission and (b) FD transmission. (a) and (b) show the total density of susceptibles (green); the total density of infected (magenta); the total density of recovered/immune (orange); and the total populations density (blue for DD (a), black for FD (b)). (c) shows the disease prevalence for DD (blue) and FD (black) transmission. Results are shown for a virulent infection, $\alpha = 4$, and with an initial endemic disease prevalence of $p_i = 10\%$. Other parameters are: $b = 1.6$, $d = 0.5$; for (i) and (ii) $\gamma = 0$; and (iii),(iv) $\gamma = 4$.

reproduction. In addition to assessing the impact of culling in systems with classical modes of directly transmitted infection (DD and FD) we have also undertaken our analysis for systems with environmental, free-living (FL) transmission [7]. The results for FL transmission are qualitatively similar to those with DD transmission and general results are detailed in Appendix 5A.3. To emphasize the breadth of our findings the results for systems with FL transmission are highlighted in the case study on the impact of culling on wild boar tuberculosis interactions.

5.4 Results

5.4.1 The effects of culling in populations with virulent infection and no recovery

Figure 5.1a(i-ii) shows that culling does not greatly decrease population density in systems with DD transmission in the absence of recovery. Indeed, after the initial culling events, the resultant density immediately prior to the next cull reaches a level exceeding the initial density $N_e = 1$. Moreover, the density can reach higher levels under a 25% cull than under a 10% cull. Here, culling leads to compensatory (even over-compensatory) growth as a result of changes to the disease dynamics. In particular, there is a reduction in the infected density and increase in susceptible density (Figure 5.1a(i-ii)) and therefore, as the total population density is not diminished, there is a reduction in disease prevalence (Figure 5.1c(i-ii)) which reduces the level of disease-induced mortality suffered by the population. The reduction in prevalence is greater under the higher level of culling and so the compensatory growth due to infection processes is greater under higher culling. Under FD transmission the total population size increases less in response to culling (Figure 5.1b(i-ii)) but again there is a reduction in the infected density and increase in susceptible density that mitigates some of the mortality due to culling. The reduction in disease prevalence due to culling is smaller under FD compared to DD transmission (Figure 5.1c(i-ii)), which may explain the lower compensatory response.

To understand these findings more clearly we examine the results for a 25% cull in population phase space (Figure 5.2i) and in terms of changes in the force of infection (Figure 5.2ii). Under DD transmission the population response following the initial culls is an increase in susceptibles but a decrease in infectives (Figure 5.2a(i)), since culling reduces the force of infection (Figure 5.2a(ii)). Eventually, the density prior to the next cull stabilises, with an increased density of susceptibles, a decreased level of infecteds and a decreased force of infection. In this way the increased mortality due to culling is compensated by population level decreases in mortality due to the disease. Under FD transmission the population response following initial culls is an increase in susceptible and infected density (Figure 5.2b(i)). In particular, culling does not reduce the force of infection under FD transmission (Figure 5.2b(ii)) as much, particularly in the initial culling events. The resultant population therefore supports a higher level of infecteds compared to DD transmission, and therefore while the compensatory effects due to reduced population level disease-induced mortality are still significant they are smaller under FD transmission.

The compensatory population growth in response to culling can result from two mechanisms: a reduction in the impact of density dependence on reproduction; and a population level reduction in disease-induced mortality due to changes in the disease dynamics. Both these mechanisms could occur for the population level

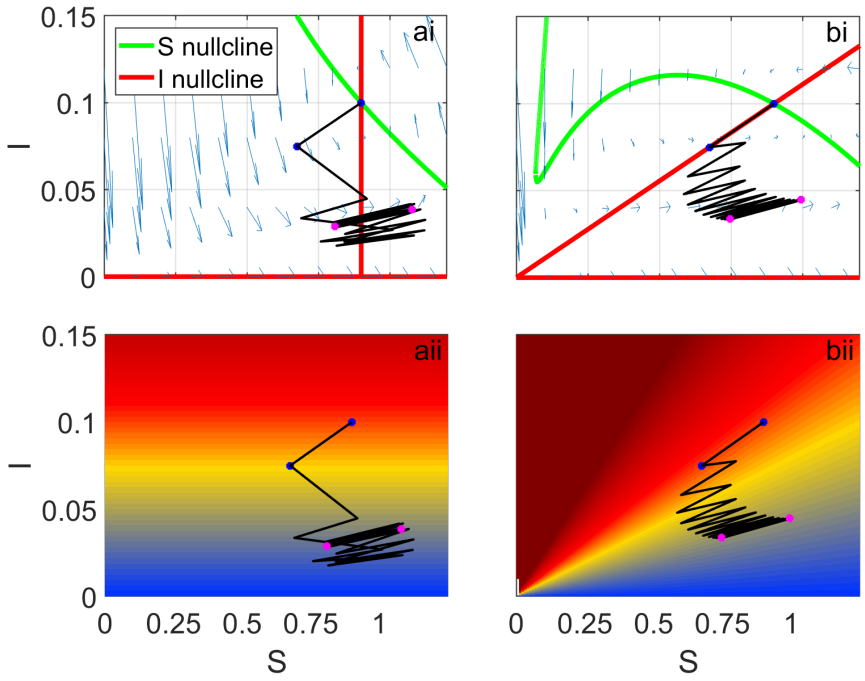

Figure 5.2: The population density response to repeated culling of 25% of the population for the SI model for (a) DD and (b) FD transmission. The figures show a population trajectory (solid black line) over the 30 cull events, with values immediately prior to and after the first cull highlighted with blue circles and before and after the 30th cull with magenta circles. In (i) the population trajectory is shown in phase space with the red lines showing the boundary between regions where I is decreasing and increasing; and the green lines show the boundary where S is decreasing and increasing (as indicated by the flux arrows in the figures). In (ii) the population trajectory is superimposed over the force of infection $\theta(I, N)$ with the colour changing from dark blue to dark red as the force of infection increases. Results are shown for a virulent infection, $\alpha = 4$, and with an initial endemic disease prevalence of $p_i = 10\%$. Parameters are as in Figures 5.1a(ii) and 5.1b(ii) for DD and FD transmission respectively.

response to culling for our full model (Equations (5.1)). In Figures 5.3a(i-ii) & 5.3b(i-ii) we compare the results from the full model with the demographic effects only model (Equation (5.3)) and in Figure 5.3b(i) we compare the results from the full model with the disease effects only model (Equation (5.5)), noting that this latter comparison is only valid for DD transmission. The difference between the full model and disease effects only model represents the compensation that is solely due to demographic effects and here this compensation is minimal (Figure 5.3b(i)). The difference between the full model and the demographic effects only model represents the compensation due to the population level reduction in disease-induced mortality and accounts for most of the compensatory growth (Figures 5.3b(i) & 5.3b(ii)). A key result is that compensation due to disease effects in response to culling can be substantial under both DD and FD transmission.

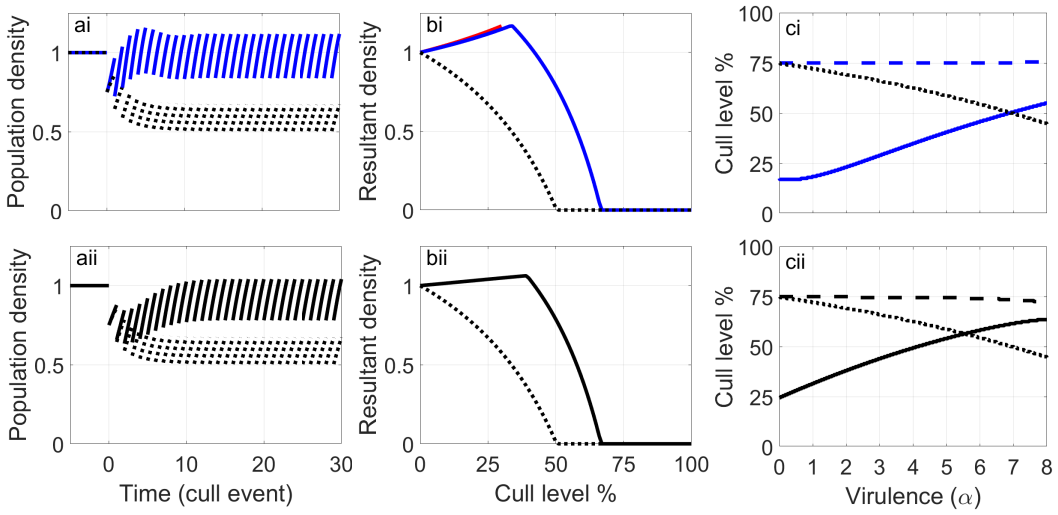

Figure 5.3: The population density compensatory response to culling for the SI model. (a) the population density response to repeated culling of 25% of the population for the full model, Equations (5.1), under SI ($\gamma = 0$) dynamics for (i) DD transmission (blue) and (ii) FD transmission (black) and for the demographic effects only model (dotted). (b) the resultant population density at the end of sequential cull and subsequent regrowth periods for different levels of culling for the full model with (i) DD transmission (blue) and (ii) FD transmission (black), the demographic effects only model (dotted) and in b(i) the disease effects only model (red). Note this (red) line is only valid for culling levels less than 30% with higher culling levels leading to disease and population extinction. The difference between the solid blue and the dotted line (b(i)) and the difference between the solid black line and the dotted line (b(ii)) represent the amount of compensation due to the disease effects and in (b(i)) the difference between the red line and the blue line represents the compensation due to demographic effects. (c) plot of virulence against the level of culling required to eradicate the infection (solid line) and the population (dashed line) as well as the level of culling to eradicate the population in the demographic effects only model (dotted line) for (i) DD transmission and (ii) FD transmission. Results are shown for a virulent infection, $\alpha = 4$, (except in (c) where α varies) and with an initial endemic disease prevalence of $p_i = 10\%$. Other parameters are as in Figure 5.1.

5.4.2 The effects of culling in populations with virulent infection and recovery to immunity

Figures 5.1a(iii-iv) & 5.1b(iii-iv) show that compensatory growth due to a population level release from disease-induced mortality is not evident in systems with life-long immunity following infection. Here, culling leads to a significant reduction in the population density and an increase in infected prevalence (Figure 5.1c(iii-iv)). This effect is most pronounced under FD transmission as here the force of infection remains high when the population abundance is reduced. In systems with life-long immunity the population composition in the absence of culling includes a relatively large proportion of recovered/immune individuals. Culling removes all classes

equally, but it takes time for individuals to move through the infection stages to reach the recovered class and therefore culling leads to a larger relative reduction to the recovered class density and so the proportion of the population that suffers virulence (I/N) increases. Figures 5.4a(i) & 5.4(ii) show that culling leads to a greater reduction in population density in the full SIR model than in the demographic effects only model. Also, for DD transmission (Figure 5.4b(i)) culling decreases population density less in the full SIR model than in the disease effects only model. Therefore culled populations that support virulent infections with recovery to life-long immunity do not benefit from reduced disease-induced mortality but, as shown here for DD transmission, do exhibit compensation due to demographic effects which mitigate some of the mortality due to culling. A key point is that when there is life-long immunity there can be a significant reduction in the population density and therefore less resilience to harvesting as the population may be reduced to such a low density that it is more susceptible to stochastic processes that may cause population extinction.

5.4.3 The impact of culling on population management

Culling is often used as a strategy for population eradication, for instance to remove pest or invasive species. We can use our model to investigate how the presence of virulent infection changes the level of culling required to eradicate a population. Figures 5.3b(i)&(ii) show that in systems without life-long immunity the compensatory effects due to changes in the disease dynamics mean that an increased level of culling is required to eradicate the population. In systems that have life-long immunity (Figures 5.4b(i) & (ii)) the presence of virulent disease makes the population harder to eradicate under DD transmission but easier to eradicate under FD transmission. Here, under FD transmission, culling leads to an increase in infection prevalence and so increases the population disease-induced mortality in addition to culling mortality. In contrast, under DD transmission, high levels of culling reduce the proportion of recovered individuals to such an extent that the system acts like one in which life-long immunity is absent. Our work therefore indicates that programmes to eradicate invasive species will be hindered if the invasive species harbours a virulent non-immunising parasite or immunising parasite under DD transmission but facilitated for strongly immunising virulent parasites with FD transmission. It is critical therefore to understand the nature of transmission and immunity to the key virulent infectious diseases of a target species prior to the use of culling for population elimination.

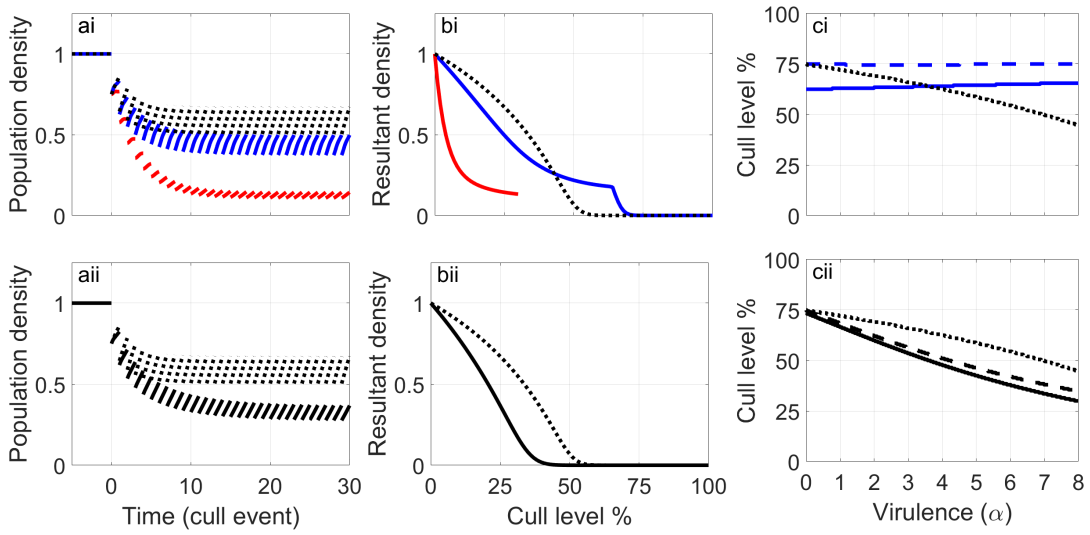

Figure 5.4: The population density compensatory response to culling for the SIR model. (a) the population density response to repeated culling of 25% of the population for the full model, Equations (5.1), under SIR ($\gamma = 4$) dynamics for (i) DD transmission (blue) and (ii) FD transmission (black), for the demographic effects only model (dotted) and for the disease effects only model (red). Here the presence of the disease leads to a lower population in response to culling. (b) the resultant population density at the end of sequential cull and subsequent regrowth periods for different levels of culling the full model with (i) DD transmission (blue) and (ii) FD transmission (black), the demographic effects only model (dotted) and the disease effects only model (red). Note this (red) line is only valid for culling levels less than 30% with higher culling levels leading to disease and population extinction. The difference between the solid blue and the dotted line (b(i)) and the difference between the solid black line and the dotted line (b(ii)) represent the amount of compensation due to the disease effects and in (b(i)) the difference between the red line and the blue line represents the compensation due to demographic effects. (c) plot of virulence against the level of culling required to eradicate the infection (solid line) and the population (dashed line) as well as the level of culling to eradicate the population in the demographic effects only model (dotted line) for (i) DD transmission and (ii) FD transmission. Results are shown for a virulent infection, $\alpha = 4$, (except in (c) where α varies) and with an initial endemic disease prevalence of $p_i = 10\%$. Other parameters are as in Figure 5.1.

5.4.4 The impact of culling on disease management

Culling is also used as a strategy to manage or eradicate a disease. Here the goal may be to eliminate the disease while maintaining viable or maximum levels of host density [78, 43, 18, 23], or the impact on the host density is of less concern [108]. Our study indicates that the level of culling required to eradicate the disease increases as the virulence increases for DD transmission under both the SI and SIR model frameworks (Figures 5.3c(i) & 5.4c(i)). Under FD transmission the level of culling required to eradicate the disease increases in the absence of immunity and decreases in the presence of life-long immunity (Figures 5.3c(ii) & 5.4c(ii)). A key result is that the interval between the level of culling required for disease eradication

and population extinction is narrow at high virulence in the absence of immunity and narrow at all levels of virulence with immunity. These results highlight the importance of understanding the infection status of a population before culling for disease management as the level of culling required for disease eradication may put the population at risk of extinction.

5.4.5 Generality of model findings

Our analysis has shown how culling can lead to positive compensatory growth due to a population reduction in disease-induced mortality in systems without immunity and can lead to larger decreases in population density in systems with life-long immunity. It is therefore important to ascertain the threshold in the level of immunity that partitions the positive and negative impacts on growth in response to culling. To do this we examine how the long-term density responds to culling in an SIRS model in which infection leads to immunity but where immunity can wane. For both DD and FD transmission, positive compensatory growth due to infection feedbacks in response to culling occurs except when the recovery rate is high and the loss of immunity is low (Figure 5.5). Therefore, our results indicate that culling can lead to a population level reduction in disease-induced mortality that mitigates the impact of culling on population abundance, provided the infection does not lead to long-lasting immunity.

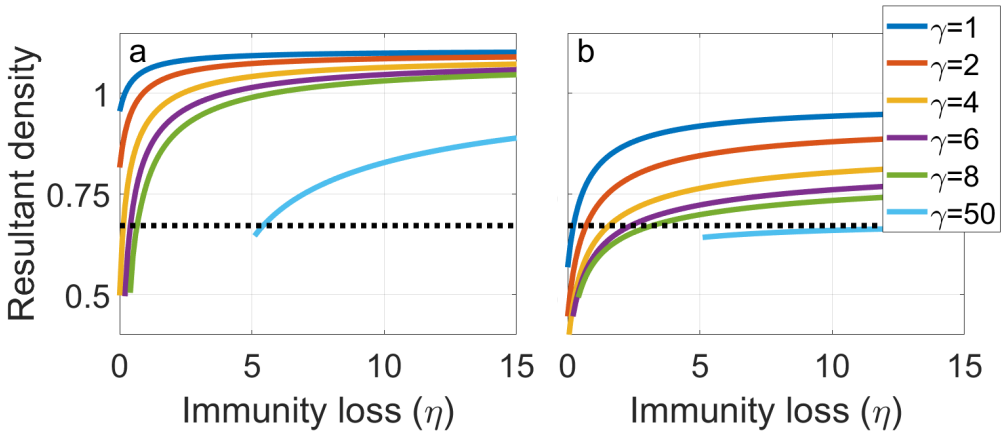

Figure 5.5: The resultant population density after 30 sequential cull and subsequent regrowth periods culling 25% of the population for the SIRS model (Equations (5.1)) plotted against waning immunity, η, for different levels of recovery, γ, for (a) DD and (b) FD transmission. The dotted line represents the resultant population density for the demographic effects only model. The difference between the solid lines and dotted line represents the positive or negative compensatory effect due to changes in the disease dynamics. Results are shown for an initial endemic disease prevalence of $p_i = 10\%$. Other parameters are as in Figure 5.1. Truncated results indicate parameter levels that do not satisfy requirements for valid solutions (Equations (5A4) & (5A5)).

We confirm our findings for discrete culling in a model of continuous culling (the detailed analysis is presented in Appendices 5A.2 and 5A.4). The results for the continuous cull model approximate the average density of those for the equivalent discrete cull (Figures 5A.1, 5A.3 & 5A.4). As such, the model for continuous culling exhibits the compensation due to a release from disease-induced mortality that we are investigating, although as an average does not show the potential increase in resultant density above the endemic steady state illustrated in Figure 5.3. However, it does allow a robust comparison of steady states for our different model formulations. In particular, we compare the steady states for total density in the full model for DD and FD transmission, N_{DD} and N_{FD} respectively, with the demographic effects only model, N_{dem}, and the disease effects only model, N_{dis}, and compare these values with the density prior to culling, N_e. For the SI model with DD transmission we show that $N_e > N_{DD} > N_{dis} > N_{dem}$ and for FD transmission $N_e > N_{FD} > N_{dem}$, which confirms the findings of Figures 5.3 & 5A.2(i). In our illustrated results (Figure 5A.2a(i)) we see that $N_{DD} - N_{dem} \gg N_{DD} - N_{dis}$ and therefore the release from disease-induced mortality contributes most of the compensation in response to culling (a similar result holds for FD transmission, Figure 5A.2b(i)). These results also hold for the SIRS model when there is a low rate of recovery or a high rate of loss of immunity. When immunity is sufficiently long-lived (e.g. high recovery and low loss of immunity) then for DD transmission $N_e > N_{dem} > N_{DD} > N_{dis}$ and for FD transmission $N_e > N_{dem} > N_{FD}$, which again confirms the findings in Figures 5.4 & 5A.2(ii). These analytical results hold for all valid parameter values and confirm our key finding that the compensation due to disease effects exceeds those due to demographic effects in systems without long-lived immunity.

We also examine the impact of culling that is targeted on infected individuals and find that compensation due to changes in the disease dynamics still occurs under the SI model, but is greater under FD than DD transmission (see Appendix 5A.4 and Figure 5A.7). The amplified compensatory growth under FD transmission occurs as targeted culling leads to a direct decrease in the force of infection since infected density decreases more rapidly than total density (under indiscriminate culling infected and total density decrease at the same rate due to culling). For the SIR model targeted culling has little effect on density and prevalence and therefore the negative impacts of culling and disease are no longer observed, but the level of compensation is minimal. For the SIR model targeted culling does initially reduce the force of infection but as a consequence fewer individuals progress to the recovered and immune class; overall these two effects balance. In general, the findings for the model with targeted culling confirm our previous results that compensation due to disease effects occurs in the absence of long-lasting immunity. We also compare the steady states for total density under continuous targeted infected culling for DD

and FD transmission, N^T_{DD} and N^T_{FD} respectively. We show that for a sufficient level of targeted infected culling and low rate of recovery or high rate of loss of immunity, then $N^T_{FD} > N^T_{DD} > N_e$, confirming the findings in Figures 5A.7 & 5A.8, and supports our finding of the potential for targeted infected culling to induce an over-compensatory population growth response.

The full model (Equations (5.1)) includes demographic crowding effects on birth only. In Appendix 5A.5 we examine the impact of culling on compensatory growth for a version of the full model that can include density-dependent birth and/or death. The results are unchanged under DD transmission regardless of whether density dependence is on birth, death or a combination of both. Under FD transmission the compensatory effect due to a release from disease mortality decreases as the level of density-dependent death increases relative to density-dependent birth. The only scenario in which there is no compensatory effect due to changes in disease dynamics is when there is purely density-dependent death (under FD transmission). Therefore our key finding that culling can lead to compensatory growth due to changes in the disease dynamics is evident for almost all scenarios of density-dependent birth and death. An analytical explanation of these findings is presented in Appendix 5A.5. A parameter sensitivity analysis examining how the level of compensatory growth varies with disease virulence, initial prevalence and cull period is presented in Appendix 5A.6.

5.5 Case Study

We highlight the applicability of our findings by considering a case study of the use of culling to manage tuberculosis in Eurasian wild boar (*Sus scrofa*) in central Spain. Here, environmental drivers, such as summer drought, can lead to aggregation with associated high prevalence of infection of *Mycobacterium tuberculosis* complex (MTC) which are the causative agents of animal tuberculosis (TB) [138]. We assume that the driver of infection in the wild boar TB system is through environmental contact with free-living MTC pathogen which is shed from the most infectious individuals [14]. It is appropriate to assume the population is well-mixed in terms of transmission as on managed estates infection is likely to occur at scarce water holes where free-living MTC can persist and which are utilised frequently by the whole population. Therefore the free-living (FL) transmission mode is used in this case study (see Appendix 5A.3 and recall that FL transmission produces qualitatively similar findings to DD transmission). In central Spain wild boar are the primary reservoir host for MTC and in some regions up to 70% of the population can be infected with MTC of which half (35% of the total population) may exhibit generalised infection (infected and infectious) [137, 126]. Individuals with generalised infection suffer high levels of disease-induced mortality [14]. Since

wild boar have an economic and cultural value for the hunting community in Spain there has been a reluctance to use additional culling to control TB as it may result in decreased population abundance. However, since the wild boar TB system is characterised by high disease-induced mortality and no recovery from infection [12] our earlier general results indicate that culling could result in compensatory growth due to reduced disease-induced mortality offsetting the mortality associated with culling and thus sustaining population abundance.

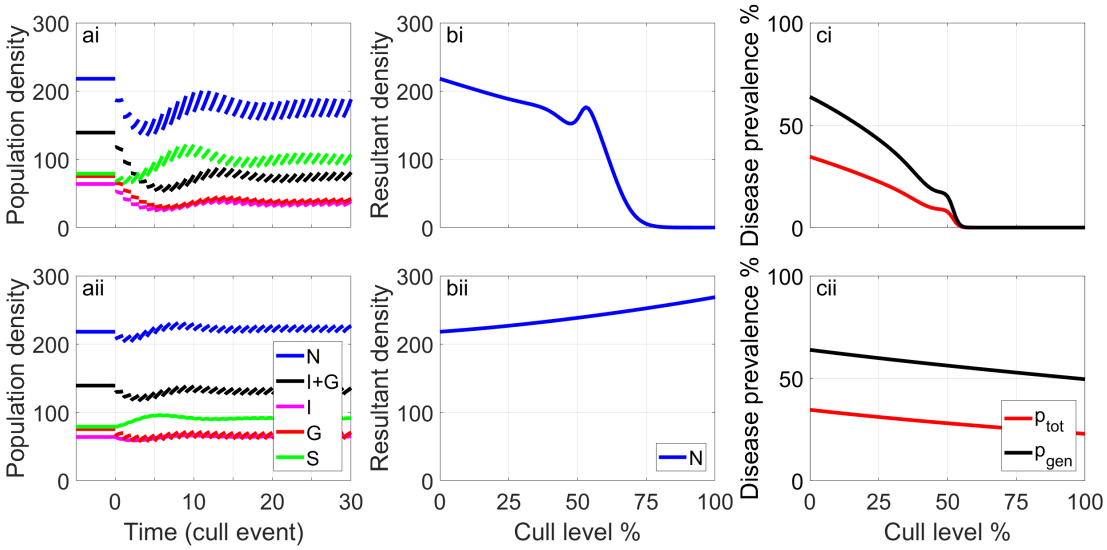

Figure 5.6: Results for the wild boar TB model in response to 30 cull events of 25% for (i) indiscriminate culling of the yearling and adult population and (ii) targeted culling of generalised yearlings and adults. The population dynamics over time are shown in (a) for total density (blue); infected and generalised density (black); infected density (magenta); generalised density (red) and susceptible density (green). The initial population assumes a TB prevalence, (I+G)/N, of 64% and a generalised prevalence, G/N, of 35%. (b) shows the resultant total population (blue) and (c) the total prevalence (black) and generalised prevalence (red) after 30 sequential cull and subsequent regrowth periods for different levels of hunting. The model and its parameters are outlined in Appendix 5A.7.

We extend our model framework to represent the wild boar TB systems for a single geographical managed estate containing a homogeneously mixed population covering an area of $3 \times 3\text{km}^2$. The population density of wild boar is separated into different age classes to capture distinct disease and reproductive characteristics for piglets (aged 0-1 year), yearlings (aged 1-2 years), and adults (aged 2 years+). Further, the age-classes are split into susceptible, infected and generalised (infected and infectious) classes to reflect disease status. Yearlings and adults can give birth, and in contrast to our model formulation in Equations (5.1) the crowding parameter q (Appendix 5A.7.1), used to limit the disease-free total population density to the carrying capacity, is independent of the endemic disease prevalence. Infection occurs through environmental contact with free-living MTC pathogen which is shed from individuals with the generalised infection. The population dynamics of wild boar and

TB are represented by a system of differential equations that are an extension of our general framework (Equations (5.1)). Full details of the model and parameterisation can be found in Appendix 5A.7.

When there is an indiscriminate cull on yearlings and adults the population density shows an initial drop followed by an increase with peak density only falling by 10% in response to a 25% annual cull (Figure 5.6a(i)). While total population size shows only a small reduction there is a more significant reduction in infected individuals and total prevalence drops from 64% to 43% and generalised prevalence from 35% to 22%. More generally (Figures 5.6b(i) & 5.6c(i)) there is only a shallow decline in population density in response to increased culling up to a threshold at which the disease is eradicated from the system (50% cull). After this the population level declines rapidly. When there is a targeted annual cull of 25% of generalised yearlings and adults (Figures 5.6ii) we see an increase in the total population but only a modest decrease in prevalence and in particular little change in the density of infected and generalised individuals. These results highlight that compensatory growth due to reduced disease-induced mortality may offset increased culling and may lead to a reduction in TB prevalence in wild boar without detrimental reductions in density. Our general predictions may therefore be applicable in this system and highlight the importance of detailed modelling in the context of culling in the face of disease.

5.6 Discussion

Despite the ubiquity of infectious disease in nature, there has been little work on the impact of disease on harvested populations. Our key result is that population reductions from culling and harvesting are compensated in a wide range of infectious disease scenarios due to a population level release from disease-induced mortality. The compensatory effect increases as disease virulence, the pre-culling level of prevalence and the level of culling increase and occurs for systems with density-dependent, frequency-dependent and environmental (free-living) modes of transmission. The key outcome is that culling in systems that harbour virulent parasites can lower disease prevalence without significantly reducing, or indeed can increase, population density. The population can therefore be regulated at a similar density by disease or at reduced prevalence by a combination of culling and disease.

Compensation due to changes in disease dynamics occurs in the absence of long-lasting immunity. With long-lasting immunity and indiscriminate culling, disease generally increases the impact of culling and harvesting, reducing the population density compared to systems without the disease. Although there are examples of life-long immunity in wildlife and livestock populations (rinderpest vaccine produces life-long immunity in African cattle [123]) there are also many

examples, including TB, where vaccine-derived immunity wanes [133]. This indicates that even in those diseases with acquired immunity, this protection may often be partial or wane leading to an SIRS model where individuals become susceptible again after a period of immunity. It is likely therefore that many wildlife systems that support virulent infectious disease will exhibit compensatory growth due to reduced disease-induced mortality following culling. Of course, many populations will have multiple diseases, but the key point is to understand the overall disease burden and in particular whether there is widespread immunity to the key sources of virulence. System-specific models can then determine whether the infectious disease allows increased exploitation or makes the host population more vulnerable. For example, our system-specific model of the wild boar TB interaction in central Spain predicted a strong effect of compensation due to changes in disease dynamics leading to only modest reductions in the population abundance due to hunting. This is therefore an example in which the impact of harvesting is offset in a host that harbours a virulent parasite and suggests hunting is likely to be a sustainable management option in this system if the desire is to regulate the population at similar density but with reduced prevalence.

Our results have important consequences for the use of culling to manage infectious disease. The impact of harvesting on wildlife disease has been previously considered in models with long-lasting immunity [35, 25] which reported an increase in prevalence. Our results confirm these findings since in systems with long-lasting immunity harvesting will reduce the density of immune individuals to a greater proportional extent than other classes [25, 97]. We also support previous studies [16, 141, 113, 130] which showed that indiscriminate culling is more effective at reducing disease prevalence when infection results from density-dependent rather than frequency-dependent transmission. However, we show that targeted culling is more effective when transmission is frequency-dependent. System-specific models have shown how localised culling could reduce the prevalence of classical swine fever in wild pigs [40] and reduce the prevalence and spread of chronic wasting disease in white tailed deer [130, 114], predictions that are supported by observations in the field [30, 93].

Our results highlight the difficulty of using culling to eradicate an infectious disease and may explain empirical findings that suggests that culling is not an effective disease management tool. For example, bovine tuberculosis has persisted in badger populations in Great Britain despite comprehensive culling campaigns [51]; Gortázar *et al.* (2015) [72] reviewed culling programmes worldwide reporting few that achieved 100% efficacy. Theoretical models have suggested that culling could not control white-nose syndrome in bats [78]; that very high levels of culling were required to eradicate paratuberculosis in rabbits [43] and Tasmanian devil facial tumour disease [18]; and that culling may increase disease transmission through

changes in other ecologically driven factors [115]. While our findings indicate that culling can maintain prevalence at reduced levels, they also highlight that high levels of culling are required to eradicate an infection and that there is a narrow range of culling levels between disease eradication and population extinction. System-specific models are therefore required to determine the likelihood of success and the risk of population extinction that may result from culling programmes to control disease.

Previous model studies of the wild boar TB system suggested that culling may contribute to TB management when used in conjunction with other control measures [6]. Our model of TB and wild boar shows how such system-specific models can be built to understand when and how culling can be used as a management tool in wildlife systems that harbour virulent disease. Wild boar hunting is a source of income while in some localities spillover of TB into livestock has economic impacts. Our results show that hunting could be a viable method for controlling TB in wild boar because hunting leads to a significant drop in disease prevalence with the model results supported by observations in central Spain [23, 12]. This is a 'win-win' situation for managed estates since in addition to decrease in disease prevalence a large proportion of the mortality from hunting is countered by a reduction in disease-induced mortality. The model results indicate that the largest decrease in prevalence and density of infectious individuals is for indiscriminate culling (of juveniles and adults). Here, there is a threshold at which culling eradicated the disease (60% in our model study) after which population abundance decreases rapidly leading to extinction when culling reaches 75%. It may therefore be possible to eradicate TB in wild boar through culling, but it would be critical to determine these thresholds at a regional level. Targeted culling of infectious wild boar resulted in only modest reductions in prevalence and no discernible change in the density of infecteds. This may explain the failure of targeted culling to control TB in empirical studies [33].

Over-compensatory population regrowth in response to culling events is well-known in systems that do not consider infectious disease; Abrams & Matsuda (2005) [2] termed this a 'hydra' effect. Abrams (2009) [1] outlined three possible mechanisms that may produce the hydra effect: (i) additional mortality altering pre-existing population oscillations in a way that leads to an increased density, (ii) a temporal separation of mortality and density dependence and (iii) mortality of a consumer leading to over-compensatory changes in other aspects in the food web. Our results for the model with discrete culling show that the resultant density can exceed the original density. Our results with targeted infected culling, for both discrete and continuous model set-ups, show that the resultant density may also surpass the total population density in the absence of culling. These results arise as culling induces population regrowth in an environment with reduced prevalence and therefore reduced disease-induced mortality. Therefore, our novel insight is that the

release from mortality caused by endemic disease following culling can also lead to a hydra effect. This has similarities to the hydra effect due to the consumer-resource mechanism (Abrams (2009) [1] mechanism (iii)) where additional mortality of the consumer leads to a reduction in mortality for the resource. Our scenario is different in that it occurs within a single species.

Our key finding is that mortality due to culling in systems that harbour virulent infections may be compensated by reductions in disease-induced mortality. We have also demonstrated that it is important to fully understand the infection processes and to model the specific system before using culling as a disease management tool [18].

Appendices to Chapter 5

The following appendices are the Supplementary Information to 'The critical role of infectious disease in compensatory population growth in response to culling' by Eleanor Tanner, Andy White, Peter Lurz, Christian Gortázar, Iratxe Díez-Delgado and Mike Boots.

5A.1 System steady states and restrictions

We derive expressions for the parameter q and transmission function $\theta(I, N)$ for the full model system (main paper Equations (5.1)) by setting the endemic steady state for the total population, $N = N_e$, and the endemic level of infecteds as $I_e = p_i N_e$ where p_i is the initial endemic prevalence of infecteds. This gives the endemic steady states of the system as:

$$I_e = p_i N_e \tag{5A1a}$$

$$S_e = (1 - \zeta p_i) N_e \tag{5A1b}$$

$$R_e = (\zeta - 1) p_i N_e. \tag{5A1c}$$

$$\text{where} \quad \zeta = \frac{d + \eta + \gamma}{d + \eta} \tag{5A1d}$$

The transmission function $\theta(I, N)$ is then derived as:

$$\text{DD transmission}: \quad \theta(I, N) = \frac{(d + \alpha + \gamma)}{N_e (1 - \zeta p_i)} I \tag{5A2a}$$

$$\text{FD transmission}: \quad \theta(I, N) = \frac{(d + \alpha + \gamma)}{(1 - \zeta p_i)} \frac{I}{N}. \tag{5A2b}$$

We also determine an expression for q, the parameter that controls density dependent birth, which is dependent on the constants set for N_e and p_i:

$$q = \frac{b - d - \alpha p_i}{b N_e}. \tag{5A3}$$

Given that for valid solutions we must have $q \geq 0$ and $0 \leq p_i \leq 1$, we therefore have a requirement on the system parameters for valid solutions:

$$0 \leq p_i < \frac{(b - d)}{\alpha}, \tag{5A4}$$

noting that to achieve a non-zero populated steady state in the system we must also have $b > d$. Further to these restrictions, to ensure a positive endemic steady state for the susceptible class and a positive transmission function, the initial endemic

prevalence p_i is also governed by:

$$0 \leq p_i < \frac{d+\eta}{d+\gamma+\eta}. \tag{5A5}$$

5A.2 Continuous culling

In the main paper we have presented results for compensatory growth as a response to discrete culling events. We now consider the same model with continuous culling which approximates the average behaviour of the model with discrete culling. The model with continuous culling allows us to determine conditions for the endemic steady state. We modify Equations (5.1) to include continuous culling controlled by the parameters c_S, c_I and c_R for culling susceptibles, infecteds and recovereds respectively:

$$\frac{\mathrm{d}S}{\mathrm{d}t} = Nb(N) - dS - \theta(I,N)S - c_S S + \eta R \tag{5A6a}$$

$$\frac{\mathrm{d}I}{\mathrm{d}t} = \theta(I,N)S - dI - \alpha I - \gamma I - c_I I \tag{5A6b}$$

$$\frac{\mathrm{d}R}{\mathrm{d}t} = \gamma I - dR - c_R R - \eta R \tag{5A6c}$$

Note we have replaced the explicit term for the birth rate with the more general

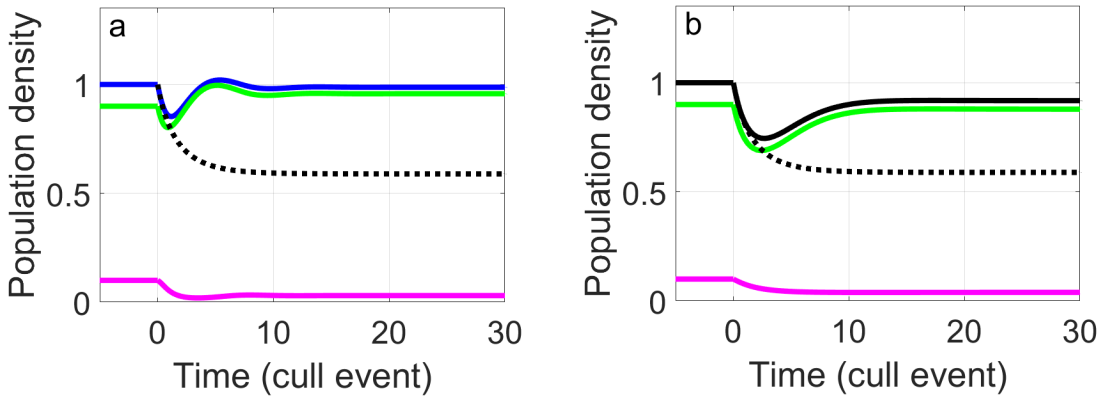

Figure 5A.1: The population density response to continuous culling at rate $c = \log\left(\frac{1}{1-0.25}\right)$ in an SI framework in Equations (5A6) (here culling is at a similar rate to in the discrete culling model). The change in population density is shown for the total population density (blue for DD (a), black for FD (b)); the total density of susceptibles (green); the total density of infected (magenta) and the demographic effects only model (Equation (5A7)) with the same level of continuous culling (black dotted). (a) shows results for DD transmission and (b) shows results for FD transmission. Results are shown for a virulent infection, $\alpha = 4$, with no recovery to immunity ($\gamma = 0$), and an initial endemic disease prevalence of $p_i = 10\%$. Other parameters are as Figure 5.1aii in the main paper.

term $b(N)$. The demographic effects only model (Equation (5.3)) is modified to

include the same rate of continuous culling as follows:

$$\frac{\mathrm{d}N}{\mathrm{d}t} = Nb(N) - dN - \alpha p_i N - c_{dem} N \tag{5A7}$$

$$\text{where} \quad c_{dem} = c_S\left(1 - \zeta p_i\right) + c_I p_i + c_R(\zeta - 1)p_i \tag{5A8}$$

The disease effects only model (Equations (5.5), (5.1b) & (5.1c)) is modified to include continuous culling by replacing Equation (5A6a) with the following equation in which the birth rate remains constant:

$$\frac{\mathrm{d}S}{\mathrm{d}t} = Nb(N_e) - dS - \theta(I, N)S - c_S S + \eta R \tag{5A9}$$

We restrict the birth function $b(N)$ to be a strictly monotonically decreasing function for $0 \leq N \leq K$ where K is the disease-free steady state for the population ($p_i = 0$) such that $b(K) = d$. Furthermore we restrict $b(N)$ to be differentiable on $0 \leq N \leq K$ so that $\dfrac{\mathrm{d}b(N)}{\mathrm{d}N} < 0$ on $0 < N < K$. Also, we define the endemic steady state without culling to be N_e such that $0 \leq N_e \leq K$. From Equation (5A7) we know that

$$b(N_e) = d + \alpha p_i \tag{5A10}$$

We consider steady states for these models under indiscriminate culling ($c_S = c_I = c_R = c$). We want to compare the endemic steady state N_e with the steady states for: the demographic effects only model (Equation (5A7)) N_{dem}; the disease effects only model (Equations (5A9), (5A6b) & (5A6c)) for DD transmission N_{dis}; and the full model (Equations (5A6) for DD transmission N_{DD} and FD transmission N_{FD}. Note that for $c = 0$ all these steady states are all equal to N_e. We wish to compare the steady states in response to culling ($c > 0$).

5A.2.1 Steady state condition for the demographic effects only model

From Equation (5A7) we see that for $c > 0$ then

$$b(N_{dem}) = d + \alpha p_i + c > b(N_e) = d + \alpha p_i \tag{5A11}$$

Since $b(N)$ is a strictly monotonically decreasing function then if $b(N_{dem}) > b(N_e)$ it implies that $N_{dem} < N_e$.

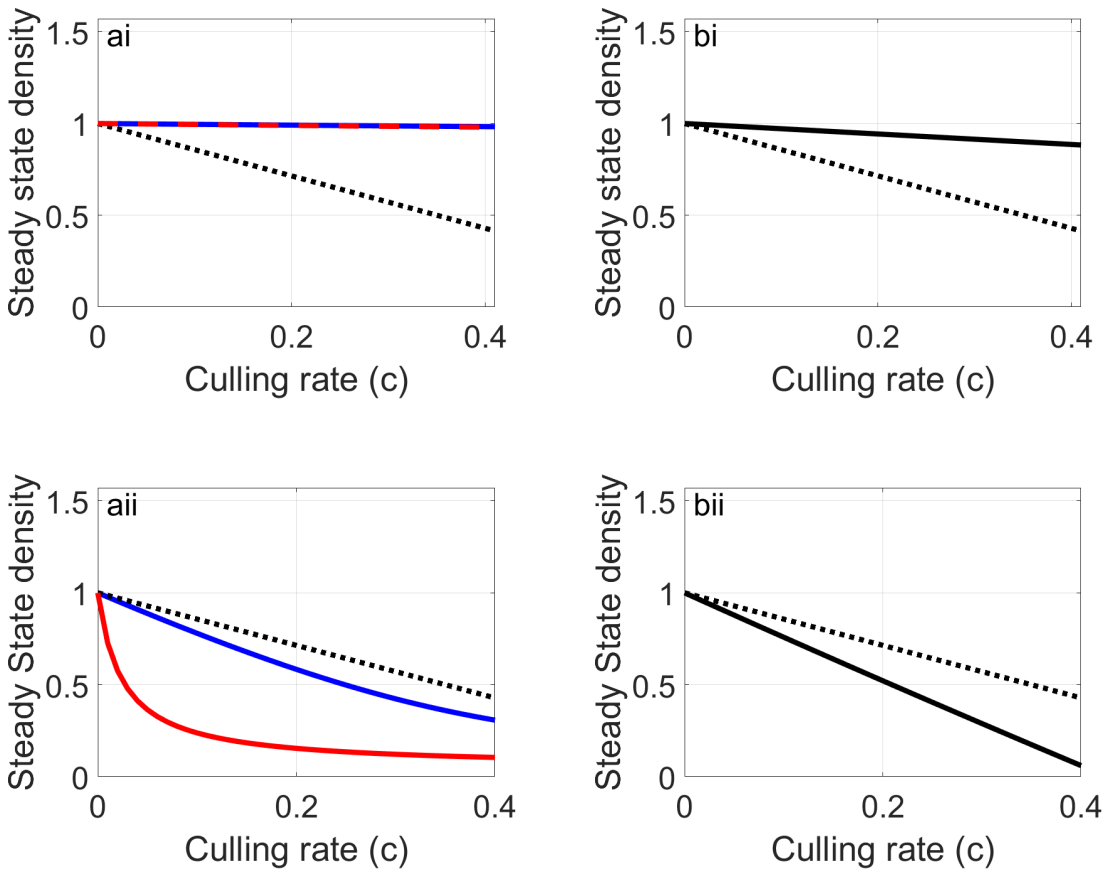

Figure 5A.2: Results for the model with continuous indiscriminate culling (Equations (5A6) with $b(N) = b(1 - qN)$) for (i) the SI model and (ii) the SIR model. The steady state density N is shown for DD transmission in (a): for the full model (blue); the disease effects only model (red); and the demographic only model (black dotted). The steady state density N is shown for FD transmission in (c) for the full model (black) and demographic only model (black dotted). Other parameters are as in the main paper Figures 5.1ii & 5.1iv for the SI model and the SIR model respectively.

5A.2.2 Steady states for continuous culling with DD transmission

Under DD transmission the steady states for the full DD model and the disease effects only model are:

$$N_{DD} = N_e\,[1 - \zeta p_i]\left[1 + \frac{c}{d+\alpha+\gamma}\right]\left[\frac{\alpha}{\alpha + \xi(d+c) - \xi b(N_{DD})}\right] \tag{5A12}$$

$$N_{dis} = N_e\,[1 - \zeta p_i]\left[1 + \frac{c}{d+\alpha+\gamma}\right]\left[\frac{\alpha}{\alpha + \xi(d+c) - \xi b(N_e)}\right] \tag{5A13}$$

$$\text{where} \quad \xi = \frac{d+\eta+c+\gamma}{d+\eta+c}, \qquad \zeta = \frac{d+\eta+\gamma}{d+\eta} \tag{5A14}$$

From Equation (5A5) we know that $1 - \zeta p_i > 0$. We assume that $\alpha + \xi(d+c) - \xi b(N) > 0$ for $N = N_e$ and $N = N_{DD}$. Note that N_{DD} is valid when $c < b(N_{DD}) - d$,

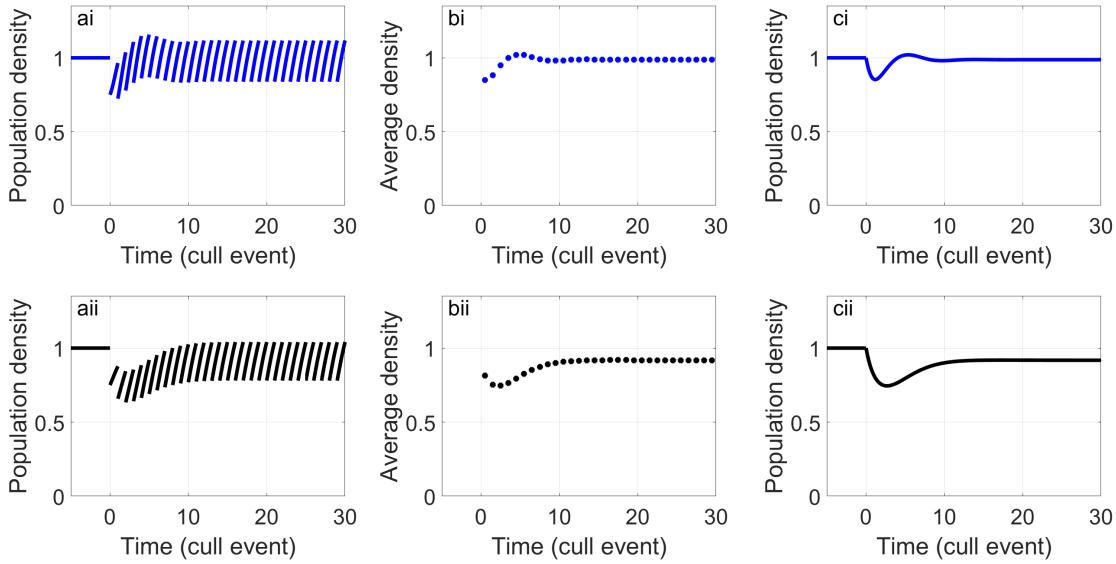

Figure 5A.3: The population density response to culling for: (a),(b) a discrete annual cull of 25% and (c) continuous culling at rate $c = \log\left(\frac{1}{1-0.25}\right)$ in an SI framework for (i) DD transmission and (ii) FD transmission. (a) shows the total population density during annual discrete culling, (b) shows the annual average total population density for the discrete cull, calculated by trapezium rule for the results obtained numerically over each regrowth period post the culling event. (c) shows the total population density under continuous culling. Other parameters are as Figure 5.1a(ii) in the main paper.

the culling threshold where I_{DD} becomes negative, and similarly N_{dis} is valid for $c < \alpha p_i$ the culling threshold where I_{Dis} becomes negative.

5A.2.3 N_{DD} and N_{dis} decrease as γ increases

Rearranging Equation (5A12) we find that

$$b(N_{DD}) = d + \alpha p_i + c - \frac{\alpha}{\xi}\left[\frac{N_e}{N_{DD}}\frac{(d+\alpha+\gamma+c)}{(d+\alpha+\gamma)}(1-\zeta p_i) - (1-\xi p_i)\right] \quad \text{(5A15)}$$

We can differentiate Equation (5A15) with respect to γ and following some algebra it can be shown that $\frac{\mathrm{d}N_{DD}}{\mathrm{d}\gamma} < 0$ and therefore N_{DD} decreases as γ increases for all valid parameters.

Using a similar process on Equation (5A13) where $b(N) = b(N_e)$, which is constant and independent of γ, it follows that $\frac{\mathrm{d}N_{dis}}{\mathrm{d}\gamma} < 0$ and so N_{dis} decreases as γ increases for all valid parameters.

5A.2.4 The relationship between N_{DD} and N_e

First we consider the relationship between N_{DD} and N_e. Let us assume that $N_{DD} > N_e$ then from Equation (5A12)

$$[1-\zeta p_i]\left[1+\frac{c}{d+\alpha+\gamma}\right]\left[\frac{\alpha}{\alpha+\xi(d+c)-\xi b(N_{DD})}\right] > 1 \tag{5A16}$$

Rearranging Equation (5A16) we find:

$$b(N_{DD}) > d+\alpha p_i + c\left[\frac{(d+\eta+c)((d+\alpha p_i)(d+\eta)+\gamma(d+\alpha p_i+\eta))+\gamma(d+\alpha+\gamma)(d+\alpha p_i+\eta)}{(d+\eta)(d+\alpha+\gamma)(d+\gamma+\eta+c)}\right] \tag{5A17}$$

and using Equation (5A10), for the inequality Equation (5A17) to hold requires that $b(N_{DD}) > b(N_e)$ which contradicts $N_{DD} > N_e$ for $c > 0$. Therefore $N_{DD} < N_e$ for $c > 0$.

5A.2.5 The relationship between N_{DD} and N_{dis}

From Appendix 5A.2.4 as $N_{DD} < N_e$ we infer that $b(N_{DD}) > b(N_e)$ for $c > 0$. Therefore for all $c > 0$,

$$\left[\frac{\alpha}{\alpha+\xi(d+c)-\xi b(N_{DD})}\right] > \left[\frac{\alpha}{\alpha+\xi(d+c)-\xi b(N_e)}\right] \tag{5A18}$$

and so from Equation (5A12) and Equation (5A13) $N_{DD} > N_{dis}$ for all $c > 0$.

5A.2.6 The relationship between N_{DD} and N_{dem}

By definition, N_{DD} equals N_{dem} when

$$b(N_{DD}) = b(N_{dem}) = d+\alpha p_i + c \tag{5A19}$$

Using Equation (5A15) and Equation (5A19) we can show that $N_{DD} = N_{dem}$ when,

$$N_{dem} = N_{DD} = N_e \frac{(d+\alpha+\gamma+c)}{(d+\alpha+\gamma)}\frac{(1-\zeta p_i)}{(1-\xi p_i)} \tag{5A20}$$

As $b(N_{dem}) > b(N_e)$ for $c > 0$ it follows that $N_{dem} < N_e$ for $c > 0$, and therefore

$$\frac{(d+\alpha+\gamma+c)}{(d+\alpha+\gamma)}\frac{(1-\zeta p_i)}{(1-\xi p_i)} < 1 \tag{5A21}$$

which is only valid for $\gamma > \gamma_{dem0} > 0$ where

$$\gamma_{dem0} = \frac{1}{2p_i}\Big[-p_i(d+\eta+c+d+\alpha)+ \sqrt{p_i^2(d+\eta+c+d+\alpha)^2+4p_i(1-p_i)(d+\eta)(d+\eta+c)}\Big] \tag{5A22}$$

so that Equation (5A21) does not hold for $\gamma = 0$, and so $b(N_{DD}\big|_{\gamma=0})$ cannot equal $d + \alpha p_i + c$ for $c > 0$. From Appendix 5A.2.3 we know that $b(N_{DD})$ increases as γ increases, therefore $b(N_{dem}) > b(N_{DD}\big|_{\gamma=0}) > b(N_e)$ and so $N_{dem} < N_{DD}\big|_{\gamma=0} < N_e$. It follows that $N_{DD} = N_{dem}$ if $\gamma = \gamma_{dem}$ (where γ_{dem} is the solution to Equation (5A20)) and $\gamma_{dem} > \gamma_{dem0}$. From Equation (5A11) we see that N_{dem} is constant with respect to changes to γ and from Appendix 5A.2.3 we know that N_{DD} decreases as γ increases. Therefore $N_{DD} > N_{dem}$ for $\gamma < \gamma_{dem}$ and $N_{DD} < N_{dem}$ for $\gamma > \gamma_{dem}$.

5A.2.7 The relationship between N_{dis} and N_{dem}

We know from Appendix 5A.2.5 that $N_{dis} < N_{DD}$ for $c > 0$, and therefore from Appendix 5A.2.6 for sufficiently large γ ($\gamma > \gamma_{dem}$) we know that $N_{dis} < N_{DD} < N_{dem}$. We want to show that for sufficiently small γ that $N_{dis} > N_{dem}$. This can be shown as follows. We know that,

$$N_{dis}\big|_{\gamma=0} = N_e\left[1-p_i\right]\left[1+\frac{c}{d+\alpha}\right]\left[\frac{\alpha}{\alpha(1-p_i)+c}\right]. \tag{5A23}$$

In Section 5A.2.6 we show that $N_{DD}|_{\gamma=\gamma_{dem0}} > N_{dem}$. We can show that $N_{dis}|_{\gamma=0} > N_{DD}|_{\gamma=\gamma_{dem0}}$ for $c < \alpha p_i$, noting that the level of susceptibles for DD transmission when $\gamma = \gamma_{dem0}$ is $S_{DD}|_{\gamma=\gamma_{dem0}} = N_e(1-\xi|_{\gamma=\gamma_{dem0}}p_i)$ and therefore the infected prevalence, $I_{DD}/N_{DD}|_{\gamma=\gamma_{dem0}}$, must be less than p_i. It follows that

$$N_{dis}|_{\gamma=0} = S_{DD}|_{\gamma=0} + I_{Dis}\big|_{\gamma=0} > S_{DD}|_{\gamma=\gamma_{dem0}} + I_{DD}|_{\gamma=\gamma_{dem0}} > N_{dem}. \tag{5A24}$$

Therefore for sufficiently low levels of recovery and valid parameter values $N_{dis} > N_{dem}$.

5A.2.8 Steady states for continuous culling with FD transmission

Under FD transmission the steady state, N_{FD}, for the full model satisfies

$$b(N_{FD}) = d + \alpha p_i + c - \frac{\alpha}{\xi}\left[\frac{(d+\alpha+\gamma+c)}{(d+\alpha+\gamma)}(1-\zeta p_i) - (1-\xi p_i)\right] \tag{5A25}$$

5A.2.9 The relationship between N_{FD} and N_e

From Equation 5A25 and using Equation (5A10), when $\gamma = 0$ then

$$b(N_{FD}) = d + \alpha p_i + \frac{c(d + \alpha p_i)}{d + \alpha} > b(N_e) \tag{5A26}$$

Hence for $\gamma = 0$ we find that $N_e > N_{FD}$. Further, Equation (5A25) shows that $b(N_{FD})$ increases as γ increases and so $N_e > N_{FD}$ for all $\gamma \geq 0$.

5A.2.10 The relationship between N_{FD} and N_{dem}

We know that $N_{FD} > N_{dem}$ if $b(N_{FD}) < b(N_{dem})$ and using Equation (5A11) and Equation (5A25) this requires that

$$\frac{(d + \alpha + \gamma + c)}{(d + \alpha + \gamma)} \frac{(1 - \zeta p_i)}{(1 - \xi p_i)} > 1 \tag{5A27}$$

so that when $\gamma < \gamma_{dem0}$, where γ_{dem0} is defined in Equation 5A22, then $b(N_{FD}) < b(N_{dem})$.

For sufficiently large γ and low η, when $\gamma > \gamma_{dem0}$, the inequality in Equation (5A27) fails and therefore $N_{dem} > N_{FD}$.

5A.2.11 Conclusion: the relationships between N_e, N_{DD}, N_{FD}, N_{dem} and N_{dis}

Gathering the results from this section, we can say that for diseases with no or short-lived immunity (little or no recovery or high loss of immunity)

$$N_e > N_{DD} > N_{dis} > N_{dem} \tag{5A28}$$

$$N_e > N_{FD} > N_{dem} \tag{5A29}$$

and for diseases with long-lived immunity (sufficiently high rate of recovery and low loss of immunity),

$$N_e > N_{dem} > N_{DD} > N_{dis} \tag{5A30}$$

$$N_e > N_{dem} > N_{FD} \tag{5A31}$$

5A.2.12 Indiscriminate continuous culling results for $b(N) = b(1 - qN)$

We present results for the continuous model using the same birth function ($b(N) = b(1 - qN)$) as used for the discrete culling results presented in the main paper. We derive the continuous culling rate, c, by equating the steady state for the continuous

demographic effects only model, Equation (5A7) with indiscriminate culling, to the average population density between culling events of the demographic effects only model, Equation (5.3), which has reached a steady state under an annual cull of $\delta\%$ each year:

$$\frac{b-d-\alpha p_i - c}{bq} = \frac{1}{bq}\ln\left[(1-\delta)\frac{\exp^{b-d-\alpha p_i}-1}{1-\exp^{-(b-d-\alpha p_i)}}\right] \tag{5A32}$$

$$\Rightarrow c = \ln\left[\frac{1}{1-\delta}\right] \tag{5A33}$$

Figures 5A.1a(i) and 5A.1b(i) show the analogous results to those with discrete culling in the main paper (Figures 5.1a(ii) and 5.1b(ii)). Also, Figure 5A.2 shows the analogous results to those with discrete culling in main paper (Figure 5.3 and Figure 5.4). Additionally, for SI models, in Figures 5A.3(i) and 5A.3(ii), for DD and FD transmission respectively, we plot the average total population density over the regrowth period following each culling event, illustrating our point that the population density represented by the continuous cull is in close agreement with the average density of the discrete cull. This is again illustrated in Figure 5A.4, for different levels of culling, showing the resultant total population density after discrete culling (Figure 5A.4a), the average total population density (Figure 5A.4b), and the continuous culling steady state (Figure 5A.4c) showing again that the resultant average population density is in close agreement with the continuous culling steady state. In all the continuous culling results the population is harvested at continuous rate $c = \log\left(\frac{1}{1-0.25}\right)$ to achieve a similar rate of a discrete cull of 25% of the population. For the SI model and DD transmission there is minimal compensation due to demographic effects with the majority of compensatory growth due to the change in disease dynamics (Figures 5A.2a(i) & 5A.2b(i)). For FD transmission, the compensation due to the change in disease dynamics is less than for DD transmission (Figure 5A.2c(i) & 5A.2d(i)). For the SIR model there is qualitatively the same level of negative disease compensation as that shown for discrete culling, and a similar level of positive compensatory growth due to demographic effects. Note that results have been plotted here up until the point that the disease endemic steady state becomes invalid ($c = \alpha p_i$), ie. where culling has eradicated the disease. The results for the specific birth function comply with the general results outlined in Appendix 5A.2 and indicate that for indiscriminate culling the findings for discrete and continuous culling are qualitatively similar.

5A.3 Free living transmission

When we consider free-living infection dynamics we assume that the free-living parasite F is excreted at a constant rate λ by infected individuals and has a decay

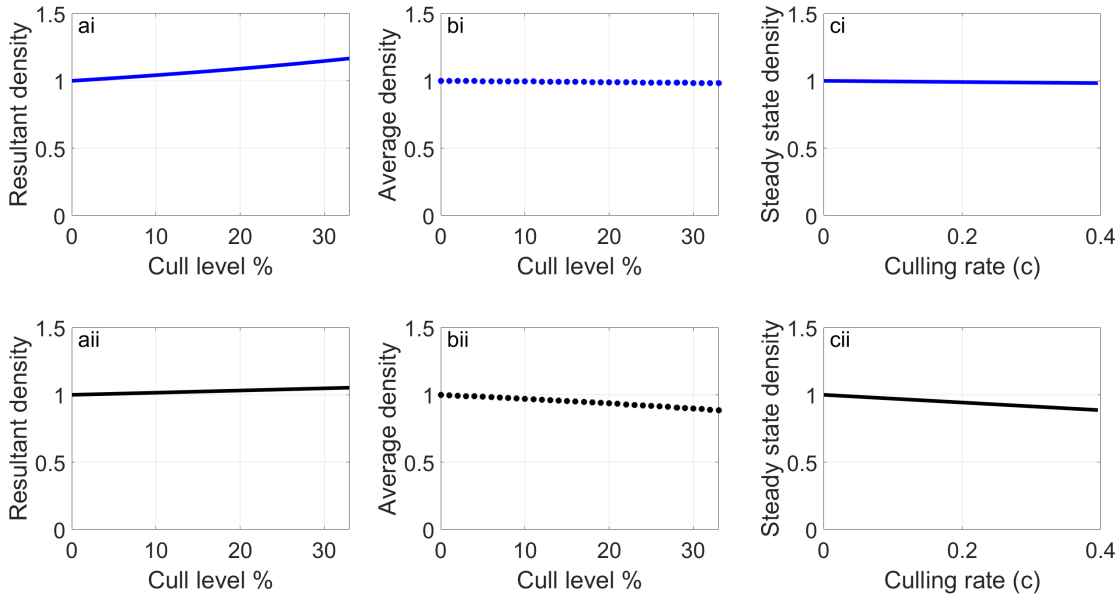

Figure 5A.4: The population density response to culling for a range of culling levels in a SI framework for: (a),(b) a discrete annual cull and (c) continuous culling where culling rate $c = \log\left(\frac{1}{1-\delta}\right)$ where δ is the equivalent discrete culling rate for (i) DD transmission and (ii) FD transmission. The change in population density is shown for the total population density (blue for DD (i), black for FD (ii)). (a) shows the resultant total population density after discrete annual culling and (b) shows the annual average total population density for the discrete cull, calculated by trapezium rule for the results obtained numerically over each regrowth period post the culling event. (c) shows the steady state total population density for the continuous culling model. Other parameters are as Figure 5.1a(ii) in the main paper.

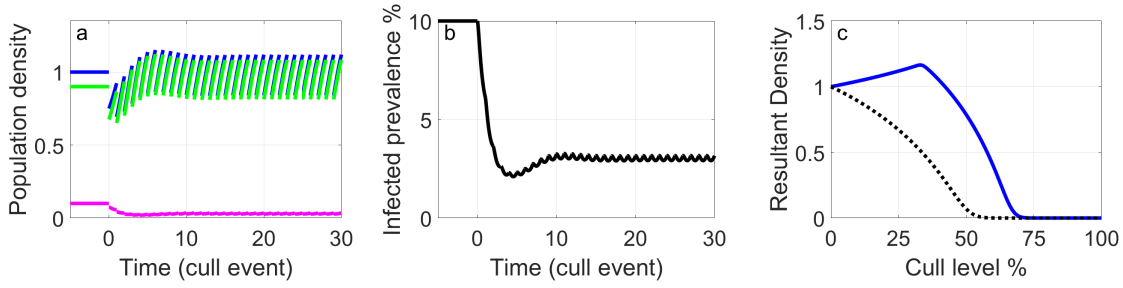

Figure 5A.5: The population density and infected prevalence ($\frac{I}{N}$) response to culling in an SI framework with free-living transmission for Equations (5A34). (a) shows the change in total population density (blue); the total density of susceptibles (green); and the total density of infected(magenta). (b) shows the change in disease prevalence over the cull events. (c) shows the resultant population density after 30 cull and subsequent regrowth events for different levels of culling for the free-living model (blue) and the demographic effects only model (Equation (5.3)) (dotted). Results are shown for a virulent infection, $\alpha = 4$, and an initial endemic disease prevalence of $p_i = 10\%$. Free-living particles are excreted at rate $\lambda = 1$ and decay at rate $\mu = 6$. Other parameters are as Figure 5.1a(ii) in the main paper.

rate μ. Susceptibles become infected through contact with the free-living parasite such that each susceptible is equally exposed and infection occurs with transmission rate function $\theta_F(F)$. We incorporate this new class into our SI framework (main paper Equations (5.1) with $\gamma = 0$), and normalise to achieve the endemic steady state N_e for a particular disease prevalence p_i, such that q takes the same value as the SI model. For this FL model we obtain the following system of ordinary differential equations:

$$\frac{\mathrm{d}S}{\mathrm{d}t} = bN(1 - qN) - dS - \theta_F(F)S \tag{5A34a}$$

$$\frac{\mathrm{d}I}{\mathrm{d}t} = \theta_F(F)S - dI - \alpha I \tag{5A34b}$$

$$\frac{\mathrm{d}F}{\mathrm{d}t} = \lambda I - \mu F \tag{5A34c}$$

$$\theta_F(F) = \frac{\mu}{\lambda}\frac{(d+\alpha)}{N_e\,(1-p_i)}F. \tag{5A34d}$$

Figure 5A.5 shows that culling populations suffering disease transmitted by free-living particles (Equations (5A34)) generates a similar compensatory response as seen for DD transmission (main paper Figure 5.1ii). In particular, Figure 5A.5c and main paper Figure 5.3b(i) for FL and DD transmission respectively demonstrate that this response is qualitatively similar for all levels of culling.

5A.4 The impact of targeted culling of infecteds

The results in the main paper focus on indiscriminate culling based on the assumption that identifying infected individuals for a targeted cull is not practicable in most settings. Here we investigate the effect on compensatory growth when only infecteds are targeted for culling. In particular in the continuous model (Equations (5A6)) we set $c_I > 0, c_S = c_R = 0$.

5A.4.1 Continuous targeted infected culling steady states

In a similar fashion to Appendix 5A.2 we derive steady state solutions for continuous targeted infecteds culling (Equations (5A6)) with $c_I > 0, c_S = c_R = 0$) to derive conditions when targeted culling induces over-compensation in the total population.

5A.4.2 Steady states for continuous targeted infected culling with DD transmission

Under DD transmission the steady state, N_{DD}^T, for the full DD model is:

$$N_{DD}^T = N_e\left[1-\zeta p_i\right]\left[1+\frac{c_I}{d+\alpha+\gamma}\right]\left[\frac{\alpha+c_I}{\alpha+c_I+\zeta d-\zeta b\left(N_{DD}^T\right)}\right] \tag{5A35}$$

$$\text{where} \quad \zeta = \frac{d+\eta+\gamma}{d+\eta} \tag{5A36}$$

Rearranging, we find that for the condition $N_{DD}^T > N_e$ to hold then the following condition on the birth function must also hold:

$$b\left(N_{DD}^T\right) < d+\alpha p_i + \frac{c_I}{\zeta(d+\alpha+\gamma)}\left[\zeta p_i(d+\alpha+\gamma)-(\alpha+c_I)(1-\zeta p_i)\right] \tag{5A37}$$

By definition if $N_{DD}^T > N_e$ then $b\left(N_{DD}^T\right) < b(N_e)$, therefore for targeted infected culling to induce a rise in population density the culling rate must satisfy the following threshold:

$$c_I > \frac{\zeta p_i(d+\alpha+\gamma)-\alpha(1-\zeta p_i)}{1-\zeta p_i} \tag{5A38}$$

Note that this threshold may be < 0 implying that any level of targeted culling will result in an increase in population above the endemic steady state. Also, as γ grows, this culling threshold grows, ameliorated by the rate of loss of immunity η so that for a sufficiently low rate of recovery or high loss of immunity, targeted culling will result in an increase in population density.

5A.4.3 Steady states for continuous targeted infected culling with FD transmission

Under FD transmission the steady state, N_{FD}^T, for the full model satisfies:

$$b\left(N_{FD}^T\right) = d+\alpha p_i + \frac{c_I}{\zeta(d+\alpha+\gamma)}\left[\zeta p_i(d+\alpha+\gamma)-(1-\zeta p_i)(\alpha+c_I)\right] \tag{5A39}$$

For the condition $N_{FD}^T > N_e$ to hold, we must have $b\left(N_{FD}^T\right) < b(N_e)$, and therefore the level of targeted culling must satisfy:

$$c_I > \frac{\zeta p_i(d+\alpha+\gamma)-\alpha(1-\zeta p_i)}{1-\zeta p_i} \tag{5A40}$$

the same condition as for DD transmission (Equation (5A38)). Therefore targeted infected culling under FD transmission will induce a rise in population density under the same model conditions as DD transmission.

5A.4.4 The relationship between N_{DD}^T and N_{FD}^T

We can further examine the relationship between N_{DD}^T and N_{FD}^T. Rearranging Equation (5A35) and from Equation (5A39) we find that:

$$b\left(N_{DD}^T\right) - b\left(N_{FD}^T\right) = \left[1 - \frac{N_e}{N_{DD}^T}\right] \frac{(\alpha + c_I)(1 - \zeta p_i)(d + \alpha + \gamma + c_I)}{\zeta(d + \alpha + \gamma)} \tag{5A41}$$

From Equation (5A41) we see that when $N_{DD}^T > N_e$ (for the appropriate level of c_I specified by Equations (5A38) and (5A40)) then $b\left(N_{DD}^T\right) - b\left(N_{FD}^T\right) > 0$ and therefore for sufficiently large targeted infected culling (which is more likely when there is low recovery to immunity or high loss of immunity), $N_{FD}^T > N_{DD}^T$. When $N_{DD}^T < N_e$ (when c_I does not satisfy the threshold specified by Equations (5A38) and (5A40)) then $b\left(N_{DD}^T\right) - b\left(N_{FD}^T\right) < 0$ and therefore when targeted culling is sufficiently low, or there is sufficiently high recovery to immunity and sufficiently low loss of immunity, $N_{FD}^T < N_{DD}^T$.

5A.4.5 Conclusion, the relationships between N_{DD}^T, N_{FD}^T and N_e

In summary, for diseases with no or short-lived immunity and a sufficient level of targeted infected culling

$$N_{FD}^T > N_{DD}^T > N_e \tag{5A42}$$

and so continuous culling can lead to an increase in population density.

5A.4.6 Targeted infected continuous culling results for $b(N) = b(1 - qN)$

For illustration, we present results for the discrete and continuous model using the same birth function ($b(N) = b(1 - qN)$) as used for the discrete culling results presented in the main paper. Figures 5A.6 and 5A.7 show the population response for discrete targeted culling for both SI and SIR models with DD and FD transmission. Note the same culling rate is used in indiscriminate culling and targeted culling, so that the culling effort is the same however there are a greater number of individuals culled during indiscriminate culling. Also, for discrete targeted culling, we also modify the rate of culling in the demographic effects only model to be multiplied by p_i to remove the equivalent number of infecteds at the endemic steady state. For the SI model targeting infecteds only for DD transmission leads to compensatory growth (Figure 5A.6a(i) & Figure 5A.7a(i)), but the compensatory effect is lower than with indiscriminate culling. For FD transmission (Figure 5A.6b(i) & Figure 5A.7b(i)), culling infecteds causes a greater

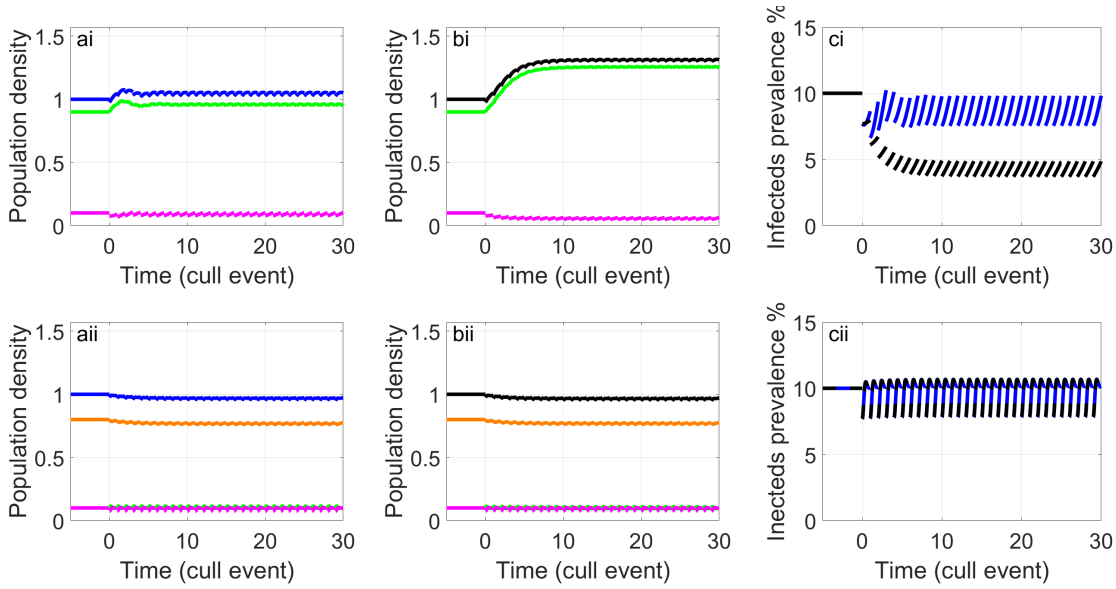

Figure 5A.6: The population density and infected prevalence ($\frac{I}{N}$) response to targeted culling of 25% of infecteds only for Equations (5.1)). (i) shows results for the SI model, (ii) shows results for SIR model and (a) for DD transmission and (b) for FD transmission. Results show the total population density (blue for DD (a), black for FD (b)); the total density of susceptibles (green); the total density of infected (magenta); and the total density of recovered/immune (orange). (c) shows the disease prevalence for DD transmission (blue) and FD transmission (black), noting the prevalence response to culling is near identical for DD and FD transmission. Parameters are as in the main paper Figures 5.1ii & 5.1iv for the SI model and the SIR model respectively.

release from disease-induced mortality as this causes a greater reduction in the force of infection. This leads to increased compensatory growth and a greater reduction in disease prevalence than for indiscriminate culling (Figure 5A.6c(i) black line).

For the SIR model, targeting infecteds brings no resultant compensatory growth for discrete culling (Figures 5A.7a(ii) & 5A.7b(ii)), but also does not cause large population depletion (Figures 5A.6a(ii) & 5A.6b(ii)) as with indiscriminate culling. This is the same for both DD transmission and FD transmission. This is because targeted culling does not deplete the level of recovered and immune individuals in the population.

In the continuous model with targeted culling ($c_I > 0, c_S = c_R = 0$) the steady

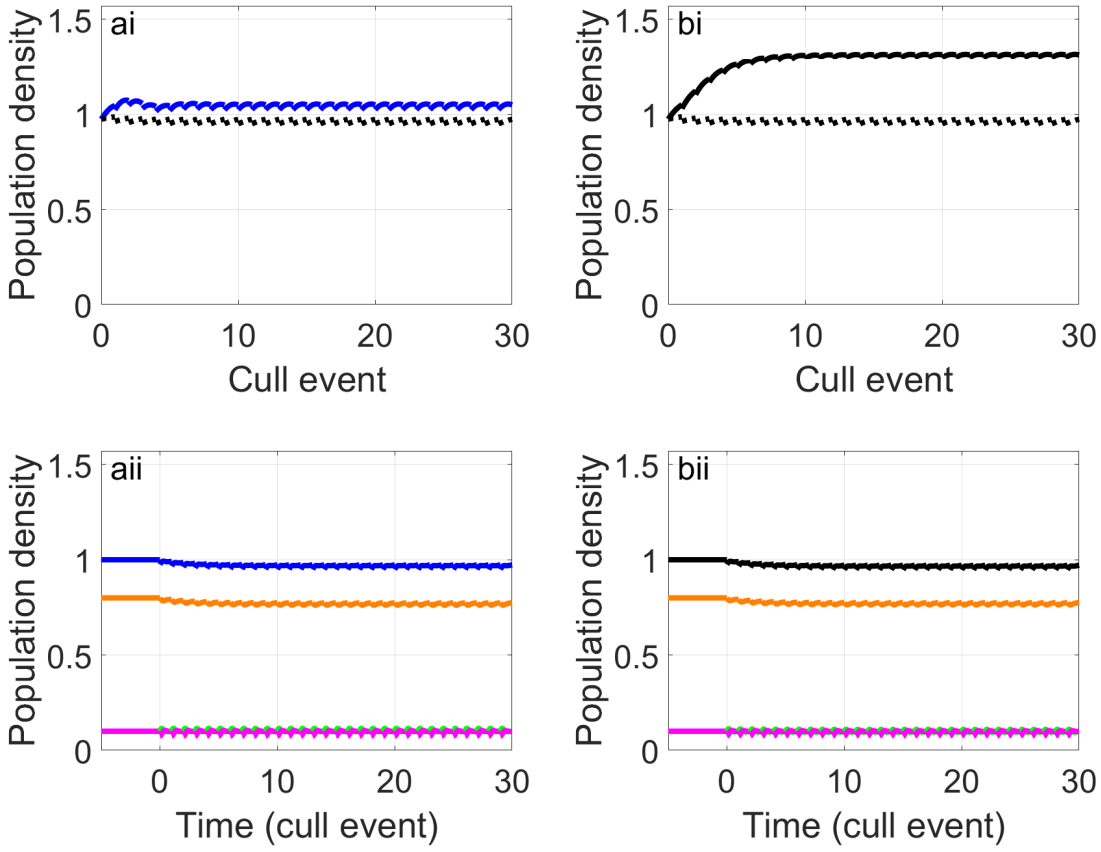

Figure 5A.7: The resultant population density after 30 sequential discrete cull and subsequent regrowth periods for (i) the SI model and (ii) the SIR model for targeted culling 25% of infecteds only and an equivalent cull of $0.25 \times p_i$ in the demographic effects only model (Equation (5.3)). (a) shows results for DD transmission (blue) and the demographic effects only model (black dotted) and (b) shows results for FD transmission (black) and the demographic effects only model (black dotted). Parameters are as in the main paper Figures 5.1ii & 5.1iv for the SI model and the SIR model respectively.

states can be determined analytically. For DD transmission these are

$$S^T_{DD} = \frac{d+\alpha+\gamma+c_I}{\beta} \qquad \text{where} \quad \beta = \frac{d+\alpha+\gamma}{N_e\left(1-p_i\dfrac{d+\gamma}{d}\right)} \tag{5A43}$$

$$N^T_{DD} = \frac{d}{2bq(\gamma+d)}\left[b\frac{d+\gamma}{d} - d - \alpha - \gamma - c_I + \right. \tag{5A44}$$

$$\left. \sqrt{\left(b\frac{d+\gamma}{d} - d - \alpha - \gamma - c_I\right)^2 + 4bqS^T_{DD}\frac{\gamma+d}{d}(\alpha+c_I)} \right] \tag{5A45}$$

The total population steady state for the demographic effects only model is:

$$N^T_{dem} = \frac{b-d-\alpha p_i - p_i c_I}{bq} \tag{5A46}$$

The steady state for the disease effects only model is:

$$S^T_{dis} = \frac{d+\alpha+\gamma+c_I}{\beta} \qquad \text{where} \quad \beta = \frac{d+\alpha+\gamma}{N_e\left(1-p_i\dfrac{d+\gamma}{d}\right)} \tag{5A47}$$

$$N^T_{dis} = S^T_{dis}\frac{d(\alpha+c_I)}{d(d+\alpha+\gamma+c_I)-(\gamma+d)b(1-qN_e)}. \tag{5A48}$$

For FD transmission and targeted culling the steady state is:

$$S^T_{FD} = \frac{(d+\alpha+\gamma+c_I)^2}{bq\beta^2}\left[\frac{b\beta}{d+\alpha+\gamma+c_I}+\frac{d}{d+\gamma}(\alpha+c_I-\beta)\right] \tag{5A49}$$

$$N^T_{FD} = \frac{\beta}{(d+\alpha+\gamma+c_I)}S^T_{FD} \qquad \text{where} \quad \beta = \frac{d+\alpha+\gamma}{\left(1-p_i\dfrac{d+\gamma}{d}\right)} \tag{5A50}$$

Figure 5A.8 shows the same set of results for the total population steady states as Figure 5A.2 with targeted culling of infecteds. For the SI model as the culling rate of infecteds increases, compensation due to the change in disease dynamics also increases under DD transmission (Figures 5A.8a(i) & 5A.8b(i)) and to a greater extent under FD transmission (Figures 5A.8c(i) & 5A.8d(i)). For DD transmission we again note that disease effects drive the majority of the compensation in response to culling. For the SIR model for DD transmission (Figures 5A.8a(ii) & 5A.8b(ii)) both the full model and the demographic effects only model show no change in steady state density as the targeted culling of infecteds grows, however the disease effects only steady population density reduces as targeted culling of infecteds grows. For FD transmission (Figures 5A.8c(ii) & 5A.8d(ii)) there is no compensatory growth due to disease dynamics. We note that in our illustrative results we set parameters $\alpha = 4$, $d = 0.5$, $p_i = 0.1$, $c_I = 0.25$, $\eta = 0$ and $\gamma = 0$ or $\gamma = 4$ for SI or SIR models respectively. The threshold specified in Equation (5A38) is therefore $c_I > 0$ for SI models and $c_I > 72.5$ for SIR models and therefore predict that there will be over-compensation for the SI results and not for the SIR results as shown in the figures. The results for continuous targeted culling confirm the results for targeted culling in the discrete model (Figure 5A.7).

5A.5 Density dependent mortality

Our system formulation (main paper Equations (5.1)) models the population growth function with density dependent birth. To examine whether density dependent death impacts the compensatory growth effect that we present in the main paper we also consider results for a similarly formulated system that includes density dependent death. We modify Equations (5.1) to include non-negative parameters q_b and q_d which control the levels of density dependent birth and death (notably a positive q_d

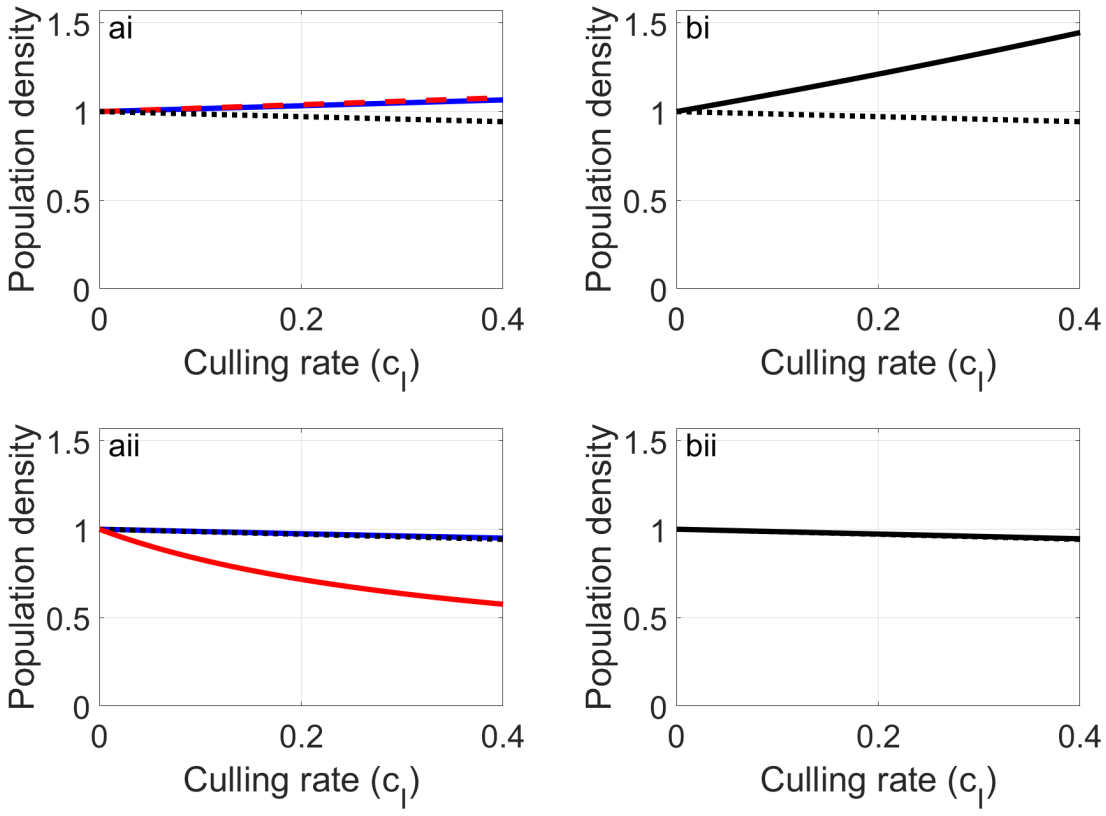

Figure 5A.8: Results for the model with targeted infected cull level c_I for the continuous disease model (Equations 5A6) with $b(N) = b(1-qN)$ for (i) the SI model and (ii) the SIR model. The steady state density N is shown for DD transmission in (a): for the full model (blue); the disease effects only model (red); and the demographic only model (black dotted). The steady state density N is shown for FD transmission in (b) for the full model (black) and demographic only model (black dotted). Parameters are as in the main paper Figures 5.1ii & 5.1iv for the SI model and the SIR model respectively.

indicating a level of density dependent death):

$$\frac{\mathrm{d}S}{\mathrm{d}t} = b(1-q_bN)N - d(1+q_dN)S - \theta_D(I,N)S \tag{5A51a}$$

$$\frac{\mathrm{d}I}{\mathrm{d}t} = \theta_D(I,N)S - d(1+q_dN)I - \alpha I - \gamma I \tag{5A51b}$$

$$\frac{\mathrm{d}R}{\mathrm{d}t} = \gamma I - d(1+q_dN)R \tag{5A51c}$$

Considering the system without recovery (an SI framework), but maintaining the same disease-free steady state and endemic steady state $N = N_e$ where $I_e = p_iN_e$ and $S_e = (1-p_i)N_e$, the transmission function $\theta_D(I,N)$ is defined for DD and FD

transmission as:

$$\text{DD transmission}: \quad \theta_D(I,N) = \frac{(d\,(1+q_dN_e)+\alpha)}{N_e\,(1-p_i)}I \tag{5A52a}$$

$$= \frac{(b\,(1-q_bN_e)+(1-p_i)\alpha)}{N_e\,(1-p_i)}I \tag{5A52b}$$

$$\text{FD transmission}: \quad \theta_D(I,N) = \frac{(d\,(1+q_dN_e)+\alpha)}{(1-p_i)}\frac{I}{N} \tag{5A52c}$$

$$= \frac{(b\,(1-q_bN_e)+(1-p_i)\alpha)}{(1-p_i)}\frac{I}{N}. \tag{5A52d}$$

where, to achieve the required steady states, q_b and q_d must satisfy:

$$q_d = \frac{b-d-\alpha p_i - bq_bN_e}{dN_e} \tag{5A53a}$$

$$0 \leq q_b \leq \frac{b-d-\alpha p_i}{bN_e}. \tag{5A53b}$$

q_b and q_d are therefore constrained by each others value in this model such that when q_b takes values between 0 to $\frac{b-d-\alpha p_i}{bN_e}$, correspondingly q_d takes values from $\frac{b-d-\alpha p_i}{dN_e}$ to 0. Thus, when $q_b = 0$ we have a system with only density dependent death, when $0 < q_b < \frac{b-d-\alpha p_i}{bN_e}$ we have a system with both density dependent birth and density dependent death and when $q_b = \frac{b-d-\alpha p_i}{bN_e}$ then $q_d = 0$ and we recover our original model formulation with only density dependent birth.

Varying values of q_b from 0 to $\frac{b-d-\alpha p_i}{bN_e}$ (i.e. from having zero density dependence on birth and density dependent death only to zero density dependence on death and density dependent birth only) we examine the effect of the difference between the model that includes epidemiological dynamics (Equations (5A51)) and a corresponding demographic effects only model containing the equivalent density dependent birth and death formulations as follows:

$$\frac{\mathrm{d}N}{\mathrm{d}t} = bN(1-q_bN) - d(1+q_dN)N - \alpha p_iN. \tag{5A54}$$

Figure 5A.9 shows that culling generates compensatory growth due to disease dynamics regardless of the level of density dependent birth relative to density dependent death except in the singular case where there is density dependent death only under FD transmission. Figure 5A.9a shows that varying q_b has no effect on the resultant population density following culling for DD transmission. The results reported in the main text therefore hold under DD transmission. Our results also hold under FD transmission except in the singular case when $q_b = 0$, indicating that there is density dependent death only.

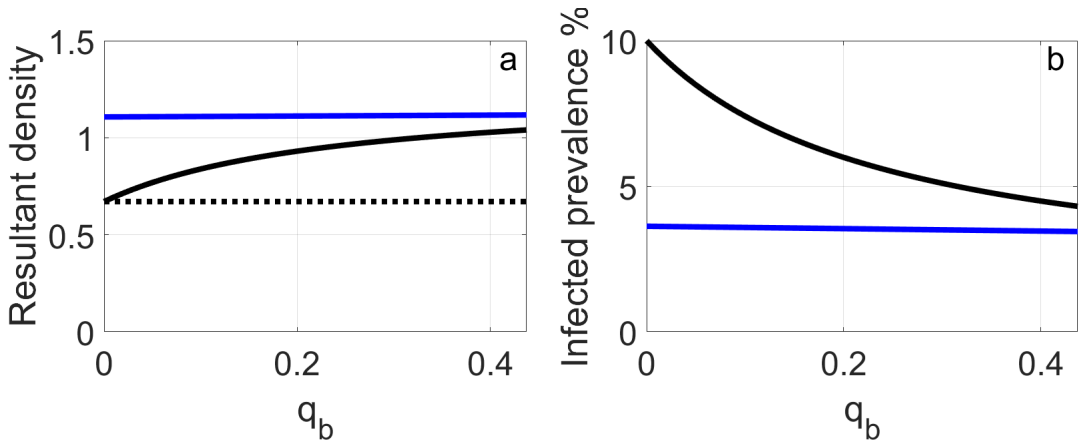

Figure 5A.9: The resultant population density and infected prevalence ($\frac{I}{N}$) after 30 sequential cull and subsequent regrowth periods showing the response to 25% culling in an SI framework when varying q_b in Equations (5A51). q_b runs from $q_b = 0$ representing density dependent death only to $q_b = \dfrac{b-d-\alpha p_i}{bN_e}$ representing density dependent birth only which is equivalent to the original model (SI framework Equations (5.1)). (a) shows the resultant population density and (b) shows the change in infected prevalence as q_b varies for DD transmission (blue) FD transmission (black) and the demographic effects only model (Equation (5A54)) (black dotted). Results are shown for a virulent infection, $\alpha = 4$, and an initial endemic disease prevalence of $p_i = 10\%$. Other parameters are as Figure 5.1a(ii) in the main paper.

5A.5.1 Why the demographic effects only model remains invariant to changes in q_b

Figure 5A.9a shows that for the demographic effects only model (Equation (5A54)), the resultant population density following the culling regime does not vary as q_b varies. To explain this we substitute Equation (5A53a) into the demographic effects only model (Equation (5A54)) as follows:

$$\frac{\mathrm{d}N}{\mathrm{d}t} = bN(1-q_bN) - d(1+q_dN)N - \alpha p_iN \tag{5A55a}$$

$$= bN - N^2\left(bq_b + \frac{b-d-\alpha p_i - bq_bN_e}{N_e}\right) - dN - \alpha p_iN \tag{5A55b}$$

$$= bN - \frac{b-d-\alpha p_i}{N_e}N^2 - dN - \alpha p_iN \tag{5A55c}$$

$$= bN\left(1 - \frac{b-d-\alpha p_i}{bN_e}N\right) - dN - \alpha p_iN \tag{5A55d}$$

and thus we recover the original demographic effects only model from the main paper (Equation(5.3)). This shows that the change in population for this new formulation of the demographic effects model (Equation (5A54)) does not vary as q_b varies and therefore does not exhibit any change in behaviour from the original demographic effects only model (Equation (5.3)) in response to culling.

5A.5.2 Density dependent mortality with FD transmission

To understand why the model with FD transmission and no density dependent birth ($q_b = 0$) does not show any additional compensatory growth above the demographic effects only model (Equation (5A54)) we examine the rate of change of the disease prevalence for Equations (5A51).

$$\frac{\mathrm{d}}{\mathrm{d}t}\left(\frac{I}{N}\right) = \frac{N\frac{\mathrm{d}I}{\mathrm{d}t} - I\frac{\mathrm{d}N}{\mathrm{d}t}}{N^2} \tag{5A56a}$$

$$= \frac{1}{N^2}\Big[N\left(\theta_D S - d(1+q_d N)I - \alpha I\right) \tag{5A56b}$$

$$- I\left(b(1-q_b N)N - d(1+q_d N) - \alpha I\right)\Big] \tag{5A56c}$$

$$= \frac{1}{N^2}\left[\theta_D SN - \alpha I(N-I) - bNI(1-q_b N)\right] \tag{5A56d}$$

$$= \frac{I}{(1-p_i)N^2}\left[-b(I-p_i N) - bq_b(N_e S - N^2(1-p_i))\right] \tag{5A56e}$$

We see that when $q_b = 0$, an initial condition that satisfies $I = p_i N$ will give a solution that does not vary from this initial prevalence. Therefore, as our culling regime starts with an initial prevalence p_i, the prevalence of the disease throughout the culling regime does not change and therefore culling does not yield any compensatory growth due to reduction in disease mortality. Therefore the full model matches the demographic effects only model. When $q_b > 0$, we note that after an initial cull when the disease prevalence is still p_i (so that $I = p_i N$), the first term in Equation (5A56e) is zero and the second term is negative indicating that after the initial cull the prevalence will start to decrease leading to a reduction in disease-induced mortality in the population, supporting our results in the main paper.

5A.5.3 Density dependent mortality with DD transmission

Our result in Figure 5A.9 for DD transmission shows varying q_b does not affect the compensatory growth response to culling. We explain this by examining the rate of change of the population density N:

$$\frac{\mathrm{d}N}{\mathrm{d}t} = b(1-q_b N)N - d(1+q_d N)N - \alpha I \tag{5A57a}$$

$$= bN - bq_b N^2 - N\left[b - (b-d) + \frac{N}{N_e}(b - d - \alpha p_i - bq_b N_e)\right] - \alpha I \tag{5A57b}$$

$$= N\left[(b-d) - \frac{N}{N_e}(b - d - \alpha p_i)\right] - \alpha I \tag{5A57c}$$

which shows that the growth in population density is independent of the density dependent birth and death parameters, q_b and q_d. Therefore varying q_b has no effect on the population rate of regrowth following a cull. Also note that q_b has little

influence in affecting the resultant value of I as $S/(1-p_i) - N \simeq 0$. To compare with FD transmission we also examine the rate of change of the disease prevalence:

$$\frac{\mathrm{d}}{\mathrm{d}t}\left(\frac{I}{N}\right) = \frac{1}{N^2}\Big[N\left(\theta_D S - d(1+q_d N)I - \alpha I\right) \tag{5A58a}$$

$$- I\left(b(1-q_b N)N - d(1+q_d N) - \alpha I\right)\Big] \tag{5A58b}$$

$$= \frac{1}{N^2}\left[\theta_D SN - \alpha I(N-I) - bNI(1-q_b N)\right] \tag{5A58c}$$

$$= \frac{I}{N^2}\left[\frac{(b - bq_b N_e + \alpha(1-p_i))}{(1-p_i)N_e}SN - \alpha(N-I) - bN + bq_b N^2\right] \tag{5A58d}$$

$$= \frac{I}{N^2(1-p_i)N_e}\Big[-bN((1-p_i)N_e - S) \tag{5A58e}$$

$$- bq_b N_e N(S - (1-p_i)N) - \alpha(1-p_i)S(N_e - N)\Big] \tag{5A58f}$$

noting in Equation (5A58f), given the maximum value of q_b, that the first term is negative whilst S remains below the endemic susceptible density, the second term is negative whilst the infected prevalence is lower than the endemic prevalence and the third term is negative when N is below the total population endemic steady state. From this we can determine that a cull taking the population below the endemic steady state, and the susceptibles below the endemic susceptible density must lead to a reduction in disease prevalence, which therefore leads to a reduction in the proportion of the population suffering disease-induced mortality, supporting our results in the main paper.

5A.6 Parameter sensitivity

In Figure 5A.10 we undertake a parameter sensitivity analysis to assess the magnitude of the compensatory effect for a range of model parameters in the SI and SIR model framework: the level of disease-induced mortality α; the initial endemic prevalence p_i; and the cull period (the length of time between each sequential cull event). As intuitively expected for the SI model framework the compensatory effect (the difference between the dotted lines and solid line in Figure 5A.10) increases as virulence increases (Figure 5A.10a(i)) and as the initial disease prevalence, p_i, increases (Figure 5A.10b(i)) and as the culling period decreases (the frequency of culling increases) (Figure 5A.10c(i)). For the SIR model with FD transmission the disease induced negative impact of culling increases as the virulence and initial infected prevalence increases whereas there is less change in the impact under DD transmission (Figure 5A.10a(ii) & 5A.10b(ii)). The compensatory effect shows only low sensitivity to changes in the cull period for DD and FD transmission in the SIR model (Figure 5A.10c(ii)).

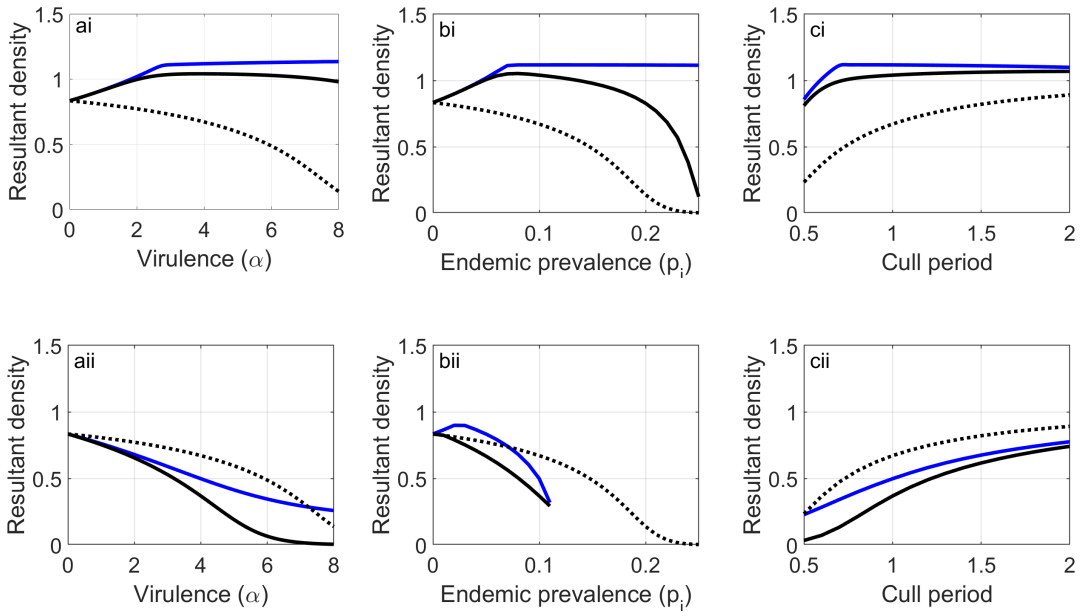

Figure 5A.10: Parameter sensitivity for main paper Equations (5.1). The resultant population density after 30 sequential cull (of 25% of the population) and subsequent regrowth periods for (i) the SI and (ii) the SIR model plotted against (a) virulence α, (b) initial endemic prevalence, p_i and (c) cull period (the time between sequential cull events) for DD transmission (blue), FD transmission (black) and the demographic effects only model (Equation (5.3)) (dotted line). The difference between the solid lines and dotted line represents the positive or negative compensatory effect due to changes in the disease dynamics. When not varied in the figures the parameters are $\alpha = 4$, $p_i = 10\%$ and cull period $= 1$. Other parameters are as in the main paper Figures 5.1ii & 5.1iv for the SI model and the SIR model respectively. Truncated results (bii) indicate parameter levels that do not obey requirements for valid solutions (Equations (5A4) & (5A5)).

5A.7 Wild boar TB model

We introduce a mathematical model that can represent the key processes influencing TB infection in wild boar in Spain. Our model reflects a single geographical managed estate containing a homogeneously mixed population covering an area representative of a hunting estate. The population density of wild boar is separated into different age classes to capture distinct disease and reproductive characteristics for piglets (aged 0-1 year) P, yearlings (aged 1-2 years) Y, and adults (aged 2 years+) A. Further, the age-classes are split into susceptible, infected and generalised (super-shedder) classes (subscripts S, I, G, respectively) to reflect the disease status of the population. The population dynamics of the wild boar TB system are represented by the following set of non-linear differential equations (which is an extension of classical disease modelling frameworks (see Anderson & May 1981 [7]; Keeling & Rohani 2008 [84])):

$$\frac{\mathrm{d}P_S}{\mathrm{d}t} =(b_Y(Y_S + Y_I) + b_A(A_S + A_I) + b_G(Y_G + A_G))(1 - qN) \tag{5A59a}$$

$$- mP_S - d_P P_S - \beta_P P_S F \tag{5A59b}$$

$$\frac{\mathrm{d}P_I}{\mathrm{d}t} =\beta_P P_S F - mP_I - d_P P_I - \varepsilon_P P_I \tag{5A59c}$$

$$\frac{\mathrm{d}P_G}{\mathrm{d}t} =\varepsilon_P P_I - mP_G - d_P P_G - \alpha P_G \tag{5A59d}$$

$$\frac{\mathrm{d}Y_S}{\mathrm{d}t} =mP_S - mY_S - d_Y Y_S - \beta_Y Y_S F \tag{5A59e}$$

$$\frac{\mathrm{d}Y_I}{\mathrm{d}t} =\beta_Y Y_S F + mP_I - mY_I - d_Y Y_I - \varepsilon_Y Y_I \tag{5A59f}$$

$$\frac{\mathrm{d}Y_G}{\mathrm{d}t} =\varepsilon_Y Y_I + mP_G - mY_G - d_Y Y_G - \alpha Y_G \tag{5A59g}$$

$$\frac{\mathrm{d}A_S}{\mathrm{d}t} =mY_S - d_A A_S - \beta_A A_S F \tag{5A59h}$$

$$\frac{\mathrm{d}A_I}{\mathrm{d}t} =\beta_A A_S F + mY_I - d_A A_I - \varepsilon_A A_I \tag{5A59i}$$

$$\frac{\mathrm{d}A_G}{\mathrm{d}t} =\varepsilon_A A_I + mY_G - d_A A_G - \alpha A_G \tag{5A59j}$$

$$\frac{\mathrm{d}F}{\mathrm{d}t} =\lambda(P_G + Y_G + A_G) - \mu F \tag{5A59k}$$

Here, N represents the total wild boar population. Susceptible and infected yearlings and adults give birth to susceptible piglets at rates b_Y and b_A respectively. Generalised yearlings and adults give birth to piglets at rate b_G. The total population is regulated through a crowding parameter, q, that acts to stabilise the total population to a carrying capacity, $N = K$, in the absence of disease. Maturity from piglets to yearlings and yearlings to adults occurs at rate m and piglets, yearlings and adults may die of natural causes at rates d_P , d_Y , d_A respectively. Here we assume $d_P = d_Y = d_A$.

The prime driver for infection in the wild boar TB system is through environmental contact with free-living MTC particles, with density F. We assume that free-living particles are shed from generalised wild boar at rate λ and decay at rate μ. Susceptibles may become infected through contact with free-living MTC particles with transmission coefficients β_P, β_Y and β_A and infecteds can progress to the generalised class at rates ε_P, ε_Y and ε_A for the different age classes respectively. We assume that individuals in the generalised class suffer an additional disease-induced mortality at rate α. We assume piglets and yearlings are more susceptible to MTC infection than adults and so set $\beta_P = \beta_Y$, which we assume to be three times greater than transmission for adults, $\beta_A = 3\beta_Y$. Similarly we set

the rate of progression to generalised infection for piglets and yearlings to be the same, $\varepsilon_P = \varepsilon_Y$, and three times the rate for adults, $\varepsilon_A = \frac{1}{3}\varepsilon_Y$. In this way we have set the model so that the yearling class is the same as the piglet class in terms of disease characteristics, but the yearling class is the same as the adult class in terms of reproductive processes.

5A.7.1 Wild boar TB model parameters

We set the model parameters to be representative of the wild boar TB system in Central Spain [48]. The parameters are as follows:

$b_Y = b_A = b_G = \log(4)$ The population birth rate in a disease-free population when resources are unlimited. This constant rate means that for each reproductive member of the population, 3 piglets will be born, averaged over the population over a year. (This has been derived by assuming that there is a 50% sex ratio and that each female produces an average of 6 offspring per year when resources are not limited.) Units: $year^{-1}$.

$K = 500$ The carrying capacity for the total population in the target area in the absence of disease. Units: $population \times area^{-1}$.

$q = \frac{1}{K}\left(1 - \frac{d_A(d_P+m)(d_Y+m)}{m(b_A m + b_Y d_A)}\right)$ This parameter limits the total population to the carrying capacity K in the populated disease-free steady state, and is derived from steady-state analysis of the model without infection. Units: $density^{-1}$.

$m = 1$ The rate that piglets mature to yearlings and yearlings mature to adults. These rates assume that it takes on average 1 year to enter the next age class. Units: $year^{-1}$.

$d_P = d_Y = d_A = \frac{1}{7}$ The natural death rate of all classes which implies an average life expectancy of 7 years. Units: $year^{-1}$.

$\beta_P = \beta_Y = c_\beta \beta_A = \frac{20}{K}$ The infection rates are fitted to give prevalence levels observed in the wild boar TB system in central Spain. We assume that $c_\beta = 3$ and so disease transmission to piglets and yearlings is three times that of the adult rate under the assumption that transmission is higher for piglets and yearlings than it is for adults. Units: $density^{-1} \times year^{-1}$.

$\varepsilon_P = \varepsilon_Y = 2$ The rate that infected piglets and yearlings become generalised. This assumes that it takes on average 6 months for an infected piglet or yearling to progress to the generalised class. Units: $year^{-1}$.

$\varepsilon_A = 2/3$ This is the rate that infectious adults become generalised. This assumes that it takes on average 18 months for an infected adult to progress to the generalised class. Units: $year^{-1}$.

$\alpha = 1$ This is the additional disease induced death rate of the generalised class and assumes that on average individuals spend 1 year in the generalised class before death. Units: $year^{-1}$.

$\lambda = 1$ The rate of shedding of infectious particles by generalised classes. We normalise this value to 1. This is valid as we have explored a range of values for β_P, β_Y and β_A which scale with the size of λ and the density of free-particles, F. Units: $year^{-1}$.

$\mu = 6$ This is the decay rate for free-living particles, indicating that they have an average life expectancy of 2 months. Units: $year^{-1}$.

Chapter 6

Wild boar model with predation

Figure 6.1: Wolf (*Canis lupus*).

The wild boar TB model introduced in Chapter 3 is tuned specifically to central Spain and the environmental issues that affect disease transmission for this region. In Asturias, in the north-west of Spain, wild boar densities are increasing whilst TB infection is endemic but at low prevalence. Within this area there are also a number of well-established wolf packs (*Canis lupus*, Figure 6.1) which are known to prey on wild boar. In this chapter we investigate the relationship between wolf predation and the control of TB infection in Asturias, and use this understanding to hypothesize the effect of the introduction of a predator on wild boar populations suffering endemic TB in areas of high prevalence such as central Spain. This work has been accepted for publication by Scientific Reports, to be titled 'Wolves contribute to disease control in a multi-host system' by Eleanor Tanner, Andy White, Pelayo Acevedo, Ana Balseiro, Jaime Marcos and Christian Gortázar. I played the lead role in developing this work and writing the article and undertook the mathematical modelling and analysis. The paper is reproduced here verbatim, with contents as

in the original submission to Scientific Reports. The supplementary information to the paper is contained in Appendices 6A.1-6A.2.

6.1 Abstract

We combine model results with field data for the case study system of wolves (*Canis lupus*) that prey on wild boar (*Sus scrofa*), a wildlife reservoir of tuberculosis, to examine how predation may contribute to disease control in multi-host systems. Results show that predation can lead to a marked reduction in the prevalence of infection without leading to a reduction in host population density since mortality due to predation can be compensated by a reduction in disease induced mortality. A key finding therefore is that a population that harbours a virulent infection can be regulated at a similar density by disease at high prevalence or predation at low prevalence. Predators can therefore provide a key ecosystem service which should be recognised when considering human-carnivore conflicts and the conservation and re-establishment of carnivore populations.

6.2 Introduction

Infectious agents that can be transmitted to more than one host species form the majority of pathogens that infect wildlife, domestic and human systems [80]. Wildlife species play a key role in maintaining reservoirs of infection [42] and therefore disease management requires strategies to reduce transmission of pathogens from wildlife reservoirs to target hosts [80]. It has been shown that predation may contribute to disease control in multi-host systems leading to reduced spillover to livestock and human populations [111, 110]. Therefore predators can provide a key ecosystem service that is often underappreciated by society [122, 91].

Mathematical models have played a key role in uncovering the potential of predators to control zoonotic disease. Here, theory has shown that predators may act to alter the epidemiological dynamics to decrease infected and increase susceptible host density and thereby reduce prevalence [110, 4, 62]. Furthermore, selective predation on infected individuals can reduce the force of infection and in extreme scenarios prevent pathogen establishment [77, 143]. However, model analysis has also outlined scenarios in which predation may lead to an increase in disease prevalence – notably when the disease induces a long-lasting immune response [81]. This highlights the importance of understanding the case-specific infection dynamics of pathogens in reservoir populations that are subject to predation. Empirical evidence to underpin the theory on the interplay between predation and host infection is however limited. Hudson *et al.* (1998)[82] suggested that macroparasite incidence in grouse (*Lagopus lagopus scotica*) populations decreased when predator

levels increased and Levi *et al.* (2012)[92] showed that increases in the incidence of Lyme disease correlated with a decline in small mammal predators. More recently, observational and experimental studies have indicated that parasites can increase host susceptibility to predation ([62, 5]; see [109] for a recent review). Therefore combining theory and empirical data at the system specific level has the potential to further clarify the role of predation in the control of infectious disease reservoirs in wildlife [91]. We investigate this by combining model results with field data for the case study system of wolves (*Canis lupus*), that prey on wild boar (*Sus scrofa*), a reservoir of tuberculosis, in Asturias in northern Spain.

Animal tuberculosis (TB), caused by infection with *Mycobacterium bovis* and closely related members of the *M. tuberculosis* complex (MTC), is a widespread multi-host infection with a profile of moderately increasing prevalence among cattle herds in infected regions of western Europe (from 1.05% in 2010 to 1.49% herd prevalence in 2015; [100]). TB causes severe economic losses to the livestock industry due to movement restrictions and compulsory test and slaughter schemes [127, 70]. TB also causes host mortality [12] and creates conservation concerns [75, 76]. The role of wildlife reservoirs in maintaining TB is now well recognised with reservoir species including cervids in North America, European badgers (*Meles meles*) in the British Isles, brushtail possums (*Trichosurus vulpecula*) in New Zealand and buffalo (*Syncerus caffir*) in South Africa, among others [70, 56]. In Europe, and in particular on the Iberian Peninsula, infection is maintained in a complex network of domestic and wild hosts, including abundant wild ungulates such as the Eurasian wild boar which acts as the primary reservoir of infection [70, 106, 71].

In multi-host settings, TB control at the wildlife-livestock interface often targets aspects such as direct and indirect contacts between host species [15, 88, 146] and TB control in reservoir hosts [48]. It has been shown that culling of wild boar can reduce TB prevalence in wild boar and sympatric host species [23, 59]. However, the role of ecosystem functioning in regulating infection transmission has not been assessed in detail. The wolf is the most widely distributed top predator of the northern hemisphere [32] where wild boar and deer are its main prey [101, 37] and wolf presence has been linked with lower ungulate prey densities [122]. It has also been found that when wolf populations decrease, wild boar populations tend to increase ([125, 63]; but see [98]). Mathematical modelling studies have suggested that wolves may contribute to disease control in their prey in the case of Chronic Wasting Disease in North American deer (*Odocoileus sp*) [143]. Moreover, empirical evidence suggested that anthrax infection in bison (*Bison bison*) might increase wolf predation risk ([21]). It has also been suggested that pathogens targeting the lung may predispose ungulate prey to wolf predation [99, 83]. Hence, maintaining viable wolf populations might contribute to disease control in wildlife and thereby reduce transmission from wildlife reservoirs.

Asturias, in north-western Spain, is a region with an established wolf population that occupies two-thirds of the region [69]. TB is present in Asturias although the current overall prevalence in wild boar (2-13%) and the level of generalised cases (17% from tests on 6 infected individuals) are lower than in TB-endemic regions of southern Spain where TB prevalence can be >50% (with 80% prevalence reported in some regions; [137]) and where a greater proportion (58%) of infected individuals are generalised [102]. Asturias is also a cattle-breeding region, with 360,735 heads in 16,312 herds in 2014 and TB is one of the main concerns of cattle farmers [39, 36]. However, the potential role of wolf predation as a natural regulator of disease in wild ungulates is not widely recognised by farmers [131]. Asturias can therefore be used as a case study region in which to test the impact of wolf predation on TB prevalence in a wildlife reservoir species (wild boar) and on TB control in the target species (cattle).

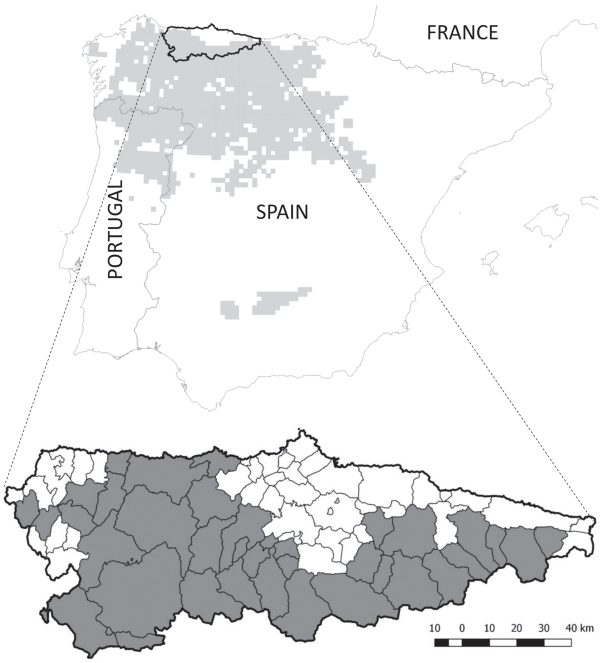

Figure 6.2: Wolf (*Canis lupus*) distribution maps where the distribution in the Iberian Peninsula is shown in light grey [112, 19] expanded to show the municipalities in Asturias, northern Spain, where wolves are present (dark grey) or absent (white).

In this study we combine field observations from Asturias with mathematical modelling to test the hypothesis that wolf presence may contribute to TB control. The results provide important insights into the role predators can play in disease control and therefore inform on the debate related to human-carnivore conflicts and the conservation and re-establishment of carnivore populations [122, 91, 135, 104].

6.3 Methods

6.3.1 Ethics statement

All animal sampling took place post-mortem. The wildlife samples were obtained from hunter-harvested individuals that were shot in the legal hunting seasons and independently and prior to our research. According to EU and National legislation (2010/63/UE Directive and Spanish Royal Decree 53/2013) and to the University of Castilla-La Mancha guidelines, no permission or consent is required to conduct the research reported herein.

6.3.2 Study area and target species

Asturias, a province of 10,604 km^2, is located in northwestern Spain (Figure 6.2). Wolf population data were obtained from the Asturias Government. Wolf presence is established in two-thirds of Asturias. In the remaining third, containing the majority of coastal regions and the urban and industrial corridors in the centre-north-east of the region (Figure 6.2; [112, 19]), wolves are absent or only sporadically recorded. Wolf monitoring is conducted during the breeding period and allows for an estimate of wolf population size. We combine the estimate of wolf abundance for 2003-2004[68] with data on wolf attack rate on livestock to give a profile of wolf abundance from 2000 to 2014. The regional government also records the number of wild boar harvested on hunting sites annually [117]. Hunting is predominantly non-commercial and traditional among rural inhabitants taking place in 17 game reserves and 60 municipal hunting estates, covering 91% of the province [117]. After standardisation by hunting effort, hunting bag statistics can be used as reliable indices of wild boar relative abundance [24]. We use data describing the temporal variation in the number of wild boar annually hunted (Figure 6.3) and in particular generate estimates of wild boar population abundance in 2000-01 and 2013-14.

6.3.3 TB prevalence

We used serum antibodies against the MTC as an indicator of TB prevalence in wild boar. Serum samples were tested by means of an indirect ELISA using bovine-purified protein derivative (bPPD) following the protocol previously described in Boadella *et al.* (2011)[22]. Sample results were expressed as an ELISA percentage (E%) that was calculated using the formula [Sample E% = (sample OD/2 x mean negative control OD) x 100]. Serum samples with E% values greater than 100 were considered positive. Wild boar TB prevalence was available at the municipality level from 2000 to 2014. All cattle herds are tested annually for TB by individual skin testing. This testing is performed and recorded by the Asturias

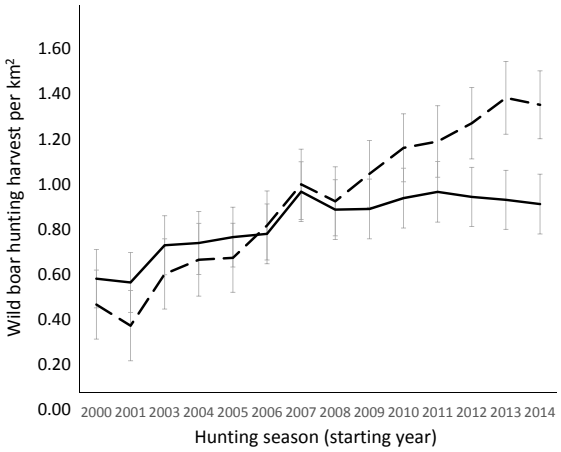

Figure 6.3: The mean annual wild boar hunting harvest/km^2 in Asturias, for the period 2000-2014. The dotted line represents areas where wolves are absent and the solid line those where wolves are present. Bars represent 95% confidence intervals.

Government. Individual and herd-level data on cattle TB was available from 2005 to 2014, at the municipality scale.

6.3.4 Asturias: estimating wolf population

We derive an estimate of wolf population abundance for the period 2000-2014 as follows. We use data on wolf population abundance for the period 2003-2004 [68] to obtain an estimate of 252 wolves in Asturias in 2004. We fit a least squares regression on wolf attack rate data for the period 2000-2014 (Figure S1) to give a rate of increase of wolf abundance. Combining this rate of increase with our wolf abundance estimate for 2004 we estimate that wolf numbers increase linearly from 196 in 2000 to 392 in 2014.

6.3.5 Mathematical Modelling

We develop a mathematical model that represents the interaction between wild boar, MTC infection and predation. In the model we set disease transmission rates and the wild boar intraspecific competition parameter so the model matches observations for the prevalence of infection and for wild boar density in 2000 and 2014 for the regions of Asturias with wolves. The model findings are extended to consider the areas of Asturias in which wolves are absent, to assess the role of future wolf density in TB control and the potential impact of wolf predation on TB in regions where TB is endemic and prevalence is high.

We separate the population density of wild boar into different age classes to capture distinct disease and reproductive characteristics for piglets (aged 0-1 year) P, yearlings (aged 1-2 years) Y, and adults (aged 2 years+) A. Further, the age-classes are split into susceptible, infected and generalised classes (subscripts

S, I, G, respectively) to reflect the disease status of the population. Generalised individuals can also release free-living pathogen with density F into the environment. This model framework has been used successfully to understand the impact of vaccination on TB prevalence in the wild boar TB system [48]. The model also includes predation by wolves, W, and we assume a range of scenarios of wolf density change. The population dynamics of the wild boar, TB and wolf system are represented by the following set of non-linear differential equations (which is an extension of classical disease modelling frameworks [7, 84]).

$$\frac{\mathrm{d}P_S}{\mathrm{d}t} = b_A(Y+A)(1-qN) - mP_S - d_P P_S - \beta_{DP} P_S \frac{G}{N} - \omega\beta_{FP} P_S F - a_P P_S W \tag{6.1a}$$

$$\frac{\mathrm{d}P_I}{\mathrm{d}t} = \beta_{DP} P_S \frac{G}{N} + \omega\beta_{FP} P_S F - mP_I - d_P P_I - \varepsilon_P P_I - a_P P_I W \tag{6.1b}$$

$$\frac{\mathrm{d}P_G}{\mathrm{d}t} = \varepsilon_P P_I - mP_G - \alpha P_G - d_P P_G - a_{PG} P_G W \tag{6.1c}$$

$$\frac{\mathrm{d}Y_S}{\mathrm{d}t} = mP_S - mY_S - d_Y Y_S - \beta_{DY} Y_S \frac{G}{N} - \omega\beta_{FY} Y_S F - cY_S - a_{YA} Y_S W \tag{6.1d}$$

$$\frac{\mathrm{d}Y_I}{\mathrm{d}t} = \beta_{DY} Y_S \frac{G}{N} + \omega\beta_{FY} Y_S F + mP_I - mY_I - d_Y Y_I - \varepsilon_Y Y_I - cY_I - a_{YA} Y_I W \tag{6.1e}$$

$$\frac{\mathrm{d}Y_G}{\mathrm{d}t} = \varepsilon_Y Y_I + mP_G - mY_G - \alpha Y_G - d_Y Y_G - cY_G - a_G Y_G W \tag{6.1f}$$

$$\frac{\mathrm{d}A_S}{\mathrm{d}t} = mY_S - d_A A_S - \beta_{DA} A_S \frac{G}{N} - \omega\beta_{FA} A_S F - cA_S - a_{YA} A_S W \tag{6.1g}$$

$$\frac{\mathrm{d}A_I}{\mathrm{d}t} = \beta_{DA} A_S \frac{G}{N} + \omega\beta_{FA} A_S F + mY_I - d_A A_I - \varepsilon_A A_I - cA_I - a_{YA} A_I W \tag{6.1h}$$

$$\frac{\mathrm{d}A_G}{\mathrm{d}t} = \varepsilon_A A_I + mY_G - \alpha A_G - d_A A_G - cA_G - a_G A_G W \tag{6.1i}$$

$$W = W(t) \tag{6.1j}$$

Here, $N = P + Y + A$ represents the total wild boar population where $P = P_S + P_I + P_G$, $Y = Y_S + Y_I + Y_G$, $A = A_S + A_I + A_G$ and G is the total number of generalised, $G = P_G + Y_G + A_G$. Susceptible and infected yearlings and adults give birth to susceptible piglets at rates b_Y and b_A respectively. Generalised yearlings and adults give birth to piglets at rate b_G. Here we assume that $b_A = b_Y = b_G$. The total population is regulated through a crowding parameter, q, that acts on the birth rate. Maturity from piglets to yearlings and yearlings to adults occurs at rate m and piglets, yearlings and adults may die of natural causes at rates d_P , d_Y, d_A respectively. Here we assume $d_P = d_Y = d_A$.

We assume infection can occur through direct frequency-dependent interactions between susceptible and generalised individuals with transmission coefficients β_{DP}, β_{DY} and β_{DA} or through environmental contact with free-living MTC, with transmission coefficients β_{FP}, β_{FY} and β_{FA} for the different age classes respectively. We assume piglets and yearlings are three times more susceptible to direct and environmental infection than adults. In this way we have set the model so that the yearling class is the same as the piglet class in terms of disease characteristics, but the yearling class is the same as the adult class in terms of reproductive processes. Infected individuals are not infectious but can progress to the generalised (infectious) class at rates ε_P, ε_Y and ε_A. In Asturias where resources are not limited we assume $\varepsilon_P = \varepsilon_Y = \varepsilon_A$. Later we consider regions where resources (particularly water) are scarce and overall health is impaired (similar to conditions in central and southern Spain). Then we assume that piglets and yearlings progress from the infected to the generalised class at three times the rate of adults (ε_P=$\varepsilon_Y = 3\varepsilon_A$). We assume that free-living MTC is shed from generalised wild boar at rate λ and decays at rate μ. The level of environmental transmission is scaled through the parameter ω which increases when environmental conditions become more severe to reflect, for example, aggregation at limited water holes ($\omega = 0.1$ in Asturias and $\omega = 1$ in resource limited regions).

We assume that wild boar suffer mortality, in addition to natural death, from three causes: individuals in the generalised class suffer an additional disease induced mortality at rate α; all adult and yearling classes are culled due to hunting at constant rate c; and predation by wolves successfully attack susceptible and infected piglets at rate a_P, generalised piglets at rate a_{PG}, generalised yearlings and adults at rate a_G and susceptible and infected yearlings and adults at rate a_{YA}. Our baseline assumption is that $a_{YA} = 0$ and $a_P = a_{PG} = a_G$ implying that wolves prey on piglets and generalised individuals only (although we do consider alternative predation assumptions). Further parameter description and the parameter values used in this study are shown in Appendix 6A.1.

6.4 Results

6.4.1 Wolf population

The annual number of reported wolf attacks on livestock increased from 1481 in 2000 to 3024 in 2014 (100% increase; Figure 6.4). Reports of wolf predation on livestock were unrelated to livestock numbers. Instead they correlated positively to the number of wolf packs and to wolves culled during the previous season [54]. Therefore we extrapolate wolf numbers from this wolf attack data using linear regression to ascertain the linear growth rate of the wolf population over this period (Figure S1). Using the data on wolf numbers for 2003-2004 as 252 [68], we estimate

the number of wolves in 2000 as 196 growing linearly to 392 in 2014.

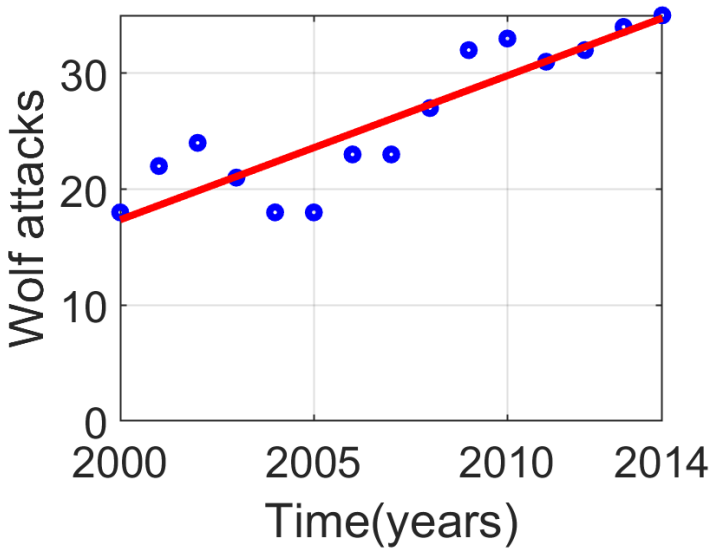

Figure 6.4: Asturias: the rate of increase in wolf attacks. Rate of increase in Asturias wolf attacks for 2000-2014 derived from least-squares linear regression on wolf attack data, Asturias government data. Blue spots show the annual wolf attack data count. The red line is the least-squares linear regression of the wolf attack data.

6.4.2 Wild boar population

Areas with and without wolves, had similar wild boar harvest rates in year 2000 (0.52 and 0.40 wild boar/km^2, respectively). By 2014 harvest rates had increased to 0.85 in areas with wolves but had a greater increase to 1.32 in areas without wolves. Between 2008 and 2014, the wild boar hunting harvest grew steadily in areas without wolves but remained stable in areas with wolves. Assuming the annual hunting harvest as a proxy for wild boar density, in 2014 this density was 50% higher in areas without wolves than areas with wolves (Figure 6.3). Therefore in the areas with wolves we estimate wild boar density as 1.65/km^2 in 2000 rising to 2.55/km^2 in 2014. In the areas without wolves we estimate wild boar density as 1.2/km^2 in 2000 rising to 3.6/km^2 in 2014.

6.4.3 TB prevalence

A total of 1051 wild boar sera were tested for antibodies against MTC, yielding a mean seroprevalence of 5.42% (95%CI 4.21-6.98) for the whole study period. The reduction in seroprevalence between periods was significant in sites with wolves (the southern more mountainous regions) where prevalence declined by 77% from

16.67% ± 7.47% in 2000-2007 to 3.87% ± 1.76% in 2008-2014 (Fisher's p<0.0001). In sites without wolves prevalence was initially lower and no significant change in prevalence was recorded: 6.89% ± 10% in 2000-2007 and 3.08% ± 3.5% in 2008-2014 (Figure 6.5). The mean annual cattle herd TB prevalence from 2005 to 2007 was 0.19%. Herd prevalence grew slightly in 2008-2014, reaching a mean of 0.22%. In areas with wolves, cattle TB herd prevalence remained almost stable during the study period (0.22% in 2005-2007; 0.19% in 2008-2014; Yates Chi^2=0.45, 1 d.f., p=0.5 supporting the hypothesis that infection prevalence has remained stable). By contrast, in areas without wolves herd prevalence increased by 56% in the same period: 0.16% in 2005-2007; 0.25% in 2008-2014; Yates Chi^2=7.18, 1 d.f., p=0.0074 indicating rejection of the hypothesis (Figure 6.5.

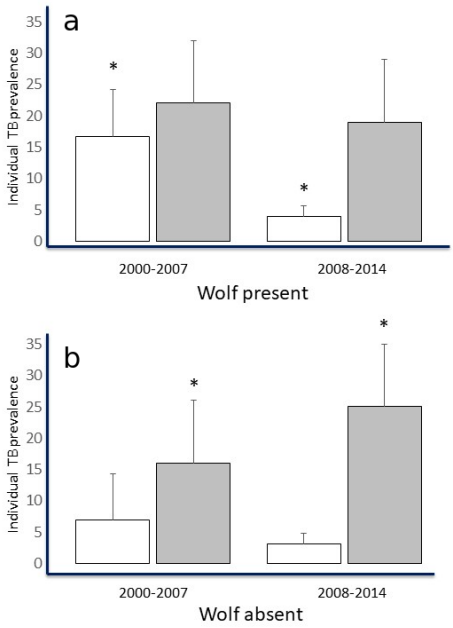

Figure 6.5: Asturias: mean TB prevalence for wild boar and cattle. Mean individual TB prevalence for wild boar (serum antibodies; white columns) and cattle (×100; skin test reactors; grey columns) in Asturias. The upper panel (a) represents areas where wolves are present and the lower one (b) those where wolves are absent. Cattle data were only available for the period between 2005 and 2014. Bars represent 95% confidence intervals and asterisks indicate significant differences at p<0.01.

6.4.4 The model comparison to data for regions with wolves

The model results for the wild boar population density, TB prevalence and the percentage change in the level of pathogen in the environment in response to a linear increase in wolf density are shown in Figure 6.6 for the period 2000-2014. As wolf density increases there is a decrease in TB prevalence from 17% in 2000 to 3.8% in 2014. The level of generalised infection remains relatively constant at 29% of the total infected population throughout the study period. The reduction in prevalence

leads to more than 50% reduction in the level of pathogen in the environment by 2014. Wild boar density increases and then starts to saturate from 2008 such that by 2014 there has been an increase in wild boar density from 1.65/km^2 to 2.55/km^2 as per the observational data, and highlight that predation by wolves could be a key factor in reducing TB prevalence in wild boar.

A key finding is that although wolf numbers increase, which will increase overall predation, there is also an increase in wild boar density. This increase in wild boar density can be attributed to an assumption that wild boar were below their carrying capacity in 2000 and so positive growth would be expected, but also because predation decreases TB prevalence and therefore decreases the population level mortality due to TB. Hence, the increased mortality due to predation is compensated by a reduced TB induced mortality. An implication of the approximately two-fold increase in wild boar population density and four-fold decrease in prevalence is that the level of pathogen in the environment decreases by more than 50% over the 14-year period. This is significant since a reduction in the free-living particles reduces the risk of infection in other animals, in particular livestock, which share the same environment as the wild boar.

The pronounced reduction in TB prevalence (from 17% in 2000 to 3.8% in 2014) assumes selective predation by wolves on wild boar piglets and generalised individuals. In comparison (Supplementary Information and Figure 6A.1), if wolves prey indiscriminately on all wild boar classes the prevalence reduction is 17% to 8.3% but the wild boar density only grows to 2.10/km^2 in 2007 before declining to 1.93/km^2 in 2014. If wolves prey on piglets only prevalence shows a reduction from 17 to 9.5% over the 2000 to 2014 period (Figure 6A.2). The model results therefore suggest that predation on generalised individuals is key to the significant reduction of prevalence since the removal of generalised individuals reduces infection from both direct contact and environmental contamination.

6.4.5 The impact of wolves on TB prevalence in the long-term

We examine the long-term impact of predation by wolves on TB prevalence in wild boar for different trends of wolf density (Figure 6.6). In Figure 6.6a we assume wolf numbers remain constant after 2014 (reflecting that wild boar are a key component of wolf diet). There is a small increase in wild boar density due to reduced disease-induced mortality as a consequence of the further reduction in TB prevalence, but in general, predation by wolves is sufficient to stabilise wild boar numbers. TB prevalence and the level of environmental pathogen decrease to low levels. This emphasises how predation can control virulent infection in a prey species and also reduce the risk of infection to other host species. In Figure 6.6b we assume wolf density will decrease and reach zero in 2042. This represents a scenario where

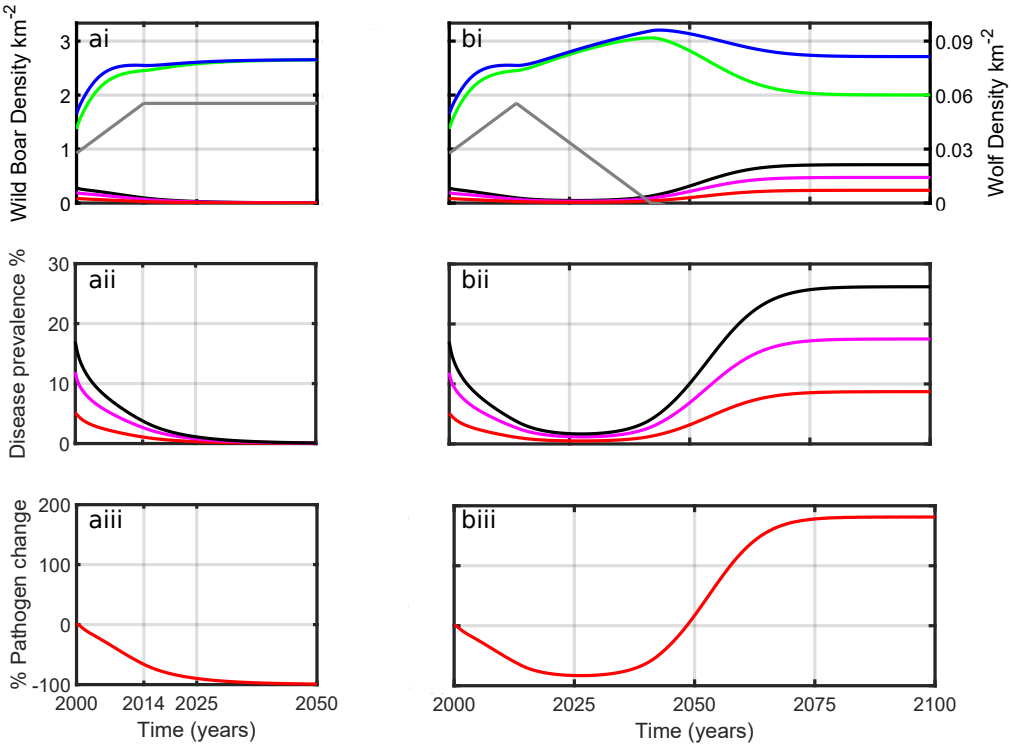

Figure 6.6: Model results for the sub-region of Asturias inhabited by wolves. (a) wolf numbers rise from 196 (2000) to 392 (2014) and then remain constant until 2050. (b) wolf numbers rise from 196 (2000) to 392 (2014) and then decrease at the rate at which they increased until they die out. Initial conditions set wild boar and wolf densities to their 2000 values taken from the field data, and the initial prevalence in 2000 is 17% (of which 29% are generalised). (A): changes in wild boar population density - total population (blue); total susceptible (green); total infected and generalised (black); infected (magenta); generalised (red); wolves (grey). (B): changes in prevalence – total prevalence (black), infected prevalence (magenta) generalised prevalence (red). (C): % change in the density of environmental pathogen. For parameters see Supplementary Information.

wolves are intentionally removed. Here, as wolf numbers initially decrease there is a rise in wild boar density with TB prevalence in wild boar remaining low. However, as wolf numbers decrease further TB prevalence increases leading to a downturn in wild boar density in response to increased disease induced mortality. It is notable that the final stable wild boar numbers in the absence of wolves (Figure 6.6b) are similar to the level in the presence of wolves (Figure 6.6a). However, a key difference is that TB prevalence is low (0.1%) in the presence of wolves and high (26%) in their absence. This has significant consequences for potential environmental transmission of MTC from wild boar to other species. The underlying mechanism responsible for this difference is that wild boar density is largely regulated by the disease in the absence of wolves whereas it is regulated by predation in their presence. This is a key insight from the mathematical model. It highlights how restrictions to predator growth may have only minor impacts on prey density but a major detrimental impact

on the prevalence of infection in prey species.

6.4.6 Model comparison to data in areas of Asturias without wolves

The results for the model that reflect the region of Asturias in which wolves are absent are shown in Figure 6.7. Here, there is a rapid increase in wild boar density, with close to a 3-fold increase in density between 2000 and 2014 (which reflects the increase in density observed in the field data). TB prevalence initially remains constant (at around 3%) but from 2007 onwards shows an increasing trend reaching a prevalence of 7.8% by 2014. This relatively low increase in prevalence coupled with a large increase in population density leads to a large increase (over 500%) in the level of environmental pathogen and therefore a potentially increased risk of infection spillover to co-habiting domestic and wild animals.

6.4.7 The potential impact of predation in regions of high TB prevalence in wild boar

To represent areas of high TB prevalence we modify the baseline parameters for Asturias to reflect increased prevalence and generalised infection. In such regions wild boar density is typically high (due to management and artificial feeding) even though environmental conditions are harsh and in particular severely diminished water availability necessitates the sharing of water holes and leads to overall poor body condition [14]. This increases the level of environmental transmission and leads to a more rapid transition from the infected to the generalised class for piglets and yearlings ([48]; see also Supplementary Information). We assume here that wild boar live at endemic density $8/\text{km}^2$, and adjust K and q to reflect this (see Supplementary Information). Other parameters remain as in the set-up in Asturias and in particular note that to maintain the comparison with Asturias we do not change the background culling rate. In the absence of wolves the model results indicate a prevalence of 57% of which around 54% are individuals with generalised infection (this is in good agreement with Muñoz-Mendoza *et al.* 2013[102]). In Figure 6A.3 we introduce wolves at constant density of $0.08/\text{km}^2$ which represents an initial wolf to wild boar ratio of 1:100. Initial predation by wolves reduces wild boar density, but primarily affects infected and generalised individuals. This causes a reduction in TB prevalence and therefore reduced population level disease-induced mortality. This drives an increase in susceptible individuals and an increase in wild boar population density which promotes a resurgence in disease prevalence. Infection and population recovery oscillates until after 50 years the population has increased wild boar numbers ($10.1/\text{km}^2$), reduced TB prevalence to 26.5% and reduced levels of environmental pathogen by 54%.

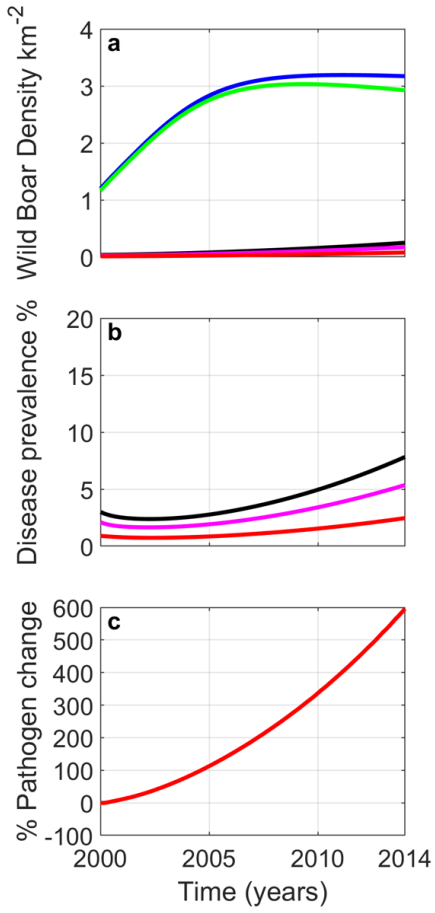

Figure 6.7: Model results for the sub-region of Asturias not inhabited by wolves. Initial conditions set wild boar and wolf densities to their 2000 values, and the initial prevalence in 2000 is 3% (of which 30% are generalised). (a): changes in wild boar population density - total population (blue); total susceptible (green); total infected and generalised (black); infected (magenta); generalised (red); wolves (grey). (b): changes in prevalence – total prevalence (black), infected prevalence (magenta) generalised prevalence (red). (c): % change in the density of environmental pathogen. For parameters see Supplementary Information.

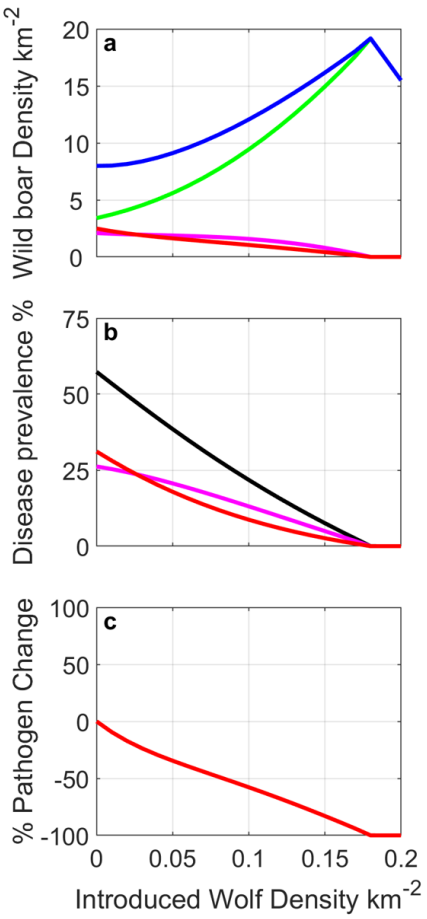

Figure 6.8: Model results for areas with high TB prevalence showing the long-term outcome after different constant densities of wolves are added to a wild boar population at steady endemic state. (a): changes in wild boar population density - total population (blue); total susceptible(green); infected (magenta); and generalised (red). (b): changes in prevalence total prevalence (black), infected prevalence (magenta) generalised prevalence (red). (c): % change in the density of environmental pathogen. For parameters see Supplementary Information.

Figure 6.8 shows the impact of wolf density on the steady state level of wild boar density, disease prevalence and environmental contamination. In the absence of wolves the model results indicate a prevalence of 57% of which around 54% are

individuals with generalised infection (this is in good agreement with [102] for wild boar TB prevalence in Mediterranean Spain). As wolf numbers increase the level of disease prevalence and risk of environmental contamination decrease. However, the density of wild boar increases as wolf density (and predation) increases. This increase in wild boar density is a direct result of the decrease in TB prevalence as the mortality from predation is lower than disease induced mortality due to TB that was experienced in the absence of wolves. There is a threshold in wolf density that leads to disease eradication and for wolf densities above this threshold there is a decrease in wild boar density (since mortality from predation is no longer compensated following eradication of the disease).

6.5 Discussion

Our modelling results show good agreement with the field data for our case study system. However there are specific aspects where the model and field study disagree. The model differs from field data in that it predicts a prevalence of generalised individuals of 25-30% whereas existing data for Asturias suggests 16.7% [102]. However, this lower prevalence was derived from a small data set (1 out of 6 being reported as generalised) and recent unpublished results from Asturias would now indicate a higher prevalence of generalised in closer agreement with model findings. Also, in areas with wolves the empirical results indicated that cattle TB stayed constant rather than declining. The model results indicated that there would be an increase in wild boar density, a reduction in TB prevalence in wild boar and a reduction in generalised infected wild boar and MTC in the environment, therefore reducing the risk of transmission of MTC to livestock. This can be explained by: firstly, the wildlife reservoir in the Atlantic regions of Spain is composed of two main hosts, wild boar and badger [102], and wolves are not likely to significantly interfere with badger population dynamics; secondly, the wildlife reservoir contributes to MTC maintenance, but is not the only driver. In Spain, the relative contribution of wildlife to cattle TB breakdowns varies between regions depending on the epidemiological circumstances [89, 73]. Cattle movements, for instance, are likely to contribute to TB maintenance [66].

In the absence of wolves (Figure 6.7), wild boar numbers increase significantly. Model results indicate that there is a lag between the increase in wild boar growth and the increase in TB prevalence since the increase in infected individuals has a similar increasing trend to that of the overall population. This could explain the observation that TB prevalence in wild boar in the absence of wolves has remained relatively fixed. Note, however, that while TB prevalence in wild boar has remained constant the model predicts that the density of generalised wild boar and the presence of MTC in the environment increases throughout the study period.

It is notable that the empirical findings for areas of Asturias in which wolves are absent show that there is a near five-fold increase in TB detected in cattle between 2000-2014. Our model provides an explanation for how a small percentage increase in prevalence coupled with a large increase in population density in a reservoir population may lead to a large increase in environmental contamination. This could explain the observed increase in cattle TB in these regions.

The model system was adapted to examine the potential impact of predation on disease control beyond the Asturias case study system (Figure 6.8). In areas with high TB prevalence such as central and southern Spain, the observed prevalence of TB is 50% and an increased proportion of those infected exhibit generalised infection (58%). Since predators may select the most severely infected individuals, it offers the potential for predation to have a greater impact on disease control in such settings. More specifically, as there is a higher prevalence of generalised individuals, there will proportionately be more predation on these super-shedders and therefore the potential to have an exaggerated effect on removing the wild boar that are responsible for shedding the pathogen in the environment, thus having greater potential to reduce spillover to other wild and domestic hosts. In this scenario our model results show that predation by wolves does lead to an exaggerated reduction in disease prevalence while leading to an increase in overall population density and reduction in the level of environmental pathogen. This increase in wild boar density is a direct result of the decrease in TB prevalence as the mortality from predation is lower than disease-induced mortality due to TB that was experienced in the absence of wolves. This emphasises the generality of our findings and further highlights the potential role of predators in disease control.

Previous theory has shown how predation on prey that harbour virulent pathogens can reduce disease prevalence [111, 110] although empirical support for these results is limited. Here we combine field data and theory for a case study system to show that wolf predation may contribute to TB control in wild boar, reducing TB prevalence and the release of MTC into the environment. These factors are likely to contribute to reduced levels of indirect transmission from the wild boar infection reservoir to other hosts. The results can be generalised and show how predation can play a key role in the control of infectious disease in multi-host systems.

It has been postulated that MTC transmission between wild and domestic hosts is mostly indirect, mediated by contaminated vegetation, water, mud, feed or other substrates [70, 14]. Wild boar are the primary reservoir host for MTC in Spain with infection to other host species likely to be through indirect transmission in regions where multiple hosts overlap [13]. Wild boar are relatively long-lived [86] and older age classes can mount a formidable defence against predation. Therefore wolves are likely to select severely infected/generalised individuals (which are the class

responsible for shedding pathogen to the environment; [14]) or piglets (which is an age group more likely to suffer generalised infection [94]). Such selective predation has been suggested as a key mechanism which can decrease infection prevalence in prey [111] and was shown to lead to reduced prevalence of prion disease in cervids without a dramatic decrease in their density [143]. Our field observations and model study show that there is a reduction in wild boar disease prevalence without a consequent reduction in wild boar density in regions where wolves might selectively target piglets and generalised wild boar. Our results indicate that the decrease in prevalence would be less pronounced if predation targets all classes indiscriminately or if it targeted only piglets. Therefore we confirm previous findings [111, 143] that suggest the ability of predators to preferentially select the most infected prey may be key to their role in disease control. Moreover, our findings suggest that wolves could play a key role in TB control in wildlife reservoirs in Spain. In Asturias, the annual cost of compensation paid to farmers due to wolf attacks on their livestock (€1,016,860) is a quarter of the annual expenses of the cattle TB eradication scheme (€4,163,348; Regional Government 2014). The ecosystem service provided by predators in terms of disease control should form part of the debate when discussing the impact of predators since here wolves may be allies of farmers, rather than enemies.

Previous theoretical studies that have shown that, in disease regulated populations, predation can reduce the force of infection and thereby decrease the density of infected hosts, increase the density of susceptible hosts and lead to an increase in overall population density [111, 143]. We confirm this finding in our model study and show that increased mortality from predation that leads to reduced disease-induced mortality are roughly in balance. A key result is therefore that the prey population can be regulated by the disease, with consequent high prevalence in the prey species or at a similar density by a predator but with low disease prevalence. This finding highlights how restrictions to predator growth may have only minor impacts on prey density but a major detrimental impact on the prevalence of infection in prey species. The compensatory balance between predation and disease induced mortality relies on the infection being virulent with no recovery to long-lasting immunity. Then predation (and culling in general) can reduce TB prevalence and the potential spillover of infection to sympatric hosts [23, 59]. In systems where infected individuals can recover to immunity predation and culling can lead to reduced population density and increased prevalence [81]. This highlights the necessity to understand the system specific host infection dynamics that are subject to predation or culling [20, 79].

Our results agree with earlier findings that the removal of a predator from a system that is regulated by both predator-prey interactions and virulent infection, may increase disease prevalence and suppress prey abundance [111, 82, 92].

Furthermore, Lennox *et al.* (2018)[91] reviewed the impact of predator removal in a wide range of ecological scenarios concluding that the majority of enforced removal ended in failure. Our model results suggest that in the initial years of wolf removal wild boar density can increase and disease prevalence stays low. This may indicate that predator removal can be beneficial, however this is only a transitory state. When the wolf reaches sufficiently low numbers the disease is able to re-infect the increased abundance of susceptibles so that over time the population becomes regulated by disease rather than predation. This is accompanied by an increase in environmental contamination and risk of spillover to other wild and domestic hosts. This further highlights the complexity and potential negative consequences of predator removal in the need to consider disease status in predator management programmes.

Our study has highlighted the potential of predation by wolves to reduce TB prevalence in wild boar and thereby reduce the risk of transmission from a key wildlife reservoir of infection. The model framework developed in this study was tailored to the wild boar TB wolf system but the underlying processes that represent the population and epidemiological dynamics are general and therefore we expect the results to apply more broadly. In particular, when predation can regulate a prey species that was previously regulated by virulent pathogens it is likely that infection levels will be reduced. Of course, care must be taken when considering the impact of generalist predators on disease control as they may also prey on alternative species that do not harbour virulent pathogens and therefore where mortality due to predation will not be compensated. Nevertheless, the potential of predators to control infection should be recognised more widely and be contrasted with the detrimental impact of predatory losses to domestic species. The beneficial role of predators should be given more prominence particularly given the need to manage conservation conflicts associated with predator re-establishment [119].

6.6 Data availability

A reporting summary for this article is available in the Supplementary Information. The supporting MATLAB code to reproduce Figures 6.6-6.8 and 6A.1-6A.3 will be deposited in an external repository on acceptance.

6.7 Acknowledgements

This is a contribution to MINECO Plan Nacional grant WILD DRIVER ref. CGL2017-89866 and EU-FEDER. Eleanor Tanner was supported by The Maxwell Institute Graduate School in Analysis and its Applications, a Centre for Doctoral Training funded by the UK Engineering and Physical Sciences Research Council

(grant EP/L016508/01), the Scottish Funding Council, Heriot-Watt University and the University of Edinburgh. Pelayo Acevedo was supported by the Ministerio de Economía y Competitividad (MINECO) and the University of Castilla-La Mancha through a "Ramón y Cajal" contract (RYC-2012-11970).

6.8 Author contributions statement

PA, AB, JM and CG gathered and analysed field data. ET and AW performed mathematical analysis. All authors contributed to the production of the manuscript. All authors gave final approval for publication.

Appendices to Chapter 6

The following appendices are the Supplementary Information to 'The wolf as an ally of the farmer: predation reduces disease transmission in multi-host systems'by Eleanor Tanner, Andy White, Pelayo Acevedo, Ana Balseiro, Jaime Marcos and Christian Gortázar.

6A.1 Wild boar TB model parameters

The parameters for wolf wild boar TB model [48] are as follows. Note that where there are two values indicated, the first value represents the parameter value for Asturias, whereas the second value represents the parameter value for areas of high TB prevalence, for example southern Spain.

$b_A = \log(4)$ The population birth rate in a disease-free population when resources are unlimited. This constant rate means that for each reproductive member of the population, 3 piglets will be born, averaged over the population over a year. (This has been derived by assuming that there is a 50% sex ratio and that each female produces an average of 6 offspring per year when resources are not limited.) Units: $year^{-1}$.

$K = 4.59$ (Asturias); 72.78 (high prevalence region) The carrying capacity for the total population density in the absence of disease: in Asturias, set to 4.59; in a high prevalence region where wild boar live at higher density and disease is more prevalent this is set to 72.78. Units: *population density*.

$q = \frac{1}{K}\left(1 - \frac{d_A(d_P+m)(d_Y+m)}{m(b_A m+b_Y d_A)}\right)$ This parameter limits the total population to the carrying capacity K in the populated disease-free steady state, and is derived from steady-state analysis of the model without infection. Units: $density^{-1}$.

$m = 1$ The rate that piglets mature to yearlings and yearlings mature to adults. These rates assume that it takes on average 1 year to enter the next age class. Units: $year^{-1}$.

$d_P = d_Y = d_A = \frac{1}{7}$ The natural death rate of all classes which implies an average life expectancy of 7 years. Units: $year^{-1}$.

$c = 0.3$ The continuous culling rate effective on all yearlings and adults, set to achieve a total hunting bag of approximately 20% of the wild boar population in Asturias. Units: $year^{-1}$.

$\beta_{DA} = 1.06$ The rate that adults are infected by direct contact frequency dependent transmission fitted to give prevalence levels observed in the wild boar TB system in Asturias. Units: $year^{-1}$.

$\beta_{DP} = \beta_{DY} = c_\beta \beta_{DA}$ The direct contact frequency dependent infection rate for piglets and yearlings. We assume that $c_\beta = 3$ and so disease transmission to piglets and yearlings is three times that of the adult rate. Units: $year^{-1}$.

$\beta_{FA} = \frac{20}{K}$ The rate that adults are infected by contact through environmental infection fitted to give prevalence levels observed in the wild boar TB system in Asturias. Units: $density^{-1} \times year^{-1}$

$\beta_{FP} = \beta_{FY} = c_\beta \beta_{FA}$ The environmental infection rate for piglets and yearlings. We assume that $c_\beta = 3$ and so disease transmission to piglets and yearlings is three times that of the adult rate. Units: $density^{-1} \times year^{-1}$.

$\omega = 0.1$ (Asturias); 1 (high prevalence regions) This parameter scales the level of environmental transmission. Environmental transmission typically occurs at shared water holes and it therefore high when water resources are scarce. In Asturias $\omega = 0.1$ to reflect plentiful resources. In high prevalence regions (such as central and southern Spain) resources are scarce and $\omega = 1$. Units: $scalar$.

$\varepsilon_A = \frac{2}{3}$ This is the rate that infectious adults become generalised. This assumes that it takes on average 18 months for an infected adult to progress to the generalised class. Units: $year^{-1}$.

$\varepsilon_P = \varepsilon_Y = c_\epsilon \varepsilon_A$ The rate that infected piglets and yearlings become generalised. In the Asturias model these are set to the same value as that for adults ($c_\epsilon = 1$). For high prevalence regions $c_\epsilon = 3$ assuming that it takes on average 6 months for an infected piglet or yearling to progress to the generalised class. This value is 3 times that of adults, and recognises the fact that in high prevalence regions that typically have scarce resources the body condition of wild boar is generally poor and co-infections are common. It is acknowledged that the stress of co-infections can shorten the length of time to progress to generalised [90]. Units: $year^{-1}$.

$\alpha = 1$ This is the additional disease induced death rate of the generalised class and assumes that on average individuals spend 1 year in the generalised class before death. Units: $year^{-1}$.

$\lambda = 1$ The rate of shedding of infectious particles by generalised classes. We normalise this value to 1. This is valid as we have explored a range of values for β_P, β_Y and β_A which scale with the size of λ and the density of free-particles, F. Units: $year^{-1}$.

$\mu = 6$ This is the decay rate for free-living particles, indicating that they have an average life expectancy of 2 months. Units: $year^{-1}$.

$a_P = a_{PG} = a_{YG} = a_{AG} = 0.00099$ The successful predation rates for wolves on susceptible and infected piglets, generalised piglets, generalised yearlings and generalised adults respectively following Nores *et al.* (2008) [107]. Units: $(wolf\ density)^{-1} \times year^{-1}$.

6A.2 Asturias: prey selection

Figures 6A.1 and 6A.2 represent the same scenario as in Figure 6.6 for the period 2000-2014 except for changes to the classes of wild boar that wolves prey on. In both these cases wolf predation, measured as the number of wild boar taken per year per wolf, is adjusted to be similar over the first 10 years to that of Figure 6.6. This results in using the same predation rate when only piglet predation occurs, and a halved predation rate for indiscriminate predation.

Figure 6A.1 shows that when wolves prey indiscriminately, infected prevalence is reduced but not as quickly as in Figure 6.6 for the period 2000-2014. However, as now there is also predation on adult and yearling wild boar, there is less reproduction and therefore a reduction in the overall population density and the number of susceptibles available for infection. This results in a 40% decrease in the level of the pathogen in the environment, and also reduced wild boar density.

Figure 6A.2 shows that when wolves only prey on piglets, infection is not reduced as quickly as for predation on piglets and generalised individuals (Figure 6.6) such that the number of generalised wild boar in the population and hence the level of free living pathogen is not significantly reduced. The wild boar density rises, but the disease prevalence is not reduced significantly.

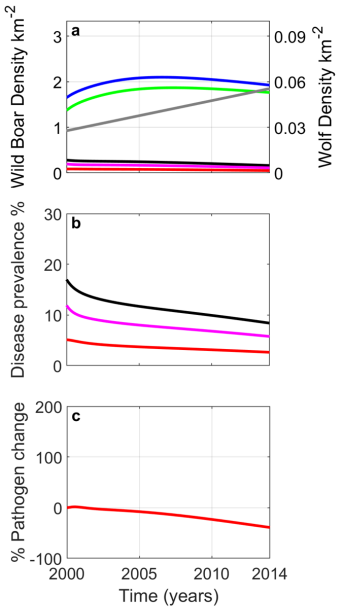

Figure 6A.1: Asturias: affect of wolves preying on all classes of wild boar. The effect on (a) wild boar density, (b) TB prevalence, (c) free-living density when predation by wolves on all classes of wild boar. For parameter values see Appendix 6A.1.

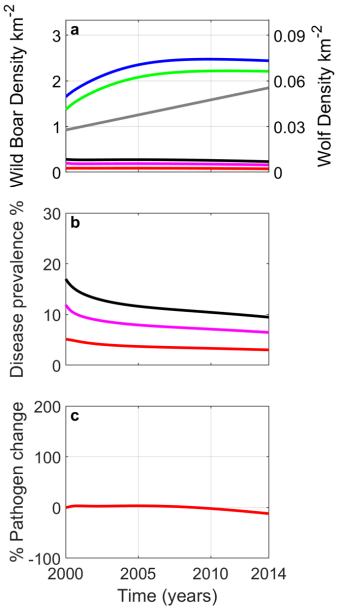

Figure 6A.2: Asturias: affect of wolves preying on wild boar piglets only. The effect on (a) wild boar density, (b) TB prevalence, (c) free-living density when predation by wolves in on wild boar piglets only. For parameter values see Appendix 6A.1.

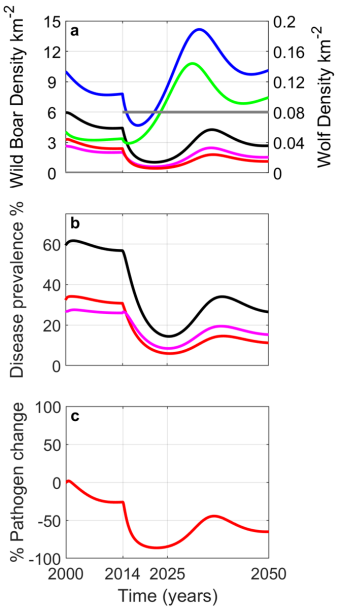

Figure 6A.3: High TB prevalence area: affect of wolves preying on wild boar. The effect on (a) wild boar density, (b) TB prevalence, (c) free-living density after a constant density of wolves ($0.08/km^2$) is added to the wild boar population at steady endemic state, preying on wild boar at the same rate as in Asturias. For parameter values see Appendix 6A.1.

Chapter 7

Discussion

In this thesis we have introduced and developed a new mathematical model to represent the dynamics of the wild boar tuberculosis system in Spain. Chapters 4, 5 and 6 consider the impact of vaccination, culling and predation on TB epidemiology. These chapters are based on work that has been published (or that is in review) and each contains a detailed discussion and review of the findings in terms of the wider literature. Therefore in this discussion we will highlight only the key findings. We will also discuss how our work could be extended to assess further questions on TB management, and developed to represent other host disease systems.

When ecological systems exhibit behaviour that doesn't match expectation or is hard to explain, mathematical models are an important tool to tease out the key factors that influence such complex interactions. The mathematical modelling used in the research for this thesis was motivated by the need to understand the mechanisms contributing to the maintenance of high density and high prevalence TB in wild boar populations in central Spain [106, 138]. In this area the predominant management controls used against TB in wild boar are vaccination and culling. Our goal was to develop mathematical models in collaboration with field experts to provide insight into the impact of long-term management control on wild boar population dynamics and TB prevalence.

In setting up this model (Chapter 3) we deliberately employed a mechanistic approach that would help uncover the dynamics driving the wild boar TB system. This model is a system of ODEs, a classical compartmental model of disease inspired by Anderson & May (1979) [9] and Keeling & Rohani (2008) [84], organised in different age classes and disease states, designed to reflect both the wild boar lifecycle and the progression of TB in wild boar from initial infection through to the most severe, generalised, form. The relative simplicity of the model framework allowed us to perform some mathematical analysis on the system as well as generate numerical solutions to illustrate behaviour and compare the model with data from the field.

A key aspect of our wild boar TB model is that it includes disease transmission from free-living infectious particles, inspired by badger modelling work of Anderson

& Trewhella (1985) [11]. Infection from free-living particles represents transmission from pathogen excreted into the environment by generalised wild boar. It assumes the population is well-mixed, which is appropriate as most of the population will utilise scarce water holes where the free-living pathogen can persist. We also represent the possibility of disease transmission via social contact for piglets by implementing pseudo-vertical transmission as a route to early infection. In itself environmental transmission is not novel in mathematical modelling, however up until recently this has been an under-used form of transmission in models of wildlife disease reservoirs, and veterinarians in the field working with wildlife disease see transmission from free-living sources as an important component for future models. Our work with free-living transmission has highlighted the need to record both density and prevalence as environmental infection is related to the actual number of diseased individuals rather than their proportion of the total population.

Our model findings that investigate the impact of vaccination on TB control (Chapter 4) show that in the short-term vaccinating wild boar piglets both reduces prevalence and the actual number of generalised individuals in the population, and increases the number of susceptibles and total population. This growth in population is a compensatory response to a release from disease-induced mortality that these piglets could have incurred but now bypass, and significantly this occurs at the time of life when they are most at risk of TB infection and progression to generalised. The subsequent increase in the number of susceptibles leads to a total population size that is significantly greater than the pre-vaccination level. This increased population size can support an increased density of infected and generalised individuals. So while long-term prevalence is reduced this is due to a rise in total population rather than a reduction in infection.Therefore the level of pathogen shed in the environment may not decrease, in fact it may increase, and the risk of spillover to other hosts may not be reduced. It should also be noted that when the vaccination regime is curtailed, there is a spike in prevalence and the number of generalised due to the increase in susceptible piglets that are no longer being vaccinated before the population reduces back to the endemic pre-vaccination levels.

Our results highlight the complex dynamics that arise when vaccinating wildlife populations against acute infections. Vaccination trials to protect against TB have been conducted in a number of wildlife reservoirs worldwide with various degrees of success. This is dependent on the appropriate delivery of the vaccine to the target age group of the population, control of the amount of vaccine consumed by each individual, and the length of protection gained [29]. Buddle (2013) [29] reports that vaccination trials in possums, white-tailed deer and badgers have shown significant protection against TB, trials in wild boar did not offer great protection and trials in buffalo showed no protection. Carter (2012) [31] reports a reduction in the incidence of TB in badger populations after a vaccination trial. However, there

are no reports that vaccination by itself has eradicated TB in wildlife reservoirs. Indeed, using vaccination to eradicate disease has had mixed results. There has been success in eradicating rabies in the western European fox population but only through a sustained campaign over many years [58]. In contrast, in order to eliminate rinderpest from cattle vaccination programmes had to be curtailed [123].

The model results for a regime of indiscriminate culling of wild boar (Chapter 4) show that initially culling reduces the the number of generalised in the population and the total population. However, this drop in the number of generalised allows the number of susceptibles to increase and hence allows compensatory growth of the total population due to the reduction in disease-induced mortality. In the long-term, as the disease has not been eradicated these susceptibles can become infected allowing the disease to persist and the number of generalised to stabilise. Thus the disease remains endemic but at a reduced prevalence. Contrary to what may be expected from a culling programme, the total wild boar population remains close to its original pre-culling level as the disease-induced mortality is replaced by the mortality from culling. This resonates with the results from the field, that prompted this research, where despite long-standing annual harvesting of wild boar the disease has remained endemic at high levels and the total population has remained buoyant. When the culling regime stops there is a spike in prevalence and the number of generalised before the population settles back to the endemic pre-culling levels.

Our results may explain why culling as a management tool to eradicate disease has not always been a success. Gortázar et al. (2015) [72] reviewed culling as a technique to control disease in wildlife, with few regimes achieving disease eradication without extreme population reduction. For example, TB in water buffalo, a non-native species in northern Australia, was eradicated through culling the buffalo to near extinction [118]. However, for badger populations in the UK where such extreme culling would be highly contested, TB has remained persistent despite a number of culling campaigns [49]. There is some evidence that selective culling may result in a significant reduction in disease without affecting host abundance [72, 144], however this may not be feasible on a large scale [144].

For the wild boar TB model including the wolf as a predator (Chapter 6) we showed that wolves preying on wild boar piglets and generalised individuals could be a factor in keeping the TB prevalence low in this region whilst the wild boar population increases. Our model shows the wolf acting in the same manner as a selective culling regime, keeping prevalence low by targeting both piglets, which are at greatest risk of infection and progression to generalised, and generalised wild boar, the individuals responsible for shedding the pathogen. When wolves are able to prey on wild boar over a number of years this leads to a wild boar population that has increased in number, has much reduced prevalence and where disease-induced mortality has been replaced by mortality due to predation by wolves.

Empirical evidence confirming the potential for a predator to limit the spread of disease is sparse, however Levi et al. (2012) [92] report that abundance of coyote and dearth of fox can act as predictors of the spread of Lyme disease. We should note, however, that when considering predation we could actually view this as a type of selective culling where the predator makes different choices of age and body condition when harvesting its prey compared to a human hunter. In this way a predator may be a more successful environmental cleanser, with some evidence from the field that predators select prey based on disease status [87].

Our results investigating the impact of wild boar control on the epidemiology of TB uncovered a new general result describing population compensatory growth arising from culling populations harbouring disease (Chapter 5). We have shown that culling a population suffering endemic disease can lead to compensatory growth due to a release from disease-induced mortality. This compensation occurs unless the disease leads to a long-lasting period of immunity. This new result will have important implications for culling wildlife reservoirs and highlights key points that wildlife managers must understand before they embark on wildlife management strategies combating endemic disease in general.

We have tested the effect of specific management strategies (culling, vaccination) on controlling TB in wild boar. Future work could also consider targeted culling; isolating infected or generalised wild boar; and combining management techniques. The model could also be extended to include livestock and thereby highlight the increase or decrease in the risk of spillover arising from TB disease management in wild boar. Also, using the preparatory work for a spatial model for badgers with dispersal between patches (Section 2B.2), it will be useful to test the effect of different levels of management control in neighbouring wild boar areas. Some of this work has been performed with an initial appraisal of targeted culling (discussed for wild boar in Section 5.5, and more generally in Section 5A.4), and one could argue that the wolf is performing targeted culling (Chapter 6) though a human would struggle to replicate selection of piglets and generalised as hunting targets. These results show that if it is possible to target culling at the individuals responsible for spreading the disease then culling is more effective at reducing both the number of generalised and the prevalence of disease in the population. Essentially, the greater the number of generalised removed, then the greater the release from disease-induced mortality in the population.

Identifying and isolating generalised wild boar may not be achievable and therefore, combining management controls may be a more fruitful step to take. Here we briefly show initial results when vaccination and culling are combined as management strategies. Considering the effect of culling a recovered class in the SIR model in Figure 5.1, there may be some concern that culling may remove vaccinated individuals that have bypassed the life-stage with the most chance of

infection and thus remove a greater proportion of healthy adults in the population. However, hunting of the wild boar population in central Spain does not include piglets, therefore an annual cull of yearlings and adults in the wild boar TB model behaves more like the SIRS-type model in Figure 5.5 whereby the immune class (in the wild boar TB model vaccinated piglets) lose their immunity as they become adult. Initial results for this combination in the wild boar TB model are shown in Figure 7.1. Here, both controls induce a release from disease-induced mortality and combine to keep the total population high and the number of generalised low: the vaccination effort prevents a large proportion of the piglets becoming infected and therefore generalised and potentially suffering mortality from the disease, so the total population grows significantly allowing the number of generalised to be maintained; the culling effort removes a proportion of yearlings and adults, including generalised, allowing a release from disease-induced mortality and compensatory population growth. Comparing Figure 7.1c with the results for culling by itself in Figure 5.6bi&ci, when vaccination and culling are combined the culling level to eradicate the disease is lower than when just culling is used. More sensitivity needs to be performed for these results to fully understand their significance, and may prove informative on a seemingly additive type of compensatory growth.

The wild boar TB model is among few mathematical models to use free-living transmission as the sole conduit for transmission. We have furthered this novelty by combining both free-living and frequency dependent transmission in our wild boar TB model including predation (Equations (6.1)). It would be very useful if the lessons taken from the modelling work in this thesis could be translated to other infections. In particular wild boar populations are increasing in density worldwide and there is concern that they may act as a reservoir for a range of infectious diseases. One such disease is African Swine Fever (ASF), a viral infection, currently affecting both wild and domestic pigs in Eastern Europe causing concern in Germany and France where there is a high level of pig farming. In infected populations the prevalence is low, with potential peaks during the summer season when disease outbreaks can lead to severe population reduction, but not disease extinction as it persists at low population levels. Individuals which have progressed to acute infection suffer a very high rate of disease-induced mortality and once infected there is no recovery. Disease transmission is currently understood to be via environmental contamination, through close contact and potentially through a vector. A starting point for modelling this disease could be to use the wild boar TB model with both free-living transmission and frequency dependent transmission, and fitting the parameters to the field data. The parameter sensitivity testing shown in Figure 3.14 gives some indication as to the effect on prevalence and density of changes to virulence, free-living decay, transmission and progression rates, and can give some assistance at setting initial values for this new model. Although the

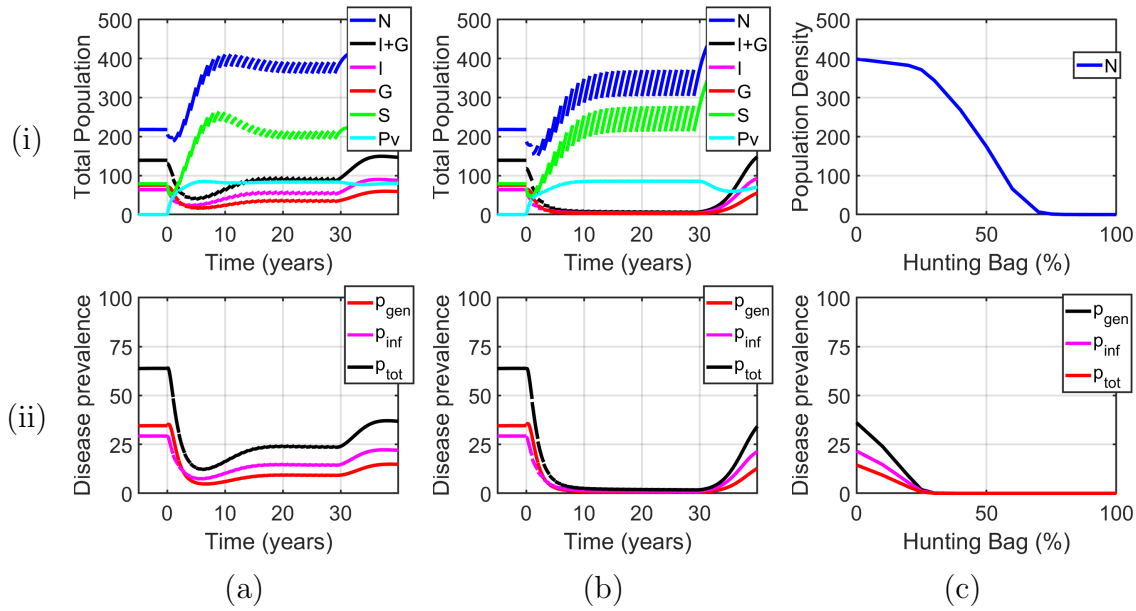

Figure 7.1: Results for the wild boar TB model (PYAG) in response to 30 cull events of indiscriminate culling of the yearling and adult population when 75% of the piglet population is successfully vaccinated. The population dynamics over time are shown in (i) for total population (blue); infected and generalised (black); infected (magenta); generalised (red), susceptible (green) and vaccinated piglets (cyan). (ii) shows the total prevalence (black); infected prevalence (magenta); and generalised prevalence (red). The initial population assumes a TB prevalence, (I+G)/N, of 64% and a generalised prevalence, G/N, of 35%. The change in population and prevalence over 30 sequential cull and subsequent regrowth periods shows when (a) 10% and (b) 25% of the yearling and adult population are hunted. Results are shown for (i) population density and (ii) disease prevalence when (a) 10%, (b) 25% of adults and yearlings are removed instantaneously from the population by hunting every year for 30 years; and (c) the resultant population and prevalence at the end of the 30 year cull and regrowth period.

wild boar TB model does not feature seasonal birth or transmission, this could be included. Transmission of ASF via a vector could be added as an extra route to infection in this model, however without firm details this could be approximated with environmental infection. The model can be used to test whether environmental or social contact is the driving force behind the disease, and how it persists at such low prevalence. Culling is currently used to manage outbreaks of ASF, with timing of these culls crucial. The new model can then be used to test management control regimes to determine optimum interventions.

In this thesis we have developed a model to understand how wild boar management can control TB infection. The specific model results have been shown to be driven by a very general property that we have highlighted - compensatory growth due to the release from disease-induced mortality. Such compensatory growth is likely to be widespread and must be considered if management methods are to control disease in wildlife reservoirs.

Bibliography

[1] P. Abrams. When does greater mortality increase population size? the long history and diverse mechanisms underlying the hydra effect. *Ecology Letters*, 12:462–474, 2009.

[2] P. Abrams and H. Matsuda. The effect of adaptive change in the prey on the dynamics of an exploited predator population. *Canadian Journal of Fisheries and Aquatic Sciences*, 62:758–766, 2005.

[3] P. Acevedo, J. Vicente, U. Höfle, J. Cassinello, F. Ruiz-Fons, and C. Gortázar. Estimation of European wild boar relative abundance and aggregation: a novel method in epidemiological risk assessment. *Epidemiology and Infection*, 135(03):519–527, 2007.

[4] F. Al-Shorbaji, B. Roche, R. Britton, D. Andreou, and R. Gozlan. Influence of predation on community resilience to disease. *Journal of Animal Ecology*, 8(5):1147–1158, 2017.

[5] V. Alzaga, J. Vicente, D. Villanua, P. Acevedo, F. Casas, and C. Gortázar. Body condition and parasite intensity correlates with escape capacity in Iberian hares (*Lepus granatensis*). *Behavioral Ecology and Sociobiology*, 62(5):769–775, 2008.

[6] L. Anderson, C. Gortázar, J. Vicente, M. Hutchings, and P. White. Modelling the effectiveness of vaccination in controlling bovine tuberculosis in wild boar. *Wildlife Research*, 40(5):367–376, 2013.

[7] R. Anderson and R. May. The population dynamics of microparasites and their invertebrate hosts. *Philosophical Transactions of the Royal Society of London. B, Biological Sciences*, 291:451–524, 1981.

[8] R. M. Anderson, H. C. Jackson, R. M. May, and A. M. Smith. Population dynamics of fox rabies in Europe. *Nature*, 289(5800):765, 1981.

[9] R. M. Anderson and R. M. May. Population biology of infectious diseases: Part I. *Nature*, 280(5721):361, 1979.

[10] R. M. Anderson and R. M. May. *Infectious diseases of humans: dynamics and control*. Oxford university press, 1992.

[11] R. M. Anderson and W. Trewhella. Population dynamics of the badger (*Meles meles*) and the epidemiology of bovine tuberculosis (*Mycobacterium bovis*). *Philosophical Transactions of the Royal Society of London. B, Biological Sciences*, 310(1145):327–381, 1985.

[12] J. Barasona, P. Acevedo, I. Díez-Delgado, J. Queiros, R. Carrasco-García, C. Gortázar, and V. J. Tuberculosis–associated death among adult wild boars, Spain, 2009–2014. *Emerging Infectious Diseases*, 22:2178–2180, 2016.

[13] J. Barasona, M. Latham, P. Acevedo, J. Armenteros, D. Latham, C. Gortázar, F. Carro, R. Soriguer, and J. Vicente. Spatiotemporal interactions between wild boar and cattle: implications for cross-species disease transmission. *Veterinary Research*, 45(1):122, 2014.

[14] J. Barasona, J. Vicente, I. Díez-Delgado, J. Aznar, C. Gortázar, and M. Torres. Environmental presence of *Mycobacterium tuberculosis* complex in aggregation points at the wildlife/livestock interface. *Transboundary and Emerging Diseases*, 64(4):1148–58, 2017.

[15] J. A. Barasona, K. VerCauteren, N. Saklou, C. Gortazar, and J. Vicente. Effectiveness of cattle operated bump gates and exclusion fences in preventing ungulate multi-host sanitary interaction. *Preventive Veterinary Medicine*, 111(1-2):42–50, 2013.

[16] N. Barlow. The ecology of wildlife disease control: simple models revisited. *Journal of Applied Ecology*, 33:303–314, 1996.

[17] N. Barlow. Non-linear transmission and simple models for bovine tuberculosis. *Journal of Animal Ecology*, 69(4):703–713, 2000.

[18] N. Beeton and H. McCallum. Models predict that culling is not a feasible strategy to prevent extinction of Tasmanian devils from facial tumour disease. *Journal of Applied Ecology*, 48:1315–1323, 2011.

[19] J. Bencatel, F. Álvares, A. E. Moura, and A. M. Barbosa. Atlas de Mamíferos de Portugal, 2017.

[20] J. Bielby, C. A. Donnelly, L. C. Pope, T. Burke, and R. Woodroffe. Badger responses to small-scale culling may compromise targeted control of bovine tuberculosis. *Proceedings of the National Academy of Sciences*, page 201401503, 2014.

[21] J. Blackburn, V. Asher, S. Stokke, D. Hunter, and K. Alexander. Dances with anthrax: wolves (*Canis lupus*) kill anthrax bacteremic plains bison (*Bison bison*) in southwestern Montana. *Journal of Wildlife Diseases*, 50(2):393–396, 2014.

[22] M. Boadella, K. Lyashchenko, R. Greenwald, J. Esfandiari, R. Jaroso, T. Carta, J. Garrido, J. Vicente, J. de la Fuente, and C. Gortázar. Serologic tests for detecting antibodies against *Mycobacterium bovis* and *Mycobacterium avium* subspecies paratuberculosis in Eurasian wild boar (*Sus scrofa*). *Journal of Veterinary Diagnostic Investigation*, 23(1):77—83, 2011.

[23] M. Boadella, J. Vicente, F. Ruiz-Fons, J. de la Fuente, and C. Gortázar. Effects of culling Eurasian wild boar on the prevalence of *Mycobacterium bovis* and Aujeszky's disease virus. *Preventive Veterinary Medicine*, 107:214–221, 2012.

[24] L. Boitani, P. Trapanese, and L. Mattei. Methods of population estimates of a hunted wild boar (*Sus scrofa* l.) population in Tuscany (Italy). *Journal of Mountain Ecology*, 3, 2014.

[25] L. Bolzoni, L. Real, and G. De Leo. Transmission heterogeneity and control strategies for infectious disease emergence. *PLoS ONE*, 2:e747, 2007.

[26] J. Bourn. Identifying and tracking livestock in england. *National Audit Office*, 2003.

[27] J. Bourne, C. Donnelly, D. Cox, G. Gettinby, J. McInerney, W. Morrison, and R. Woodroffe. Bovine TB: the scientific evidence. The final report of the Independent Scientific Group on Cattle TB. London. Department of Environment. *Food and Rural Affairs*, 2007.

[28] E. Brooks-Pollock, G. O. Roberts, and M. J. Keeling. A dynamic model of bovine tuberculosis spread and control in Great Britain. *Nature*, 511(7508):228, 2014.

[29] B. Buddle, N. Parlane, D. Wedlock, and A. Heiser. Overview of vaccination trials for control of tuberculosis in cattle, wildlife and humans. *Transboundary and Emerging Diseases*, 60:136–146, 2013.

[30] M. Carstensen, D. J. O'Brien, and S. M. Schmitt. Public acceptance as a determinant of management strategies for bovine tuberculosis in free-ranging US wildlife. *Veterinary Microbiology*, 151(1-2):200–204, 2011.

[31] S. P. Carter, M. A. Chambers, S. P. Rushton, M. D. Shirley, P. Schuchert, S. Pietravalle, A. Murray, F. Rogers, G. Gettinby, G. C. Smith, et al. BCG vaccination reduces risk of tuberculosis infection in vaccinated badgers and unvaccinated badger cubs. *PLoS ONE*, 7(12):e49833, 2012.

[32] G. Chapron, P. Kaczensky, J. D. Linnell, M. von Arx, D. Huber, H. Andrén, J. V. López-Bao, M. Adamec, F. Álvares, O. Anders, et al. Recovery of large carnivores in Europe's modern human-dominated landscapes. *Science*, 346(6216):1517–1519, 2014.

[33] A. Che'Amat, J. A. Armenteros, D. González-Barrio, J. Lima, I. Díez-Delgado, J. A. Barasona, B. Romero, K. P. Lyashchenko, et al. Is targeted removal a suitable means for tuberculosis control in wild boar? *Preventive Veterinary Medicine*, 135:132–135, 2016.

[34] A. Che'Amat, D. González-Barrio, J. Ortiz, I. Díez-Delgado, M. Boadella, J. Barasona, J. Bezos, B. Romero, J. Armenteros, K. Lyashchenko, et al. Testing Eurasian wild boar piglets for serum antibodies against *Mycobacterium bovis*. *Preventive Veterinary Medicine*, 121(1-2):93–98, 2015.

[35] M. Choisy and P. Rohani. Harvesting can increase severity of wildlife disease epidemics. *Proceedings of the Royal Society of London B: Biological Sciences*, 273:2025–2034, 2006.

[36] G. Ciaravino, P. Ibarra, E. Casal, S. Lopez, J. Espluga, J. Casal, S. Napp, and A. Allepuz. Farmer and veterinarian attitudes towards the bovine tuberculosis eradication programme in Spain: what is going on in the field? *Frontiers in Veterinary Science*, 4:202, 2017.

[37] P. Ciucci, L. Artoni, F. Crispino, E. Tosoni, and L. Boitani. Inter-pack, seasonal and annual variation in prey consumed by wolves in Pollino National Park, southern Italy. *European Journal of Wildlife Research*, 64(1):5, 2018.

[38] H. Comins, M. Hassell, and R. May. The spatial dynamics of host–parasitoid systems. *Journal of Animal Ecology*, pages 735–748, 1992.

[39] C. Cowie, N. Marreos, C. Gortázar, R. Jaroso, P. White, and A. Balseiro. Shared risk factors for multiple livestock diseases: a case study of bovine tuberculosis and brucellosis. *Research in Veterinary Science*, 97(3):491–497, 2014.

[40] B. Cowled, M. Garner, K. Negus, and M. Ward. Controlling disease outbreaks in wildlife using limited culling: modelling classical swine fever incursions in wild pigs in Australia. *Veterinary Research*, 43(3), 2012).

[41] D. Cox, C. A. Donnelly, F. J. Bourne, G. Gettinby, J. P. McInerney, W. I. Morrison, and R. Woodroffe. Simple model for tuberculosis in cattle and badgers. *Proceedings of the National Academy of Sciences*, 102(49):17588–17593, 2005.

[42] P. Daszak, A. Cunningham, and A. Hyatt. Emerging infectious diseases of wildlife–threats to biodiversity and human health. *Science*, 287(5452):443, 2000.

[43] R. Davidson, G. Marion, P. White, and M. Hutchings. Use of host population reduction to control wildlife infection: rabbits and paratuberculosis. *Epidemiology & Infection*, 137:131–138, 2009.

[44] R. De la Rua-Domenech. Human *Mycobacterium bovis* infection in the United Kingdom: incidence, risks, control measures and review of the zoonotic aspects of bovine tuberculosis. *Tuberculosis*, 86(2):77–109, 2006.

[45] Defra. The Strategy for Achieving Officially Bovine Tuberculosis Free Status for England, 2014.

[46] Defra. 2010 to 2015 government policy: bovine tuberculosis (bovine TB), 2015.

[47] K. Dietz. Epidemics and rumours: a survey. *Journal of the Royal Statistical Society. Series A (General)*, pages 505–528, 1967.

[48] I. Díez-Delgado, I. A. Sevilla, B. Romero, E. Tanner, J. A. Barasona, A. R. White, P. W. Lurz, M. Boots, J. de la Fuente, L. Dominguez, et al. Impact of piglet oral vaccination against tuberculosis in endemic free-ranging wild boar populations. *Preventive Veterinary Medicine*, 155:11–20, 2018.

[49] C. Donnelly, G. Wei, W. Johnston, D. Cox, R. Woodroffe, F. Bourne, C. Cheeseman, R. Clifton-Hadley, G. Gettinby, P. Gilks, and H. Jenkins. Impacts of widespread badger culling on cattle tuberculosis: concluding analyses from a large–scale field trial. *International Journal of Infectious Diseases*, 11(4):300–308, 2007.

[50] C. A. Donnelly and J. Hone. Is there an association between levels of bovine tuberculosis in cattle herds and badgers? *Statistical Communications in Infectious Diseases*, 2(1), 2010.

[51] C. A. Donnelly, R. Woodroffe, D. Cox, F. J. Bourne, C. Cheeseman, R. S. Clifton-Hadley, G. Wei, G. Gettinby, P. Gilks, H. Jenkins, et al. Positive and negative effects of widespread badger culling on tuberculosis in cattle. *Nature*, 439(7078):843, 2006.

[52] J. Drewe, H. O'connor, N. Weber, R. McDonald, and R. Delahay. Patterns of direct and indirect contact between cattle and badgers naturally infected with tuberculosis. *Epidemiology and Infection*, 141(07):1467–1475, 2013.

[53] G. Enticott. Public attitudes to badger culling to control bovine tuberculosis in rural Wales. *European Journal of Wildlife Research*, 61(3):387–398, 2015.

[54] A. Fernández-Gil, J. Naves, A. Ordiz, M. Quevedo, E. Revilla, and M. Delibes. Conflict misleads large carnivore management and conservation: brown bears and wolves in Spain. *PLoS ONE*, 11(3):e0151541, 2016.

[55] A. E. Fine, C. A. Bolin, J. C. Gardiner, and J. B. Kaneene. A study of the persistence of *Mycobacterium bovis* in the environment under natural weather conditions in Michigan, USA. *Veterinary Medicine International*, 2011, 2011.

[56] S. Fitzgerald and J. Kaneene. Wildlife reservoirs of bovine tuberculosis worldwide: hosts, pathology, surveillance, and control. *Veterinary Pathology*, 50(3):488–499, 2013.

[57] C. W. Fowler. Density dependence as related to life history strategy. *Ecology*, 62(3):602–610, 1981.

[58] C. M. Freuling, K. Hampson, T. Selhorst, R. Schröder, F. X. Meslin, T. C. Mettenleiter, and T. Müller. The elimination of fox rabies from Europe: determinants of success and lessons for the future. *Philosophical Transactions of the Royal Society B: Biological Sciences*, 368(1623):20120142, 2013.

[59] W. García-Jiménez, P. Fernández-Llario, J. Benítez-Medina, R. Cerrato, J. Cuesta, A. García-Sánchez, P. Gonçalves, R. Martínez, D. Risco, F. Salguero, and E. Serrano. Reducing Eurasian wild boar (*Sus scrofa*) population density as a measure for bovine tuberculosis control: effects in wild boar and a sympatric fallow deer (*Dama dama*) population in central Spain. *Preventive Veterinary Medicine*, 110(3-4):435–446, 2013.

[60] J. M. Garrido, I. A. Sevilla, B. Beltrán-Beck, E. Minguijón, C. Ballesteros, R. C. Galindo, M. Boadella, K. P. Lyashchenko, B. Romero, M. V. Geijo, et al. Protection against tuberculosis in Eurasian wild boar vaccinated with heat-inactivated *Mycobacterium bovis*. *PLoS ONE*, 6(9):e24905, 2011.

[61] D. Gavier-Widén, K. Ståhl, A. Neimanis, C. H. av Segerstad, C. Gortázar, S. Rossi, and T. Kuiken. African swine fever in wild boar in Europe: a notable challenge. *Veterinary Record*, 176(8):199–200, 2015.

[62] A. Gehman and J. Byers. Non-native parasite enhances susceptibility of host to native predators. *Oecologia*, 183(4):919–926, 2017.

[63] J.-F. Gerard, B. Cargnelutti, F. Spitz, G. Valet, and T. Sardin. Habitat use of wild boar in a French agroecosystem from late winter to early summer. *Acta Theriologica*, 36(1-2):119–129, 1991.

[64] F. Gethöffer, G. Sodeikat, and K. Pohlmeyer. Reproductive parameters of wild boar (*Sus scrofa*) in three different parts of Germany. *European Journal of Wildlife Research*, 53(4):287–297, 2007.

[65] R. Ghodbane, F. M. Medie, H. Lepidi, C. Nappez, and M. Drancourt. Long-term survival of tuberculosis complex mycobacteria in soil. *Microbiology*, 160(3):496–501, 2014.

[66] M. Gilbert, A. Mitchell, D. Bourn, J. Mawdsley, R. Clifton-Hadley, and W. Wint. Cattle movements and bovine tuberculosis in Great Britain. *Nature*, 435(7041):491, 2005.

[67] D. T. Gillespie. A general method for numerically simulating the stochastic time evolution of coupled chemical reactions. *Journal of Computational Physics*, 22(4):403–434, 1976.

[68] Gobierno del Principado de Asturias. Situación de lobo en Asturias, 2003. Consejería de Medio Ambiente, ordenación del Territorio e Infraestructuras del Principado de Asturias. Unpublished report, 102p, 2003.

[69] Gobierno del Principado de Asturias. Diagnóstico de la situación del lobo en Asturias, 2014. Estimación de la población por unidades reproductoras. Unpublished report 28p, 2014.

[70] C. Gortázar, A. Che'Amat, and D. O' Brien. Open questions and recent advances in the control of a multi-host infectious disease: animal tuberculosis. *Mammal Review*, 45(3):160–175, 2015.

[71] C. Gortazar, R. Delahay, R. Mcdonald, M. Boadella, G. Wilson, D. Gavier-Widen, and P. Acevedo. The status of tuberculosis in European wild mammals. *Mammal Review*, 42(3):193–206, 2012.

[72] C. Gortázar, I. Díez-Delgado, J. A. Barasona, J. Vicente, J. De La Fuente, and M. Boadella. The wild side of disease control at the wildlife-livestock-human interface: a review. *Frontiers in Veterinary Science*, 1:27, 2015.

[73] C. Gortázar, L. Fernández-Calle, J. Collazos-Martínez, O. Mínguez-González, and P. Acevedo. Animal tuberculosis maintenance at low abundance of suitable wildlife reservoir hosts: a case study in northern Spain. *Preventive Veterinary Medicine*, 146:150–157, 2017.

[74] C. Gortázar, E. Ferroglio, U. Höfle, K. Frölich, and J. Vicente. Diseases shared between wildlife and livestock: a European perspective. *European Journal of Wildlife Research*, 53(4):241, 2007.

[75] C. Gortázar, M. Torres, J. Vicente, P. Acevedo, M. Reglero, J. De la Fuente, J. Negro, and J. Aznar-Martín. Bovine tuberculosis in Doñana Biosphere Reserve: the role of wild ungulates as disease reservoirs in the last Iberian lynx strongholds. *PLoS ONE*, 3(7):e2776, 2008.

[76] C. Gortázar, J. Vicente, M. Boadella, C. Ballesteros, R. Galindo, J. Garrido, A. Aranaz, and J. De La Fuente. Progress in the control of bovine tuberculosis in Spanish wildlife. *Veterinary Microbiology*, 151(1):170–178, 2011.

[77] S. Hall, M. Duffy, and C. Cáceres. Selective predation and productivity jointly drive complex behavior in host-parasite systems. *The American Naturalist*, 165(1):70–81, 2004.

[78] T. G. Hallam and G. F. McCracken. Management of the panzootic white–nose syndrome through culling of bats. *Conservation Biology*, 25(1):189–194, 2011.

[79] A. Harrison, S. Newey, L. Gilbert, D. T. Haydon, and S. Thirgood. Culling wildlife hosts to control disease: mountain hares, red grouse and louping ill virus. *Journal of Applied Ecology*, 47(4):926–930, 2010.

[80] D. Haydon. Identifying reservoirs of infection: a conceptual and practical challenge. *Emerging Infectious Diseases*, 8(12):1468–1473, 2002.

[81] R. Holt and M. Roy. Predation can increase the prevalence of infectious disease. *The American Naturalist*, 169(5):690–699, 2007.

[82] P. Hudson, A. Dobson, and D. Newborn. Do parasites make prey vulnerable to predation? red grouse and parasites. *Journal of Animal Ecology*, pages 681–692, 1992.

[83] D. O. Joly and F. Messier. The distribution of *Echinococcus granulosus* in moose: evidence for parasite-induced vulnerability to predation by wolves? *Oecologia*, 140:586—-590, 2004.

[84] M. J. Keeling and P. Rohani. *Modeling infectious diseases in humans and animals*. Princeton University Press, 2008.

[85] W. O. Kermack and A. G. McKendrick. A contribution to the mathematical theory of epidemics. *Proceedings of the Royal Society of London. Series A, Containing papers of a mathematical and physical character*, 115(772):700–721, 1927.

[86] O. Keuling, E. Baubet, A. Duscher, C. Ebert, C. Fischer, A. Monaco, T. Podgórski, C. Prevot, K. Ronnenberg, G. Sodeikat, and N. Stier. Mortality rates of wild boar *Sus scrofa* l. in central Europe. *European Journal of Wildlife Research*, 59(6):805–814, 2013.

[87] C. E. Krumm, M. M. Conner, N. T. Hobbs, D. O. Hunter, and M. W. Miller. Mountain lions prey selectively on prion-infected mule deer. *Biology Letters*, page rsbl20090742, 2009.

[88] E. Kukielka, J. Barasona, C. Cowie, J. Drewe, C. Gortazar, I. Cotarelo, and J. Vicente. Spatial and temporal interactions between livestock and wildlife in south central Spain assessed by camera traps. *Preventive Veterinary Medicine*, 112(3-4):213–221, 2013.

[89] N. LaHue, J. Baños, P. Acevedo, C. Gortázar, and B. Martínez-López. Spatially explicit modeling of animal tuberculosis at the wildlife-livestock interface in Ciudad Real province, Spain. *Preventive Veterinary Medicine*, 128:101–111, 2016.

[90] S. Lass, P. J. Hudson, J. Thakar, J. Saric, E. Harvill, R. Albert, and S. E. Perkins. Generating super-shedders: co-infection increases bacterial load and egg production of a gastrointestinal helminth. *Journal of the Royal Society Interface*, 10(80):20120588, 2013.

[91] R. J. Lennox, A. J. Gallagher, E. G. Ritchie, and S. J. Cooke. Evaluating the efficacy of predator removal in a conflict-prone world. *Biological Conservation*, 224:277–289, 2018.

[92] T. Levi, A. M. Kilpatrick, M. Mangel, and C. C. Wilmers. Deer, predators, and the emergence of Lyme disease. *Proceedings of the National Academy of Sciences*, 109(27):10942–10947, 2012.

[93] M. Manjerovic, M. Green, N. Mateus-Pinilla, and J. Novakofski. The importance of localized culling in stabilizing chronic wasting disease prevalence in white-tailed deer populations. *Preventive Veterinary Medicine*, 113:139–145, 2014.

[94] M. P. Martín-Hernando, U. Höfle, J. Vicente, F. Ruiz-Fons, D. Vidal, M. Barral, J. M. Garrido, J. de la Fuente, and C. Gortazar. Lesions associated with *Mycobacterium tuberculosis* complex infection in the European wild boar. *Tuberculosis*, 87(4):360–367, 2007.

[95] R. May and A. R. McLean. *Theoretical ecology: principles and applications*. Oxford University Press on Demand, 2007.

[96] R. M. May. *Complexity and stability in model ecosystems*. Princeton University Press, 1973.

[97] H. McCallum. Models for managing wildlife disease. *Parasitology*, 143:805–820, 2016.

[98] C. Melis, P. A. Szafrańska, B. Jedrzejewska, and K. Bartoń. Biogeographical variation in the population density of wild boar (*Sus scrofa*) in western Eurasia. *Journal of Biogeography*, 33(5):803–811, 2006.

[99] F. Messier, M. E. Rau, and M. A. McNeill. *Echinococcus granulosus* (Cestoda: Taeniidae) infections and moose–wolf population dynamics in southwestern Quebec. *Canadian Journal of Zoology*, 67(1):216–219, 1989.

[100] S. More, A. Bøtner, A. Butterworth, P. Calistri, K. Depner, S. Edwards, B. Garin-Bastuji, M. Good, C. Gortázar Schmidt, V. Michel, et al. Scientific opinion on the assessment of listing and categorisation of animal diseases within the framework of the Animal Health Law (Regulation (EU) No 2016/429): bovine tuberculosis. *EFSA Journal*, 15(7):4959, 2017.

[101] E. Mori, L. Benatti, S. Lovari, and F. Ferretti. What does the wild boar mean to the wolf? *European Journal of Wildlife Research*, 63(1):9, 2017.

[102] M. Muñoz-Mendoza, N. Marreros, M. Boadella, C. Gortázar, S. Menéndez, L. de Juan, J. Bezos, B. Romero, M. F. Copano, J. Amado, et al. Wild boar tuberculosis in Iberian Atlantic Spain: a different picture from Mediterranean habitats. *BMC Veterinary Research*, 9(1):176, 2013.

[103] J. D. J. D. Murray. *Mathematical biology. 1, An introduction.* Interdisciplinary applied mathematics ; v. 17. Springer-Verlag, New York, third edition.. edition, 2002.

[104] S. Mykrä, M. Pohja-Mykrä, and T. Vuorisalo. Hunters' attitudes matter: diverging bear and wolf population trajectories in finland in the late nineteenth century and today. *European Journal of Wildlife Research*, 63(5):76, 2017.

[105] A. Náhlik and G. Sándor. Birth rate and offspring survival in a free-ranging wild boar *Sus scrofa* population. *Wildlife Biology*, 9(SUPPL 1):37–42, 2003.

[106] V. Naranjo, C. Gortázar, J. Vicente, and J. De La Fuente. Evidence of the role of European wild boar as a reservoir of *Mycobacterium tuberculosis* complex. *Veterinary Microbiology*, 127(1):1–9, 2008.

[107] C. Nores, L. Llaneza, and A. Álvarez. Wild boar *Sus scrofa* mortality by hunting and wolf *Canis lupus* predation: an example in northern Spain. *Wildlife Biology*, 14(1):44–51, 2008.

[108] D. J. O'Brien, S. M. Schmitt, B. A. Rudolph, and G. Nugent. Recent advances in the management of bovine tuberculosis in free-ranging wildlife. *Veterinary Microbiology*, 151(1-2):23–33, 2011.

[109] C. J. O'Bryan, A. R. Braczkowski, H. L. Beyer, N. H. Carter, J. E. Watson, and E. McDonald-Madden. The contribution of predators and scavengers to human well-being. *Nature Ecology & Evolution*, page 1, 2018.

[110] R. Ostfeld and R. Holt. Are predators good for your health? Evaluating evidence for top-down regulation of zoonotic disease reservoirs. *Frontiers in Ecology and the Environment*, 2(1):13–20, 2004.

[111] C. Packer, R. Holt, P. Hudson, K. Lafferty, and A. Dobson. Keeping the herds healthy and alert: implications of predator control for infectious disease. *Ecology Letters*, 6(9):797–802, 2003.

[112] L. J. Palomo, J. Gisbert, and J. C. Blanco. *Atlas y libro rojo de los mamíferos terrestres de España*. Organismo Autónomo de Parques Nacionales Madrid, 2007.

[113] A. Potapov, E. Merrill, and M. Lewis. Wildlife disease elimination and density dependence. *Proceedings of the Royal Society of London B: Biological Sciences*, 279:3139–3145, 2012.

[114] A. Potapov, E. Merrill, M. Pybus, and M. Lewis. Chronic wasting disease: Transmission mechanisms and the possibility of harvest management. *PLoS ONE*, 11:e0151039, 2016.

[115] J. C. Prentice, G. Marion, P. C. White, R. S. Davidson, and M. R. Hutchings. Demographic processes drive increases in wildlife disease following population reduction. *PLoS ONE*, 9(5):e86563, 2014.

[116] Public Health England. Tuberculosis in the UK 2014 report. `www.gov.ukpublicationsgatewaynumber:2014353`.

[117] F. Quirós-Fernández, J. Marcos, P. Acevedo, and C. Gortázar. Hunters serving the ecosystem: the contribution of recreational hunting to wild boar population control. *European Journal of Wildlife Research*, 63(3):57, 2017.

[118] B. Radunz. Surveillance and risk management during the latter stages of eradication: experiences from Australia. *Veterinary Microbiology*, 112(2-4):283–290, 2006.

[119] S. Redpath, J. Young, A. Evely, W. Adams, W. Sutherland, A. Whitehouse, A. Amar, R. Lambert, J. Linnell, A. Watt, and R. Gutierrez. Understanding and managing conservation conflicts. *Trends in Ecology & Evolution*, 28(2):100–109, 2013.

[120] E. Renshaw. *Modelling biological populations in space and time*, volume 11. Cambridge University Press, 1993.

[121] W. Ricker. Stock and recruitment. *Journal of the Fisheries Board of Canada*, 11:559–623, 1954.

[122] W. J. Ripple, J. A. Estes, R. L. Beschta, C. C. Wilmers, E. G. Ritchie, M. Hebblewhite, J. Berger, B. Elmhagen, M. Letnic, M. P. Nelson, et al. Status and ecological effects of the world's largest carnivores. *Science*, 343(6167):1241484, 2014.

[123] P. Roeder, J. Mariner, and R. Kock. Rinderpest: the veterinary perspective on eradication. *Philosophical Transactions of the Royal Society B: Biological Sciences*, 368(20120139), 2013.

[124] F. Ruiz-Fons, J. Vicente, D. Vidal, U. Höfle, D. Villanúa, C. Gauss, J. Segalés, S. Almería, V. Montoro, and C. Gortázar. Seroprevalence of six reproductive pathogens in European wild boar (*Sus scrofa*) from Spain: the effect on wild boar female reproductive performance. *Theriogenology*, 65(4):731–743, 2006.

[125] C. Sáez-Royuela and J. Tellería. The increased population of the wild boar (*Sus scrofa* l.) in Europe. *Mammal Review*, 16(2):97–101, 1986.

[126] N. Santos, V. Almeida, C. Gortázar, and M. Correia-Neves. Patterns of *Mycobacterium tuberculosis*-complex excretion and characterization of super-shedders in naturally-infected wild boar and red deer. *Veterinary Research*, 46:129, 2015.

[127] I. Schiller, W. RayWaters, H. M. Vordermeier, T. Jemmi, M. Welsh, N. Keck, A. Whelan, E. Gormley, M. L. Boschiroli, J. L. Moyen, et al. Bovine tuberculosis in Europe from the perspective of an officially tuberculosis free country: trade, surveillance and diagnostics. *Veterinary Microbiology*, 151(1-2):153–159, 2011.

[128] G. Smith and C. Cheeseman. A mathematical model for the control of diseases in wildlife populations: culling, vaccination and fertility control. *Ecological Modelling*, 150(1-2):45–53, 2002.

[129] G. Smith, C. Cheeseman, R. Clifton-Hadley, and D. Wilkinson. A model of bovine tuberculosis in the badger *Meles meles*: the inclusion of cattle and the use of a live test. *Journal of Applied Ecology*, 38(3):520–535, 2001.

[130] D. Storm, M. Samuel, R. Rolley, P. Shelton, N. Keuler, B. Richards, and T. Van Deelen. Deer density and disease prevalence influence transmission of chronic wasting disease in white-tailed deer. *Ecosphere*, 4:1–14, 2013.

[131] A. Stronen, R. Brook, P. Paquet, and S. Mclachlan. Farmer attitudes toward wolves: implications for the role of predators in managing disease. *Biological Conservation*, 135:1–10, 2007.

[132] M. Tanner and A. L. Michel. Investigation of the viability of *M. bovis* under different environmental conditions in the Kruger National Park. *Onderstepoort Journal of Veterinary Research*, 66:185–190, 1999.

[133] M. Thom, M. McAulay, H. Vordermeier, D. Clifford, R. Hewinson, B. Villarreal-Ramos, and J. Hope. Duration of immunity against *Mycobacterium bovis* following neonatal vaccination with bacillus Calmette-Guérin Danish: significant protection against infection at 12, but not 24, months. *Clinical and Vaccine Immunology*, 19:1254–1260, 2012.

[134] C. Toïgo, S. Servanty, J.-M. Gaillard, S. Brandt, and E. Baubet. Disentangling natural from hunting mortality in an intensively hunted wild boar population. *The Journal of Wildlife Management*, 72(7):1532–1539, 2008.

[135] A. Treves and K. Karanth. Human–carnivore conflict and perspectives on carnivore management worldwide. *Conservation biology*, 17(6):1491–1499, 2003.

[136] F. Uehlinger, A. Johnston, T. Bollinger, and C. Waldner. Systematic review of management strategies to control chronic wasting disease in wild deer populations in North America. *BMC Veterinary Research*, 12:173, 2016.

[137] J. Vicente, J. Barasona, P. Acevedo, J. Ruiz-Fons, M. Boadella, I. Díez-Delgado, B. Beltran-Beck, and C. Gortázar. Temporal trend of tuberculosis in wild ungulates from Mediterranean Spain. *Transboundary and Emerging Diseases*, 60(s1):92–103, 2013.

[138] J. Vicente, U. Höfle, J. Garrido, P. Acevedo, R. Juste, M. Barral, and C. Gortázar. Risk factors associated with the prevalence of tuberculosis–like lesions in fenced wild boar and red deer in south central Spain. *Veterinary Research*, 38(3):451–464, 2007.

[139] J. Vicente, U. Höfle, J. Garrido, I. Fernández-De-Mera, R. Juste, M. Barral, and C. Gortázar. Wild boar and red deer display high prevalences of tuberculosis–like lesions in Spain. *Veterinary Research*, 37(1):107–119, 2006.

[140] J. Vicente, J. Segalés, U. Höfle, M. Balasch, J. Plana-Durán, M. Domingo, and C. Gortázar. Epidemiological study on porcine circovirus type 2 (PCV2) infection in the European wild boar (*Sus scrofa*). *Veterinary Research*, 35(2):243–253, 2004.

[141] G. Wasserberg, E. Osnas, R. Rolley, and M. Samuel. Host culling as an adaptive management tool for chronic wasting disease in white-tailed deer: a modelling study. *Journal of Applied Ecology*, 46:457–466, 2009.

[142] A. White and P. Lurz. A modelling assessment of control strategies to prevent/reduce Squirrelpox spread. Scittusg Natural Heritage Commissioned Report No. 627, 2014.

[143] M. Wild, N. Hobbs, M. Graham, and M. W. Miller. The role of predation in disease control: a comparison of selective and nonselective removal on prion disease dynamics in deer. *Journal of Wildlife Diseases*, 47(1):78–93, 2011.

[144] L. L. Wolfe, M. W. Miller, and E. S. Williams. Feasibility of "test-and-cull" for managing chronic wasting disease in urban mule deer. *Wildlife Society Bulletin*, 32(2):500–505, 2004.

[145] R. Woodroffe. Managing disease threats to wild mammals. *Animal Conservation*, 2(3):185–193, 1999.

[146] R. Woodroffe, C. Donnelly, C. Ham, S. Jackson, K. Moyes, K. Chapman, N. Stratton, and S. Cartwright. Badgers prefer cattle pasture but avoid cattle: implications for bovine tuberculosis control. *Ecology Letters*, 19(10):1201–1208, 2016.